

T  
✓ F-83  
AGK

# NUCLEATE POOL BOILING OF SATURATED LIQUIDS ON HORIZONTAL CYLINDERS

A THESIS  
*submitted in fulfilment of the requirements  
for the award of the degree  
of*  
DOCTOR OF PHILOSOPHY  
*in*  
CHEMICAL ENGINEERING

By  
SUBODH KUMAR AGRAWAL



DEPARTMENT OF CHEMICAL ENGINEERING  
UNIVERSITY OF ROORKEE  
ROORKEE-247 667 (INDIA)

August, 1983



## *Candidate's Declaration*

I hereby certify that the work, which is being presented in the thesis entitled "*Nucleate Pool Boiling of Saturated Liquids on Horizontal Cylinders*" in fulfilment of the requirements for the award of the degree of Doctor of Philosophy, submitted in the Department of CHEMICAL ENGINEERING of the University is an authentic record of my own work carried out during a period from January, 1980 to August, 1983 under the supervision of Dr. B. S. Varshney, Professor & Head and Dr. S. C. Gupta, Reader, Department of Chemical Engineering, University of Roorkee, Roorkee.

The matter embodied in this thesis has not been submitted by me for the award of any other degree.

(Subodh Kumar Agrawal)  
Candidate's Signature

This is to certify that the above statement made by the candidate is correct to the best of our knowledge.

(S. C. Gupta)

Reader

Department of Chemical Engineering  
University of Roorkee  
Roorkee-247667

(B. S. Varshney)

Professor & Head

Department of Chemical Engineering  
University of Roorkee  
Roorkee-247667

August 9, 1983

## ABSTRACT

The present thesis pertains to nucleate pool boiling heat transfer from electrically heated horizontal cylinder(s) to the pool of saturated liquids : distilled water, benzene and toluene under low heat flux values for atmospheric and subatmospheric pressures both experimentally and theoretically. The heat flux ranged from  $16.168 \text{ kW/m}^2$  to  $48.504 \text{ kW/m}^2$  and the pressure from  $29.86 \text{ kN/m}^2$  to  $98.00 \text{ kN/m}^2$ . Both the heating cylinders were of identical surface characteristics and they were kept apart horizontally one over the other at a distance of 75 mm.

The experimental data were conducted for the above parameters for the heat transfer from one of the heating cylinders to saturated liquids. These data provide an equation for the calculation of average wall superheat from the knowledge of heat flux and pressure for a given surface liquid combination. Further, they also reveal that the value of wall superheat is not constant over the circumference of the heating cylinder. It increases from top- to side- to bottom- position of the electrically heated cylinders.

A semi-theoretical analysis has led to a generalized correlation which provides a procedure to predict the values of average wall superheat for the boiling of a liquid under atmospheric and subatmospheric pressures on a given heating surface from the knowledge of the average wall superheat

for the boiling of same liquid on the same heating surface but at a known value of pressure and heat flux. The correlation has successfully correlated the experimental data for the boiling of distilled water, benzene, toluene, methanol, isopropanol and carbon tetra-chloride conducted on differing heating surfaces at atmospheric and subatmospheric pressures within  $\pm 10$  per cent error. Thus, it can also be profitably used for checking the consistency of experimental data of nucleate pool boiling heat transfer obtained at different values of atmospheric and subatmospheric pressures.

Based on the experimental data, it has been found that the ratio of average wall superheat for the boiling of benzene to that of distilled water for a given heating surface, heat flux and pressure bears a constant value equal to 1.98. However this ratio is equal to 1.85 for the boiling of toluene and distilled water. Thus, the heat transfer data for the boiling of benzene and toluene over a heating surface for the desired values of heat flux and pressure can be predicted from the values of boiling heat transfer data for distilled water on the same heating surface and for the same values of heat flux and pressure.

The experimental data, when both the heating cylinders were energized simultaneously, show that the heat transfer from the lower heating cylinder is not affected whereas that from the upper heating cylinder is influenced considerably by the vapour bubbles emerging out from the lower heating cylinder. As a result of it the wall superheat of the upper

heating cylinder decreases from top- to side- to bottom- position of the cylinder indicating that the induced turbulence in the vicinity of bottom- position becomes more than in the vicinity of the top- position. It is equally important to mention that for a given heat flux, pressure and boiling liquid the average wall superheat for the upper heating cylinder is less than that of the lower heating cylinder. Further, for the value of heat flux lying between 16.168 to 24.252 kW/m<sup>2</sup>, the heat transfer coefficient,  $h$  for the boiling of liquids on upper heating cylinder has been found to be a function of heat flux,  $q$  raised to the power of 0.55 whereas that of on the lower heating cylinder varies with heat flux according to the relationship,  $haq^{0.7}$ . Furthermore, the ratio of heat transfer coefficient for the boiling of distilled water from upper heating cylinder to that of from the lower heating cylinder is 1.75 whereas it is 1.50 for the boiling of benzene and 1.30 for the boiling of toluene. In the range of heat flux from 24.252 to 28.294 kW/m<sup>2</sup> the variation of heat transfer coefficient with heat flux for the boiling of liquids on upper heating cylinder is represented by a 'dome' shaped curve, however for the lower heating cylinder it remains unaltered i.e.  $haq^{0.7}$ . For the region of heat flux from 28.294 to 48.504 kW/m<sup>2</sup> the heat transfer coefficient for the boiling of liquids from upper cylinder varied with heat flux raised to the power of 0.45. But, for the lower heating cylinder the variation of heat transfer coefficient with heat flux remains the same as observed for the low values of heat flux.

## ACKNOWLEDGEMENTS

The author expresses his deep sense of gratitude and indebtedness to his august guides and supervisors Dr. B.S. Varshney, Professor and Head and Dr. S.C. Gupta, Reader, Department of Chemical Engineering, University of Roorkee, Roorkee, who provided inspirational guidance, cooperation and encouragement throughout the duration of this work. Their painstaking efforts in going through the manuscript, giving valuable suggestions for its improvement and personal interest into the work can not be described in the words and the author can only recall with gratitude the long tiring but indefatigable hours spent in discussing and thrashing out the minutest details of the work.

The author deeply appreciates the enthusiastic association, cooperation and help rendered by his friend Sri Bikash Mohanty, Lecturer in Chemical Engineering Department, University of Roorkee, Roorkee.

Many thanks are due to

Dr. L.R. Sharma, Professor and Chairman, Department of Chemical Engineering and Technology, Panjab University, Chandigarh for providing necessary assistance as and when required;

Sri Chandrahas, Lecturer, Institute of Paper Technology (University of Roorkee), Saharanpur, a friend of the author, for his help and assistance during the work;

Sri Subhash Sharma, Lecturer in Chemical Engineering, Regional Engineering College, Srinagar and Sri G.D. Bansal, Senior Research Scholar under Quality Improvement Programme, University of Roorkee, Roorkee and Km. Sadhana Arya, a M.E. student for their cooperation and help during the course of the work ;

Faculty members of Chemical Engineering Department for their cooperation;

Members of the technical staff of Chemical Engineering Department for their help in fabrication and erection of the experimental set-up ;

Mrs. B.S. Varshney and Mrs. S.C. Gupta for their affection and encouragement during the total span of this work ;

and finally to his parents and wife for inspiration and understanding.

# CONTENTS

	Page
ABSTRACT	i
ACKNOWLEDGEMENTS	iv
CONTENTS	vi
LIST OF FIGURES	x
LIST OF TABLES	xv
NOMENCLATURE	xvi
CHAPTER 1 INTRODUCTION	1
CHAPTER 2 LITERATURE REVIEW	6
2.1 Nucleate pool boiling of liquids from heating surface	6
2.1.1 Nucleation site density	6
2.1.2 Bubble departure diameter	11
2.1.3 Bubble emission frequency	20
2.1.4 Nucleate boiling heat transfer models	26
2.1.5 Correlations for nucleate pool boiling	31
CHAPTER 3 EXPERIMENTAL SET-UP	54
3.1 Design considerations	54
3.2 Experimental set-up	55
3.3 Testing of the experimental set-up	66
CHAPTER 4 EXPERIMENTAL PROCEDURE	67
4.1 Cleaning, rinsing and charging the vessel	67
4.2 Stabilization of surface characteristics of heating cylinders	67



## Contents contd.

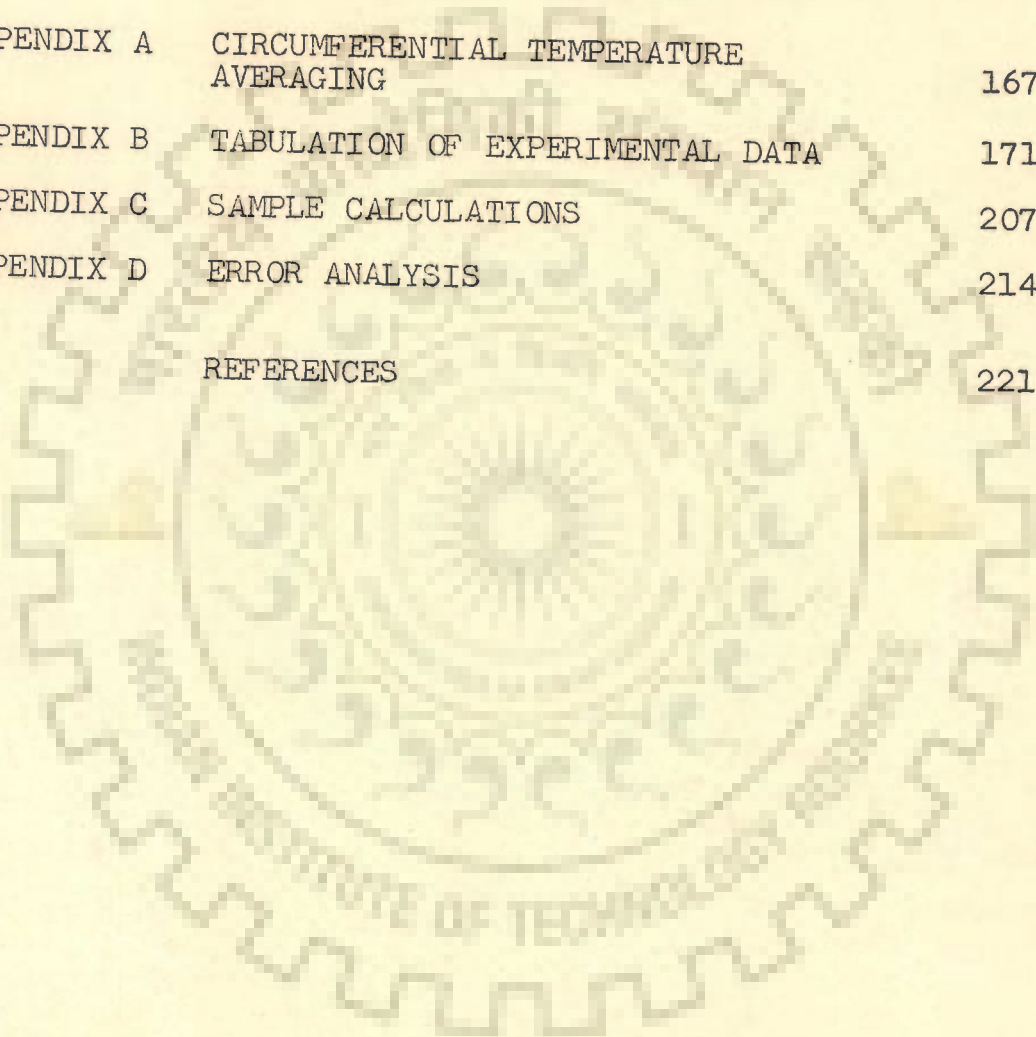
	4.3	Deagration of the test liquid	68
	4.4	Conduction of experimental data	68
	4.5	Reproducibility of experimental data	71
	4.6	Operational constraints	71
CHAPTER 5		ANALYTICAL INVESTIGATIONS	73
	5.1	Analysis	73
	5.2	Boiling heat transfer rate	75
CHAPTER 6		RESULTS AND DISCUSSION	81
	6.1	Constraints for data analysis	81
	6.2	Nucleate pool boiling of liquids on a single heating horizontal cylinder	82
	6.2.1	Surface characteristics of lower and upper heating cylinders	83
	6.2.2	Effect of heat flux on wall- and liquid- temperature distribution around the heating cylinder	87
	6.2.3	Effect of pressure on wall temperature distribution around the heating cylinder	91
	6.2.4	Effect of boiling liquids on wall temperature distribution around the heating cylinder	93
	6.2.5	Effect of heat flux on local wall superheat	97
	6.2.6	Effect of pressure on local wall superheat	101
	6.2.7	Effect of boiling liquid on local wall superheat	105
	6.2.8	Average wall superheat	105

## Contents contd.

6.2.9	Effect of heat flux on average wall superheat	107
6.2.10	Variation of $\Delta \bar{t}_w / q^{0.3}$ with pressure	112
6.2.11	Effect of heating surface on constant, $C_2$ of Eq(6.2)	114
6.2.12	Prediction of average wall superheat from the Alad'ev correlation	115
6.2.13	Determination of $\Psi(p/p_1)$ of Eq (5.17)	124
6.2.14	General correlation for wall superheat	124
6.2.15	Relationship between the values of average wall superheat of a heating cylinder for the boiling of organic liquids and the distilled water	128
6.2.16	Prediction of average wall superheat of benzene and toluene	132
6.3	Boiling heat transfer from an assembly consisting of two heating cylinders oriented horizontally one over the other	133
6.3.1	Wall- and the liquid-temperature distribution around the heating cylinders	134
6.3.2	Local wall temperature distribution around the lower heating cylinder	138
6.3.3	Wall superheat of the upper and the lower heating cylinders	142
6.3.4	Effect of heat flux on average wall superheat	146

## Contents contd.

6.3.5	Effect of pressure on average wall superheat	146
6.3.6	Effect of heat flux on heat transfer coefficient	153
CHAPTER 7	CONCLUSIONS AND RECOMMENDATIONS	160
APPENDIX A	CIRCUMFERENTIAL TEMPERATURE AVERAGING	167
APPENDIX B	TABULATION OF EXPERIMENTAL DATA	171
APPENDIX C	SAMPLE CALCULATIONS	207
APPENDIX D	ERROR ANALYSIS	214
	REFERENCES	221



## LIST OF FIGURES

		Page
Fig. 3.1	Schematic diagram of the experimental set-up	56
Fig. 3.2	Photographic view of experimental set-up	57
Fig. 3.3	Details of test vessel	58
Fig. 3.4	Details of a heating cylinder with heater	60
Fig. 3.5	Heating cylinder with test vessel wall	62
Fig. 3.6	Position of mounted thermocouples	64
Fig. 6.1	Circumferential wall temperature distribution for the upper and lower heating cylinders	84
Fig. 6.2	Circumferential wall temperature distribution for the upper and lower heating cylinders	85
Fig. 6.3	Circumferential wall temperature distribution for the upper and lower heating cylinders	86
Fig. 6.4	Effect of heat flux on wall and liquid temperature distribution around the heating cylinder	88
Fig. 6.5	Effect of heat flux on wall liquid temperature distribution around the heating cylinder	89
Fig. 6.6	Effect of heat flux on wall and liquid temperature distribution around the heating cylinder	90
Fig. 6.7	Effect of pressure on wall temperature distribution along the circumference of the heating cylinder	92

## List of Figures contd.

Page

Fig. 6.8	Effect of pressure on wall temperature distribution along the circumference of the heating cylinder	94
Fig. 6.9	Effect of pressure on wall temperature distribution along the circumference of the heating cylinder	95
Fig. 6.10	Effect of boiling liquids on wall temperature distribution along the circumference of the heating cylinder	96
Fig. 6.11	Effect of heat flux on wall superheat distribution along the circumference of the heating cylinder	98
Fig. 6.12	Effect of heat flux on wall superheat distribution along the circumference of the heating cylinder	99
Fig. 6.13	Effect of heat flux on wall superheat distribution along the circumference of the heating cylinder	100
Fig. 6.14	Effect of pressure on wall superheat distribution along the circumference of the heating cylinder	102
Fig. 6.15	Effect of pressure on wall superheat distribution along the circumference of the heating cylinder	103
Fig. 6.16	Effect of pressure on wall superheat distribution along the circumference of the heating cylinder	104
Fig. 6.17	Effect of boiling liquids on wall superheat distribution along the circumference of the heating cylinder	106
Fig. 6.18	Variation of average wall superheat with heat flux for the boiling of distilled water on upper heating cylinder	108

## List of Figures contd.

Page

- Fig. 6.19 Variation of average wall superheat with heat flux for the boiling of benzene on upper heating cylinder 109
- Fig. 6.20 Variation of average wall superheat with heat flux for the boiling of toluene on upper heating cylinder 110
- Fig. 6.21 Variation of average wall superheat with heat flux for the boiling of different liquids 111
- Fig. 6.22  $\Delta\bar{t}_w/q^{0.3}$  as a function of  $p$  113
- Fig. 6.23 Present experimental data compared with the Alad'ev equation, Eq (2.105) 117
- Fig. 6.24 Relationship between  $\Delta\bar{t}_w / \left[ \frac{10^{-6} q \lambda}{k_l T_s g} \right]^{0.3}$  and  $\left[ \frac{\lambda}{c_l T_s} \right]^{1.2} T_s$  and  $\rho_l/\rho_v$  119
- Fig. 6.25 A plot of  $\Delta\bar{t}_w$  Vs  $\left[ \frac{10^{-6} q \lambda}{k_l T_s g} \right]^{0.3} \left[ \frac{\lambda}{c_l T_s} \right]^{1.2} \left[ \frac{\rho_l}{\rho_v} \right]^{-0.24} T_s$  for nucleate boiling of saturated liquids 120
- Fig. 6.26 Experimental wall superheat compared with predicted values from the modified Alad'ev equation, Eq (6.4) 121
- Fig. 6.27 A plot of  $\Psi(p/p_1)$  Vs  $(p/p_1)$  for the boiling of saturated benzene of present investigation 125
- Fig. 6.28 Comparison of experimental data of various investigators from present analysis, Eq (6.8) 127

List of Figures contd.	Page
Fig. 6.29 $(\Delta\bar{t}_w)_b/(\Delta\bar{t}_w)_w$ as a function of heat flux	130
Fig. 6.30 $(\Delta\bar{t}_w)_t/(\Delta\bar{t}_w)_w$ as a function of heat flux	131
Fig. 6.31 Effect of heat flux on wall and liquid temperature distribution around the upper and lower heating cylinders	135
Fig. 6.32 Effect of heat flux on wall and liquid temperature distribution around the upper and lower heating cylinders	136
Fig. 6.33 Effect of heat flux on wall and liquid temperature distribution around the upper and lower heating cylinders	137
Fig. 6.34 Wall temperature distribution around the lower heating cylinder for the boiling of distilled water	139
Fig. 6.35 Wall temperature distribution around the lower heating cylinder for the boiling of benzene	140
Fig. 6.36 Wall temperature distribution around the lower heating cylinder for the boiling of toluene	141
Fig. 6.37 Wall superheat distribution along the circumference of the upper and lower heating cylinders	143
Fig. 6.38 Wall superheat distribution along the circumference of the upper and lower heating cylinders	144
Fig. 6.39 Wall superheat distribution along the circumference of the upper and lower heating cylinders	145

## List of Figures contd.

Page

Fig. 6.40	Variation of average wall superheat with heat flux for the boiling of distilled water on upper heating cylinder	147
Fig. 6.41	Variation of average wall superheat with heat flux for the boiling of benzene on upper heating cylinder	148
Fig. 6.42	Variation of average wall superheat with heat flux for the boiling of toluene on upper heating cylinder	149
Fig. 6.43	Variation of average wall superheat with pressure for upper heating cylinder	150
Fig. 6.44	Variation of average wall superheat with pressure for upper heating cylinder	151
Fig. 6.45	Variation of average wall superheat with pressure for upper heating cylinder	152
Fig. 6.46	Variation of heat transfer coefficient with heat flux for upper and lower heating cylinders	154
Fig. 6.47	Variation of heat transfer coefficient with heat flux for upper and lower heating cylinders	155
Fig. 6.48	Variation of heat transfer coefficient with heat flux for upper and lower heating cylinders	156



## LIST OF TABLES

		Page
Table 2.1	Expressions for bubble emission frequency	24
Table 2.2	Values of constants, a and b in Eqs (2.72 and 2.73)	34
Table 2.3	Values of constant, C and exponent, n in Eq (2.77)	38
Table 2.4	Range of operating variables [69]	39
Table 2.5	Values of constant, E in Eq (2.78)	40
Table 2.6	Values of c, n and m in Eq (2.82)	42
Table 2.7	Some empirical correlations of nucleate pool boiling of liquids	43
Table 2.8	Values of constant, $C_{sf}$ and exponent, s in Eq (2.89)	48
Table 2.9	Some of the analytical correlations of pool boiling of liquids	53
Table 4.1	Operating parameters of present investigation	69
Table 6.1	Values of constant, $C_2$ of Eq (6.2) for different boiling liquids on stainless steel heating cylinder	114
Table 6.2	Values of constant, $C_2$ of Eq (6.2) for different heating surfaces	115
Table 6.3	Values of constant, $C_3$ in Eq (6.3)	118
Table 6.4	Values of exponent, n of Eq (6.5)	123

## NOMENCLATURE

A	heat transfer area	$m^2$
c	specific heat	$J/kg \text{ } ^\circ K$
$C_{sf}$	surface-liquid combination factor	
d	diameter	m
D	diameter of the heating surface	m
$D_b$	diameter of bubble at departure	m
f	bubble emission frequency	1/s
g	acceleration due to gravity	$m/s^2$
h	heat transfer coefficient	$W/m^2 \text{ } K$
k	thermal conductivity	$W/m \text{ } K$
$l$	length of the heating surface	m
n	number of active sites per unit area of the heating surface	$1/m^2$
N	number of active sites	
p	Pressure	$N/m^2$
$\Delta p$	pressure difference	$N/m^2$
q	heat flux	$W/m^2$
Q	heat transfer rate	W
$r_c$	critical radius of active site	m
R	radius	m
t	temperature	K or $^\circ C$
$\bar{t}$	average temperature	K or $^\circ C$
$\Delta t$	temperature difference	K or $^\circ C$
$\Delta t_w$	wall superheat, $(t_w - t_s)$	K or $^\circ C$
$\Delta \bar{t}_w$	average wall superheat	K or $^\circ C$
V	volume	$m^3$
W	power input	W

## Greek Symbols

$\sigma$	surface tension	N/m
$\rho$	density	kg/m <sup>3</sup>
$\lambda$	latent heat of vaporization	J/kg
$\mu$	dynamic viscosity	Ns/m <sup>2</sup>
$\nu$	kinematic viscosity, $\mu/\rho$	m <sup>2</sup> /s
$\alpha$	thermal diffusivity, $k/\rho c$	m <sup>2</sup> /s
$\beta$	contact angle	deg or radian
$\theta$	time	s
$\theta_d$	departure period	s
$\theta_w$	waiting period	s
$\delta$	transient thermal layer thickness	m

## Dimensionless Modulii

Ar	Archimedes number	$\frac{g}{\nu^2} \left[ \frac{\sigma}{g(\rho_l - \rho_v)} \right]^{3/2} \left( \frac{\rho_l - \rho_v}{\rho_l} \right)$
Bu	Buoyancy number	$(\rho_l - \rho_v) / \rho_l$
Ga	Gallilean number	$\frac{g}{\nu^2} \left[ \frac{\sigma}{g(\rho_l - \rho_v)} \right]^{3/2}$
Ja	Jakob number	$\frac{\rho_l c_l \Delta \bar{t}_w}{\lambda \rho_v}$
K	Criterion	$\frac{\sigma}{\rho_v \lambda D_b f}$
$K_p$	Criterion for pressure term in boiling	$\frac{p}{\sqrt{g\sigma(\rho_l - \rho_v)}}$
$K_{sub}$	criterion for subcooling term	$\left[ 1 + \sqrt{\frac{\rho_l}{\rho_v}} \frac{(t_s - t_l)}{t_s} \right]$

$K_t$	Criterion for bubble break-off frequency	$\frac{(\rho_v \lambda)^2}{c_{\ell} T_s \rho_{\ell} \sqrt{g \sigma (\rho_{\ell} - \rho_v)}} = \frac{1}{Ku}$
$K_q$	Criterion for number of active sites	$\frac{q \rho_v \lambda}{T_s k_{\ell} (\rho_{\ell} - \rho_v) g}$
$Nu_B$	Nusselt number for boiling	$\frac{h}{k_{\ell}} \sqrt{\frac{\sigma}{g (\rho_{\ell} - \rho_v)}}$
$Pe_B$	Peclet number for boiling	$\frac{q}{\rho_v \lambda \alpha} \sqrt{\frac{\sigma}{g (\rho_{\ell} - \rho_v)}}$
$Pr$	Prandtl number	$c_{\ell} \mu_{\ell} / k_{\ell}$
$Re_B$	Reynolds number for boiling	$\frac{q \rho_{\ell}}{\lambda \rho_v \mu_{\ell}} \sqrt{\frac{\sigma}{g (\rho_{\ell} - \rho_v)}}$

## Subscripts

B	boiling
b	bubble, benzene
c	critical
d	departure
i	inside
$\ell$	liquid
o	outside
s	saturation
t	toluene
v	vapour
w	wall, water
Pred.	predicted
Expt.	experimental
l	reference pressure

## CHAPTER 1

### INTRODUCTION

Nucleate pool boiling occurs commonly in evaporators, reboilers, vaporisers and many others, which are largely employed in chemical, petro-chemical, power plant, refrigeration and allied industries. The design and fabrication of these equipment involve huge amount of money every year. Therefore, a large amount of money and material can be saved by their optimal design. One of the important factors to this is the precise knowledge of boiling heat transfer data.

Boiling heat transfer is a surface phenomenon. High rates of heat transfer are achieved during boiling heat transfer due to the dynamics of the vapour bubbles on and near the heating surface. As a matter of fact the vapour bubbles originate on the sites of the surface having values of wall superheat exceeding a minimum value. The minimum wall superheat required for bubble birth on a given size of nucleation site depends upon the physico-thermal properties of the boiling liquid. When the value of wall superheat is further raised, the bubble birth takes place on the sites of smaller size. Thus the magnitude of wall superheat is of far reaching consequence for the boiling heat transfer. The vapour bubbles growing on the top-position of a heating cylinder escape at a faster rate than those on the side-position and at still faster rate than those on the bottom-position. Due to this the wall superheat

increases from the top- to the side- to the bottom-position of a given electrically heated heating cylinder for a given liquid, pressure and heat flux and thereby the heat transfer coefficient decreases from top- to side- to bottom-position of the cylinder. Hence the surface area recommended for a given duty, based on the heat transfer coefficient at the top-position and the bottom-position, will prove to be undersized and oversized, respectively. Consequently, the former would lead to non-functioning of the equipment, whereas the latter to increase the fixed cost of it unnecessarily. Therefore, a knowledge of variation of wall superheat and heat transfer coefficient along the circumference of a cylinder as a functional relationship to heat flux, pressure, heating surface characteristics and physico-thermal properties of the boiling liquid would help the designer to judiciously compute the surface requirement for a given condition of parameters. Unfortunately, this information is not available adequately in the literature.

Process industries have many such situations where the boiling heat transfer is carried out for low heat flux values at atmospheric and subatmospheric pressures for liquids other than distilled water. Literature shows that the experimental data for such liquids are scarce. Therefore, there is a distinct need to obtain boiling heat transfer data pertinent to low heat flux conditions for liquids other than water under atmospheric and subatmospheric pressures.

The experimental data for the nucleate boiling of liquids, as reported in the literature, differ from investigation to investigation. Thus, unlike many other situations of heat transfer, no generalised correlation seems to exist which can correlate the boiling heat transfer data of different investigations. The non-existence of generalized correlations is attributed to the dubious nature of the heating surface characteristics which plays an important role on the boiling heat transfer data. But the characteristics of the heating surface differs from surface to surface in a peculiar manner and its value cannot be determined explicitly for a given heating surface. Therefore the effect of heating surface on the boiling heat transfer data cannot be predicted. Due to this reason one is unable to scrutinize the data of nucleate boiling heat transfer of different investigations. Besides, there is another problem related to checking the consistency of the experimental data for the boiling of a liquid on a given heating surface at different pressures. With the above in view there is a need to investigate these aspects also.

Another peculiar aspect of boiling heat transfer is from the outer surface of a tube bundle to the shell liquid in which the tubes of the bottom-most row pass on vapour bubbles to the tubes lying in the row above it. The tubes in latter row, in turn, do the same to the tubes of the row above it and so on. Thus the vapour bubbles from a given row to the next row above contribute to further increase the turbulence around the tubes lying in the next row in

addition to that due to the generation of bubbles on it. Consequently, the boiling heat transfer coefficient from a tube of a given heating surface, pressure, heat flux and liquid would depend on in which row the tube lies. Hence, a designer would want to know the functional relationship between heat transfer coefficient and heat flux, pressure, physico-thermal properties of a boiling liquid for tubes lying in different rows of a multitubular exchanger. However, the literature seems to be silent in this regard.

The above summarises that the knowledge of local values of boiling heat transfer coefficient along the circumference of tubes lying in different rows of a shell and tube exchanger is of great significance to a designer. To quantise the local boiling heat transfer coefficient as a function of heat flux, pressure, surface characteristics and physico-thermal properties of a boiling liquid in multitubular exchanger an elaborate research experimental set-up is required. However, the practical difficulties limited the present investigation to two horizontal tubes kept one over the other in a vertical plane submerged in a pool of boiling liquid. As a matter of fact, this investigation would be helpful to the furtherance of knowledge in the area of boiling heat transfer taking place on the tubes of a bundle of a shell and tube exchanger.

Keeping the above considerations in view the present experimental investigation on nucleate pool boiling of liquids on electrically heated horizontal cylinder(s) was undertaken with the following objectives :



1. To conduct the experiments of boiling heat transfer from a horizontal cylinder to the pool of saturated liquids of differing physico-thermal properties under atmospheric and subatmospheric pressures for values of low heat flux.
2. To obtain the wall superheat distribution around a heating cylinder for the boiling of liquids for low values of heat flux and atmospheric and sub-atmospheric pressures.
3. To establish the relationship between average wall superheat and operating parameters - heat flux, pressure and physico-thermal properties of the boiling liquids.
4. To derive a theoretical equation based on available models for predicting the average wall superheat of a given heating surface for the boiling of liquids under atmospheric and subatmospheric pressures.
5. To determine the effect of vapour bubbles emerging out from a horizontal heating cylinder on the boiling heat transfer data from another horizontal heating cylinder above it at some distance.

## CHAPTER 2

### LITERATURE REVIEW

This chapter contains the literature review pertaining to various aspects of nucleate pool boiling heat transfer from a heating surface to liquids and also the experimental data of earlier studies relevant to the present investigation.

#### 2.1 NUCLEATE POOL BOILING HEAT TRANSFER FROM HEATING SURFACE TO LIQUIDS

To understand the principles of nucleate pool boiling a number of investigators have carried out studies. These are either empirical or semi-empirical in nature and cover various aspects, namely; nucleation site density, bubble emission frequency, bubble departure diameter, boiling heat transfer mechanism and correlations. Some of the important studies are reviewed in the following Sections.

##### 2.1.1 NUCLEATION SITE DENSITY

In nucleate pool boiling vapour bubbles form on the preferred sites which are in the form of cracks, irregularities, scratches, etc. on the heating surface. These sites, known as nucleation sites, are distributed at random on the heating surface and can not be determined directly by measurement. However, some inference about their population

can be obtained from the experimental studies. Based on this approach, a large number of investigators conducted experiments to study the functional relationship of nucleation site density with the operating variables like heat flux, pressure, physico-thermal properties of the liquid and surface characteristics of the heating surface.

Jakob and Linke [1,2] were perhaps the first to carry out a systematic study of boiling heat transfer. Their experimentation included the boiling of water upto a heat flux of  $56,790 \text{ W/m}^2$ . Based on these data they recommended a linear relationship between heat flux and nucleation site density.

The above observation has been questioned by later investigators [4,5,6] who have shown the non-linear dependence of heat flux on nucleation site density.

Corty and Foust [3] investigated the effect of surface variables in nucleate boiling by conducting experiments for the saturated boiling of ethane, pentane and Freon-113 at atmospheric pressure. Their heating surfaces were of copper and nickel having different degrees of roughness (4/0, 2/0, 0, 1 and 3). They obtained that a rough clean surface is better for boiling heat transfer than a smooth clean one. Further, they also concluded that wall superheat is a strong function of surface roughness.

Gaertner and Westwater[4] carried out experiments for nucleate pool boiling of nickel-water solution on a horizontal copper plate. The heat flux ranged from 7,680 to

5,35,000 BTU/hr.ft<sup>2</sup> and the number of nucleation sites from 0 to 1130 per square inch at a heat flux of 3,17,000 BTU/hr.ft<sup>2</sup>. They found the linear relationship proposed by Jakob [1] to be invalid and recommended the following equations based on their own experimental data :

$$q = 1400 n^{0.47} \quad \dots(2.1)$$

$$h = 49 n^{0.43} \quad \dots(2.2)$$

Nishikawa and Urakawa [5] conducted experiments for the boiling of distilled water on a horizontal brass plate. The pressure ranged from 0.4 kgf/cm<sup>2</sup> to 1.03 kgf/cm<sup>2</sup> and the heat flux from 9,000 to 30,000 kcal/hr.m<sup>2</sup> with a maximum count of 8 nucleation sites per square inch. They recommended the following relationship :

$$h \propto n^{0.33} \quad (2.3)$$

However, for atmospheric pressure their relationship is of the following form :

$$n \propto q^2 \quad \dots(2.4)$$

They also reported that the above relationships, Eqs (2.3 and 2.4) are not affected by the surface contamination, surface-active agents, dissolved salts and surface roughness.

Kurihara and Myers [6] undertook an investigation to study the parametric effect of nucleation site density on boiling heat transfer coefficient of water and organic liquids. Their operating variables included heat flux upto a value of 19,000 BTU/hr.ft<sup>2</sup> and the nucleation sites upto a maximum count of 28 per square inch. Based on their data, they

corroborated the Nishikawa's relationship, Eq (2.3).

Griffith and Wallis [7] investigated the effect of heating surface conditions on nucleate pool boiling of water, methanol and ethanol. The boiling took place on an artificial cavity made on the copper surface having different degrees of roughness. They concluded that the shape and the size of the cavity strongly affected the value of wall superheat required for boiling to take place. Further, they also established that the parameter group  $[r_c = 2\sigma T_s / \lambda \rho_v (t_w - t_s)]$  had a functional relationship with nucleation site density for all the investigated fluids.

Gaertner [8] made a statistical analysis of the existing data of nucleation site density and obtained the following equation to correlate them :

$$n = n_0 \exp(-k/t_w^3) \quad \dots(2.5)$$

where  $k$  is a constant which depends upon the surface conditions and the boiling liquid and  $n_0$  is a constant.

Semeria [9] recommended the following correlation for predicting nucleation site density for the boiling of water at pressures ranging from 3 to 100 atmosphere :

$$n = 0.012 q^2 p \quad \dots(2.6)$$

where  $n$  is in  $\text{cm}^{-2}$ ,  $q$  in  $\text{W}/\text{cm}^2$  and  $p$  in atmosphere.

Gaertner [10] attempted to obtain the parametric effect of heat flux on nucleation site density for the boiling of distilled water on a copper surface having the roughness of 4/0. The maximum value of heat flux was

58,600 BTU/hr.ft<sup>2</sup>. The equation recommended by him is :

$$q \propto n^{2/3} \quad \dots(2.7)$$

Kirby and Westwater [11] carried out an extensive investigation of boiling heat transfer of different liquids on different heating surfaces. They concluded the following :

$$q \propto n^b \quad \dots(2.8)$$

where the value of exponent, b lies between 0.33 and 0.50 for the metallic surfaces and 0.73 for glass.

The following correlations of heat flux with nucleation site density and bubble emission frequency for the boiling of water are due to Wiebe and Judd [12].

For  $nf < 55 \times 10^3$  bubbles/inch<sup>2</sup>s.

$$q \propto (nf)^{1/2} \Delta \bar{t}_w \quad \dots(2.9)$$

and for  $nf > 55 \times 10^3$  bubbles/inch<sup>2</sup>s.

$$q \propto (nf)^{1/3} \Delta \bar{t}_w \quad \dots(2.10)$$

Brown [13] recommended the following power law for calculating the value of nucleation site density, n of the radii equal to or greater than  $r_c$  :

$$n = C_0 \left( \frac{r_r}{r_c} \right)^m \quad \dots(2.11)$$

where  $C_0$  is a dimensional constant having the dimensions of (area)<sup>-1</sup>; exponent, m is a constant characterizing the heating surface and  $r_r$  is the radius for which n would be one per unit area. The value of  $r_c$  is given by the following

expression :

$$r_c = \frac{2 \sigma T_s}{\rho_v \lambda (t_w - t_s)} \quad \dots(2.12)$$

Shoukri and Judd [14] used the above relationship, Eq (2.11) along with the parameter group, Eq (2.12) for correlating the experimental data and recommended that the Brown's equation along with Eq (2.12) was a sufficient method for describing the nucleation characteristics of a boiling surface.

Danilova [15] correlated the experimental data of pool boiling of water and Freon-113 by the following expression :

$$q \propto n^b \quad \dots(2.13)$$

where  $b = 4/9$  for Freon-113  
 $= 1/3$  for water.

### 2.1.2 BUBBLE DEPARTURE DIAMETER

Bubble departure diameter is an important parameter in nucleate pool boiling as it represents the amount of heat transfer from a cavity. As the bubble forms and grows on the heating surface a number of forces act upon it. These are : static forces comprising of surface tension and the inertial force; the dynamic forces comprising of viscous drag force, buoyancy force and excess pressure force. Some of these forces tends to keep the bubble in contact with the heating

surface while the other tends to take it away from the heating surface. As soon as the magnitude of the forces tending to take the vapour bubble away from the heating surface exceeds the other forces, the vapour bubble detaches and starts travelling upward in the pool of liquid. Therefore, the bubble departure diameter can be calculated by the analysis and balance of the forces. These forces [16-20] are:

**SURFACE TENSION FORCE,  $F_s$  :** This is due to the interfacial tension between the liquid and vapour phase [17,19] and is given by :

$$F_s = \pi D_b \sigma \sin \beta \quad \dots(2.14)$$

where  $\beta$  is the contact angle.

**BUOYANCY FORCE,  $F_b$  :** This force acts upward and is due to the difference between the liquid and vapour density of the boiling liquid. This can be represented mathematically as :

$$F_b = V_b (\rho_l - \rho_v) g \quad \dots(2.15)$$

where  $V_b$  is the volume of the vapour bubble.

**INERTIAL FORCE,  $F_i$  :** As the bubble grows the vapour in the bubble moves and consequently the surrounding liquid also undergoes movement. This gives rise to bubble inertial force,  $F_{ib}$  and liquid inertial force,  $F_{il}$ . Vapour inertial force [22] :

$$F_{ib} = V_b \rho_v \frac{dV}{d\theta} g \quad \dots(2.16)$$



and the liquid inertial force

$$F_{il} = V_{\ell} \rho_v \frac{d V_n}{d\theta} \quad \dots(2.17)$$

where  $V_g$  and  $V_n$  represent the velocities of bubble centre and the bubble top surface.  $V_{\ell}$  is the volume of affected liquid which is equal to  $V_b$ .

**VISCOUS DRAG FORCE :** This is due to the interfacial drag forces acting on the surface of the vapour bubble. It is assumed to depend upon the velocity of advance of bubble front i.e.

$$F_{CD} = C_d \rho_{\ell} \frac{\pi D_b^2}{4} \frac{V_n^2}{2} \quad \dots(2.18)$$

Hatton and Hall [20] assumed  $C_d$  in Eq (2.18) to be constant. Hughes and Gilliland [21] recommended the following equation for  $C_d$  in laminar flow :

$$C_d = \frac{C_{do}}{[V_g/V_t]} \quad \dots(2.19)$$

where  $V_t$  is the terminal velocity and is given by :

$$V_t = \sqrt{\frac{4 D_b (\rho_{\ell} - \rho_v) g}{3 C_{do} \rho_{\ell}}} \quad \dots(2.20)$$

If  $V_g$  is characteristic velocity in Reynolds number, then

$$C_d = \frac{D_b}{4X^2} \sqrt{\frac{4 C_{do} D_b g (\rho_{\ell} - \rho_v)}{3 \rho_{\ell}}} \quad \dots(2.21)$$

where  $C_{do}$  is a constant equal to 2.0 [22] and X is given by

$$X = \frac{k\ell\sqrt{3} \Delta\bar{t}_w}{\rho_v \sqrt{\pi\alpha}} \quad \dots(2.22)$$

EXCESS PRESSURE AT BUBBLE BASE : It is equivalent to a loss of buoyancy due to the fact that liquid pressure does not act over the bubble base and is expressed by :

$$F_{EX} = \frac{\pi D_c^2 (\rho_v - \rho_l)}{4} \quad \dots(2.23)$$

At equilibrium the balance of these forces at a bubble is :

$$F_s + F_{CD} + F_{il} + F_{ib} + F_{EX} = F_b \quad \dots(2.24)$$

This equation has been solved by investigators [23-26] in different ways.

Fritz [23] calculated the bubble departure diameter by making a balance of buoyancy force and the surface tension force. He neglected all other forces. His relationship is :

$$D_b = 0.0208 \beta \sqrt{\frac{g_c \sigma}{g(\rho_l - \rho_v)}} \quad \dots(2.25)$$

This expression was verified for the experimental data of steam bubbles at low heat flux and atmospheric pressure and that of hydrogen bubbles [23,24].

Staniszewski [37] modified Eq (2.25), applicable for bubbles of very low growth rate, for the bubbles of high growth rate. He carried out experiments for boiling water and methanol at 14.7 psia and 28 psia. Based on his data he found that the bubble departure diameter was linearly

proportional to the bubble growth rate at the last stage and recommended the following equation :

$$D_b = 0.0071 \beta \sqrt{\frac{2 g_c \sigma}{g(\rho_l - \rho_v)}} \left(1 + 0.435 \frac{d D_b}{d \theta}\right) \dots(2.26)$$

where  $dD_b/d\theta$  is in inch/s.

Eq (2.26) reduced to Eq (2.25) for low growth rates approaching to zero.

Zuber [28] obtained the following expression for bubble departure diameter by equating the buoyancy and the surface tension forces acting on a gas bubble formed at an orific and assuming  $\sin \beta$  to be unity :

$$D_b = \left[ 12 \frac{r_o g_c \sigma}{g(\rho_l - \rho_v)} \right]^{1/3} \dots(2.27)$$

Eq (2.27) simplifies to Eq (2.25) if  $r_o$  is the bubble radius and  $\sin \beta$  is proportional to  $\beta$ . Later, Zuber [25] substituted orific radius,  $r_o$  by the expression of cavity radius  $r_c$  and reduced Eq (2.27) to :

$$D_b = \left[ \frac{6 g_c \sigma k_l \Delta \bar{t}_w}{g(\rho_l - \rho_v) Q} \right]^{1/3} \dots(2.28)$$

In a similar analysis, Ruckenstein [29] obtained the following expression for bubble departure diameter by considering the buoyancy and drag forces and taking drag coefficient to be unity :

$$D_b = \left[ \frac{3\pi^2 \rho_l \alpha^2}{g(\rho_l - \rho_v)} \right] Ja^{4/3} \quad \dots(2.29)$$

Roll and Myers [26] considered buoyancy, viscous drag and liquid inertial forces in determining the value of bubble departure diameter. The surface-tension force and the bubble inertial force were considered to be negligible. They reported the following expression of  $D_b$  :

$$D_b = \left[ \pi Ja^2 \alpha \right]^{2/3} \left[ \frac{3(C_d - 11/12)}{g(\rho_l - \rho_v)} \right]^{1/3} \quad \dots(2.30)$$

Nishikawa and Urakawa[5] obtained bubble departure diameter for the boiling of water at pressures ranging from 300 to 760 mm Hg. Their data were correlated by :

$$D_b = 0.672 p^{-0.0575} \quad \dots(2.31)$$

where  $D_b$  is in inch and  $p$  is in psia.

Semeria [30] obtained the following expression for the bubble departure diameter in the range 2 to 20 atmospheric pressure :

$$D_b = 0.242 p^{-0.5} \quad \dots(2.32)$$

where  $D_b$  is in inch and  $p$  is in psia. He further extended the pressure range to approximately 140 atmosphere and for this range recommended the following correlation :

$$D_b = 26.8 p^{-1.5} \quad \dots(2.33)$$

Cole and Shulman [25] examined the existing correlations and showed that none of the expressions correlated

satisfactorily bubble departure diameter for subatmospheric pressure range. Therefore they modified the Fritz equation, Eq (2.25) by incorporating a term for accounting the effect of pressure. The resulting expression is :

$$D_b = \left( \frac{133.3}{p} \right) \sqrt{\frac{\sigma}{g(\rho_l - \rho_v)}} \quad \dots(2.34)$$

Eq (2.34) successfully correlated the data of subatmospheric pressure ranging from 48 to 760 mm Hg. Based on his observations, Cole [27] proposed that the dimensionless departure diameter is directly proportional to the wall superheat,  $\Delta \bar{t}_w$  expressed through Jakob number, as given below :

$$\frac{D_b}{\sqrt{\frac{\sigma g_c}{g(\rho_l - \rho_v)}}} = 4 \times 10^{-2} \text{ Ja} \quad \dots(2.35)$$

The above variation of departure diameter with wall superheat has also been reported by Preckshot and Denny [97]. However, Gaertner [8] experimentally showed that increase in heat flux and wall superheat counteracted the effect of each other.

Cole and Rohsenow [98] modified the correlations of Cole and Shulman [25] and Cole [27] because both these correlations required the knowledge of wall superheat for calculating the value of  $D_b$ . For this, they modified the Jakob number, Ja to make the correlation free from wall superheat as given by the following expression :

$$\text{Ja}^* = \frac{\rho_l c_l T_s}{\rho_v \lambda} \quad \dots(2.36)$$

The correlations proposed by them are :

For water ( $Pr < 0.2$ ),

$$\frac{D_b}{\sqrt{\frac{\sigma}{g(\rho_l - \rho_v)}}} = 1.5 \times 10^{-4} (Ja^*)^{5/4} \quad \dots(2.37)$$

and for organic liquids ( $Pr > 0.2$ ),

$$\frac{D_b}{\sqrt{\frac{\sigma}{g(\rho_l - \rho_v)}}} = 4.65 \times 10^{-4} (Ja^*)^{5/4} \quad \dots(2.38)$$

Eq (2.37) is based on the experimental data of Semeria[30] for pressure 2 to 140 atmosphere; Tolubinskii and Ostrovsky[31] for pressure ranging from 0.2 to 10 atmosphere; Cole[27] for pressure ranging from 0.066 to 0.47 atmosphere; Hatton and Hall[20] for pressure ranging from 0.12 to 1 atmosphere and Siegel and Keshock [32] for 1 atmosphere. Eq(2.38) is based on the experimental data of Wanninger[33] for propane at 8.5, 11 and 14 atmosphere and iso-pentane at 1 atmosphere; Cole[27] for toluene, n-pentane, carbon-tetrachloride and acetone for pressure ranging from 0.066 to 1 atmosphere; Tolubinskii and Ostrovsky[31] for benzene, n-butanol and Freon-12 at 1 atmosphere; McFadden and Grassmann [86] for methanol at 1 atmosphere, Preckshoot and Denny [97] and Jakob [1] for carbon-tetrachloride at 1 atmosphere. Deviation of the order of  $\pm 50$  per cent had been reported between the experimental values and the predicted ones due to Eqs (2.37 and 2.38). The authors pointed out that this discrepancy was due to the result of neglecting the effect of

nucleation site density, contact angle, cavity size and wall superheat on bubble departure diameter.

Hatton et al [22] considered the buoyancy, surface tension, pressure at the bubble base and the dynamic forces for the study of bubble dynamics during the boiling of liquids and obtained the following equation :

$$\frac{D_b^3 (\rho_l - \rho_v)}{6} = \frac{64 X^4}{g} \left[ \frac{C_d \rho_l}{8} - \frac{\rho_l}{12} + \frac{\rho_v}{6} \right] - \frac{\sigma}{g} \left[ \frac{D_c^2}{D_b} - D_c \sin \theta \right] \quad \dots(2.39)$$

where

$$C_d = \frac{D_b}{4 X^2} \sqrt{\frac{4 C_{do} D_b g (\rho_l - \rho_v)}{3 \rho_l}}$$

and  $X = \frac{12 \sqrt{3} k_l \sigma T_s}{\lambda^2 \rho_v^2 \sqrt{\pi \alpha \delta}}$

$C_{do}$  is an empirical constant which is approximately equal to 2.0 and  $\delta$  is the thermal boundary layer thickness.

Saini et al [99] made a critical analysis of the forces taking part in the bubble dynamics and recommended the following expressions for the bubble departure diameter:

$$\left( \frac{g}{\alpha^2} \right)^{1/3} D_b = \left[ \frac{6.6 c_l \Delta T_w \sigma}{\alpha q} \right]^{1/3} ; \text{ for } Ja \leq 16 \quad \dots(2.40)$$

$$\left( \frac{g}{\alpha^2} \right)^{1/3} D_b = 1.35 Ja^{4/3} \left[ 1.22 + \sqrt{1 + \frac{2.67 c_l \Delta T_w \sigma}{\alpha q Ja^4}} \right]^{2/3} ;$$

for  $16 < Ja < 100$

$$\dots(2.41)$$

$$\left(\frac{g}{\alpha^2}\right)^{1/3} D_b = 9.18 Ja \quad ; \quad \text{for } Ja \geq 100 \quad \dots(2.42)$$

### 2.1.3 BUBBLE EMISSION FREQUENCY

To predict the rate of heat transfer in nucleate pool boiling the precise knowledge of the bubble emission frequency,  $f$  and bubble departure diameter,  $D_b$  is essential. Therefore many investigators have attempted to obtain expressions of bubble emission frequency but there has not been any single expression which can be used for the exclusive determination of bubble emission frequency. Most of the available equations predict the product of bubble emission frequency and bubble departure diameter.

The study of bubble emission frequency started with the pioneer work of Jakob [1] who made a photographic study of boiling of water and carbontetrachloride on a heating surface. They found that the value of the product  $fD_b$  was a constant ( $= 280 \text{ m/hr}$ ) for low to moderate heat flux range at a given pressure.

Jicina-Molazhin and Kutateladze [35] examined the Jakob observation for the boiling of carbontetrachloride, 26 % water-glycyrene solution, 24 aqueous sodium-chloride solution, water and mercury for the pressure ranging from 0.15 to 10  $\text{kg/cm}^2$ . They found that the value of  $fD_b$  did not remain constant with pressure and recommended the following relationship :



$$f D_b = C_{sf} \sqrt{\frac{g \rho_l \sigma}{p \rho_v}} \quad \dots(2.43)$$

Zuber [28] recommended the following relationship for the calculation of  $f D_b$ :

$$f D_b = 0.59 \left[ \frac{g \sigma (\rho_l - \rho_v)}{\rho_l^2 \lambda} \right]^{1/4} \quad \dots(2.44)$$

Rallis and Jawurek [36] showed that the mean product of bubble emission frequency and the departure volume,  $f V_b$  increased with heat flux. However, at the same heat flux and pressure the product  $f V_b$  was same for each bubble source within reasonable scatter.

Perkins and Westwater [34] carried out experiments for the boiling of methanol for medium and high heat fluxes. They reported that the mean frequency and mean departure diameter remained constant upto 80 % of the critical heat flux value.

Han and Griffith[38] determined  $f$  by the calculation of departure time,  $\theta_d$  and the waiting period,  $\theta_w$  by the following equation :

$$f = \frac{1}{\theta_d + \theta_w} \quad \dots(2.45)$$

where

$$\theta_w = \frac{\delta^2}{\pi \alpha} = \frac{9}{4\pi\alpha} \left[ \frac{(T_w - T_\infty) R_c}{T_w - T_s \left\{ 1 + (2\sigma/R_c \rho_v \lambda) \right\}} \right]^2 \quad \dots(2.46)$$

The value of  $\theta_d$  was calculated by solving the following equations :

$$R_d = 0.4251 \varphi [2\sigma/g(\rho_l - \rho_v)] \quad \dots(2.47)$$

and

$$R_d - R_c = \frac{\varphi_s \varphi_c \alpha c_l \rho_l}{\varphi_v \rho_v \lambda} \left[ \frac{2(T_w - T_s) \sqrt{\theta_d}}{\sqrt{\pi \alpha}} - \frac{(T_w - T_s) \delta^2}{\delta 4 \alpha} \right. \\ \left. \times \left\{ \frac{4 \alpha \theta_d}{\delta^2} \operatorname{erf} \frac{\delta}{\sqrt{4 \alpha \theta_d}} + \frac{2}{\sqrt{\pi}} \frac{\sqrt{4 \alpha \theta_d}}{\delta} \exp\left(\frac{-\delta^2}{4 \alpha \theta_d}\right) \right. \right. \\ \left. \left. - 2 \operatorname{erfc} \frac{\delta}{\sqrt{4 \alpha \theta_d}} \right\} \right] + \frac{\varphi_b h_v (T_w - T_s)}{\varphi_v \rho_v \lambda} \theta_d \quad \dots(2.48)$$

where  $\varphi_c$  = curvature factor  $1 < \varphi_c < \sqrt{3}$

$\varphi_s$  = surface factor  $1 + \cos \varphi / 2$

$\varphi_v$  = volume factor  $\frac{2 + \cos \varphi (2 + \sin^2 \varphi)}{4}$

$\varphi$  = contact angle

and  $h_v$  = coefficient of heat transfer from heating surface to steam bubble through its base area.

Hatton and Hall [20] used the expression of Plesset and Zwick [39] for departure time,  $\theta_d$  and Hsu [9] and Han and Griffith [38] for bubble nucleation under the assumption of waiting period,  $\theta_w$  to be zero. The expression recommended by them is :

$$f = \frac{1}{\theta_d} = \frac{3}{\pi \alpha} \left[ \frac{16 k_l \sigma T_s}{(\lambda \rho_v)^2 D_b D_c} \right]^2 \quad \dots(2.49)$$

Rallis and Jawurek [36] established that the volumetric vapour flow rate,  $fV_b$  for the isolated bubble region is a function of heat flux and pressure. Based on this concept, Cole [27] modified the works of earlier investigators for subatmospheric pressure range. He included the effect of

heat flux and pressure through Jakob number and thus recommended the following expression to correlate the experimental data :

$$f D_b^3 \propto \left[ \frac{\sigma^{5/3}}{g \rho_\ell^{2/3} (\rho_\ell - \rho_v)} \right]^{3/4} [Ja]^2 \quad \dots(2.50)$$

where

$$Ja = \frac{\rho_\ell c_\ell \Delta \bar{t}_w}{\rho_v \lambda} \quad \dots(2.51)$$

and the volumetric vapour flow rate per cross-section is

$$f D_b \propto \left[ \frac{g(\rho_\ell - \rho_v) \sigma}{\rho_\ell^2} \right]^{1/4} \quad \dots(2.52)$$

which is independent of Jakob number.

Ivey [40] scrutinised the existing correlations of bubble frequency and found that a single correlation can not adequately correlate the bubble emission frequency with bubble diameter for all bubble diameters in nucleate pool boiling. He suggested three separate regions - hydrodynamic, transition and thermodynamic for relating bubble frequency and diameter. Following are the relationships advocated by him :

Hydrodynamic region :

$$f D_b^{0.5} = 0.90 g^{0.5} \quad \dots(2.53)$$

Transition region :

$$f D_b^{0.75} = 0.44 g^{0.5} \quad \dots(2.54)$$

Thermodynamic region :

$$fD_b^2 = \text{constant} \quad \dots(2.55)$$

Some other investigators have also given the expressions of bubble emission frequency as a function of bubble departure diameter, physico-thermal properties of the liquid and other system parameters. They are listed in Table 2.1.

Table 2.1 Expressions for bubble emission frequency

Region	Investigator(s)	Expression
Hydro-dynamic	Cole [27]	$fD_b^{0.5} = 1.15 g^{0.5}$
	McFadden and Grassmann [86]	$fD_b^{0.5} = 0.56 g^{0.5}$
	Zuber [28]	$fD_b = 0.59 \left[ \frac{g\sigma(\rho_l - \rho_v)}{\rho_l^2} \right]^{1/2}$
Transition	Jakob and Linke [2]	$fD_b = \text{constant}$
	Siegel and Keshock [32]	$fD_b \propto g^{0.5}$
	Rallis and Jawurek [36]	$fD_b^3 = \text{constant}$
	Nishikawa and Urakawa [5]	$fD_b^3 = \text{constant}$
Thermo-dynamic	Jicina-Molazhin and Kutateladze [35]	$fD_b = \frac{2q}{\lambda \rho_v}$
	Hatton and Hall [20]	$fD_b^2 = \frac{3}{\pi\alpha} \left[ \frac{16k_l \sigma T_s}{\lambda^2 \rho_v^2 D_c} \right]^2$
	Staniszewski [37]	$fD_b = \frac{2k_l}{\lambda \rho_v} \left( \frac{dT}{dr} \right)_{r=R}$

Saini et al [100 and 101] recommended the following correlations for the calculation of bubble emission frequency for different ranges of Jakob number :

For  $Ja \leq 16$

$$f = \frac{1}{\frac{0.865}{\alpha} \left( \frac{k \Delta \bar{t}_w}{q} \right)^2 + \left( \frac{\alpha}{g^2} \right)^{1/3} \left[ \frac{(6.6 c_p \Delta \bar{t}_w \sigma / \alpha q)^{2/3}}{\pi Ja^2} \right]} \quad \dots(2.56)$$

For  $16 < Ja < 100$

$$f = \frac{1}{\frac{0.865}{\alpha} \left( \frac{k \Delta \bar{t}_w}{q} \right)^2 + \left( \frac{\alpha}{g^2} \right)^{1/3} \left[ 0.578 Ja^{2/3} \left\{ 1.22 + \sqrt{1 + 2.67 \left( \frac{c_p \Delta \bar{t}_w \sigma}{\alpha q Ja^4} \right)} \right\} \right]} \quad \dots(2.57)$$

For  $Ja \geq 100$

$$f = \frac{1}{\frac{0.865}{\alpha} \left( \frac{k \Delta \bar{t}_w}{q} \right)^2 + \left( \frac{\alpha}{g^2} \right)^{1/3} (3.4 Ja^{1/2})} \quad \dots(2.58)$$

Tolubinskii and Ostrovsky [31] verified the Cole correlations Eqs (2.50 and 2.52) experimentally. Their results showed that the average value of  $fD_b$  depends upon the physical properties of the liquid and the vapour and is independent of the material of the heating surface.

Duskus and Westwater [41] investigated the effect of traces of additives on boiling heat transfer and reported

that the frequency of bubble release in some cases was upto three times greater than its corresponding value for pure solvent.

Costello and Tuthil [42] investigated the effect of acceleration on departure diameter and bubble emission frequency. They found that wall superheat increased with acceleration and the buoyancy force acting on the bubble imposed a larger force enhanced by high frequency of the bubbles. As a result of it the bubble spent less time on the heating surface and the total growth is reduced. This in turn, also decreased the bubble departure diameter.

#### 2.1.4 NUCLEATE BOILING HEAT TRANSFER MODELS

Nucleate boiling heat transfer has been the subject of active research in the past few decades for generating experimental data and to understand the mechanism responsible for high heat transfer rates. As a result, various models have appeared in the literature. These models present different mechanisms for the transportation of heat from heating surface to the liquid bulk. As a matter of fact, they are diversified in nature and give conflicting opinions about the boiling heat transfer mechanism. Some of the important models are reviewed here in the following Sub-sections:

a. LATENT HEAT TRANSPORT MODEL

Rallis and Jawurek [36] developed a model on the postulation that the latent heat transport by vapour-bubbles can explain high rate of heat transfer during nucleate boiling. This model considers that a bubble volume of latent heat is transported by the bubble during the growth, departure or collapse at the heating surface. Mathematically, it can be expressed by the following relationship :

$$Q = \frac{\pi D_b^3}{6} \rho_v \lambda N f \quad \dots(2.59)$$

b. MICRO-CONVECTION MODEL

Forster and Zuber [56] developed micro-convection model which considers the importance of bubble agitation (micro-convection) in removing the high thermal resistance of thin superheated boundary layer adjacent to the heating surface. Their model is

$$Nu = 0.0015 Re^{0.62} Pr^{0.33} \quad \dots(2.60)$$

This model could not correlate the experimental data of Addoms [52].

c. VAPOUR-LIQUID EXCHANGE MODEL

This model, developed by Forster and Greif [57] proposes a mechanism to explain high rate of heat transfer during nucleate boiling. According to this model individual vapour bubble acts as tiny, efficient pump, pushing hot liquid from

the thermal boundary layer into the bulk liquid and drawing cooler liquid from the bulk to the heating surface. This liquid stays on the surface during which it is heated up. After some time, this is transported out into the bulk liquid due to either the collapse or departure of bubbles from the surface. This cycle continues. This model can be represented by the following expression :

$$q = c_{\ell} \rho_{\ell} \left( \frac{2}{3} \pi R_b^3 \right) \left( \frac{t_w + t_s}{2} - t_s \right) n f \quad \dots(2.61)$$

#### d. ENTHALPY TRANSPORT MODEL

Han and Griffith [38] developed a model which considered heat flow from heating surface to liquid bulk composed of two portions - one by natural convection in the portion uninfluenced by departing bubbles and another by conduction to the cold fluid that replaces the departing bubble and the associated thermal layer drawn up in its wake in the portion affected by departing bubbles. Mathematically it can be represented by :

$$q = 2 \rho_{\ell} c_{\ell} \Delta t_w \left[ R_b^2 \delta - \frac{1}{3} R_b^2 (\delta - \delta') \right] n f \quad \dots(2.62)$$

where

$$\delta = \sqrt{\pi \alpha (\tau_a + \tau_i)}$$

$$\delta' = \sqrt{\pi \alpha_i \tau_i}$$

$\tau$  = elapsed time

subscripts a,i and b represent active, inactive and bulk respectively.



## e. SOURCE FLOW MODEL

Bankoff [75] considered the combined action of convection at the heating surface due to bubble agitation and transient heat conduction. They gave the following expression:

$$q = 1.25 \sqrt{\rho_{\ell} c_{\ell} k_{\ell} \tau_a} \Psi\left(\frac{\tau_i}{\tau_a}\right) D_b^2 \Delta \bar{t}_w n \beta$$

$$+ (\text{a constant}) \rho_{\ell} c_{\ell} \frac{D_b}{\tau_a} \left(\frac{2F}{1-F}\right)^{1/2} (1-\eta) \Delta \bar{t}_w \quad \dots (2.63)$$

where  $\Psi\left(\frac{\tau_i}{\tau_a}\right) = \int_{1/2}^1 \left(\frac{D}{D_0}\right) \frac{d}{d(t/\tau_a)} \frac{D}{D_b} \sqrt{\left(1 + \frac{\tau_i}{\tau_a}\right) - \left(\frac{t}{\tau_a}\right)} d(t/\tau_a)$

$\tau$  = elapsed time

$F$  = instantaneous area fraction covered by bubbles

$\eta$  = time average area fraction covered by bubbles

subscripts a, i and b represent active, inactive and bulk respectively.

## f. TURBULENT-NATURAL CONVECTION MODEL

Zuber [76] proposed that isolated bubble regime in nucleate pool boiling is similar to a single phase turbulent-natural convection; in both cases 'up draught' induced circulation governs heat flow. He observed that the buoyancy of the vapour bubbles in the liquid adjacent to the heating surface augments the thermally induced buoyancy of the liquid which in turn increases convective heat transfer process. The model is as given below :

$$\frac{h\lambda}{k} = \text{constant} \left[ \frac{g\lambda^3}{\nu\alpha} (\beta \Delta \bar{t}_w + \epsilon_w \frac{\rho_{\ell,w} - \rho_v}{\rho_{\ell}}) \right]^{1/3} \quad \dots(2.64)$$

where  $\epsilon_w$  represents vapour hold up which is defined as the volume fraction of the mixture that is in vapour phase. It is given by the following expression :

$$\epsilon_w = \frac{\pi}{6} D_b^3 \frac{n_f}{U_t} \quad \dots(2.65)$$

$U_t$  in Eq (2.65) is the terminal velocity of a single bubble rising in an infinite medium. It is expressed by

$$U_t = 1.18 \left[ \frac{\sigma g (\rho_{\ell} - \rho_v)}{\rho_{\ell}^2} \right]^{1/4} \quad \dots(2.66)$$

Zuber used 0.16 as the value of constant in Eq (2.64) and successfully correlated the data of Corty and Foust [3]. Later on, Judd and Merte [77] substituted 0.32 for the constant in Eq (2.64).

#### g. INVERTED STAGNATION FLOW MODEL

Tien [78] noted the hydrodynamic analogy between an inverted stagnation flow and the flow field associated with a rising bubble column. Based on this, he developed a model which is represented by the following expression :

$$h = 1.32 Y^{0.5} Pr^{0.333} n^{0.5} \quad \dots(2.67)$$

where  $Y$  is a parameter which relates heat transfer to the strength of inverted stagnation flow. Based upon the data of Yamagata [79], Tien determined  $Y$  to be 2150 for water.

The parameter  $Y$  is related to thickness of thermal boundary layer,  $\zeta$  in nucleate boiling of water by the following relationship :

$$\zeta = 2.44 / (\sqrt{Y} Pr^{1/3} n^{1/2}) \quad \dots(2.68)$$

Comparison with the experimental data of Yamagata [79] and of Gaertner and Westwater [80] shows that the model is not adequate to deal with the experimental data.

#### 2.1.5 CORRELATIONS FOR NUCLEATE POOL BOILING

A large number of heat transfer correlations for nucleate pool boiling of liquids are available in literature. They are in both dimensional and non-dimensional forms. The correlations, in dimensional form generally express heat transfer coefficient as a function of heat flux and pressure through heating surface characteristics as represented by the following equation :

$$h = (\text{a constant}) q^a p^b \quad \dots(2.69)$$

The value of constant in Eq (2.69) depends upon the heating surface and the liquid boiling on it.

In non-dimensional form, different dimensionless groups have been used by various investigators for fitting their experimental data. The general form of the non-dimensional correlations is

$$Nu = (\text{a constant})(Re)^{n_1}(Pr)^{n_2}(Ga)^{n_3}(K_p)^{n_4}(K_t)^{n_5}$$

## EMPIRICAL CORRELATIONS

One of the earliest correlations of nucleate pool boiling was presented by Cryder and Gilliland [43]. They applied the method of dimensional analysis for combining all the quantities pertaining to boiling heat transfer. Their resulting expression is :

$$h = (\text{constant}) \frac{(\Delta \bar{t}_w)^{2.39} k_\ell^{2.97} c_\ell^{0.43} \rho_\ell^{3.1} D^{2.1}}{\sigma^{1.65} \mu^{3.45}} \quad \dots(2.70)$$

Akin and McAdams [44] conducted experiments for the boiling of water, isopropanol, isobutanol and n-butanol at atmospheric pressure. The heating surface was a chrome-plated horizontal cylinder of  $1.905 \times 10^{-4}$  m diameter. They also studied the boiling of distilled water for subatmospheric pressures ranging from 0.16 to 0.68 atmosphere.

Insinger and Bliss [45] carried out experiments for the boiling of water, carbon tetrachloride, isopropanol and 40 % sucrose solution at atmospheric pressure on a vertical heating cylinder of 1.25 inch in diameter and 6 inch in length and recommended the following correlation based on their own data :

$$h = (\text{constant}) \left( \frac{k_\ell c_\ell}{\sigma \rho_v} \right)^{1.6} \frac{\rho_\ell^{2.6} (\Delta \bar{t}_w)^{2.1}}{\lambda^{0.85}} \quad \dots(2.71)$$

Eq (2.71) has correlated the experimental data of Jakob and Linke [2] for water and carbon-tetrachloride, Linden and Montillon [46] and Dunn and Vincent [47] for water

and Akin and McAdams [44] for water, isopropanol, isobutanol and n-butanol successfully.

Cryder and Finalborgo [48] carried out experimental investigations to determine heat transfer coefficient. The liquids investigated by them were distilled water, methanol, carbon-tetrachloride, n-butanol, kerosene, 26.4 % glycerol solution, 10.1 % sodium sulphate solution and 24.2 % sodium chloride solution. The heat rate varied from 439 to 2360 BTU/hr. Following equations correlated their experimental data :

$$\log h = a + 2.5 \log \Delta \bar{t}_w + b t_{\ell} \quad \dots(2.72)$$

$$\log \frac{h}{h_n} = b (t_{\ell} - t_n) \quad \dots(2.73)$$

where a and b are the constants which depend upon the nature of the boiling liquid ; subscript, n refers to normal atmospheric pressure;  $t_{\ell}$  is the temperature of the boiling liquid in  $^{\circ}\text{F}$  and h is the heat transfer coefficient in  $\text{BTU/hr ft}^2 \text{ }^{\circ}\text{F}$ . The values of the constant a and b as obtained by the authors are listed in Table 2.2.

Table 2.2 Values of constants a and b in Eqs (2.72 and 2.73)

Boiling liquid	a	b
Water	- 2.05	0.014
Methanol	- 2.23	0.015
Carbon-tetrachloride	- 2.57	0.012
n-Butanol	- 4.06	0.014
26.3 % Glycerol solution	- 2.65	0.015
Kerosene	- 5.15	0.012
10.1 % Sodium sulphate solution	- 2.62	0.016
24.2 % Sodium chloride solution	- 3.61	0.017

Bonilla and Perry [49] conducted a comprehensive investigation for the boiling of pure liquids and their binary mixtures. The pure liquids were water, ethanol, n-butanol and acetone. Based on the experimental data, they modified Jakob and Linke's equation (cf. equation 2.87) by changing exponent from 0.80 to 0.73; by introducing  $(Pr)^{0.5}$  and also changing the constant from 31.6 to 16.6. The resulting expression was :

$$\frac{h}{k_f} \sqrt{\frac{\sigma}{\rho_f}} = 16.6 \left[ \frac{\nu_a}{\nu} \right] \left[ \frac{\sigma}{\sigma_a} \frac{\rho_{f,a}}{\rho_f} \frac{q}{\rho_{v,a} \lambda W_{b,a}} \right]^{0.73} \left[ \frac{c_f \mu_f}{k_f} \right]^{0.5} \quad \dots(2.74)$$

where subscript, a in Eq (2.74) refers to normal boiling point condition and W is Jakob's constant (= 918 ft/hr).

They also examined the effect of pressure on boiling heat transfer coefficient for ethanol and also for the data of Akin and McAdams [44] for a heat flux of 50,000 BTU/hr.ft<sup>2</sup> and found the following relationship to correlate the data :

$$h = b (p)^{0.25} \quad \dots(2.75)$$

where b is a constant which depends upon the nature of the boiling liquid.

Eq (2.75) clearly shows that heating surface characteristics does not affect the ratios of heat transfer coefficients at different pressures.

Cichelli and Bonilla [50] undertook an experimental investigation for the boiling of water, benzene, ethanol, propane, n-pentane and n-heptane and their binary mixtures at atmospheric and superatmospheric pressures. An electrically heated horizontal thick copper plate was used as the heating surface. They concluded that heat transfer coefficient increased with pressure until the critical pressure where nucleate boiling ceased to be stable.

A comparison of the above correlations illustrates the disagreement existing in literature prior to 1950 on the effect of even the most fundamental variables. Thus, the calculation of boiling heat transfer coefficient at pressures other than atmosphere was very much uncertain. Therefore, the use of Cichelli and Bonilla graphs [50] for the substances investigated by them and the Insinger-Bliss equation [45]

multiplied by  $(p/p_a)^{0.4}$  was recommended.

Sternling and Tichacek [51] obtained the experimental data for the boiling of benzene, methyl-chloroform, carbon-tetrachloride, water, methanol and isopropanol. They covered a wide range of heat flux at atmospheric pressure.

Addoms [52] experimented for the boiling of distilled water on an electrically heated horizontal platinum wire for pressures ranging from 14.7 psia to 2465 psia.

Farber and Scorah [53] experimentally investigated nucleate boiling of distilled water on a horizontal wire at atmospheric pressure.

The data of above investigations have been widely used by other investigators for the purpose of comparison.

Hughmark [54] carried out a statistical analysis of nucleate boiling data of about 23 liquids. The expression obtained by him is :

$$q = 2.67 \times 10^{-7} \left[ \frac{(\Delta p)^{1.867} (\rho_l - \rho_v)_w^{2.27} (c_l)_w^{0.945} T_s^{1.618}}{(\rho_v)_w^{1.385} (\mu)_w^{1.63} (\lambda)_w^{1.15} (p/p_c)^{0.202}} \right] \quad \dots(2.76)$$

where subscript, w refers to properties evaluation at wall surface temperature; p the ambient pressure, lb/ft<sup>2</sup>; p<sub>c</sub> the critical pressure, lb/ft<sup>2</sup> and Δp the vapour pressure difference corresponding to  $\Delta \bar{t}_w$ , lb/ft<sup>2</sup>.

Drayers [55] tested the generality of existing boiling heat transfer correlations to hydrogen. He found Cryder-Gilliland [43], Forster-Zuber [56] and Forster-Greif [57]



correlations to predict heat flux values in good agreement with experimental data for  $\Delta \bar{t}_w$  of about  $1^\circ\text{F}$ . However, Insinger-Bliss [45], Hughmark [54], Levy [58], Jakob-Linke [2], Nishikawa et al [59] and Miyauchi et al [60] correlations gave poor results. He concluded that many of the existing correlations could agree well with experimental data merely by a readjustment of some of the arbitrary constants used.

Kosky and Lyon [61] undertook a comprehensive investigation of nucleate boiling of several cryogenic and non-cryogenic fluids on the heating surface of different shapes - horizontal, flat, circular and platinum plated disk. Their list of liquid included nitrogen, oxygen, argon, methane and carbon-tetrachloride. They concluded that the correlations due to Gilmour [62], Mc Nelly [63], Kutateladze [64] and Borishanskii et al [65] are superior to the Rohsenow [66], Forster-Greif [57] and Forster and Zuber [56] correlations.

Sciame et al [67] carried out experiments for the nucleate boiling of saturated hydrocarbons; namely - methane, ethane and n-butane on a horizontal gold-plated cylinder. They could not correlate their data into the Rohsenow correlation. However, the data of methane, propane and n-butane were correlated by the following equation which was obtained by modifying Rohsenow correlation;

$$q \sqrt{\frac{\sigma}{\rho_l - \rho_v}} = C \left[ \frac{c_l \Delta \bar{t}_w}{\lambda} \left( \frac{T_R}{Pr} \right)^{1.18} \right]^n \quad \dots(2.77)$$

Where  $T_R$  denotes the reduced temperature. The values of constant,  $C$  and exponent,  $n$  are given in Table 2.3.

Table 2.3 Values of constant,  $C$  and exponent,  $n$  in Eq(2.77)

Liquid	$C \times 10^{-5}$	$n$
Methane	3.25	2.89
Propane	5.77	2.60
n-Butane	2.33	2.84

Borishanskii et al [65] made an experimental investigation of nucleate boiling of water and ethanol from electrically heated tubes of different sizes having ID/OD equal to 6.12/6.94, 4.00/4.99 and 4.00/6.00. For the boiling of water pressure ranged from 1 atmosphere to 200 atmosphere and heat flux from  $50 \times 10^3$  to  $1 \times 10^6$  kcal/hr.m<sup>2</sup> and for ethanol pressure ranged from 1 to 60 atmosphere and heat flux ranged from  $22 \times 10^3$  to  $700 \times 10^3$  kcal/hr.m<sup>2</sup>. They concluded that effect of pressure on heat transfer rate can be expressed by a complex relationship ( $h \propto p^{f(p)}$ ) and cannot be described by a simple power law having a constant exponent on pressure term.

Frost and Li [68] examined the Rohsenow correlation [66] for the boiling of water under subatmospheric pressures. Their experimental set-up included a pyrex tank for holding the pool of distilled water and an electrically heated platinum wire of 0.008 inch diameter and 3 inch length as a

heating surface. The pressure ranged from 0.92 psia to 14.45 psia. They found the value of exponent,  $r$  and constant  $C_{sf}$  in Eq (2.89) not to be constant but to vary with pressure. In the subatmospheric pressure range, pressure has little effect on exponent,  $r$  while it has a marked effect on constant,  $C_{sf}$  of the Rohsenow correlation.

Rice and Calus [69] studied nucleate pool boiling of pure liquids and their binary mixtures on a nickel-aluminium wire of 0.0315 cm diameter and 8.9 cm effective heat transfer length. The pure liquids were water, toluene, carbon-tetrachloride, methanol, isopropanol and n-propanol. The range of operating variables is given in Table 2.4.

Table 2.4 Range of operating variables [69]

Liquid	Atmospheric Boiling Point, °C	Range of $\Delta \bar{t}_w$ , °C	Range of $q$ , °C
Toluene	110.8	9.6 - 33.2	9,150-4,19,560
Carbon-tetrachloride	76.8	11.9 - 24.7	35,330-3,07,570
Methanol	64.7	7.7 - 14.4	82,330-5,74,130
n-Propanol	97.8	12.2 - 28.9	9,780-4,41,000
Isopropanol	82.5	6.8 - 15.1	22,710-4,01,900
Water	100.0	7.8 - 21.7	63,720-7,06,630
Water-isopropanol azeotrope	80.4	7.7 - 16.7	37,220-5,07,890

Based on their data, they recommended the following correlation for calculating boiling heat transfer coefficient

$$\frac{Nu}{K_p^{0.7}} \left[ \frac{T_s}{T_{s,w}} \right]^4 = E Pe_B^{0.7} \quad \dots(2.78)$$

where  $T_{s,w}$  represents the absolute boiling temperature of water at the system pressure and  $E$  is a constant which depends upon the heating surface characteristics used in the investigation.

Eq (2.78) is a modification of Borishanskii et al correlation. The values of  $E$  in Eq (2.78) as obtained by various investigators, are listed in Table 2.5.

Table 2.5 Values of constant,  $E$  in Eq (2.78)

Investigators	Heating Surface	$E \times 10^4$
Rice and Calus [69]	Nickel-aluminium	6.30
Cichelli and Bonilla [50]	Copper polished with electroplated chromium	3.92
Borishanskii et al [65]	Stainless steel	8.90

Huber and Hoehme [70] investigated the boiling of benzene on a tube at pressures ranging from 13.5 to 488.5 psia. They reported that the equations of Rohsenow [66], Gilmour [62] and Levy [58] fit the experimental data excellently.

Kruzhilin [64] recommended the following dimensionless equation for the boiling of liquids at pressures ranging

from 0.2 to 100 atmosphere:

$$\text{Nu}_B = 0.082(\text{Kq})^{0.7} (\text{Ku})^{0.333} (\text{Pr})^{0.45} \quad \dots(2.79)$$

Eq (2.79) can be reduced to a simple and convenient form for the boiling of water:

$$h = 3 q^{0.7} p^{0.15} \quad \dots(2.80)$$

Veneraki [72] investigated the pool boiling of water at pressures ranging from 0.1 atmosphere to 1 atmosphere and heat flux from 4,000 kcal/hr.m<sup>2</sup> to 55,000 kcal/hr.m<sup>2</sup> on a brass pipe. He correlated his experimental data by the following equation:

$$h = C q^n p^m \quad \dots(2.81)$$

The value of  $m$  in Eq (2.81) depends upon the nature of the liquid and the orientation of the heating surface. It was 0.37 for vertical pipe and 0.17 for horizontal pipe. At high heat flux values and 1 atmosphere pressure, heat transfer coefficient for a vertical pipe was about 20 % higher than for horizontal pipe. At low heat flux this value was 40 % higher and at 0.1 atmosphere pressure it was 25 to 30 % higher.

Chi-Fang-Lin et al [73] conducted experiments for the nucleate pool boiling of water, benzene, toluene, and their mixtures. The range of heat flux was from 4,000 to 40,000 kcal/hr.m<sup>2</sup> and that of pressure from 200 to 760 mm Hg. Based on their data they recommended the following dimensional equation:

$$h = C P^n q^m \quad \dots(2.82)$$

The values of the constant, C and exponents, n and m depend upon the liquid. They are given in the Table 2.6.

Table 2.6 Values of C, n and m in Eq (2.82)

Liquid	C	n	m
Water	4.0	0.2	0.69
Benzene	4.5	0.2	0.6
Toluene	3.1	0.7	0.6

Kozitskii [74] studied the boiling of n-butane on horizontal stainless steel tube of different roughnesses. The tubes were of  $6 \times 10^{-3}$  meter OD and 0.18 meter length. The experimental data were correlated by the following equation:

$$h = \frac{4.2 T_s^{0.8} p_c^{0.3}}{T_c^{0.85} M^{0.15}} F(p/p_c) q^{0.7} \quad \dots (2.83)$$

where  $F(p/p_c)$  is a function which characterizes the effect of pressure on heat transfer coefficient. The value of this function depends upon the value of  $(p/p_c)$ .

$$F\left(\frac{p}{p_c}\right) = 2.14 \left(\frac{p}{p_c}\right)^{0.3} ; \text{ for } 0.02 \leq \frac{p}{p_c} \leq 0.127$$

$$\text{and } F\left(\frac{p}{p_c}\right) = 2.6 \left(\frac{p}{p_c}\right)^{0.4} , \text{ for } 0.127 \leq \frac{p}{p_c} \leq 0.80$$

Some of the important empirical correlations of nucleate pool boiling are listed in Table 2.7.

Table 2.7 Some empirical correlations of nucleate pool boiling of liquids

Investigators	Correlation
1 Minchenko and Firsova [81]	$Nu_B = 0.55 (K_P Pe_B)^{0.7}$
2 Kruzhilin and Averin [65]	$Nu_B = 0.082 (Pe_B)^{0.7} (Pr)^{-0.5} (K_t)^{0.377}$
3 Labuntsov [71]	$Nu_B = 0.125 (Pe_B)^{0.65} (Pr)^{-0.32} (K_t)^{0.35}$
4 Mc Nelly [63]	$Nu_B = 0.255 \left(\frac{gd}{\mu\lambda}\right)^{0.69} \left(\frac{Pd}{\sigma}\right)^{0.31} (Bu)^{0.33} (Pr)^{0.6}$
5 Gilmour [62]	$\frac{h}{CG} = 0.001 (Re_B)^{-0.3} (Pr)^{-0.6} \left(\frac{P^2}{\rho\mu\sigma}\right)^{0.425}$
6 Kutateladze [64]	$Nu_B = 7.0 \times 10^{-4} (Pe_B)^{0.7} (Pr)^{-0.35} (K_P)^{0.7}$
7 Kichigin et al [64]	$Nu_B = 1.04 \times 10^{-4} (Pe_B)^{0.7} (K_P)^{0.7} \cdot (Ar)^{0.125}$
8 Alam and Varshney [82]	$Nu_B = 0.084 (Pe_B)^{0.6} (K_{sub})^{-0.5} (K_t)^{0.37}$
9 Tolubinskii and Kostanchuk [83]	$Nu_B = 75 K^{0.7} Pr^{-0.2}$

#### SEMIEMPIRICAL CORRELATIONS

Jakob and Linke [2] studied quantitatively the role of turbulence induced by the vapour bubbles in transferring heat from heating surface to boiling liquid. They laid foundation of analytical correlations by developing an analytical equation for predicting boiling heat transfer

coefficient of liquids. These correlations had invariably used the Fritz equation [23] for bubble departure diameter and do not take into account the influence of pressure on bubble departure diameter and bubble emission frequency. As a result of it, the correlations do not predict heat transfer coefficient in agreement with the experimental values. This situation had led many investigators [35,66,59] to develop suitable analytical correlations of boiling heat transfer.

Jakob and Linke [2] in their analytical investigation considered the influence of turbulence induced by vapour bubbles on the number of nucleation sites. In their correlation, the influence of number of nucleation sites was accounted by  $nA_{b,1}/A$  and the influence of continual displacement of liquid which develops a circulation of liquid along each vapour column was taken into account by  $V_{b,1}/V_{b,2}$ . Hence, heat transfer coefficient was related to these quantities by the following equation :

$$\frac{h D_{b,1}}{k_{\ell}} = \varphi \left[ \frac{n A_{b,1}}{A} \cdot \frac{V_{b,1}}{V_{b,2}} \right] \quad \dots(2.84)$$

Further, they used linear relationship between heat flux and number of nucleation sites on the heating surface and reduced the above equation to the following form :

$$\frac{h D_{b,1}}{k_{\ell}} = \psi \left[ \frac{q}{\rho_v \lambda} \cdot \frac{1}{D_{b,1}^f} \right] \quad \dots(2.85)$$



Later Jakob [1] carried out photographic studies for the boiling of water and carbon-tetrachloride and reported  $fD_b$  to be nearly same for both liquids (equal to 280 m/hr). Jakob and Linke [2] reduced the Fritz equation [23] using photographic measurements of bubble departure diameter. Based on these observations, Eq (2.85) can be modified to the following equation :

$$\frac{h}{k_{\ell}} \sqrt{\frac{\sigma}{\rho_{\ell}}} = 30 \left[ \frac{q}{\rho_v \lambda D_{b,1} f} \right]^{0.8} \quad \dots(2.86)$$

Eq (2.86) was further modified by Jakob [1] for extending its applicability to boiling of liquids at pressures, other than 1 atmosphere. The modified form of the equation is :

$$\frac{h}{k_{\ell}} \sqrt{\frac{\sigma}{(\rho_{\ell} - \rho_v)g}} = 31.6 \frac{v_{\ell,a}}{v_{\ell}} \left[ \frac{f_{\ell,a}}{\rho_{\ell}} \frac{\sigma}{\sigma_a} \frac{q}{\rho_{v,a} \lambda_a D_{b,a} f} \right]^{0.8} \quad \dots(2.87)$$

where subscript, a denotes the value of physical property at normal boiling point. In the development of Eq (2.87)  $D_{b,a}$  and their product were considered to depend upon pressure.

Jicina-Molazhin and Kutateladze [35] scrutinized Eqs (2.85 and 2.87) for the experimental data of carbon-tetrachloride, 26 % water-glycerine, 24 % aqueous sodium chloride solution, water and mercury for pressures ranging from 0.15 to 10.0 atmosphere. They reported that Jakob's relationship, Eq (2.87) can not correlate the experimental data as it does not take into account the effect of pressure on

$fD_b$  properly. Therefore, they recommended the following modified expression of  $fD_b$  for correlating their data and that of Cryder and Finalborgo [48] :

$$\frac{h_a^*}{h_a^*} = \left( \frac{k_{l,a}}{k_{l,a}} \right) \left( \frac{D_{b,a}}{D_b} \right) \left( \frac{\lambda_a \rho_{v,a}}{\lambda \rho_v} \right)^{0.7} \left( \frac{f_a D_{b,a}}{f D_b} \right)^{0.7} \quad \dots(2.88)$$

where subscript a refers to the atmospheric pressure condition and  $h^* = h/q^{0.7}$ .

Rohsenow [66] made a comprehensive investigation for nucleate boiling of liquids in 1952. He quantified the boiling model introduced by Jakob and Linke [2] by assuming that heat is transferred directly from the heating surface to adjacent liquid as in the case of natural or forced convection and the increase in heat flux during boiling is a result of increased agitation associated with the liquid flowing behind the wake of departing bubbles.

He developed a Nu-Re-Pr type correlation using bubble Nusselt number and bubble Reynolds number. The bubble departure diameter and frequency diameter product were the same as used by Jakob and Linke [2]. Because, both the dimensionless groups, Nusselt and Reynolds number contain heat flux term, he employed the following functional form for correlating the experimental data :

$$St = C_{sf} (Re)^r (Pr)^s \quad \dots(2.89)$$

where  $C_{sf}$  is a constant which depends upon the heating surface and the boiling liquid. In literature it has been

commonly referred as surface-liquid combination factor.

The derivation of Eq (2.89) involved the following assumptions: heat flux is proportional to heat transfer to bubbles per unit surface area, product of emission frequency and bubble departure diameter,  $fD_b$  is constant and all the quantities are independent of pressure.  $C_{sf}$  is a function of surface-liquid combination involved in the investigation. Rohsenow obtained the value of exponent  $r$  to be 0.33 and  $s$  to be 1.7 for the experimental data of Addoms [52]. Thus Eq (2.89) assumes the following form :

$$\frac{c_{\ell} \Delta \bar{t}_w}{\lambda} = C_{sf} \left[ \frac{q}{\mu \lambda} \sqrt{\frac{\sigma}{g(\rho_{\ell} - \rho_v)}} \right]^{0.33} \left[ \frac{c_{\ell} \mu}{k_{\ell}} \right]^{1.7} \quad \dots(2.90)$$

Eq (2.90) can be rearranged to :

$$\frac{h}{k_{\ell}} \sqrt{\frac{\sigma}{g(\rho_{\ell} - \rho_v)}} = \frac{1}{C_{sf}} \left[ \frac{q}{\mu \lambda} \sqrt{\frac{\sigma}{g(\rho_{\ell} - \rho_v)}} \right]^{0.667} \left[ \frac{c_{\ell} \mu}{k_{\ell}} \right]^{-0.7} \quad \dots(2.91)$$

or

$$Nu_B = \frac{1}{C_{sf}} (Re_B)^{0.667} (Pr)^{-0.7} \quad \dots(2.92)$$

Various investigators [48,50,84 and 85] tested Eq (2.89) for their experimental data. They reported exponent,  $r$  to be 0.33 but different values of exponent,  $s$  and constant  $C_{sf}$ . These values are given in Table 2.8.

Table 2.8 Values of constant,  $C_{sf}$  and exponent,  $s$  in Eq (2.89)

Surface-liquid combination	$C_{sf}$	$s$
Water-nickel	0.006	1.0
Water-platinum	0.013	1.0
Water-copper	0.013	1.0
Water-brass	0.006	1.0
Carbon-tetrachloride-copper	0.013	1.7
Benzene-chromium	0.010	1.7
n- Pentane-chromium	0.015	1.7
Ethanol-chromium	0.0027	1.7
Isopropanol-copper	0.0025	1.7
35 % $K_2CO_3$ -copper	0.0054	1.7
50 % $K_2CO_3$ -copper	0.0027	1.7
n-butanol-copper	0.0030	1.7

Nishikawa et al [5,59,87] made a photographic study of nucleate boiling of water to obtain the effect of surface nucleation sites on heat flux, heat transfer coefficient and wall superheat quantitatively. Their operating variable included pressure from 0.4 to 1.03 kg/cm<sup>2</sup> and a maximum population count of 8 nucleation sites per square inch. Based on their own data they recommended following expressions:

$$h \propto (fD_b^3 n)^{1/3} \quad \dots(2.93)$$

$$\Delta \bar{t}_w \propto q^{2/3} n^{-1/6} \quad \dots(2.94)$$

Gaertner and Westwater [4] found the above relationships to hold true for their own data. Kurihara and Myers [6] successfully correlated their data of water and four organic liquids for heat flux values upto  $92,500 \text{ kcal/hr.m}^2$  and 28 nucleation sites per square inch in the above expressions. Further, they showed that surface roughness and the boiling liquids do not affect the above relationship between heat transfer coefficient and nucleation site density.

In another investigation, Nishikawa and Urakawa [88-91] analytically studied nucleate boiling of water for pressure ranging from 0.4 to 1.033 atmosphere. They recommended the following dimensionless expressions:

For laminar flow :

$$\frac{hR}{k_f} = 6.35 \left[ \left( \frac{1}{M_s^2 P} \frac{c_f \rho_f^2}{k_f \sigma \lambda \rho_v} \right)^{1/2} R^{3/2} q \right]^{2/3} \dots(2.95)$$

For turbulent flow :

$$\frac{hR}{k_f} = 8.26 \left[ \left( \frac{1}{M_s^2 P} \frac{c_f \rho_f^2}{k_f \sigma \lambda \rho_v} \right)^{1/2} R^{3/2} q \right]^{8/11} \dots(2.96)$$

where  $M_s = 900 \text{ m}^{-1}$ ,  $P = 1,699 \text{ kcal/hr}$  and  $R$  is characteristic dimension of the heating surface.

Mikic and Rohsenow [92] studied boiling heat transfer analytically. Starting with the basic mechanism for a single active cavity size they related heat flux,  $q$  with nucleation site density,  $n$ ; bubble emission frequency,  $f$  and wall superheat,  $\Delta \bar{t}_w$ . Their equation is :

$$q_b = 2 \sqrt{\pi} \sqrt{k_l \rho_l c_l} \sqrt{f} D_b^2 n \Delta \bar{t}_w \quad \dots(2.97)$$

Eq (2.97) was developed on the basis that heat transfer in nucleate boiling is due to transient heat conduction to and subsequent replacement of superheated liquid layer in contact with the heating surface. Nucleation site density,  $n$  was determined by the following expression which is a result of Brown's equation, Eq (2.11) coupled with Clausius - Clapeyron equation:

$$n = C_o r_r^m \left( \frac{\lambda \rho_v}{2 T_s \sigma} \right)^m (\Delta \bar{t}_w)^m \quad \dots(2.98)$$

Using the Cole and Rohsenow expression for  $D_b$ ; the Cole expression for  $f D_b$  and Eq (2.98) for  $n$  Eq (2.97) finally results to following form:

$$q_b = \frac{C_o C_2 C_3^{1/2} r_r^m}{\sqrt{\pi} 2^{m-1}} \sqrt{(k_l \rho_l c_l)} \left( \frac{\lambda \rho_v}{T_s \sigma} \right)^m \times \left[ \frac{\sigma g (\rho_l - \rho_v)}{\rho_l^2} \right]^{1/8} \left[ \frac{\sigma}{g (\rho_l - \rho_v)} \right]^{3/4} (Ja^*)^{15/8} \Delta \bar{t}_w^{m+1} \quad \dots(2.99)$$

where  $C_2 = 1.5 \times 10^{-4}$  for water and  $4.65 \times 10^{-4}$  for other liquids

$$C_3 = 0.6$$

$m = 2.5$  for water and  $3.0$  for other liquids.

or normalising heat flux

$$\frac{q_b \sqrt{\frac{\sigma}{g (\rho_l - \rho_v)}}}{\mu \lambda} = B (\Psi \Delta \bar{t}_w)^{m+1} \quad \dots(2.100)$$



where  $w^{m+1} = \frac{k_l^{1/2} \rho_l^{1/2} C_l^{19/8} \lambda^{(m-23/8)} \rho_v^{(m-15/8)}}{\mu(\rho_l - \rho_v)^{9/8} \sigma^{(m-11/8)} T_s^{(m-15/8)}}$

and  $B = \left(\frac{r_r J}{2}\right)^m \frac{2}{\pi^{1/2} g^{9/8}} C_2^{5/3} C_3^{1/2} C_o$

Eq (2.100) was tested against the experimental data of Addoms [52] and Cichelli and Bonilla [50]. It was found to yield results in agreement with the experimental values. The above correlation was also found to be consistent with low heat flux data of Gaertner and Westwater [4].

Wiebe and Judd [12] carried out experiments for the subcooled and saturated boiling of water on a horizontal copper surface. The heat flux ranged from 20,000 to 1,00,000 BTU/hr ft<sup>2</sup> and the liquid was subcooled from 0 to 105 °F. They recommended the following expressions for the calculation of superheated boundary layer thickness,  $\delta$ :

$$\delta \propto (nf)^{-0.5}, \text{ for } nf < 55 \times 10^3 \text{ bubbles/inch}^2 \text{ s} \quad \dots(2.101)$$

$$\delta \propto (nf)^{-0.33}, \text{ for } nf > 55 \times 10^3 \text{ bubbles/inch}^2 \text{ s} \quad \dots(2.102)$$

They also derived the following equations which relate heat flux as a function of wall superheat and  $nf$ :

$$q \propto (nf)^{0.5} \Delta \bar{t}_w, \text{ for } nf < 55 \times 10^3 \text{ bubbles/inch}^2 \text{ s} \quad \dots(2.103)$$

$$q \propto (nf)^{0.33} \Delta \bar{t}_w, \text{ for } nf > 55 \times 10^3 \text{ bubbles/inch}^2 \text{ s} \quad \dots(2.104)$$

Alad'ev [94] carried out a dimensional analysis of the variables associated in nucleate boiling of liquids. He developed following equation for the calculation of wall

superheat of boiling distilled water at pressures ranging from 0.09 to 200 atmosphere. The equation is :

$$\frac{\Delta \bar{t}_w}{T_s} = 4.7 \times 10^{-3} \left[ \frac{10^{-6} q \lambda}{k_f T_s g} \right]^{0.3} \left[ \frac{\lambda}{c_f T_s} \right]^{1.2} \dots (2.105)$$

Raben et al [95] conducted an analytical as well as experimental investigation for nucleate boiling of distilled water for identifying the dominating mechanism involved in the boiling process and to understand the influence of pressure on boiling heat transfer. They derived the following equation for heat transfer using free convection, vapour-liquid exchange and latent heat transport mechanisms :

$$Q = \frac{k_f}{\delta} a_c \Delta \bar{t}_w + \left[ \frac{\pi}{6} D_b^3 \rho_v \lambda + \frac{\pi}{3} \delta^2 \left( \frac{3}{2} D_b - \delta \right) \right. \\ \left. \times (\rho_f - \rho_v) c_f \frac{\Delta \bar{t}_w}{2} \right] Nf \dots (2.106)$$

where  $a_c$  is convective heat transfer area and  $\delta$  is the thermal boundary layer thickness.

Eq (2.106) correlated the experimental data for pressures ranging from 10 mm Hg to 760 mm Hg satisfactorily.

Singh et al [96] tested the correlation of the Mikic and Rohsenow [92] for the boiling of water and organic liquids on copper surfaces with varying degree of roughness. They reported that for a given heat flux and pressure the ratio of wall superheat of organic liquid to that of water is unaffected by surface roughness of the heating surface.



Some of the analytical investigations are listed in Table 2.9

Table 2.9 Some of the analytical correlations of pool boiling of liquids

Investigators	Correlation
Forster and Zuber [56]	$\frac{\rho_l c_l (\pi \alpha)^{0.5} q}{k_l \rho_v \lambda} \left[ \frac{2\sigma}{\Delta p} \right]^{0.5} \left[ \frac{\rho_l}{g \Delta p} \right]^{0.5}$ $= 0.0015 \left[ \frac{\rho_l c_l \Delta \bar{t}_w (\pi \alpha)^{0.5}}{\lambda \rho_v} \right]^2 \left[ \frac{\rho_l}{\mu} \right]^{0.62}$ $\times \left( \frac{c_l \mu_l}{k_l} \right)^{0.33}$
Levy [58]	$q = \frac{k_l c_l \rho_l^2}{\sigma T_s (\rho_l - \rho_v)} \frac{1}{B_l} (\Delta \bar{t}_w)^3$
Forster and Greif [57]	$q = 1.2 \times 10^{-3} \frac{\alpha c_l \rho_l T_s}{\lambda \rho_v \sigma^{0.5}} \left[ \frac{c_l T_s \alpha^{0.5}}{(\lambda \rho_v)^2} \right]^{1/4}$ $\times \left[ \frac{\rho_l}{\mu} \right]^{5/8} \left[ \frac{c_l \mu}{k_l} \right]^{1/3} \Delta p^2$
Miyauchi and Yagi [60]	$\frac{h}{k_l} = C_1 \left[ \frac{q \rho_l}{\lambda \rho_v \mu} \right]^{0.74} \left[ \frac{\rho_v}{\rho_{v,1}} \right]^{0.69} \left[ \frac{c_l \mu}{k_l} \right]^{0.63}$

## CHAPTER 3

### EXPERIMENTAL SET-UP

Figure 3.1 shows schematic diagram of the experimental set-up to conduct experimental data for heat transfer from horizontal cylinders to a pool of saturated liquids. The photographic diagram is given in Figure 3.2.

The design considerations taken into account are as follows :

#### 3.1 DESIGN CONSIDERATIONS

- a. For an electrically heated horizontal cylinder submerged in a liquid pool, the outer surface temperature changes along its circumference. To measure this variation, thermocouples should be installed at as many places as possible. Due to practical difficulties only three thermocouples could be installed at the top -, at the side - and at the bottom - position of the cylinder as shown in Figure 3.6. However, this was considered adequate as the readings at three places are sufficient for obtaining an average value.

There is a possibility of error in the measurement of surface temperature if the thermocouples are installed near an end of the cylinder due to end effects. To eliminate this the thermocouples were inserted upto an axial length equal to half of the cylinder length.

- b. Another important consideration was to measure bulk temperature of the boiling liquid corresponding to the wall thermocouples. The radial distance off the outer surface at which the thermocouple monitors the bulk temperature is variable and depends on heat flux, pressure and the physico-thermal properties of the boiling liquid. Therefore, travelling thermocouples, especially designed and fabricated, were employed for this purpose.
- c. The condensate flowing back from the condenser might affect the bubble dynamics if it falls directly on the heating cylinder. This can be eliminated if sufficient liquid height on the heating cylinder is kept. By conducting actual data with different liquid heights it was established that the height should be 93 mm.

### 3.2 EXPERIMENTAL SET-UP

Keeping the above design considerations in view, the experimental set-up was assembled as in Figure 3.1. Its essential components were (a) test vessel (b) heating surface (c) condenser (d) vacuum pump (e) agitator with its accessories and (f) instrumentation.

#### a. TEST VESSEL

Figure 3.3 shows the schematic diagram of the test vessel. It was a 304 AISI stainless steel cylindrical vessel (5) of 150 mm ID, 156 mm OD and 450 mm

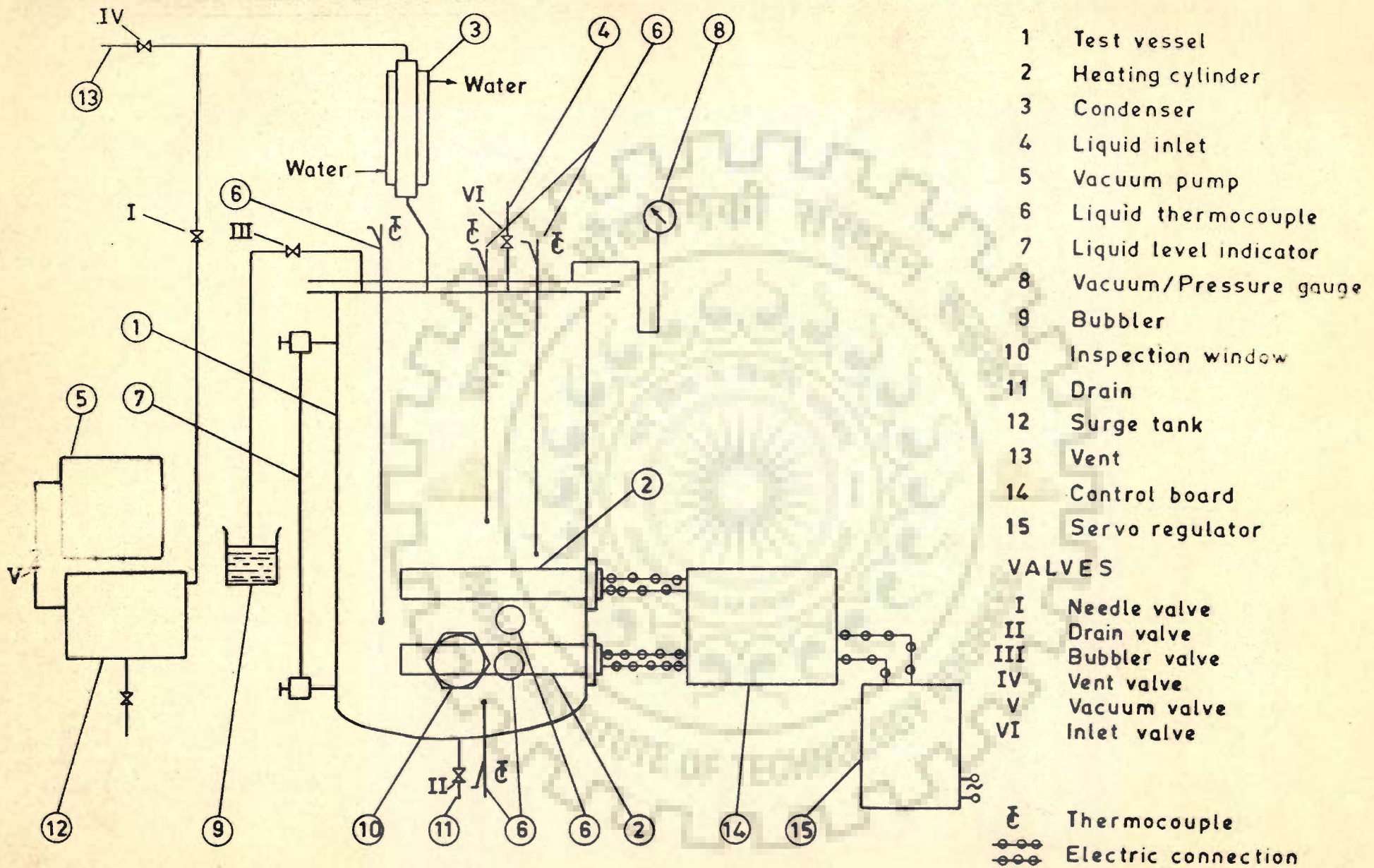


Fig 3-1 Schematic diagram of the experimental set-up

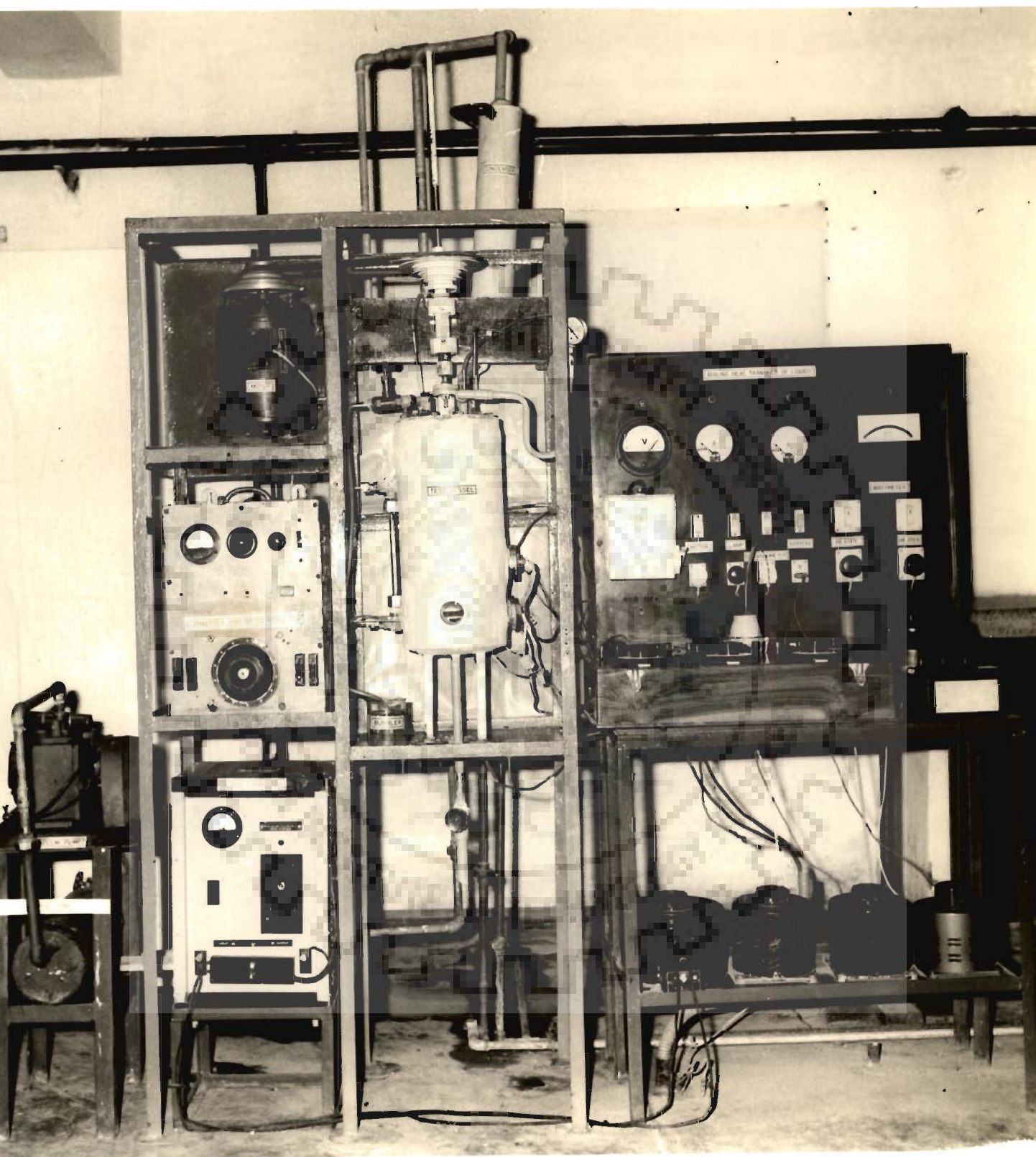
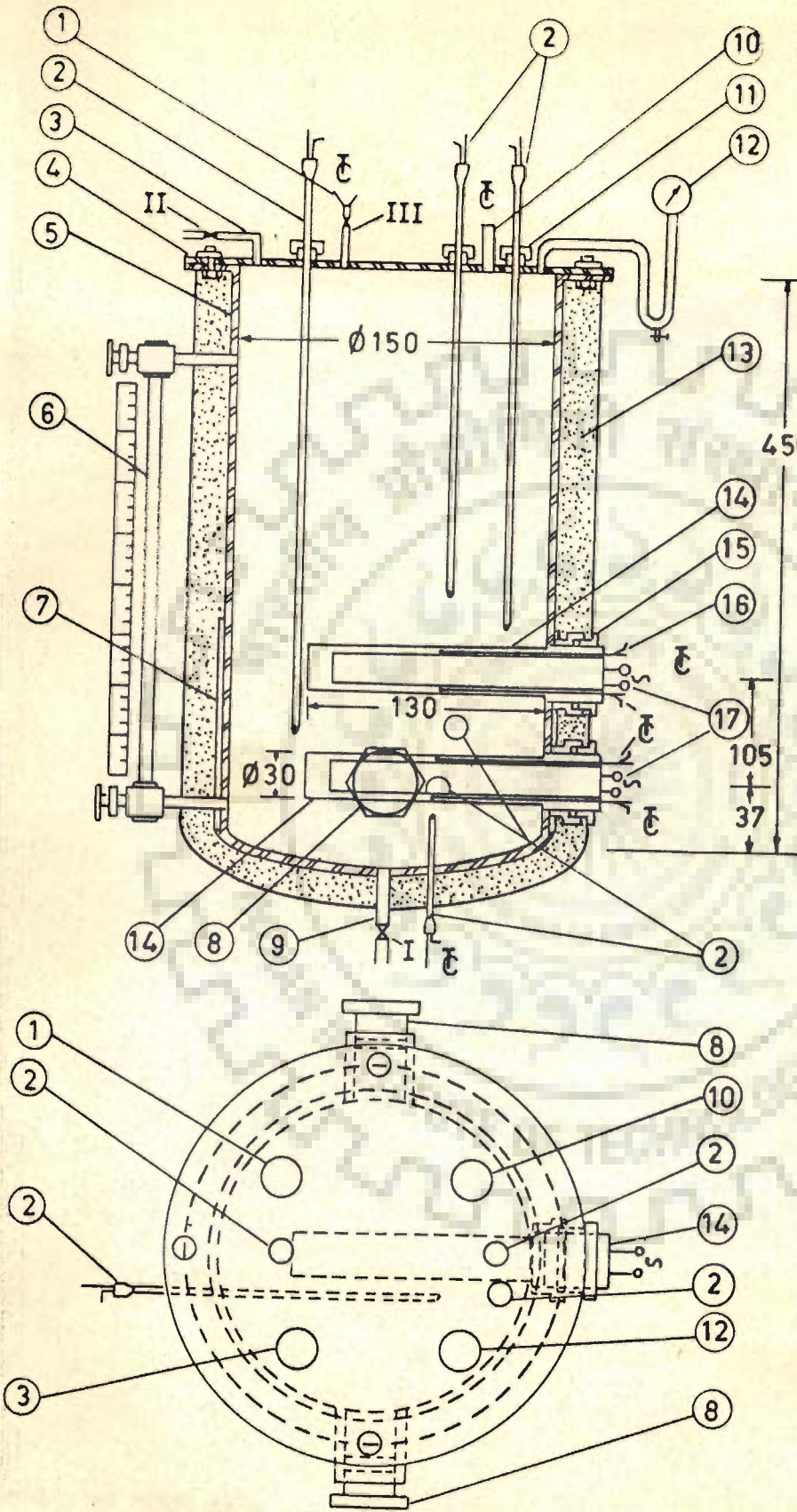


Fig 3-2 Photographic view of the experimental set-up



- 1 Liquid inlet
- 2 Liquid thermocouple
- 3 Bubbler line
- 4 Flange cover
- 5 Test vessel
- 6 Liquid level indicator
- 7 Auxiliary heater
- 8 Inspection window
- 9 Drain
- 10 To condenser
- 11 Thermocouple adapter
- 12 Vacuum/Pressure gau
- 13 Insulation
- 14 Heating cylinder
- 15 Socket check nut assembly
- 16 Wall thermocouple
- 17 Heater

**VALVES**

- I Drain valve
- II Bubbler valve
- III Inlet valve
- ⊕ Thermocouple
- ⤵ Alternating current

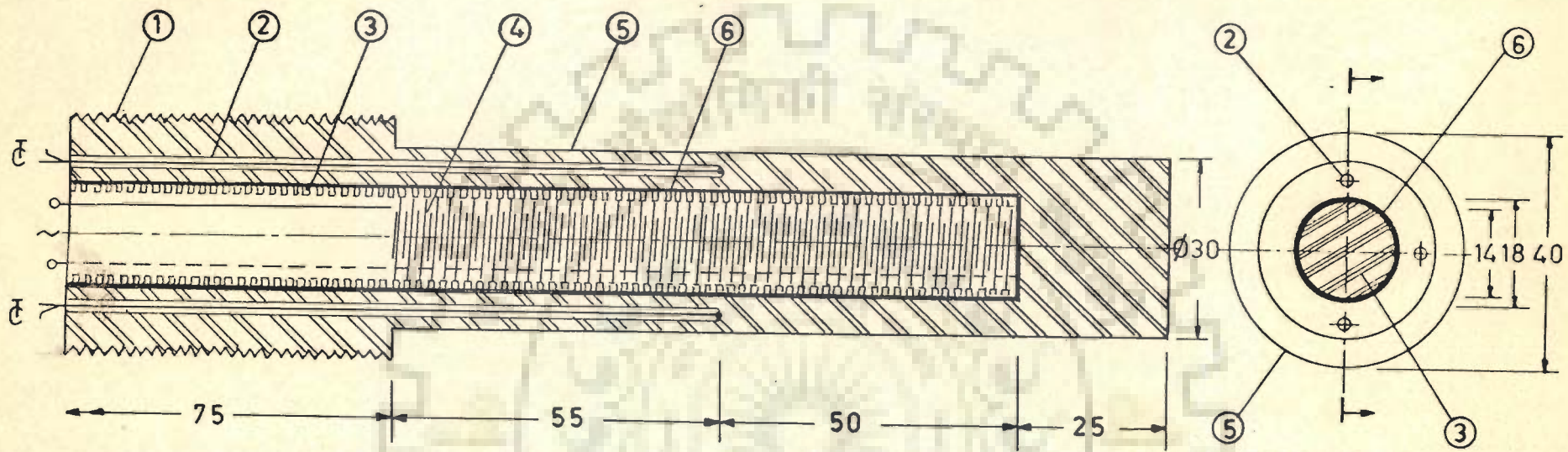
All dimensions in mm

Fig 3.3 Details of test vessel

height. Two diametrically opposite inspection windows (8) were provided on the front and rear sides of the test vessel. The vessel had the dished bottom with an opening (9) in its centre to drain the liquid from it. Its top had a flanged over (4) with mountings for liquid thermocouples (2), the liquid inlet (1), the bubbler (3), the condenser (10) and the vacuum/pressure gauge (12). Level indicator (6) was provided to observe the level of the liquid in the test vessel. A home-made electric heater was used as an auxiliary heater (7) to pre-heat the liquid in the vessel. It was made by wrapping 26 gauge nichrome wire over the outer surface of the test vessel upto the height of 150 mm from the bottom of the test vessel. The vessel body was suitably insulated (13) by a covering of asbestos rope followed by a layer of paste of 85 per cent magnesia powder and plaster of paris.

#### b. HEATING SURFACE

The heating surface consisted of two identical 304 AISI stainless steel cylinders of 105 mm length, 18 mm ID and 30 mm OD. The details of one of the identical heating cylinder are shown in Figure 3.4. The outer surface of the cylinder was prepared to have a specific surface characteristics by turning on a lathe machine and rubbing against an emery paper of standard o/o grade. As is seen from the



All dimensions in mm

- |   |                  |   |                           |   |                |   |                     |
|---|------------------|---|---------------------------|---|----------------|---|---------------------|
| 1 | Threaded end     | 2 | Wall thermocouple holes   | 3 | Porcelain tube | 4 | Nichrome wire       |
| 5 | Heating cylinder | 6 | Mica sheet and glass tape | ϕ | Thermocouple   | ⋈ | Alternating current |

Fig 3-4 Details of a heating cylinder with heater

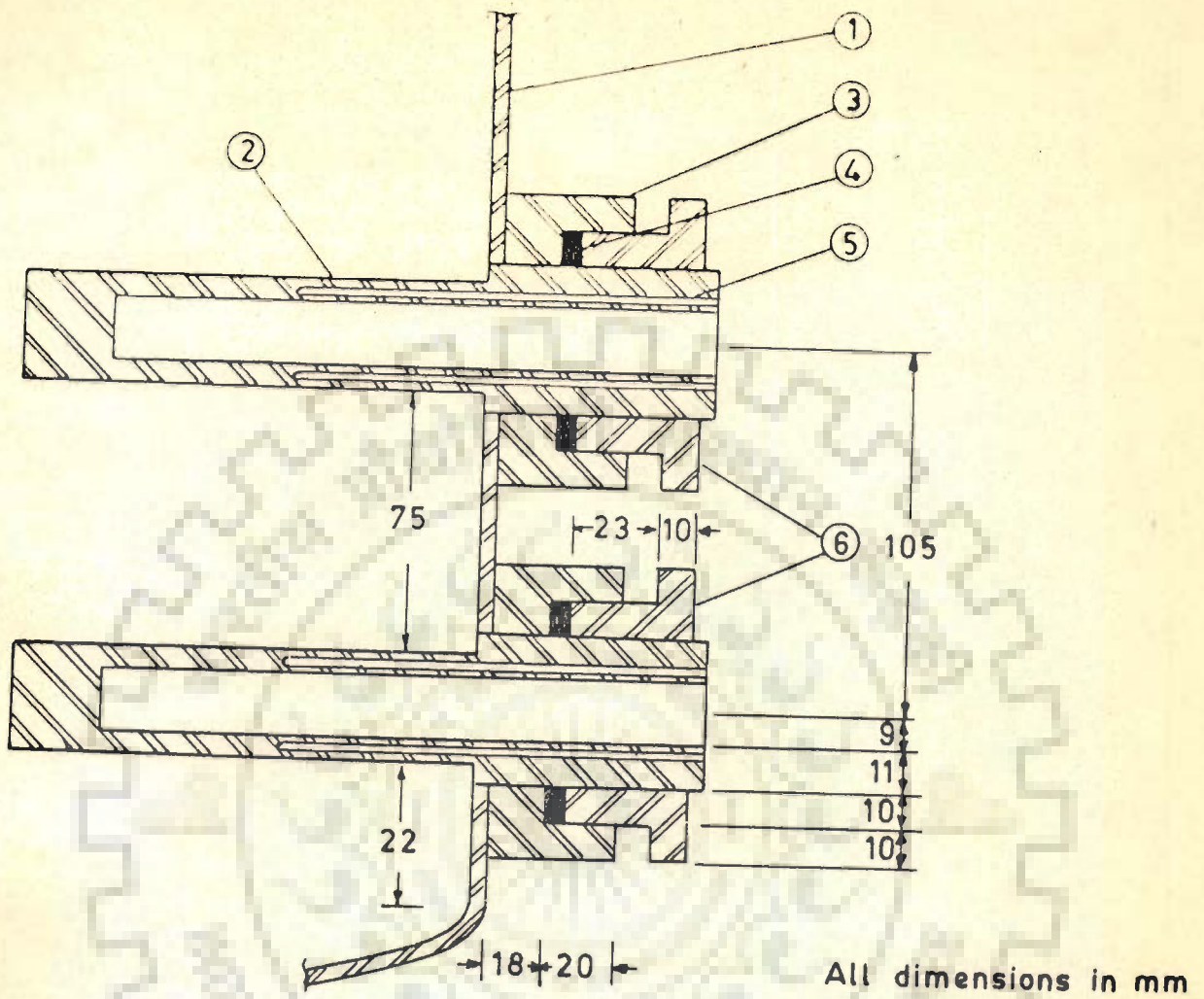


figure one of the ends of cylinder was made blind whereas the other end open. Both the ends were provided with thick flanges. The open end of the flange(1) had the thread.

The cylinder (5) was internally heated by placing electric heater inside it. The heater comprised of 26 gauge nichrome wire uniformly wound over a 14 mm diameter porcelain tube (3). The wire had the maximum current carrying capacity of 5A. Thin mica-sheet and glass tape (6) were wrapped over the heaters to provide electrical insulation between the heaters and the cylinders.

Figure 3.5 shows the orientation of the heating cylinders and the method of attaching them with the vessel wall. The cylinders were inserted into the vessel through two holes, 75 mm apart in a vertical plane, provided in the vessel. They were oriented in horizontal position such that the blind ends remained floating in the vessel and the open ends attached to the test vessel wall (1). The check-nut (6) with teflon gaskets (4) made the system leak-proof.

Each cylinder had three axial holes of 3 mm diameter and 55 mm length in its wall thickness, measured from the open end. These holes were 90° apart, at the top -, at the side- and at the bottom-position of the cylinder. Thermocouples were



- |   |                  |   |                   |   |           |
|---|------------------|---|-------------------|---|-----------|
| 1 | Test vessel wall | 2 | Heating cylinder  | 3 | Socket    |
| 4 | Teflon gasket    | 5 | Thermocouple hole | 6 | Check nut |

Fig 3.5 Heating cylinder with test-vessel wall

inserted in the holes (2) provided in the thickness of the cylinder right upto the depth of 55 mm from the open end to monitor the wall temperature at the top- , at the side- and at the bottom- position of the heating cylinders. Travelling liquid thermocouples were positioned at various locations as shown in Figure 3.6 to measure the liquid bulk temperature. They were at the respective positions corresponding to the surface thermocouples in the heating cylinders.

c. CONDENSER

The condenser was a stainless steel double pipe type heat exchanger. The inside diameter of the inner and outer tubes was 50 mm and 100 mm respectively. Tubes had a length of 560 mm. It was provided with an air vent. It was vertically placed over the test vessel. Cooling water routed in the annular space whereas the vapours, from the boiling liquid, inside the inner pipe. The condensate returned to the liquid pool in the test vessel. The cooling water flow rate helped in maintaining the vacuum in the system developed by the vacuum pump.

d. VACUUM PUMP

It was a single stage oil immersed type rotary pump driven by 0.25 HP motor having 1440 rpm. The pump was capable of producing an ultimate pressure of  $6.67 \text{ kN/m}^2$ . It was connected to the vapour space

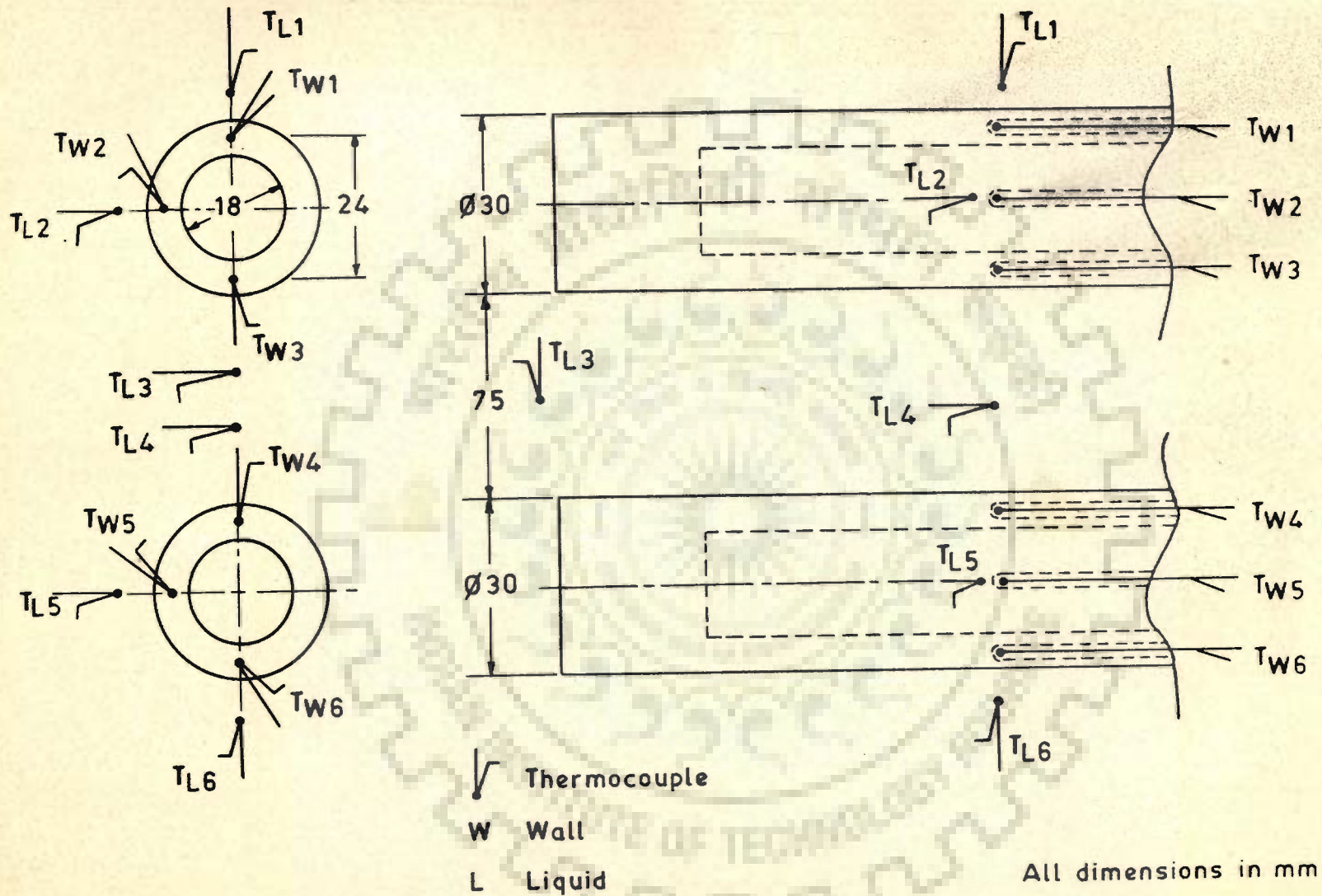


Fig 3.6 Position of mounted thermocouples

in the test vessel through condenser and an oil seal. A needle valve (I of Figure 3.1) in the line regulated the vacuum in the vessel.

e. AGITATOR WITH ITS ACCESSORIES

The test vessel had an agitator having a turbine type impeller of standard geometric configuration. However, the present investigation did not make use of it.

f. INSTRUMENTATION

The experimental set-up was properly instrumented to measure the following variables: power input to the heaters placed in the cylinders, liquid- and the wall- temperatures and the pressure in the vessel.

Stabilized alternating current modulated by autotransformers was supplied to the heaters. It was measured by calibrated wattmeters supplied by M/S Automatic Electric Ltd., Bombay. The wattmeters were of precision grade having a range of 0-720 watts with a maximum error of less than  $\pm 1$  per cent.

Liquid- and the wall- temperatures were measured by calibrated copper-constantan thermocouples of 22 gauge. The e.m.f. developed in the thermocouples was measured by means of a vernier potentiometer and a sensitive spot-galvanometer. The vernier potentiometer had a least count of 0.001 mV and an accuracy of 0.01 per cent. The thermocouple leads

were connected to the potentiometer through a 12-point selector switch and a cold junction. The cold junction was an ice box having melting ice to provide a reference temperature of  $0^{\circ}\text{C}$ . The thermocouples had maximum error of less than  $\pm 1$  per cent.

The pressure in the test vessel was measured by a calibrated vacuum gauge having a maximum error of less than  $\pm 1$  per cent.

The set-up assembled as in Figure 3.1 was tested for mechanical and electrical failures as follows:

### 3.3 TESTING OF THE EXPERIMENTAL SET-UP

To ensure the experimental set-up against any mechanical failure, the procedure used was as follows :

The system was filled with compressed air at  $300 \text{ kN/m}^2$  (3 times the maximum pressure at which the system operated for experimental data) and left for 24 hours followed by a vacuum of  $93.33 \text{ kN/m}^2$  for 24 hours. The system withstood the pressure and vacuum well.

To test the system against electrical leakage, the vessel was filled with water to a height of 260 mm such that the heating cylinders were well submerged. A current of 3A was passed through the heaters placed inside the heating cylinders for some time. On testing the system it was found that it was electric leak-proof.

## CHAPTER 4

### EXPERIMENTAL PROCEDURE

The following procedures were followed for cleaning, rinsing and charging the test vessel with the test liquid; and also for the stabilization of the surface characteristics of the heating cylinders, deaeration of the test liquid and for conducting a given set of experimental runs.

#### 4.1 CLEANING, RINSING AND CHARGING THE VESSEL

Before conducting data for a given liquid, the vessel was made empty. All the valves of experimental set-up were closed. The system was connected to a compressor through the condenser. The system was filled with compressed air at a pressure of  $200 \text{ kN/m}^2$ . The drain valve (II of Figure 3.1) was partially opened. The compressed air rushed out carrying with it the drops of the previous test-liquid. After this the vessel was rinsed and filled with the test-liquid to be investigated upto a height of 260.0 mm in the vessel.

#### 4.2 STABILIZATION OF SURFACE CHARACTERISTICS OF THE HEATING CYLINDERS

The heating cylinder surfaces were found to be stabilized after aging them in the test liquid for 72 hours and boiling of 24 hours. This was considered an important part of the experimentation after charging the fresh liquid.

#### 4.3 DEAERATION OF THE TEST LIQUID

This was carried out before starting a given set of experimental runs. It was achieved by boiling test liquid for many hours. During boiling the dissolved air came out from the liquid and bubbled through the bubbler (9 of Figure 3.1). In fact, the complete removal of the air was ensured when bubbling ceased in the bubbler.

#### 4.4 CONDUCTION OF EXPERIMENTAL DATA

The experimental data were conducted for the values of heat flux, pressure and liquids as given in Table 4.1. As is seen from the last column of the Table, the experiments were conducted when (a) the lower heating cylinder was energized, (b) the upper heating cylinder was energized and (c) both the lower and upper heating cylinders were energized simultaneously. The data for the respective cases appear in Table B.1 through B.3 of Appendix B.

First of all the data were obtained for the boiling heat transfer from the lower heating cylinder to distilled water at  $98.00 \text{ kN/m}^2$  pressure after ensuring the cleaning, rinsing and charging the vessel with test liquid, stabilization of the heating cylinder and deaeration of distilled water. The heat flux changed regularly in increasing order from lower value to higher ones. Accordingly, a heat flux of  $20,210 \text{ W/m}^2$  was adjusted. The boiling continued as visualized through the inspection windows (8 of Figure 3.3). The liquid thermocouples were moved away from the surface of the cylinder



Table 4.1 Operating parameters of present investigation

Boiling liquid	Heat flux, kW/m <sup>2</sup>	Pressure, kN/m <sup>2</sup>	Heating <sup>+</sup> surface
Distilled water	20.210, 24.252, 28.294, 32.336, 36.378, 40.420, 44.462 and 48.504	98.00, 71.16, 57.93, 44.50 and 31.26	Lower heating cylinder
	20.210, 24.252, 28.294, 32.336, 36.378, 40.420, 44.462 and 48.504	98.00, 71.16, 57.93, 44.50 and 31.26	Upper heating cylinder
	16.168, 20.210, 24.252, 28.294, 32.336, 36.378, 40.420, 44.462 and 48.504	98.40, 71, 50, 57.90 and 44.50	Both lower and upper heating cylinders
Benzene	16.168, 20.210, 24.252, 28.294, 32.336, 36.378, 40.420, 44.462 and 48.504	96.86, 70.66, 57.60, 44.00 and 33.40	Lower heating cylinder
	16.168, 20.210, 24.252, 28.294, 32.336, 36.378, 40.420, 44.462 and 48.504	96.86, 70.66, 57.66, 44.00 and 33.40	Upper heating cylinder
	16.168, 20.210, 24.252, 28.294, 32.336, 36.378, 40.420, 44.462 and 48.504	97.20, 70.60, 57.70 and 43.80	Both lower and upper heating cylinders

Table 4.1 Contd.

Boiling liquid	Heat Flux, kW/m <sup>2</sup>	Pressure, kN/m <sup>2</sup>	Heating <sup>+</sup> surface
Toluene	20.210, 24.252, 28.294, 32.336, 36.378, 40.420, 44.462 and 48.504	96.15, 69.93, 56.60, 43.45 and 29.86	Lower heating cylinder
	20.210, 24.252, 28.294, 32.336, 36.378, 40.420, 44.462 and 48.504	96.00, 69.33, 56.60, 43.19 and 29.86	Upper heating cylinder
	16.168, 20.210, 24.252, 28.294, 32.336, 36.378, 40.420, 44.462 and 48.504	96.25, 69.60, 56.40 and 43.19	Both lower and upper heating cylinders.

<sup>+</sup>304 AISI Stainless steel horizontal cylinder

till they did not show any change in their values ensuring that they were measuring the bulk temperature of the liquid surrounding the cylinder. The readings of all the surface and the liquid thermocouples were noted after attaining the steady state. The reading of wattmeter was also noted. Experiments following the above procedure, were also conducted for other values of heat flux of Table 4.1. After completing data for all the values of heat flux under atmospheric pressure, the data were conducted for subatmospheric pressures for distilled water.

Similar experiments were conducted for boiling heat transfer from the upper heating cylinder to distilled water

and when both the heating cylinders were energized simultaneously for the range of pressure and heat flux given in Table 4.1.

Experiments following the above procedure were also conducted for benzene and toluene for the condition of Table 4.1.

#### 4.5 REPRODUCIBILITY OF EXPERIMENTAL DATA

Before accepting the experimental data, they were examined for their reproducibility.

Reproducibility of the data was checked by conducting experiments under the same operating conditions at different times and comparing them. Data were found to be reproducible.

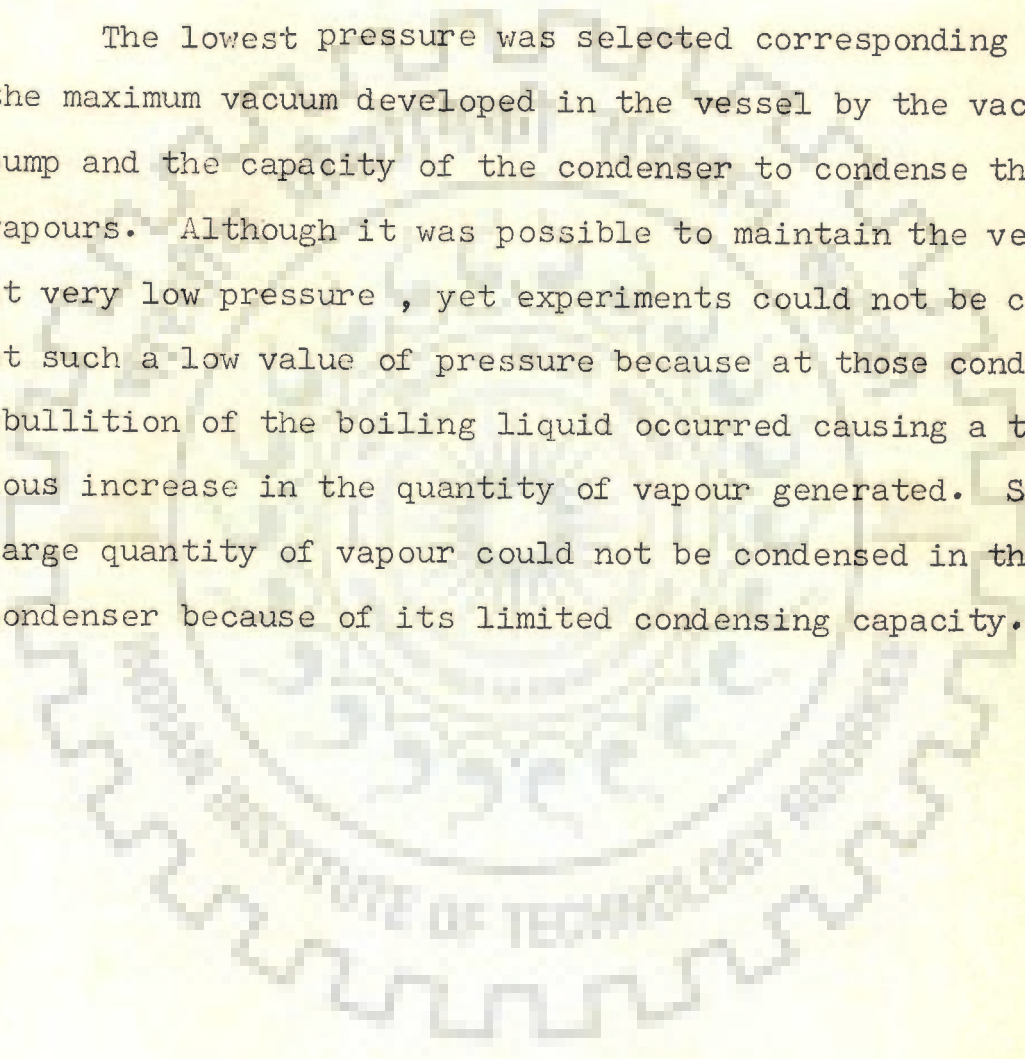
Prior to switching over a new liquid, test-check experiments were conducted with distilled water. These experiments compared excellently with the earlier data taken with distilled water. This indicated that the heating surface characteristics did not change during experimentation. Thus the data were found to be reproducible.

#### 4.6 OPERATIONAL CONSTRAINTS

Heat flux and the pressure were two of the important parameters in this investigation. Their operating ranges were fixed based on the physical limitations of the instruments used. The maximum value of heat flux was  $48.504 \text{ kW/m}^2$

corresponding to the maximum current carrying capacity of the nichrome wire used for the heater. The minimum heat flux corresponded to a condition at which the boiling could sustain on the heating cylinder for a given liquid and pressure.

The lowest pressure was selected corresponding to the maximum vacuum developed in the vessel by the vacuum pump and the capacity of the condenser to condense the vapours. Although it was possible to maintain the vessel at very low pressure, yet experiments could not be conducted at such a low value of pressure because at those conditions ebullition of the boiling liquid occurred causing a tremendous increase in the quantity of vapour generated. Such a large quantity of vapour could not be condensed in the condenser because of its limited condensing capacity.



During the last several decades a large number of research efforts has been concentrated to investigate the various aspects of nucleate pool boiling heat transfer, consequently both the theoretical and the experimental investigations have resulted in expressions for the bubble departure diameter, the bubble emission frequency, the number of nucleation sites and the models for boiling heat transfer. An examination of these expressions shows that none of them has the applicability for wide range of pressure and heat flux. However they are suitable for their respective range of parameters.

The present investigation attempts to obtain analytical expression which can correlate the data of nucleate pool boiling heat transfer of liquids for atmospheric and sub-atmospheric pressures.

## 5.1 ANALYSIS

As a matter of fact the heat taken away from the heat transfer surface during nucleate boiling is by simultaneous transient heat conduction to and subsequent replacement of the superheated liquid layer and latent heat transport. Following them and using appropriate expressions for the bubble departure diameter, the bubble emission frequency and the number of nucleation sites on the heating surface,

an expression has been derived for correlating the nucleate pool boiling heat transfer data of saturated liquids under atmospheric and subatmospheric pressures.

#### 5.1.1 TRANSIENT HEAT CONDUCTION MODEL

Mikic and Rohsenow [92] developed a semitheoretical correlation for the boiling heat transfer by considering the transient conduction to and subsequent replacement of the superheated liquid layer in contact with the heating surface. Later it has been supported by Gaertner and Westwater [4], Addoms [52] and Cichelli and Bonilla [50] for the different boiling liquids for pressure exceeding atmospheric pressure. The expression recommended is in terms of boiling liquid properties; bubble emission frequency,  $f$ ; bubble departure diameter,  $D_b$ ; number of nucleation sites,  $N$ ; and wall superheat,  $\Delta\bar{t}_w$  as given below :

$$Q = 2 \sqrt{\pi} \left( \sqrt{k_l \rho_l c_l} \right) \sqrt{f} D_b^2 \Delta\bar{t}_w N \quad \dots(5.1)$$

#### 5.1.2 LATENT HEAT TRANSPORT MODEL

Rallis and Jawurek [36] postulated a model considering that while the bubble grows it absorbs latent heat of vaporization and during its collapse it transfers this heat to the liquid pool. They derived an equation in terms of bubble departure diameter,  $D_b$ ; number of nucleation sites,  $N$ ; bubble emission frequency,  $f$  and the physico-thermal

properties of the boiling liquid in the following form :

$$Q = \frac{\pi}{6} D_b^3 \rho_v \lambda f N \quad \dots(5.2)$$

Both the above models assume the vapour bubble to be spherical in shape.

## 5.2 BOILING HEAT TRANSFER RATE

In fact both the above mentioned mechanisms operate simultaneously in the boiling process and thus the total amount of heat transferred from the heating surface to a boiling liquid is a summation of the heat transfer by the individual mechanism. It may be mentioned that the contribution of the above mechanisms is likely to depend upon the pressure of the boiling liquid. This seems logical in view of the fact that at subatmospheric pressure the latent heat of vaporization is much larger than that at the high pressures, implying that both the models will have their partial contributions depending upon pressure. Therefore, the following equation describes the boiling heat transfer rate :

$$Q = [K_1 2\sqrt{\pi} (\sqrt{k_f \rho_f c_f}) \sqrt{f} D_b^2 \Delta \bar{t}_w + K_2 \frac{\pi}{6} D_b^3 \rho_v \lambda f] N \quad \dots(5.3)$$

where  $K_1$  and  $K_2$  represent the fraction of heat transfer contributed due to transient conduction model and latent heat transport model respectively and their values depend upon pressure.

Eq (5.3) requires the knowledge of the bubble departure diameter,  $D_b$ ; the bubble emission frequency,  $f$ ; the wall superheat,  $\Delta \bar{t}_w$  and the physico-thermal properties corresponding to the pressure of boiling liquid for the computation of boiling heat transfer rate. The relevant expressions for  $f$ ,  $D_b$  and  $N$  are described as given below :

a. BUBBLE EMISSION FREQUENCY

Hatton and Hall [20] have recommended the following expression for the calculation of bubble emission frequency for the boiling of liquids under subatmospheric pressures :

$$f = \frac{3}{\pi \alpha} \left[ \frac{16 k_\ell \sigma T_s}{(\lambda \rho_v)^2 D_b D_c} \right]^2 \quad \dots(5.4)$$

where  $D_c = 2 r_c$ .

b. BUBBLE DEPARTURE DIAMETER

Cole and Rohsenow [98] have derived the following equation for the calculation of bubble departure diameter,  $D_b$  for the boiling of liquids under subatmospheric pressures:

$$D_b = C J_a^{*5/4} \sqrt{\frac{\sigma}{g(\rho_\ell - \rho_v)}} \quad \dots(5.5)$$

where  $J_a^* = \frac{\rho_\ell c_\ell T_s}{\rho_v \lambda}$

and  $C = 1.5 \times 10^{-4}$  for organic liquids  
 $= 4.6 \times 10^{-4}$  for distilled water.



Substitution of the values of  $f$  and  $D_b$  from respective Eqs (5.4) and (5.5) into Eq (5.3) results into following:

$$q = \frac{Q}{A} = \left[ 2\sqrt{3}K_1 \rho_l c_l \frac{16 k_l \sigma T_s}{\lambda \rho_v^2 D_c} \frac{D_b}{4} \Delta \bar{t}_w + \frac{128K_2 \rho_l c_l k_l \sigma^2 T_s^2 D_b}{\lambda^3 \rho_v^3 D_c^2} \right] \frac{N}{A} \quad \dots(5.6)$$

### c. NUMBER OF NUCLEATION SITES

Expression for the calculation of number of nucleation sites per unit area due to Brown [13] is as follows :

$$\frac{N}{A} = C_o \left( \frac{r_r}{r_c} \right)^m \quad \dots(5.7)$$

where  $C_o$  is a dimensional constant having the dimensions of  $(\text{area})^{-1}$  and  $r_r$  is the radius of the sites for which  $\frac{N}{A}$  would be one per unit area.

The value of  $r_c$  is obtained from the use of Laplace equation as given below :

$$r_c = \frac{2\sigma}{\Delta p} \quad \dots(5.8)$$

The pressure difference,  $\Delta p$  required for bubble formation can be expressed in term of wall superheat,  $\Delta \bar{t}_w$  in the following manner :

$$\begin{aligned} \Delta p &= p(T_s + \Delta \bar{t}_w) - p(T_s) \\ &= \left( \frac{\partial p}{\partial T} \right)_s \Delta \bar{t}_w + \left( \frac{\partial^2 p}{\partial T^2} \right)_s \frac{\Delta \bar{t}_w^2}{2!} + \dots \\ &\approx \left( \frac{\partial p}{\partial T} \right)_s \Delta \bar{t}_w \quad \dots(5.9) \end{aligned}$$

Using Clausius-Clapeyron equation and Eq (5.9) into Eq (5.8) one gets :

$$r_c = \frac{2\sigma T_s (\rho_l - \rho_v)}{\lambda \rho_l \rho_v \Delta \bar{t}_w} \quad \dots(5.10)$$

Substitution of the value of  $r_c$  from Eq (5.10) into Eq (5.7) yields the following expression for  $N/A$ .

$$\frac{N}{A} = C_o r_r^m \left[ \frac{\lambda \rho_l \rho_v \Delta \bar{t}_w}{2\sigma T_s (\rho_l - \rho_v)} \right]^m \quad \dots(5.11)$$

Using the values of  $N/A$  and  $r_c$  from the respective Eqs (5.11) and (5.10) into Eq (5.6), the expression for boiling heat flux assumes the following form for subatmospheric pressures ( $\rho_l \gg \rho_v$ ) :

$$q = (2\sqrt{3} K_1 + 8K_2) \frac{C_o r_r^m C}{2^m g^{0.5}} \left[ \frac{\rho_l^{7/4} c_l^{9/4} k_l T_s^{5/4-m}}{\lambda^{9/4-m} \rho_v^{9/4-m} \sigma^{m-0.5}} \right] \times \Delta \bar{t}_w^{m+2} \quad \dots(5.12)$$

Eq (5.12) describes the direct relationship between heat flux,  $q$  and the wall superheat,  $\Delta \bar{t}_w$ . To determine the value of  $m$  we proceed as follows : For a given heating surface, liquid and pressure the heat flux,  $q$  varies with wall superheat  $\Delta \bar{t}_w$  raised to the power of 3.33. In other words  $q \propto \Delta \bar{t}_w^{3.33}$ . Therefore, applying the above relationship of  $q$  with  $\Delta \bar{t}_w$  in Eq (5.12) one gets :

$$m + 2 = 3.33$$

$$m = 1.33$$

Now replacing the exponent,  $m$  by its numerical value ( $m = 1.33$ ) Eq (5.12) assumes the form :

$$q = K \left[ \frac{\rho_l^{1.75} c_l^{2.25} k_l}{T_s^{0.08} \lambda^{0.92} \rho_v^{0.92} \sigma^{0.83}} \right] \Delta \bar{t}_w^{3.33} \quad \dots(5.13)$$

or

$$\Delta \bar{t}_w = \frac{1}{K^{0.3}} \left[ \frac{T_s^{0.024} \lambda^{0.276} \rho_v^{0.276} \sigma^{0.249}}{\rho_l^{0.525} c_l^{0.675} k_l^{0.3}} \right] q^{0.3} \quad \dots(5.14)$$

where

$$K = (2\sqrt{3} K_1 + 8K_2) \frac{C_o r_r^{1.33} C}{2^{1.33} g^{0.5}} \quad \dots(5.15)$$

The quantity  $K$  has the terms;  $C_o$ ,  $r_r$ ,  $K_1$  and  $K_2$ . The terms,  $C_o$  and  $r_r$  depend upon the heating surface characteristics while  $K_1$  and  $K_2$  depend upon pressure. Keeping this in view one can write the following :

$$K = F_1(p) F_2(C_{sf}) \quad \dots(5.16)$$

where  $F_1(p)$  is some function of pressure,  $p$  and  $F_2(C_{sf})$  of surface liquid combination factor,  $C_{sf}$ . In other words function  $F_2(C_{sf})$  does not depend upon pressure for a given surface-liquid combination. Unfortunately, function  $F_2(C_{sf})$  cannot be generalized. Therefore, the only course is to use Eq (5.14) to attempt a relationship,  $\Delta \bar{t}_w / \Delta \bar{t}_{w,1}$  (ratio of the values of wall superheat at two different pressures) and

thereby cancel out function  $F_2(C_{sf})$ . Now from Eqs (5.14), (5.15) and (5.16) the following equation results :

$$\frac{\bar{\Delta t}_w}{\bar{\Delta t}_{w,1}} = \Psi \left[ \frac{p}{p_1} \right] \left[ \frac{\rho \ell}{\rho_{\ell,1}} \right]^{-0.525} \left[ \frac{c \ell}{c_{\ell,1}} \right]^{-0.675} \left[ \frac{k \ell}{k_{\ell,1}} \right]^{-0.3}$$

$$\left[ \frac{T_s}{T_{s,1}} \right]^{0.024} \left[ \frac{\lambda}{\lambda_1} \right]^{0.276} \left[ \frac{\rho_v}{\rho_{v,1}} \right]^{0.276}$$

$$\left[ \frac{\sigma}{\sigma_1} \right]^{0.249} \left[ \frac{q}{q_1} \right]^{0.3} \dots (5.17)$$

Subscript 1 represents a reference point for which the numerical value of wall superheat  $\bar{\Delta t}_w$  is known. Now the value of  $\Psi (p/p_1)$  can be determined by fitting the experimental data of boiling heat transfer on a given heating surface at different pressures. This is shown in Chapter 6.

## CHAPTER 6

### RESULTS AND DISCUSSION

This chapter contains the results and their interpretations based on the experimental data of present and earlier investigations. The present experimental data were for the nucleate pool boiling of liquids on a single heating cylinder and also on an assembly consisting of two heating cylinders placed one over the other horizontally.

The data for all the operating parameters of Table 4.1 of Chapter 4 are listed in Tables B.1 through B.3 of Appendix B. They include the values of wall- and boiling liquid-temperatures for the top-, the side- and the bottom-position of the heating cylinder(s), the heat flux and the pressure for the boiling of distilled water, benzene and toluene. The wall temperatures and the boiling liquid-temperatures are corresponding to the values of the e.m.f. as measured by the thermocouples.

#### 6.1 CONSTRAINTS FOR DATA ANALYSIS

In the present investigation the temperature of the outer surface of the cylinder(s) were not measured directly. In fact, the thermocouples placed in the wall thickness were employed for this purpose. Therefore, the outer surface temperatures were computed by subtracting the respective temperature drops across the wall thickness as shown in Appendix C. The longitudinal conduction of heat was neglected

since the wall thickness of the cylinder(s) was much smaller than its length.

The boiling temperatures of the liquids were found to differ from the saturation temperatures corresponding to the pressures. However, the differences were negligibly small. But measured temperatures of the boiling liquids have been used for the calculation of wall superheat and heat transfer coefficient. This was accepted in view of the unavoidable impurities present in the liquids investigated.

The wall temperatures of the heating cylinders and the temperatures of the boiling liquids were measured at three circumferential positions shown in Figure 3.6. The experimental data recorded in Appendix B show that the wall temperature varies along the circumference whereas there is no change in the liquid temperature. The Simpson rule (cf. Appendix A) was used to obtain the values of average wall temperature from the local values of wall temperature.

## 6.2 NUCLEATE POOL BOILING OF LIQUIDS ON A SINGLE HORIZONTAL HEATING CYLINDER

The following Sections discuss the surface characteristics of the heating cylinders and the effects of the parameters like heat flux, pressure and the boiling liquid on the heat transfer data from a single horizontal heating cylinder for the range of parameters given in Table 4.1. The experimental data are listed in Tables B.1 and B.2 of

Appendix B. Table B.1 lists the data points for the heat transfer from upper heating cylinder and Table B.2 from lower heating cylinder.

#### 6.2.1 SURFACE CHARACTERISTICS OF LOWER-AND UPPER-HEATING CYLINDERS

Amongst many other parameters, the surface characteristics of a heating surface plays an important role on boiling heat transfer. Due to this reason the data taken for a given heat flux, pressure and boiling liquid by different investigators differ considerably. Determination of the surface characteristics is not possible. However, the boiling heat transfer data conducted on different surfaces can establish whether the surfaces employed are identical or not. To know this for the lower and the upper heating cylinders used in the present investigation, Figures 6.1 through 6.3 were drawn. They represent the wall-temperatures at the top-, the side- and the bottom-position of the lower as well as of the upper heating cylinder for the boiling of distilled water, benzene and toluene respectively. All these plots show that for a given value of heat flux, pressure and liquid the wall temperature distribution was the same for both the cylinders. In fact, this is possible when the surface characteristics of them are the same. Thus, both the cylinders employed in present investigation were of identical surface characteristics. Therefore, to account the effects of heat flux, pressure and the liquid on the

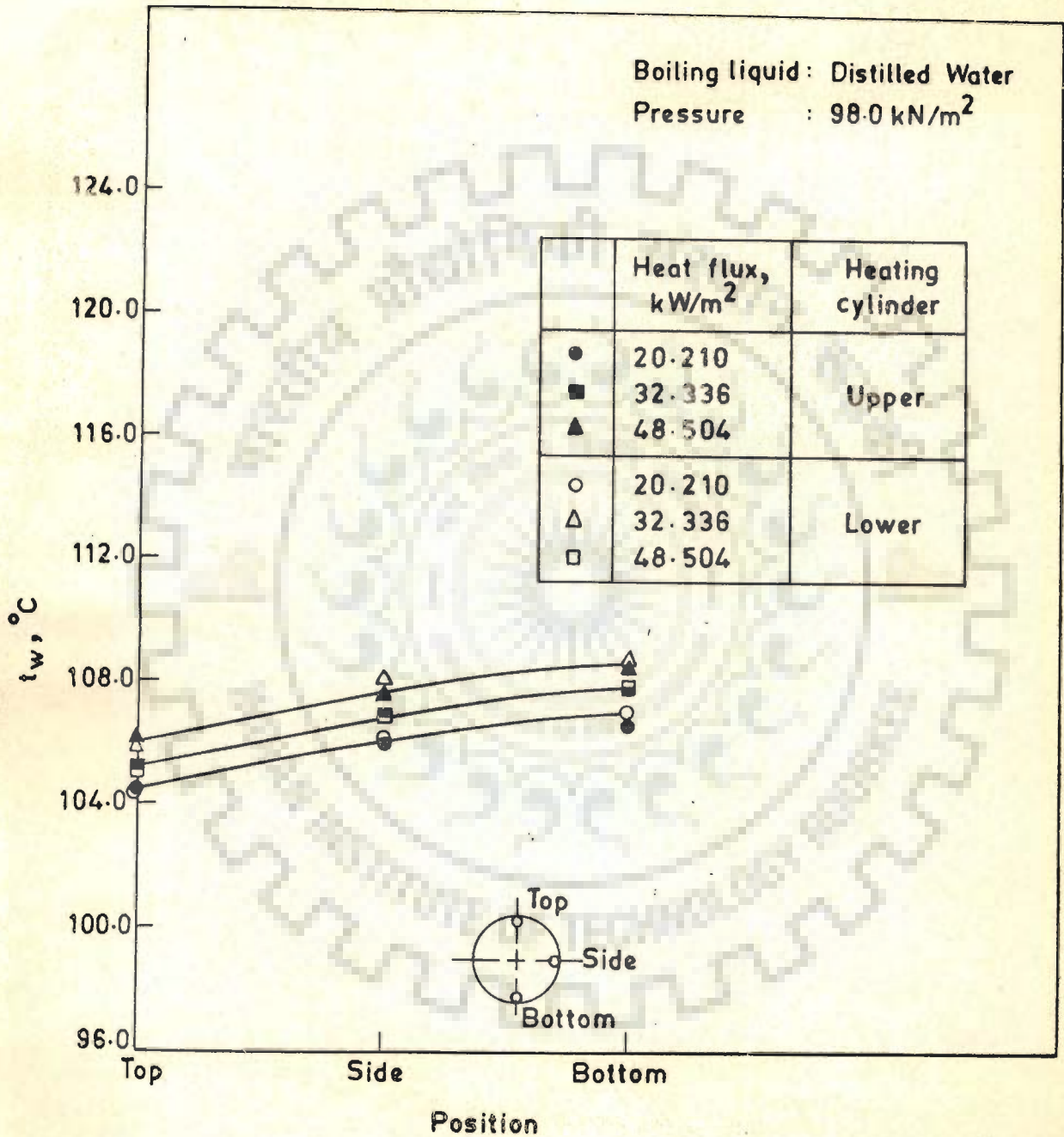


Fig 6.1 Circumferential wall temperature distribution for the upper and lower heating cylinders



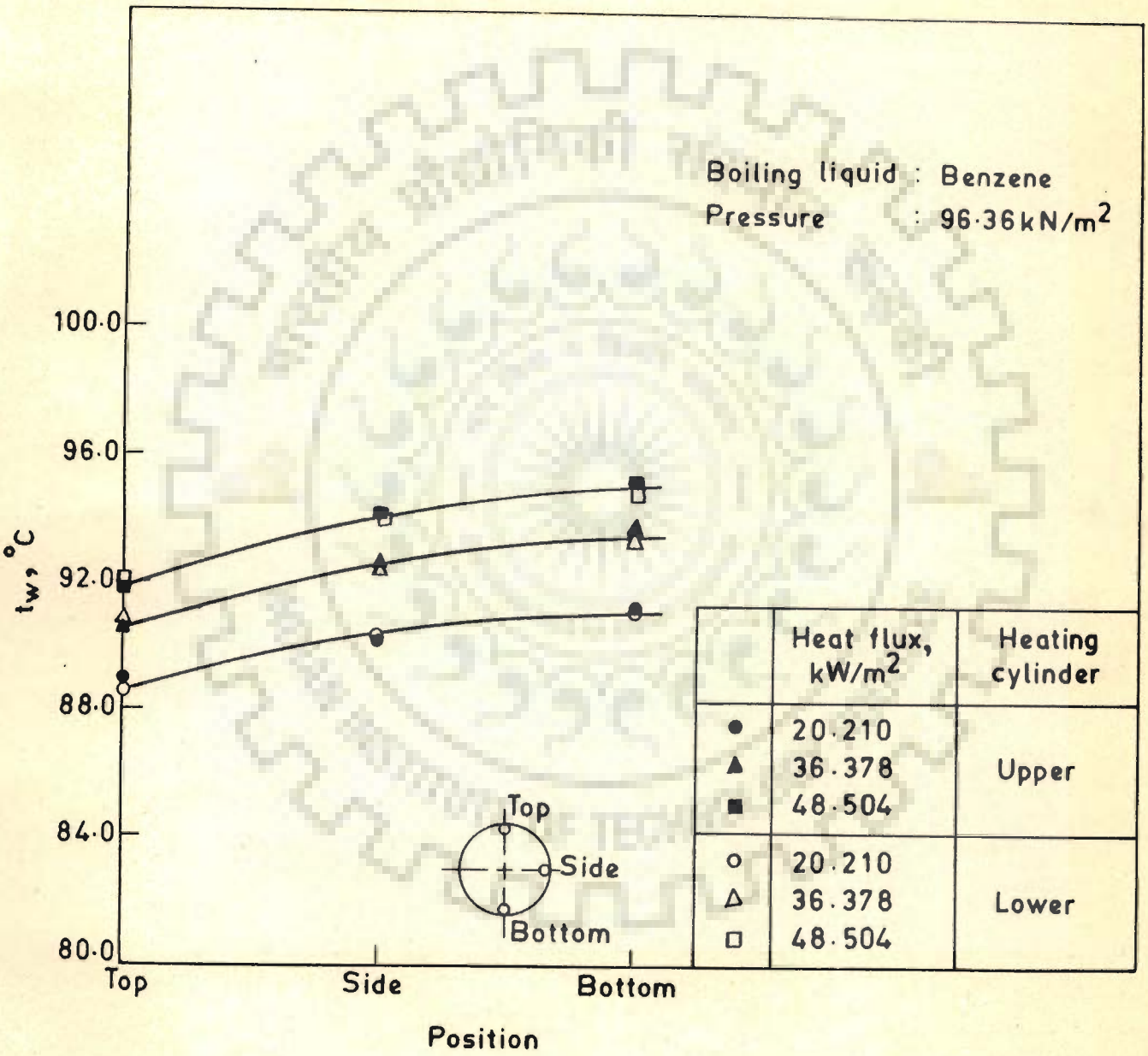


Fig 6.2 Circumferential wall temperature distribution for the upper and lower heating cylinders

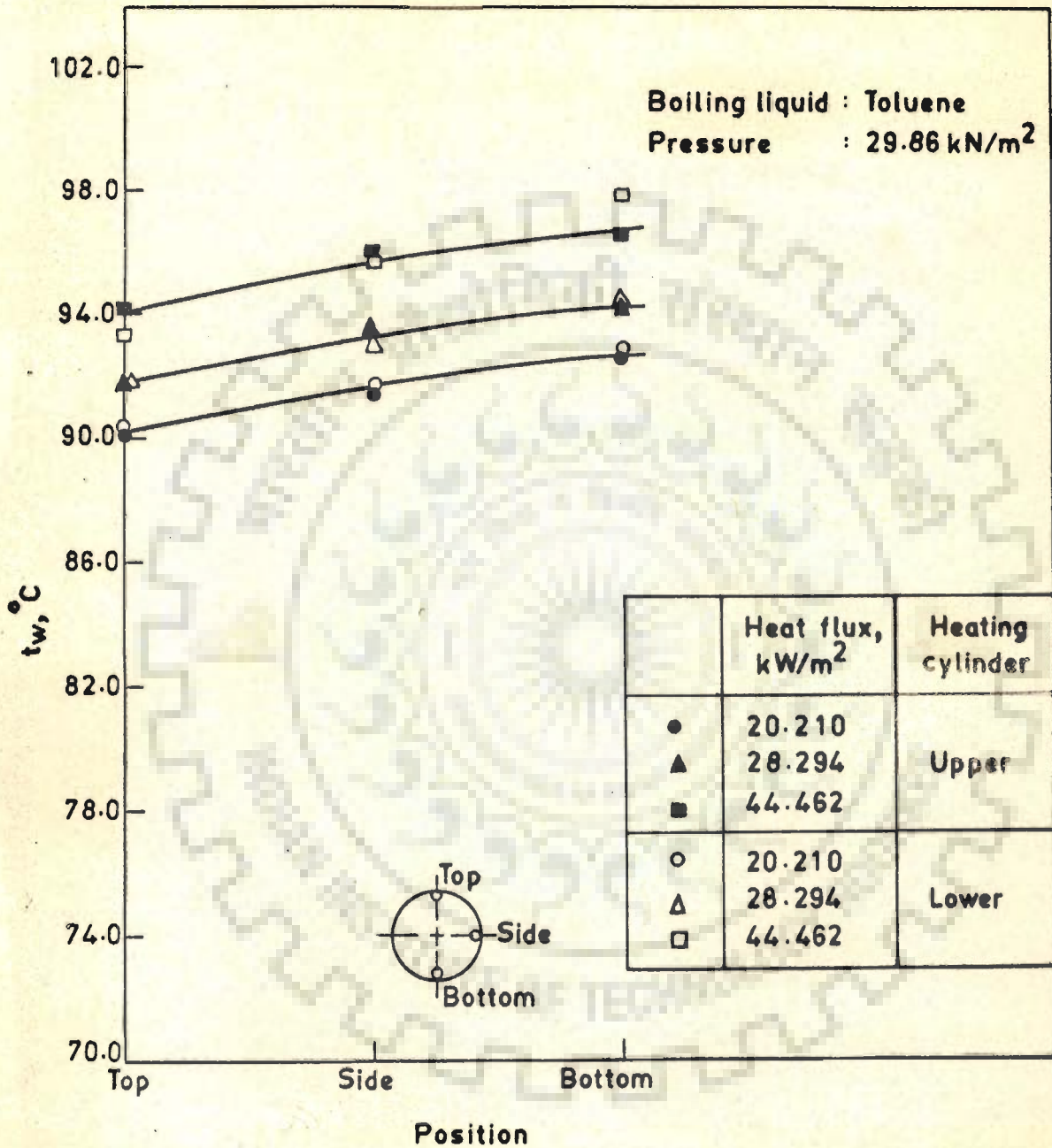


Fig 6.3 Circumferential wall temperature distribution for the upper and lower heating cylinders

boiling heat transfer from a single heating cylinder, it was sufficient to analyse the data for any of the heating cylinders. For this the data for the upper heating cylinder shown in Table B.1 of Appendix B were processed in the subsequent Sections.

#### 6.2.2 EFFECT OF HEAT FLUX ON WALL- AND LIQUID-TEMPERATURE DISTRIBUTION AROUND THE HEATING CYLINDER

Figure 6.4 is a typical plot showing the wall-temperature distribution along the circumference of the heating cylinder with heat flux as a parameter for the pool boiling of distilled water at a pressure of  $98.00 \text{ kN/m}^2$ . The liquid-temperatures for the corresponding surface positions are also shown in this plot. An examination of this plot reveals the following :

1. The wall-temperature increases continuously from the top- to the side- to the bottom- position of the heating cylinder for a given heat flux. With the increase in heat flux the curve shifts to the left indicating that the wall-temperature for a given position increases with the heat flux.
2. The liquid-temperature does not change with respect to the position around the heating cylinder.

Figures 6.5 and 6.6 also exhibit the same aforesaid characteristic features for the boiling of benzene and toluene respectively.

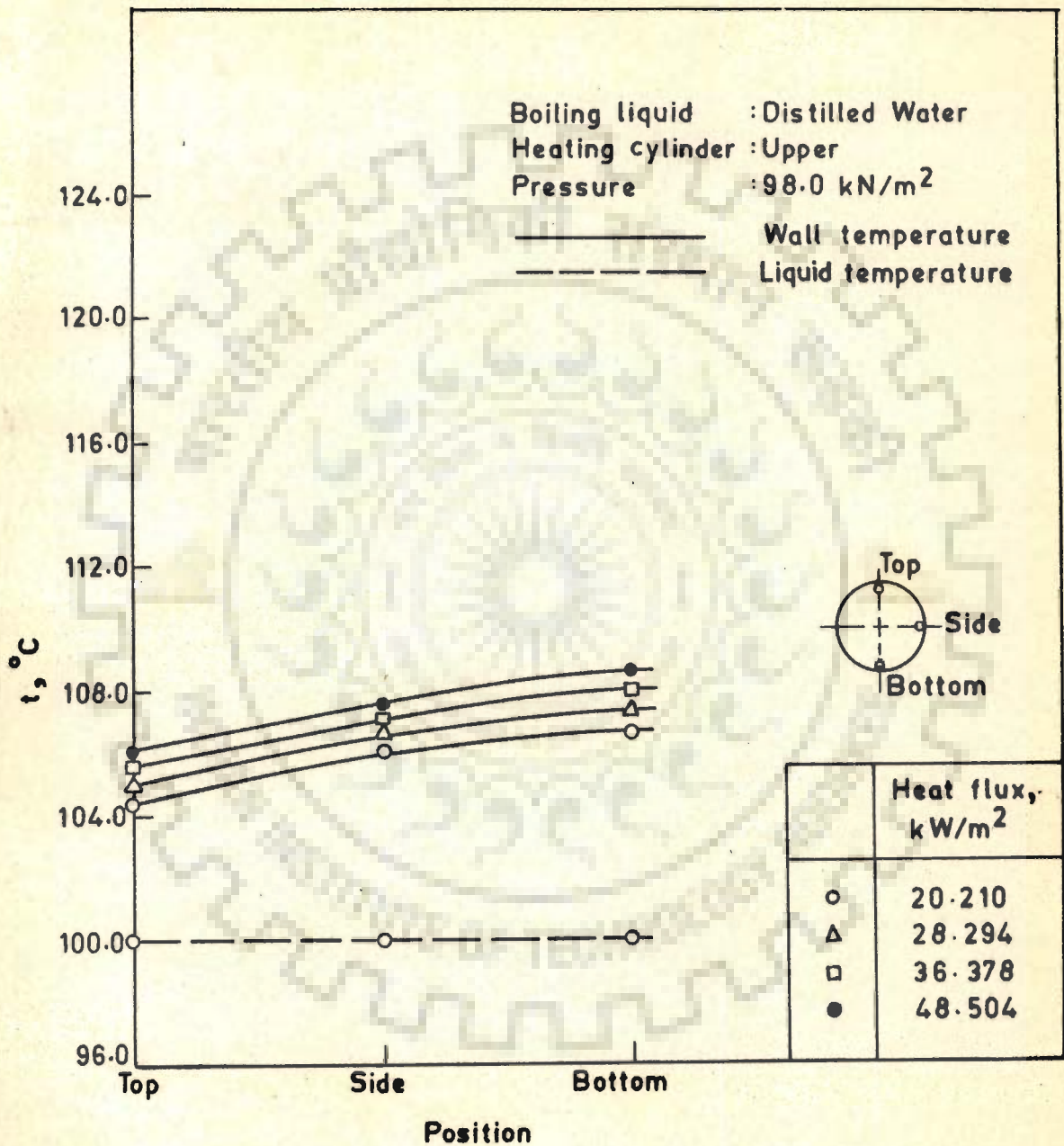


Fig 6.4 Effect of heat flux on wall and liquid temperature distribution around the heating cylinder

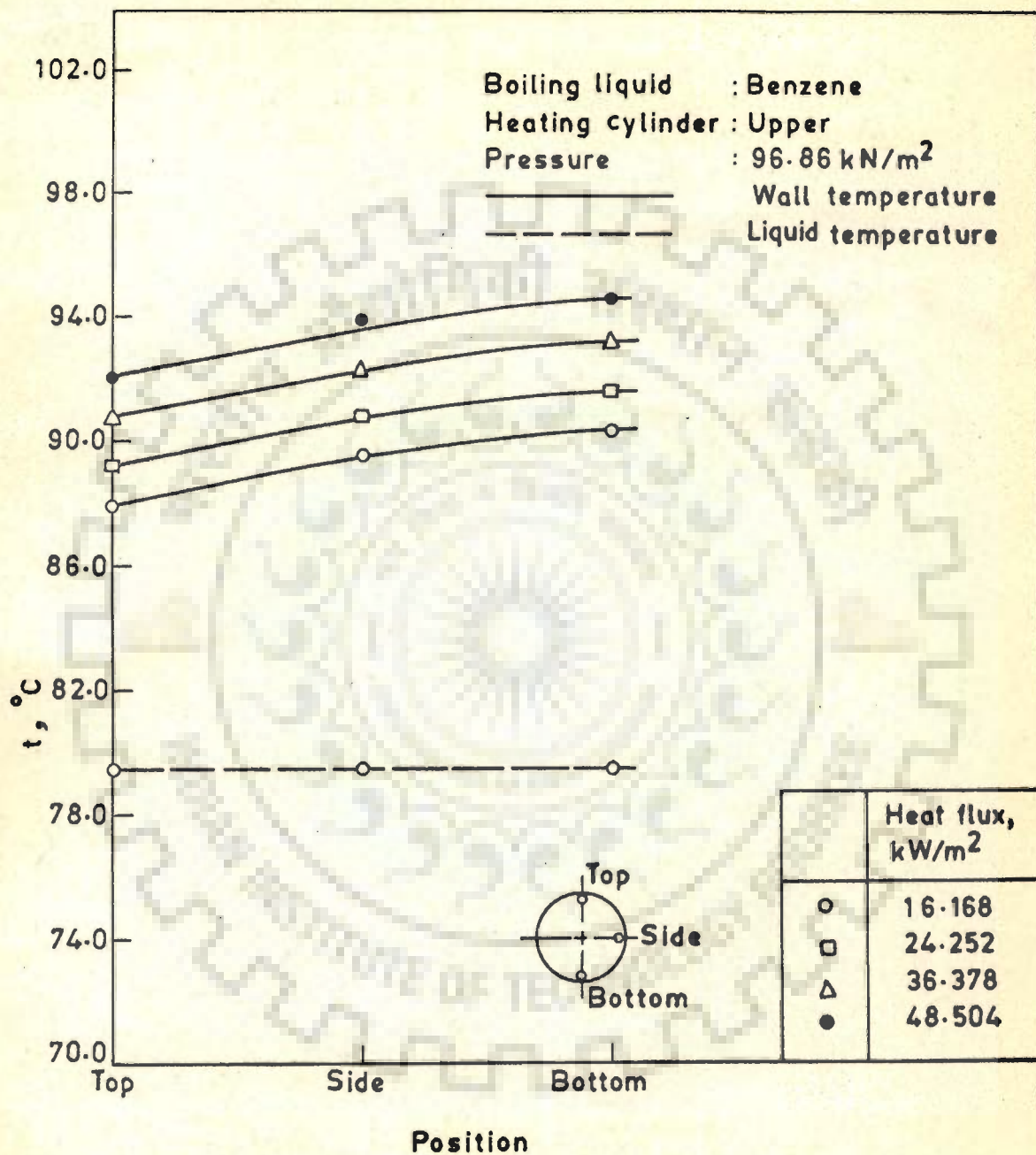


Fig 6.5 Effect of heat flux on wall and liquid temperature distribution around the heating cylinder

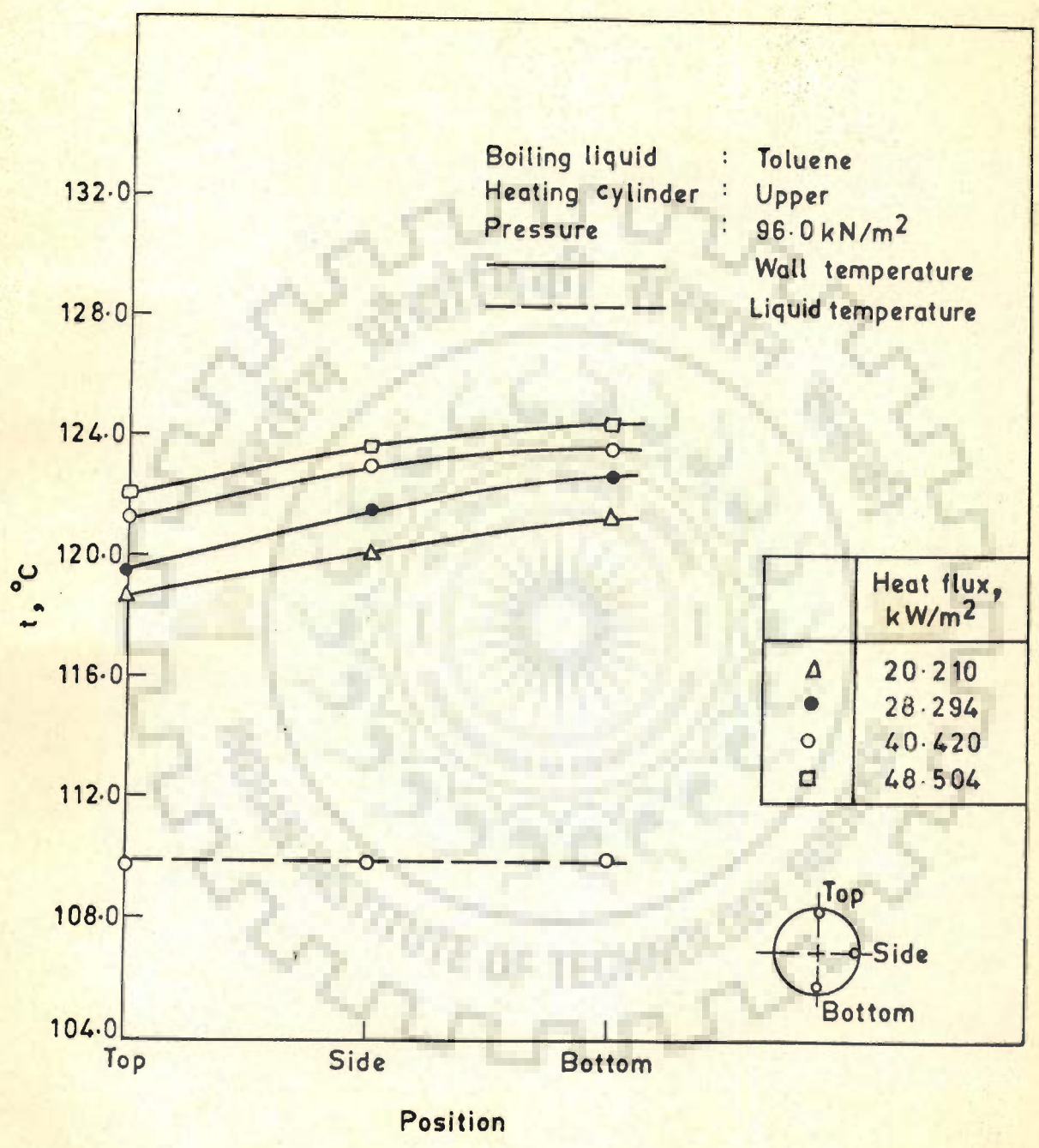


Fig 6.6 Effect of heat flux on wall and liquid temperature distribution around the heating cylinder

The behaviour of the above plots can be explained as follows :

At a given value of heat flux and the pressure the access of the vapour bubbles for their free movement in the pool of the liquid is the largest at the top- , less at the side- and the least at the bottom- position of the heating cylinder. As a consequence of it, the magnitude of the turbulence induced by the vapour bubble dynamics decreases regularly from the top- to the side- to the bottom- position. Therefore, for an electrically heated cylinder ( $q=\text{constant}$ ) the wall temperature increases from the top- to the side- to the bottom- position.

As regards the increase in wall-temperature with the heat flux one can argue as follows : It is a known fact that due to the increase in heat flux the number of nucleation sites for vapour bubble formation increases. This, in fact, is possible only when the temperature of the heating cylinder increases for a given pressure, liquid and the surface characteristics.

### 6.2.3 EFFECT OF PRESSURE ON WALL-TEMPERATURE DISTRIBUTION AROUND THE HEATING CYLINDER

Figure 6.7 represents the wall-temperature distribution along the circumference for the boiling of distilled water on the upper heating cylinder for a heat flux of  $20.210 \text{ kW/m}^2$  with pressure as a parameter. This plot shows the following characteristic features :

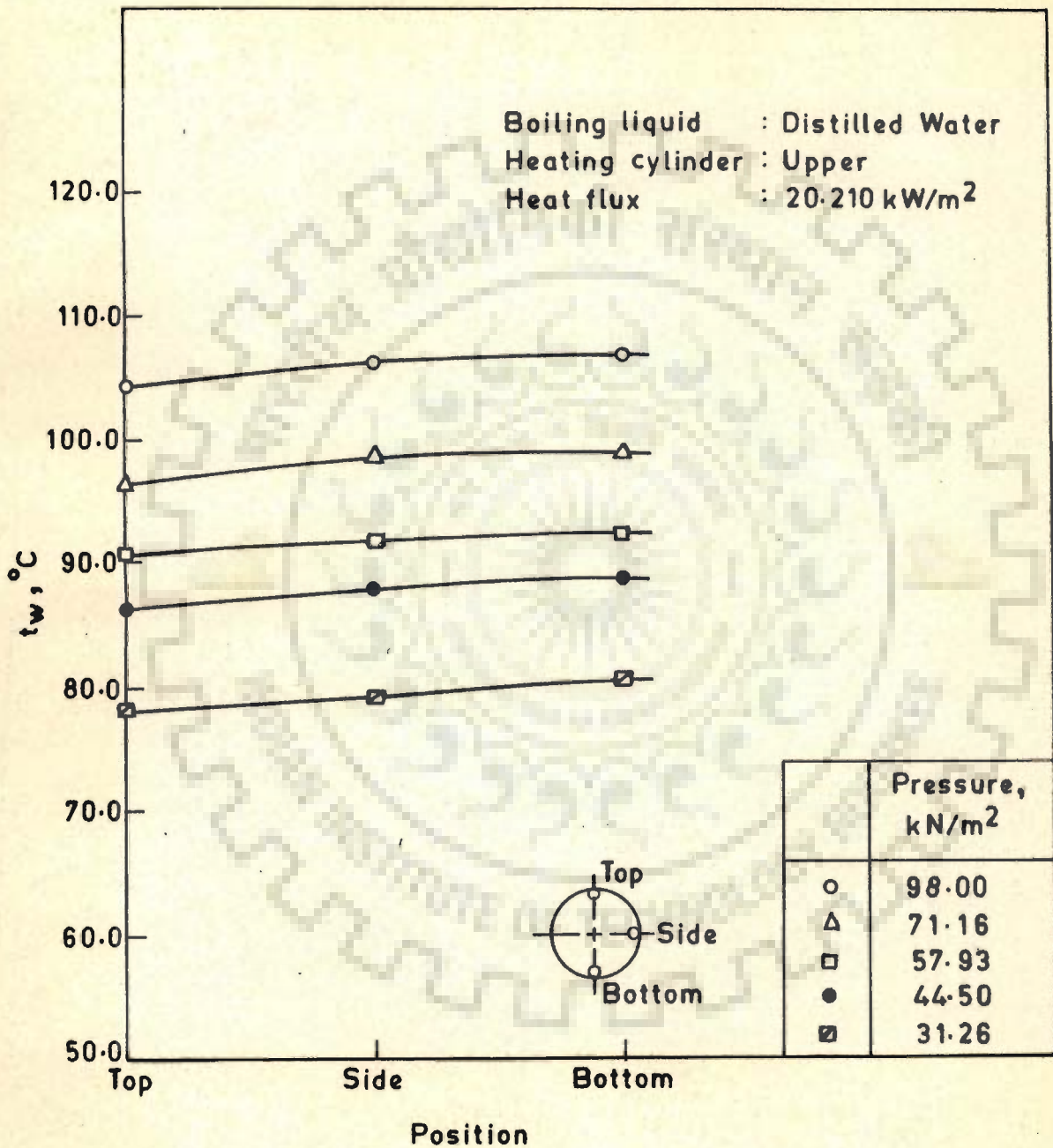


Fig 6.7 Effect of pressure on wall temperature distribution along the circumference of the heating cylinder



1. At a given pressure the wall-temperature increases regularly from the top- to the side- to the bottom- position.
2. An increase in pressure shifts the curve to the left indicating that wall-temperature at all the positions increases with the increase in pressure.

Figures 6.8 and 6.9 are the similar plots for the boiling of benzene and toluene respectively for a heat flux of  $20.210 \text{ kW/m}^2$ . These figures also exhibit the same behaviour as that of Figure 6.7 indicating that the pressure has the same effect on the boiling of benzene and toluene also.

The increase in wall-temperature from the top- to the side- to the bottom- position for a given pressure and heat flux is attributed to the same fact as under Section 6.2.2.

#### 6.2.4 EFFECT OF BOILING LIQUIDS ON WALL-TEMPERATURE DISTRIBUTION AROUND THE HEATING CYLINDER

Figure 6.10 shows the effect of the boiling liquids on the wall-temperature distribution. For this the data for the boiling of distilled water, benzene and toluene at a heat flux of  $20.210 \text{ kW/m}^2$  and atmospheric pressure were considered. From this plot the following is noted :

The wall temperature distribution curve for the boiling of distilled water lies between those for toluene and benzene. Further, they are separated apart considerably. This, in fact is due to the

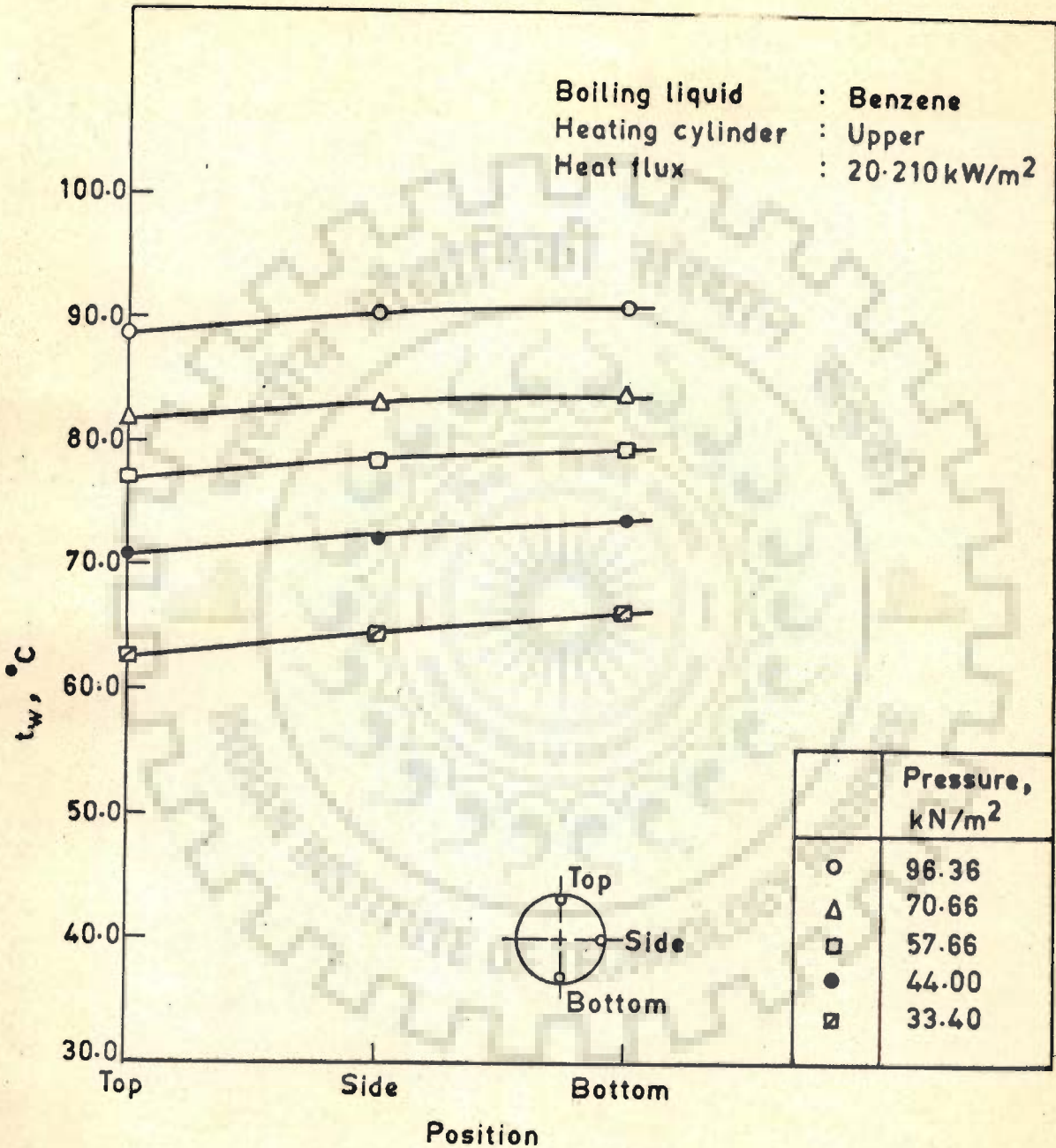


Fig 6.8 Effect of pressure on wall temperature distribution along the circumference of the heating cylinder

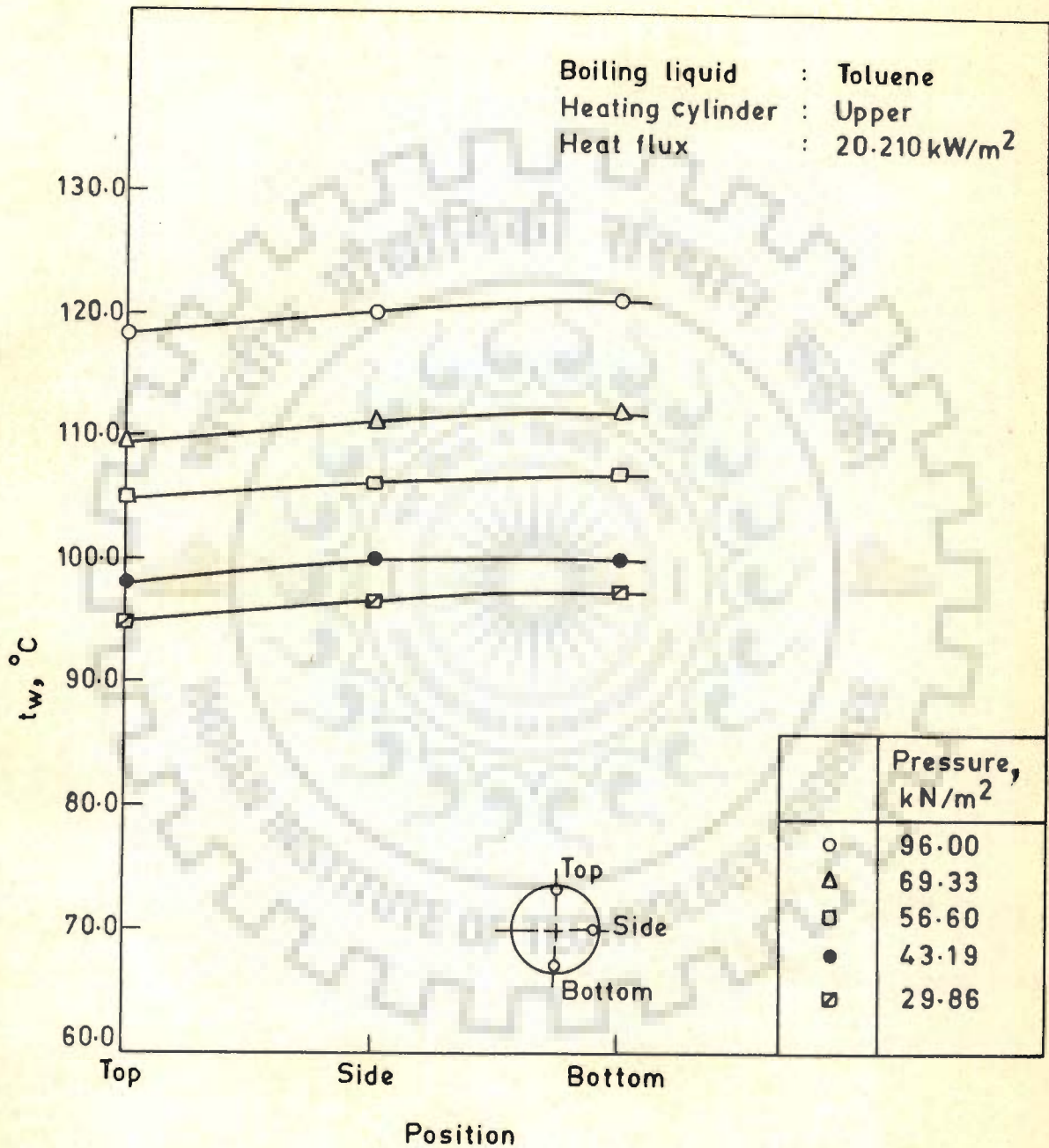


Fig 6.9 Effect of pressure on wall temperature distribution along the circumference of the heating cylinder

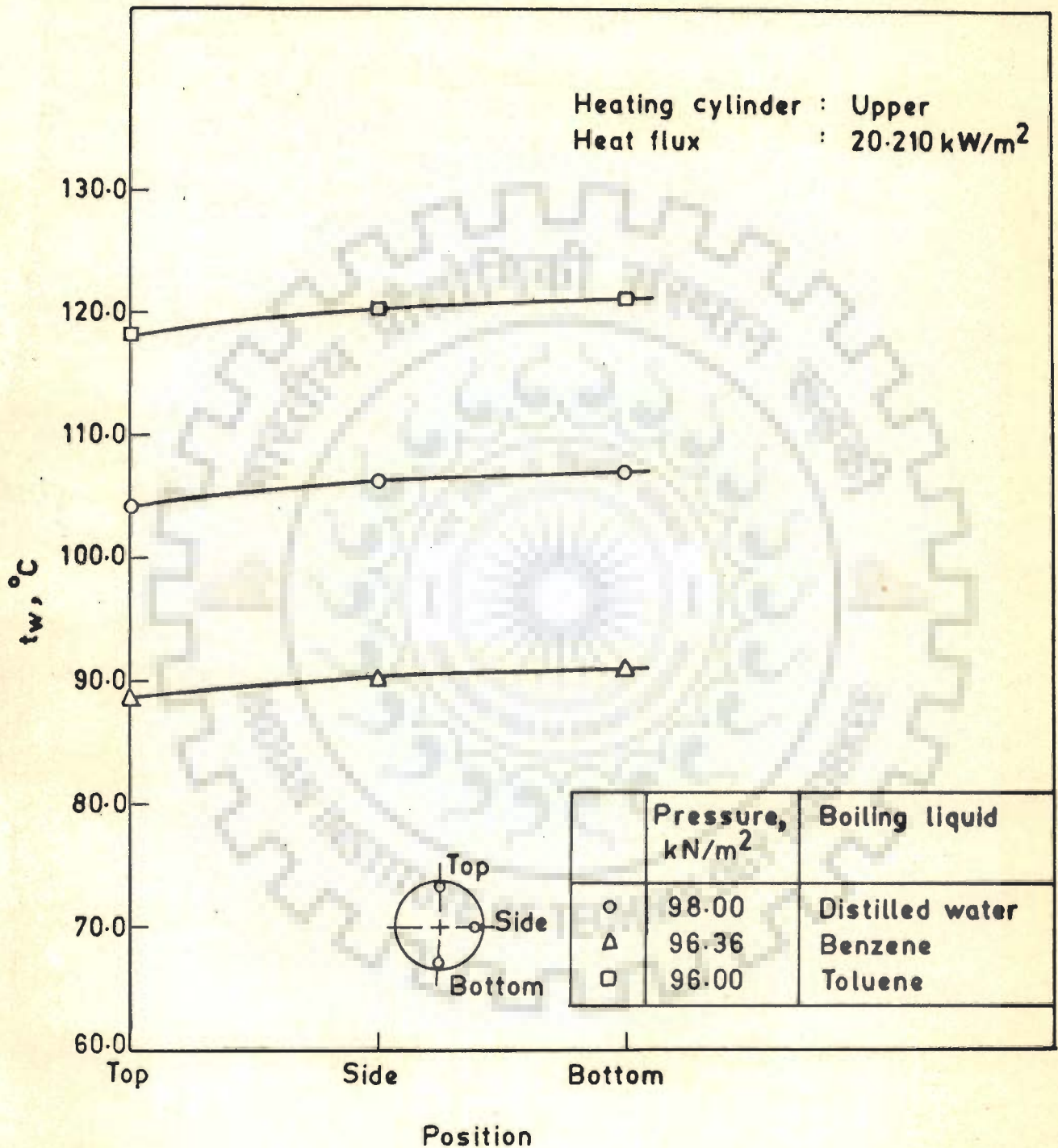


Fig 6.10 Effect of boiling liquids on wall temperature distribution along the circumference of the heating cylinder

differing physico-thermal properties of these liquids.

#### 6.2.5 EFFECT OF HEAT FLUX ON LOCAL WALL SUPERHEAT

Figures 6.11 through 6.13 represent the replot of Figures 6.4 to 6.6 to show the variation of wall superheat with circumferential position on the heating cylinder. These plots demonstrate the following characteristic features :

1. For a given pressure, the wall superheat increases regularly from the top- to the side- to the bottom- position of the cylinder proving that the turbulence induced due to the vapour bubble dynamics decreases from the top- to the side- to the bottom- position.
2. An increase in heat flux does not change the nature of the curve but shifts it to the left indicating that the wall superheat at a given circumferential position increases with the heat flux. But the increase in the wall superheat is not proportional to the increase in the heat flux suggesting that the turbulence induced due to the boiling process increases with heat flux.

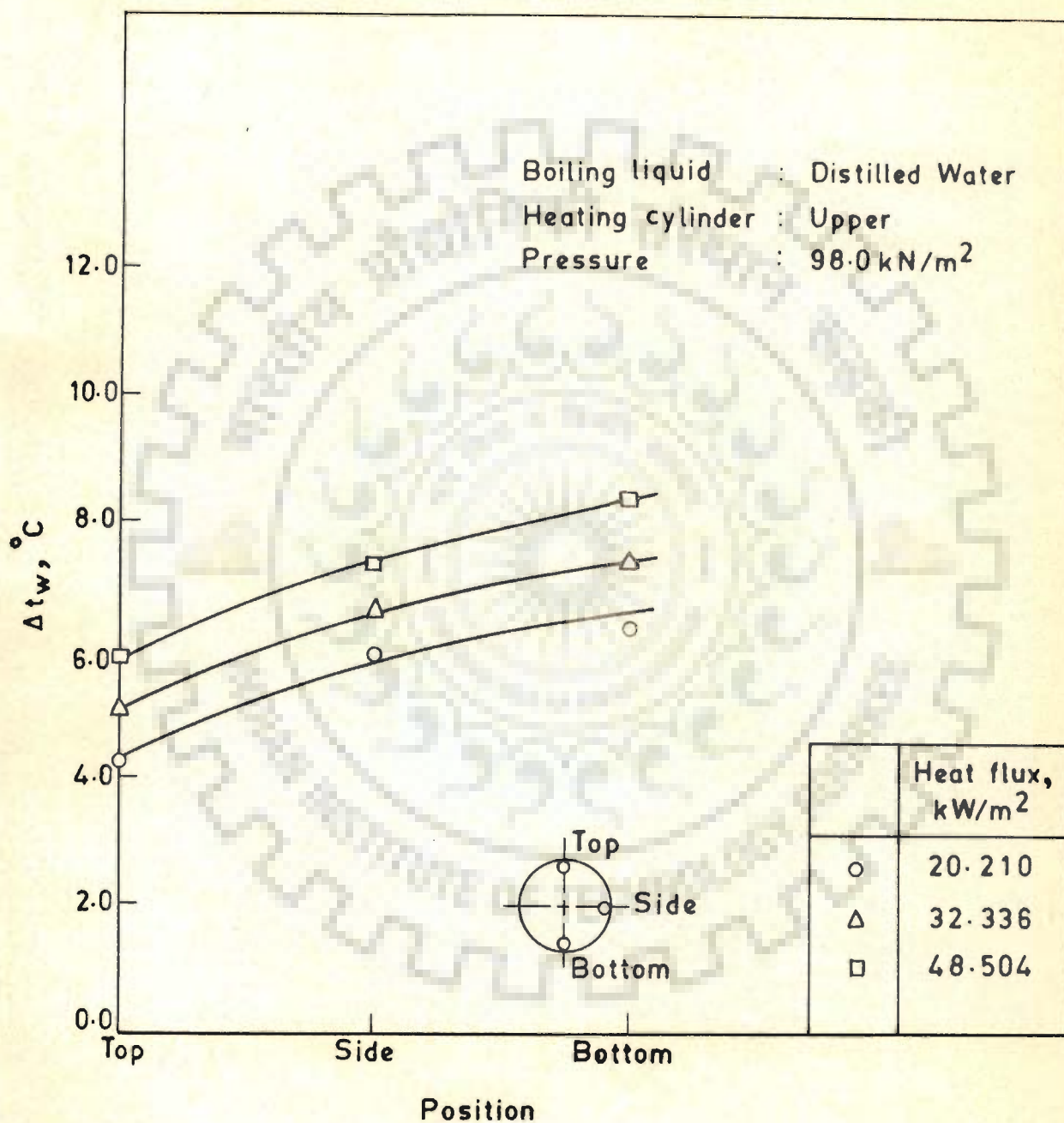


Fig 6.11 Effect of heat flux on wall superheat distribution along the circumference of the heating cylinder

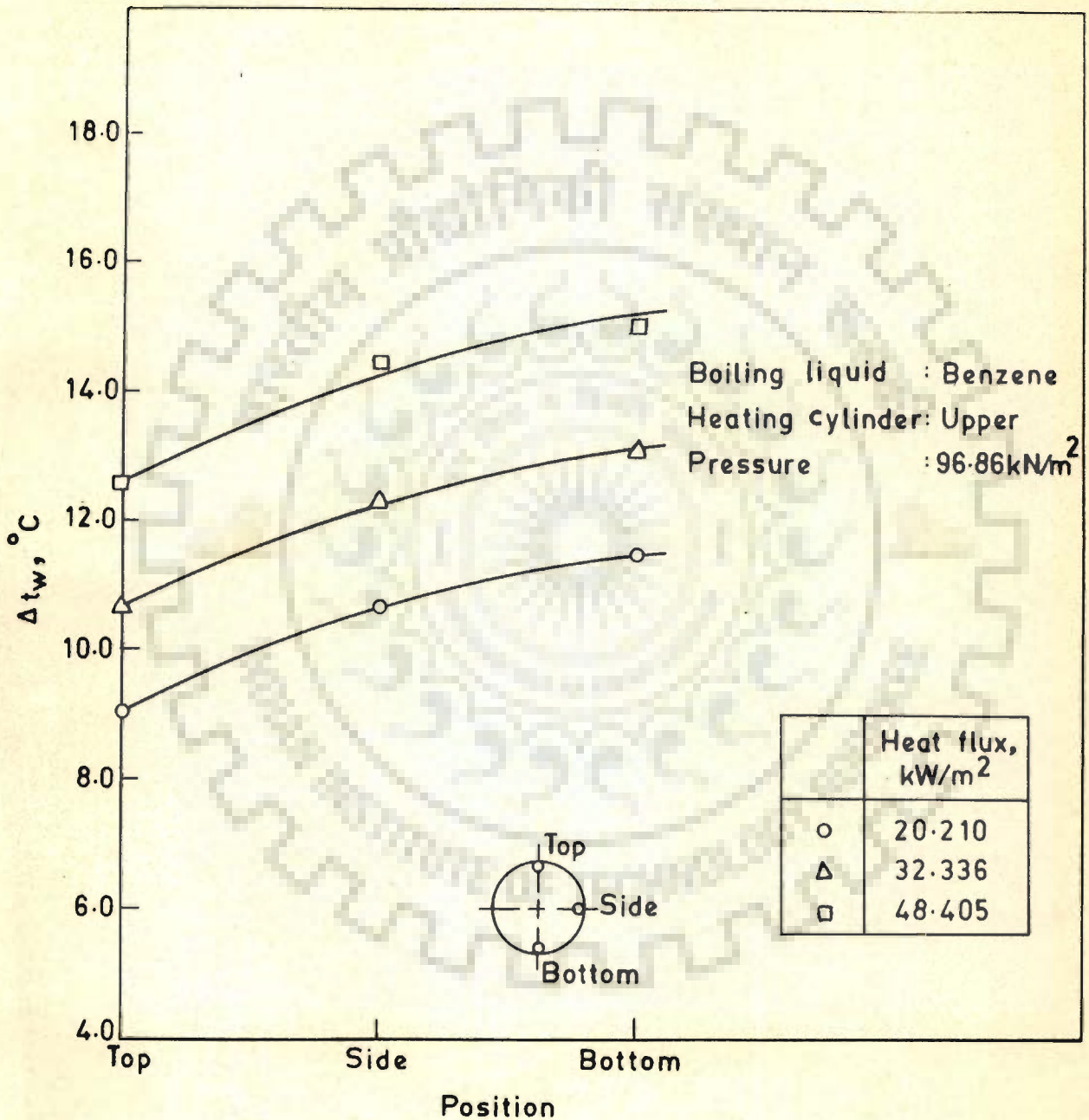


Fig 6-12 Effect of heat flux on wall superheat distribution along the circumference of the heating cylinder

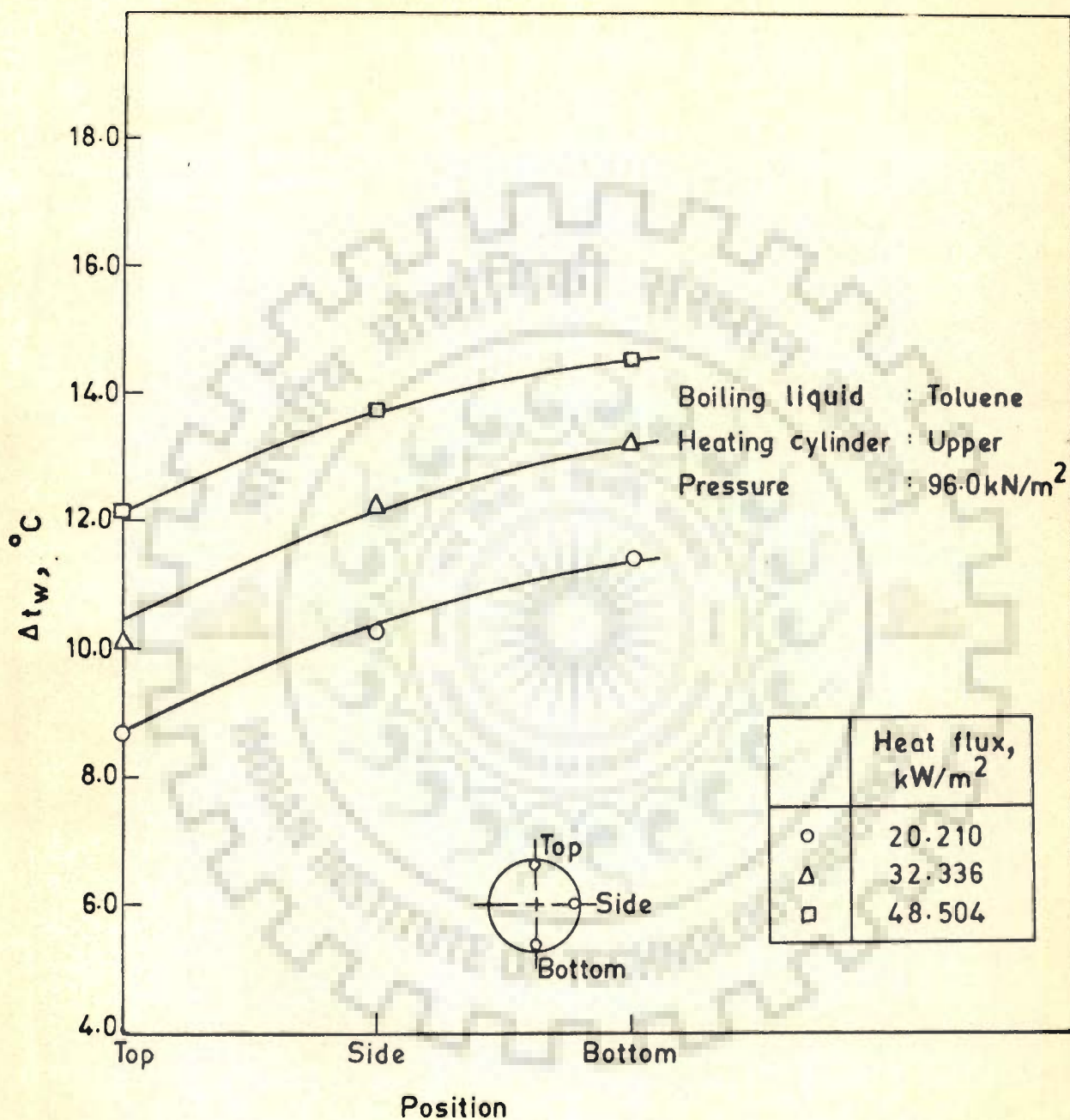


Fig 6.13 Effect of heat flux on wall superheat distribution along the circumference of the heating cylinder .



### 6.2.6 EFFECT OF PRESSURE ON LOCAL WALL SUPERHEAT

Figure 6.14 shows the distribution of local wall superheat for the boiling of distilled water at a heat flux of  $48.504 \text{ kW/m}^2$  with pressure as a parameter. This plot reveals the following :

At a given pressure the wall superheat increases regularly from the top- to the side- to the bottom-position. However, the curve shifts to the right with the increase in pressure indicating that wall superheat decreases with the increase in pressure.

The decrease in wall superheat with increase in pressure is attributed to the following :

The surface tension of the boiling liquid decreases considerably with the increase in pressure, thereby on a given heating surface the number of bubble nucleation sites rises which, in turn, causes more induced turbulence. Thus the value of wall superheat falls.

Figure 6.15 and 6.16 are the typical plots which possess the trend similar to that of Figure 6.14 for the boiling of benzene and toluene at a heat flux of  $48.504 \text{ kW/m}^2$  and  $24.252 \text{ kW/m}^2$  respectively with pressure as a parameter.

It is important to recall here the result of Figures 6.7 to 6.9 that the temperature increases with the increase in pressure while Figures 6.14 through 6.16 suggest that the wall superheat,  $(t_w - t_s)$  decreases with the increase in pressure. It is due to the fact that the saturation temperature of the liquid,  $t_s$  also increases with the increase in

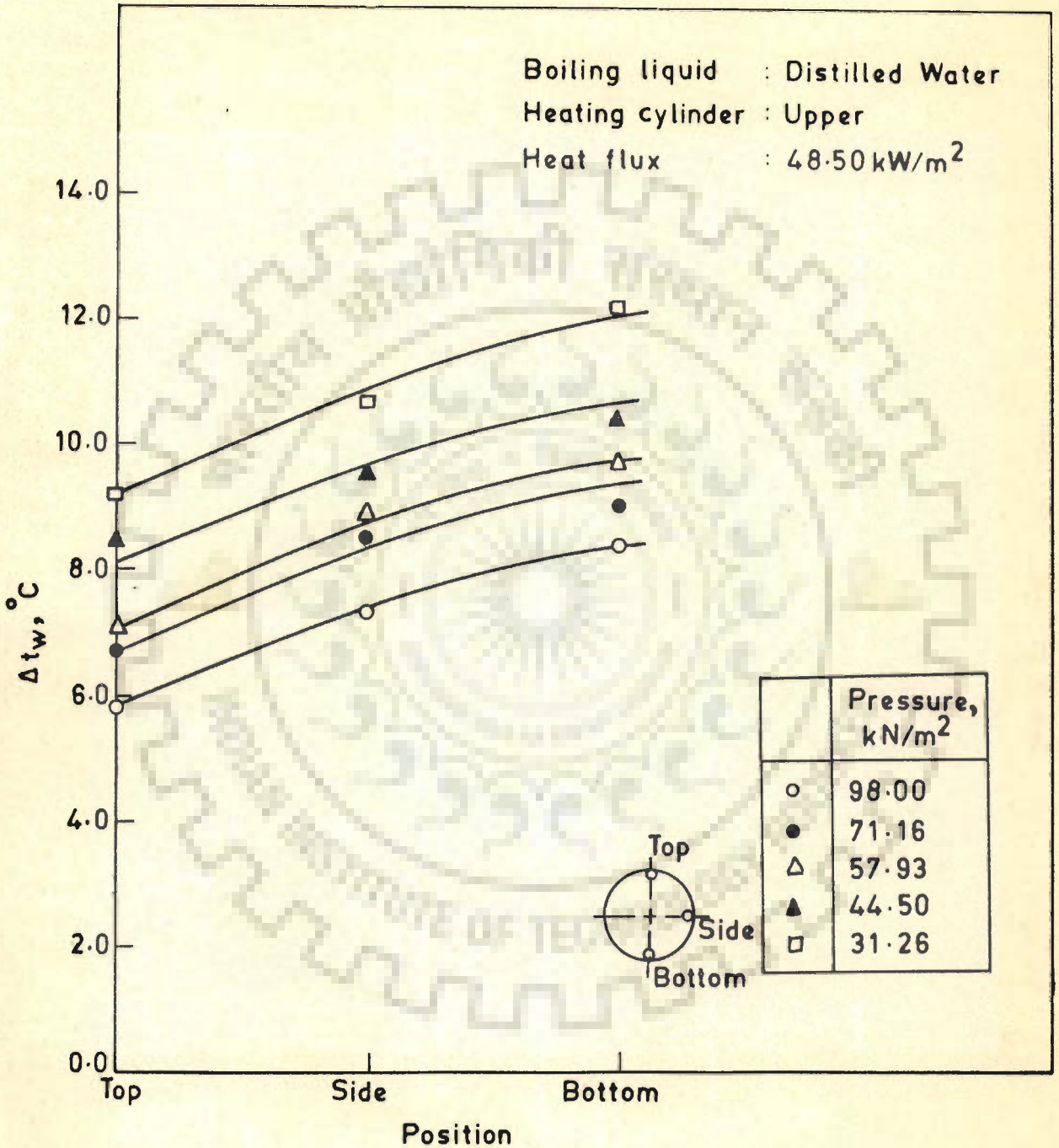


Fig 6.14 Effect of pressure on wall superheat distribution along the circumference of the heating cylinder

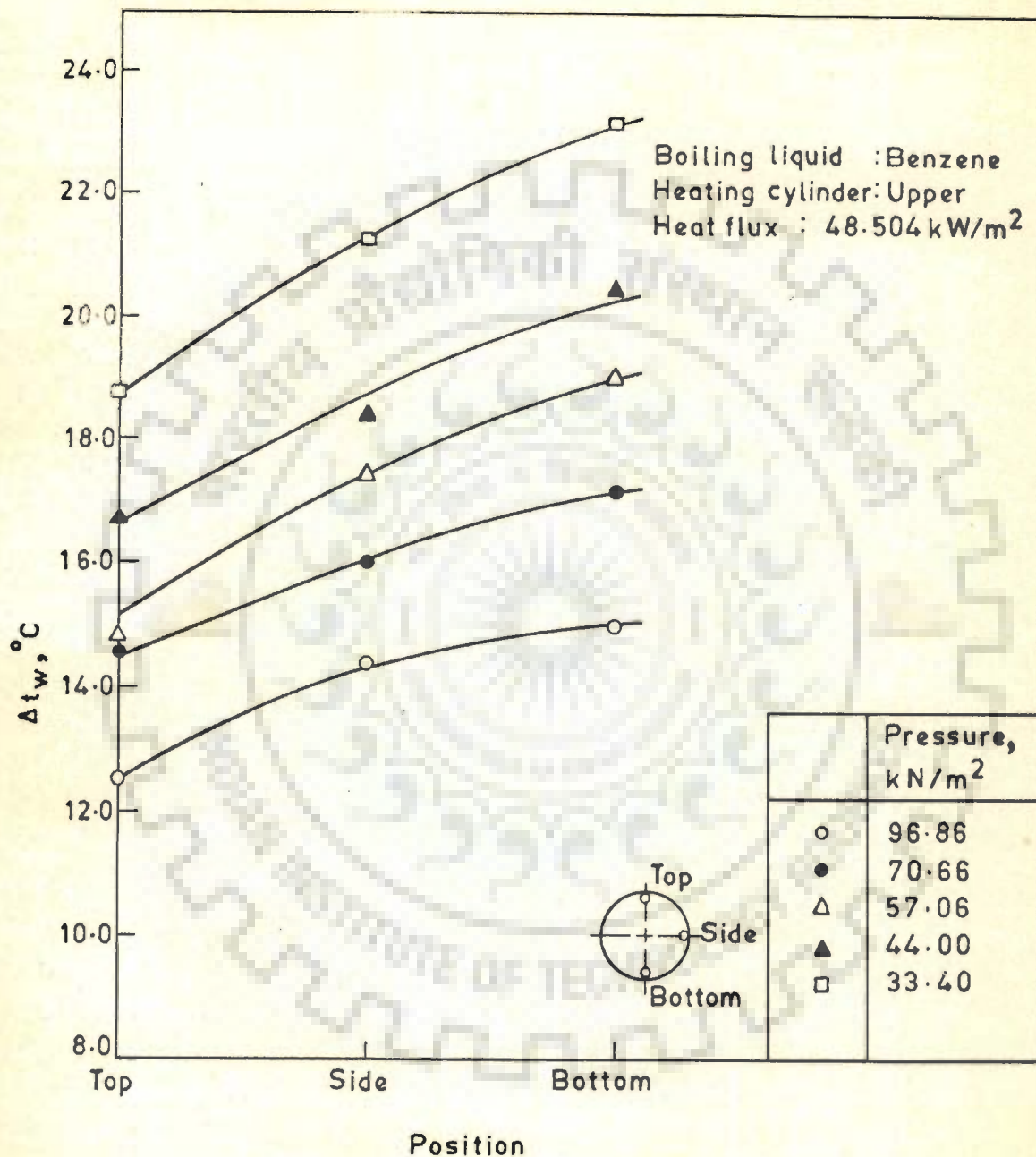


Fig 6.15 Effect of pressure on wall superheat distribution along the circumference of the heating cylinder

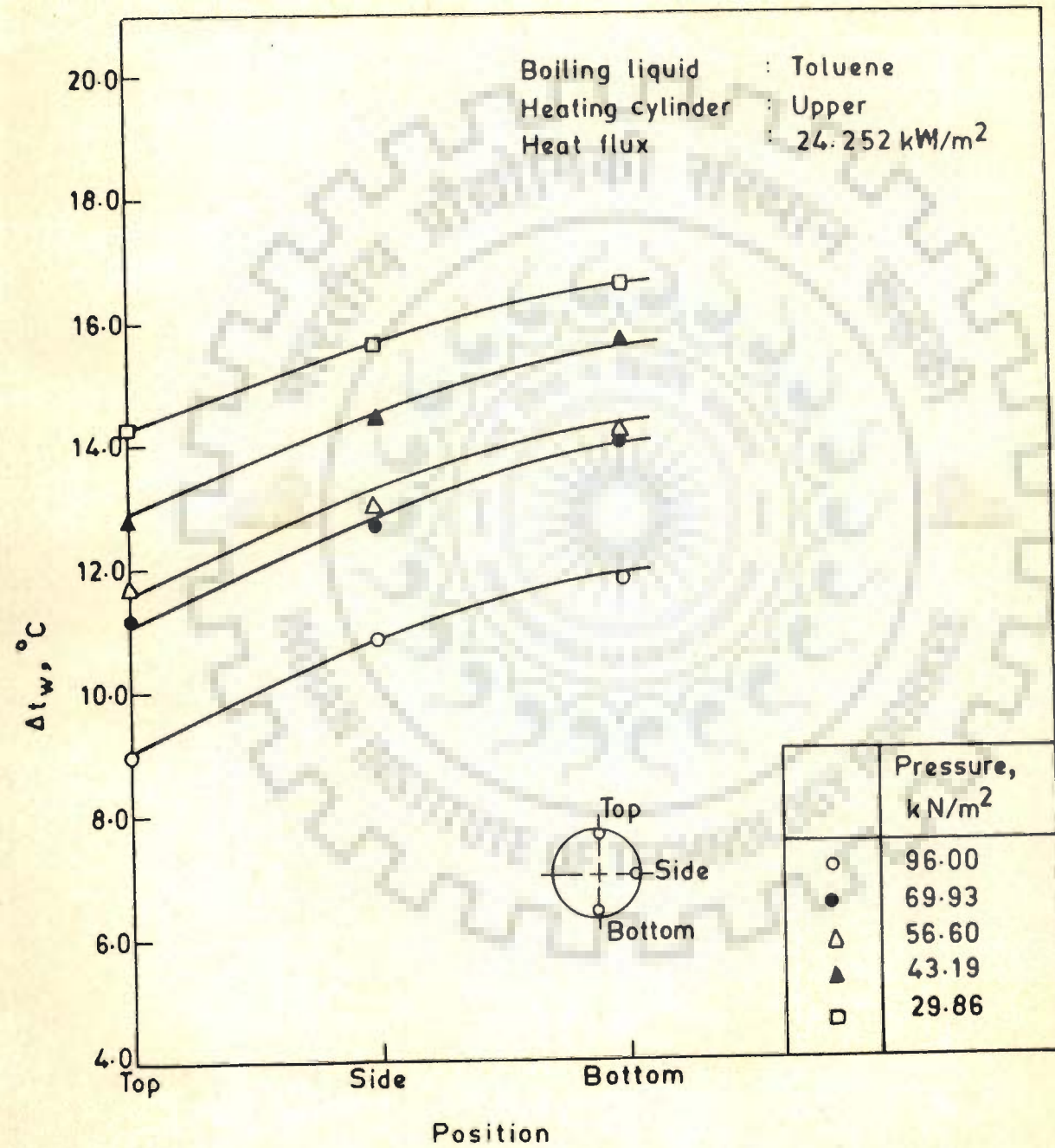


Fig 6.16 Effect of pressure on wall superheat distribution along the circumference of the heating cylinder

pressure. But the increase in liquid-temperature,  $t_s$  is more than the increase in wall-temperature,  $t_w$ . Therefore the wall superheat,  $(t_w - t_s)$  decreases with rise in pressure.

#### 6.2.7 EFFECT OF BOILING LIQUID ON LOCAL WALL SUPERHEAT

Figure 6.17 represents a typical plot of wall superheat at the top-, the side- and the bottom- position for the boiling of distilled water, benzene and toluene at a heat flux of  $20.210 \text{ kW/m}^2$  and atmospheric pressure. This plot has three distinct curves each representing a particular liquid. The upper, middle and lower curves are for benzene, toluene and distilled water respectively. It is important to mention here as shown in Figure 6.10 that the wall-temperature for benzene at a circumferential position was minimum while the wall superheat is maximum. This clearly indicates that the wall superheat depends upon the pertinent physico-thermal properties of the boiling liquids.

#### 6.2.8 AVERAGE WALL SUPERHEAT

The corrected values of the local wall-temperature at the top-, at the side- and at the bottom- position were averaged by the use of Eq (A.8) of Appendix A. The average liquid-temperature was subtracted from the average wall-temperature to obtain the average wall superheat. This was calculated for all the values of heat flux, pressure and all the liquids investigated. The following Sections discuss the effects of heat flux and pressure on the average wall superheat.

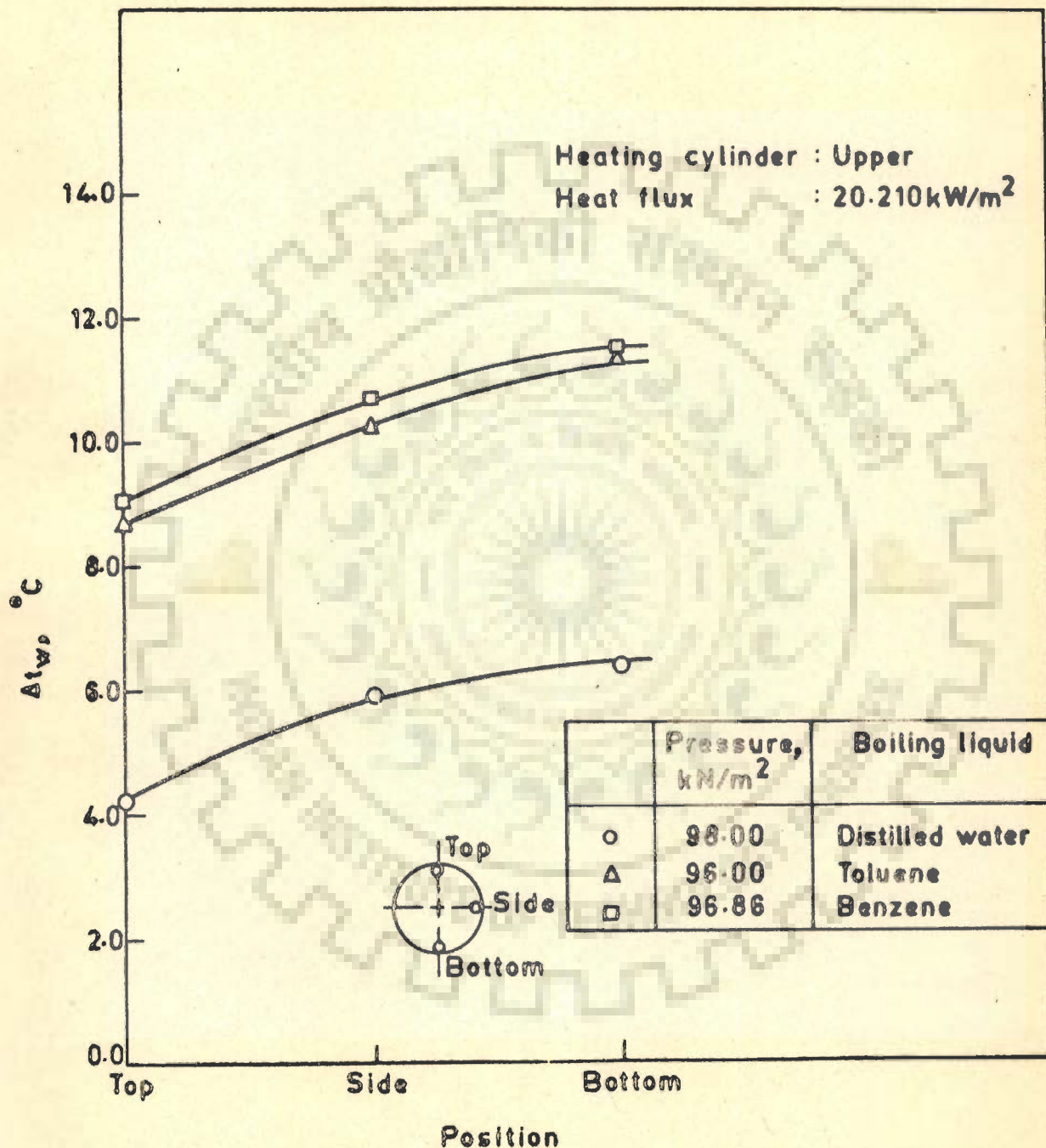


Fig 6-17 Effect of boiling liquids on wall superheat distribution along the circumference of the heating cylinder

### 6.2.9 EFFECT OF HEAT FLUX ON AVERAGE WALL SUPERHEAT

Figure 6.18 shows the relationship between average wall superheat and heat flux on a log-log plot for the boiling of distilled water with pressure as a parameter. An inspection of this plot demonstrates the following characteristic features :

1. The value of average wall superheat,  $\Delta \bar{t}_w$  increases with the rise in heat flux,  $q$  in accordance with the following mathematical relationship:

$$\Delta \bar{t}_w = C_1 q^{0.3} \quad \dots(6.1)$$

2. An increase in pressure shifts the line to the right indicating that for a given heat flux the value of  $\Delta \bar{t}_w$  decreases with the rise in pressure. As a matter of fact, the constant  $C_1$  of Eq (6.1) depends upon the pressure for a given liquid and heating cylinder.

Figures 6.19 and 6.20 contain the experimental data for the boiling of benzene and toluene respectively. It is seen that these figures also possess the same characteristic behaviour as that of Figure 6.18.

CENTRAL LIBRARY UNIVERSITY OF BOHOKI  
ADDIS ABABA

To ascertain the dependency of constant,  $C_1$  of Eq (6.1) on the boiling liquid, Figure 6.21 was drawn which is a typical plot containing the experimental data for distilled water, benzene and toluene at atmospheric pressure. The plot suggests that the data points for the boiling of these liquids are represented by different straight lines having the same slope

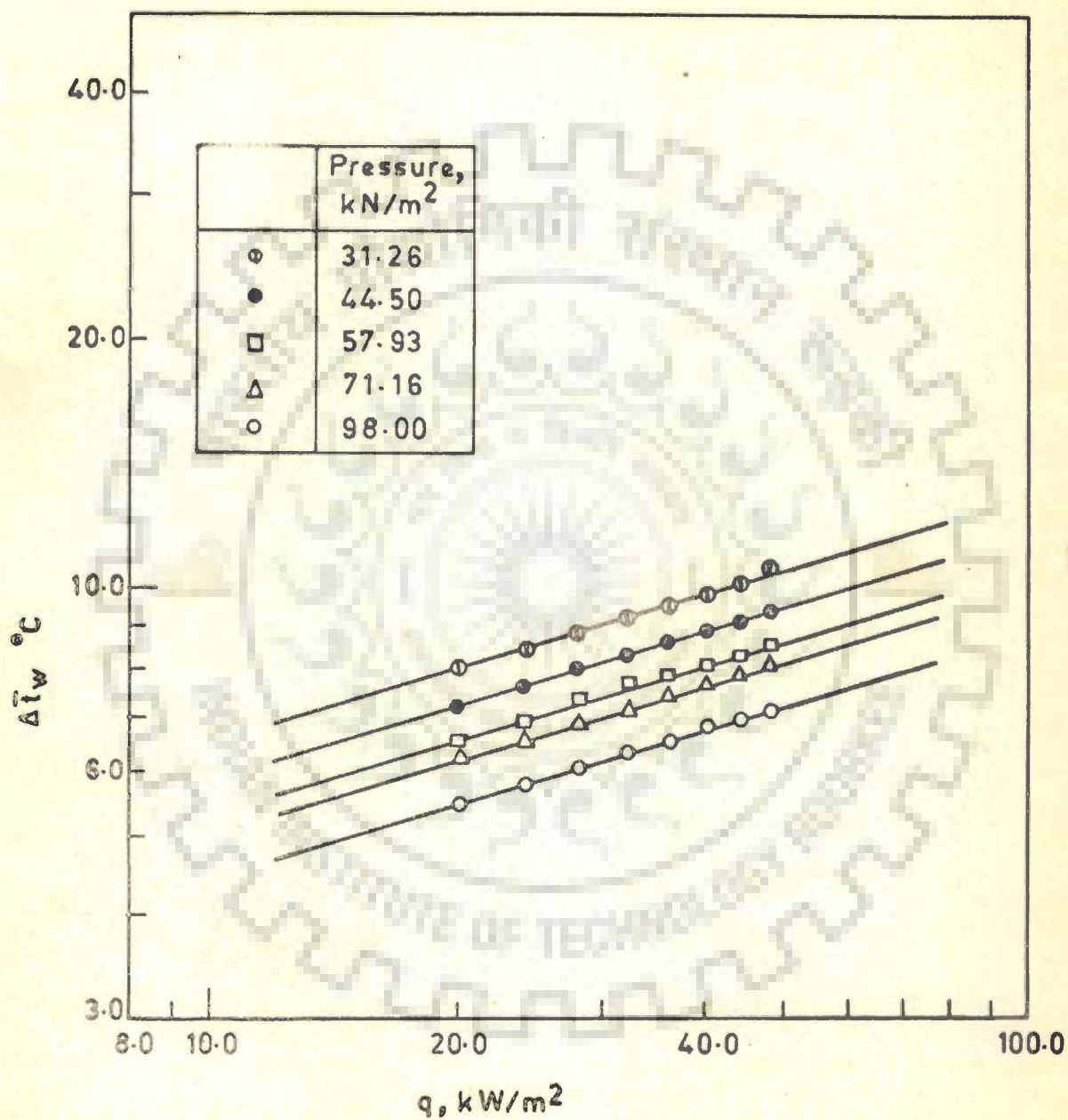


Fig 6-18 Variation of average wall superheat with heat flux for the boiling of distilled water on upper heating cylinder



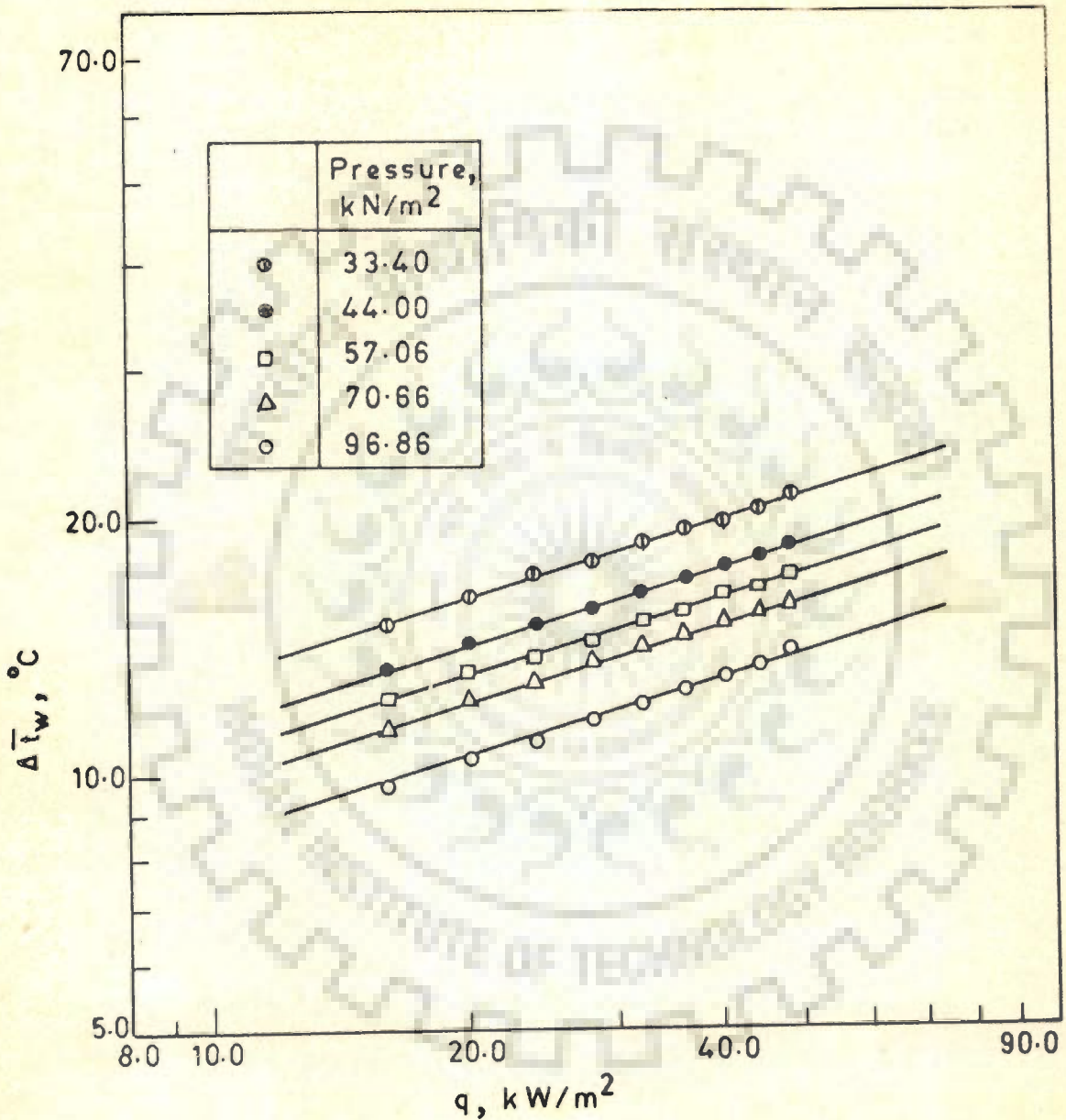


Fig 6.19 Variation of average wall superheat with heat flux for the boiling of benzene on upper heating cylinder

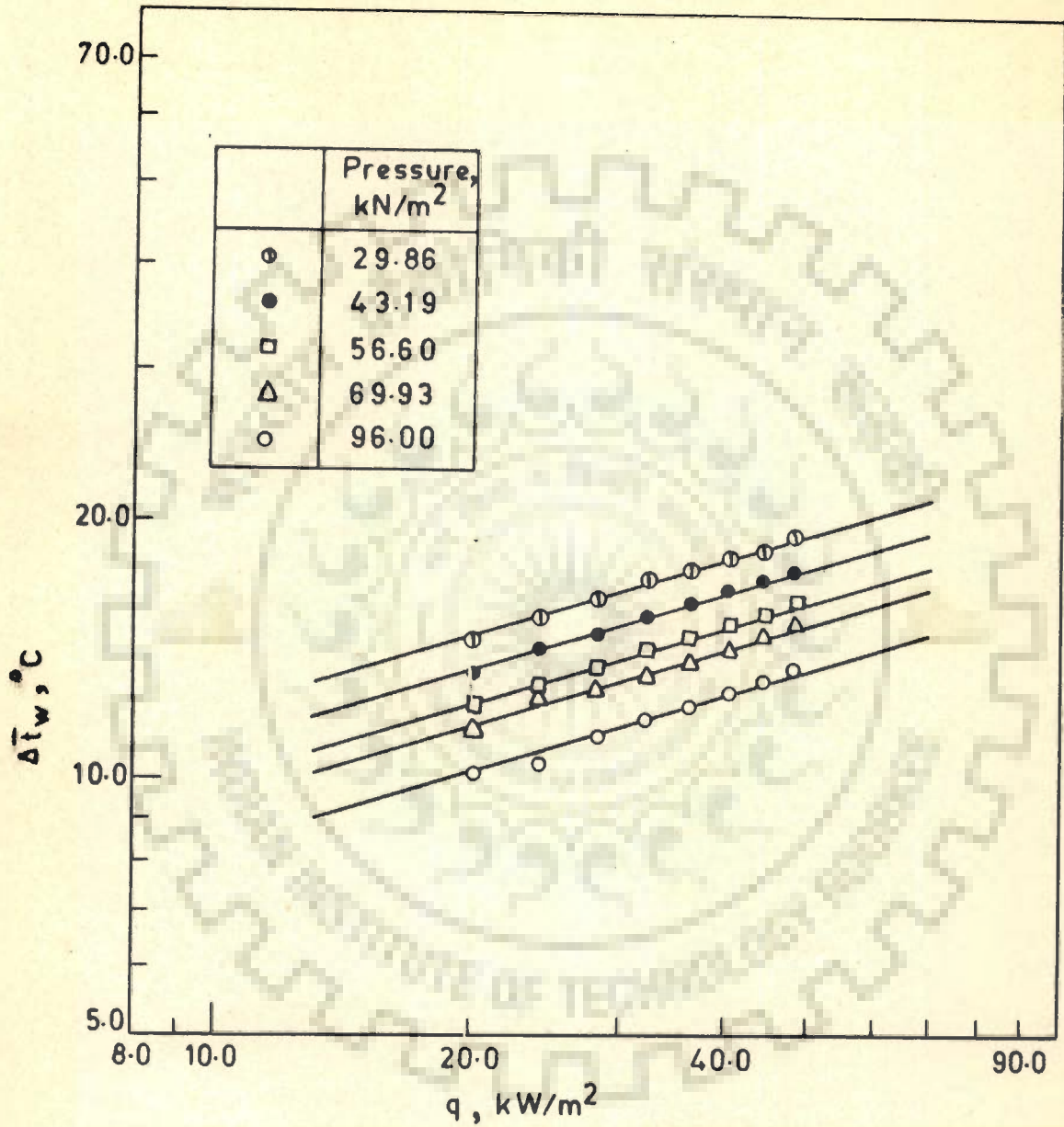


Fig 6.20 Variation of average wall superheat with heat flux for the boiling of toluene on upper heating cylinder

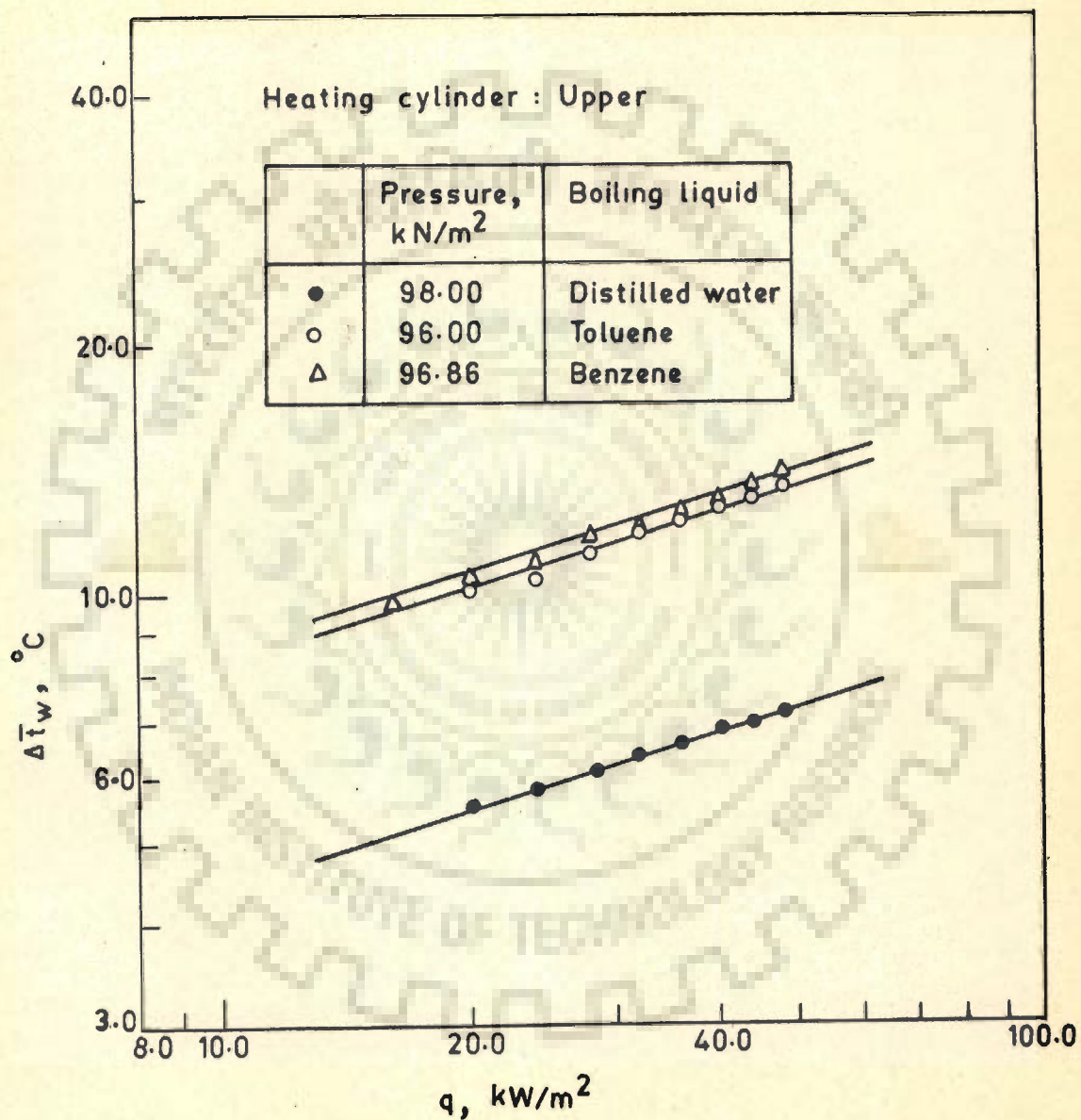


Fig 6.21 Variation of average wall superheat with heat flux for the boiling of different liquids

of 0.3. In other words they are represented by equation, Eq (6.1) but with different values of  $C_1$ , implying that the value of  $C_1$  depends upon the boiling liquid also for a given heating surface.

From Figures 6.18 through 6.21 it can be concluded that constant,  $C_1$  of Eq (6.1) depends upon pressure and the boiling liquid for a given heating surface. The effect of heating surface characteristics on constant,  $C_1$  is explained in Section 6.2.11.

#### 6.2.10 VARIATION OF $\Delta \bar{t}_w / q^{0.3}$ WITH PRESSURE

The experimental data of Figures 6.18 through 6.20 have been replotted in Figure 6.22 having  $\Delta \bar{t}_w / q^{0.3}$  and pressure,  $p$  as the ordinate and the abscissa respectively on a log-log plot. All the data points are correlated by the following equation within  $\pm 10$  per cent:

$$\Delta \bar{t}_w = C_2 q^{0.3} p^{-0.32} \quad \dots(6.2)$$

where constant,  $C_2$  depends upon the boiling liquid for a given heating surface. Table 6.1 contains the values of constant,  $C_2$  for the boiling liquids on a given stainless steel heating cylinder employed in the present investigation.

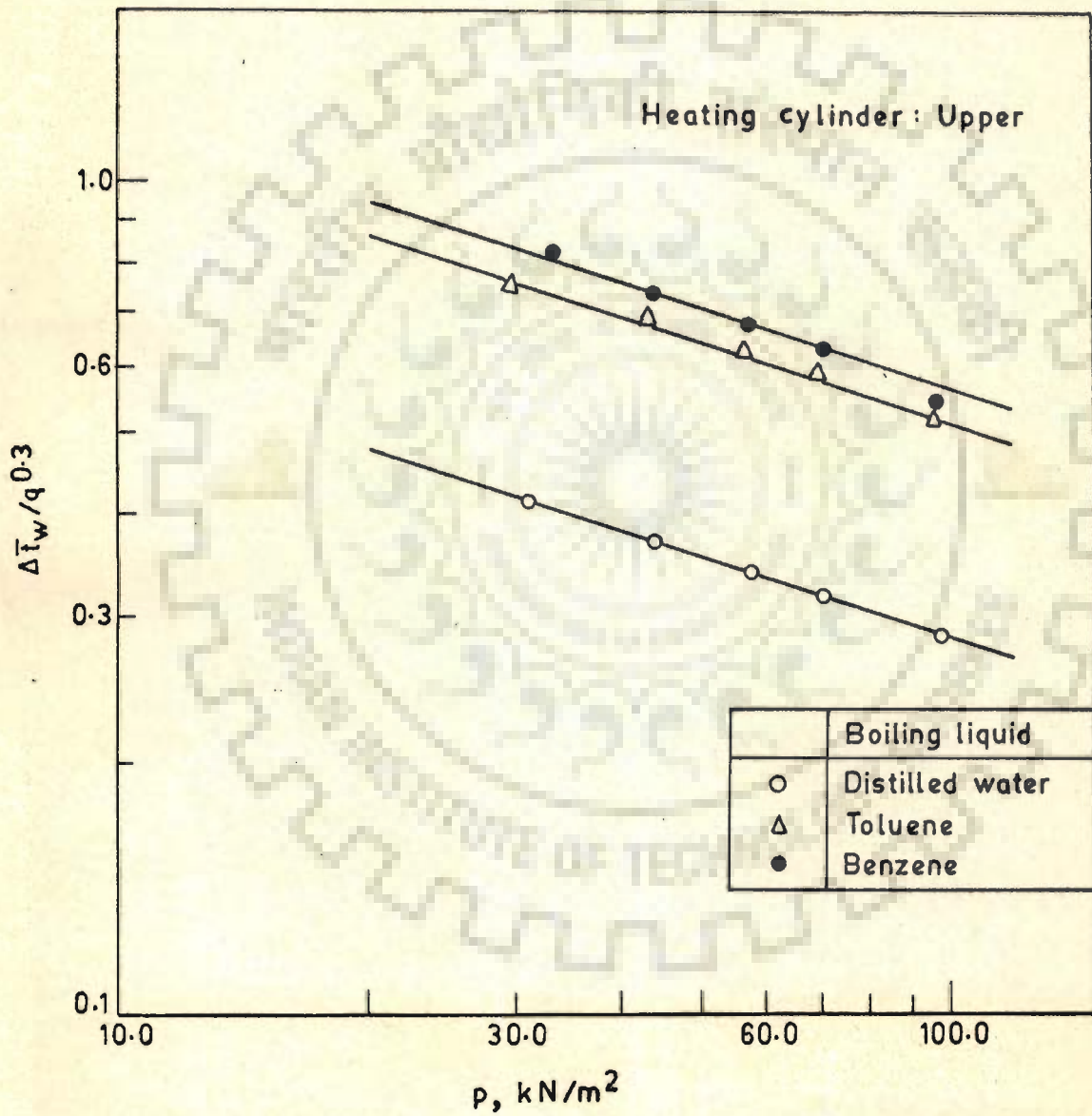


Fig 6.22  $\Delta T_w / q^{0.3}$  as a function of  $p$

Table 6.1 Values of constant,  $C_2$  of Eq (6.2) for different boiling liquids on stainless steel heating cylinder

Boiling liquid	Constant, $C_2$
Distilled water	1.23
Benzene	2.44
Toluene	2.28

#### 6.2.11 EFFECT OF HEATING SURFACE ON CONSTANT, $C_2$ OF EQ (6.2)

To determine the effect of heating surface characteristics on constant,  $C_2$  of Eq(6.2), the experimental data conducted on differing heating surfaces were analysed. Data of Cryder and Finalborgo [48] for the boiling of distilled water and methanol on brass pipe, data of Cole and Shulman [25] for distilled water and methanol on zirconium ribbon and all the data points of the present investigation were employed for this purpose. From these data, values of constant,  $C_2$  of Eq (6.2) were obtained as given in Table 6.2. They were within  $\pm 10$  per cent.

An inspection of Table 6.2 shows that for a given boiling liquid constant,  $C_2$  differs from investigation to investigation implying that constant,  $C_2$  of Eq (6.2) is affected by the surface characteristics of heating surfaces for a given boiling liquid. As a matter of fact, the value of  $C_2$  is of dubious character and still remains a subject for future investigations.

Table 6.2 Values of constant,  $C_2$  of Eq (6.2) for different heating surfaces

Boiling liquid	Constant, $C_2$	Heating surface	Investigator(s)
Distilled water	1.23	Stainless steel cylinder	Present Investigation
Benzene	2.44		
Toluene	2.28		
Distilled water	0.883	Brass pipe	Cryder and Finalborgo [48]
Methanol	1.610		
Distilled water	1.78	Zirconium ribbon	Cole and Shulman [25]
Methanol	3.26		

Eq (6.2) offers a simple convenient relation for the calculation of average wall superheat for the boiling of saturated liquids under subatmospheric pressure conditions if the value of constant,  $C_2$  is known.

#### 6.2.12 PREDICTION OF AVERAGE WALL SUPERHEAT FROM THE ALAD'EV CORRELATION

Alad'ev has recommended a correlation for the calculation of average wall superheat for the pool boiling of saturated distilled water on stainless steel tube for the pressure ranging from  $10.13 \text{ kN/m}^2$  to  $20,233 \text{ kN/m}^2$ . The

correlation has been described in Chapter 2 and is reproduced as follows :

$$\frac{\Delta \bar{t}_w}{T_s} = 4.7 \times 10^{-3} \left[ \frac{10^{-6} q \lambda}{k \ell T_s g} \right]^{0.3} \left[ \frac{\lambda}{c \ell T_s} \right]^{1.2} \quad \dots (2.105)$$

Figure 6.23 compares the predicted values of  $\Delta \bar{t}_w$  from Eq (2.105) with the experimental values of  $\Delta \bar{t}_w$  for the boiling of distilled water for different pressures of the present investigation. From this plot the following is noted :

1. The data points for different pressures fall on separate straight lines parallel to  $45^\circ$  line.
2. All the data points do not agree with the predicted values.

The above results suggest that the Alad'ev correlation is not capable to correlate the experimental data for atmospheric and subatmospheric pressures. This seems to be attributed to the fact that the Alad'ev correlation is not based purely on the data pertaining to subatmospheric pressures. In fact it is obtained from a large number of data related to high pressures (from  $101.33 \text{ kN/m}^2$  to  $20,233 \text{ kN/m}^2$ ) and a limited number of data for subatmospheric pressures. Due to this reason this correlation seems to be more suitable for the data at high pressures.

To extend the validity of this correlation for atmospheric and subatmospheric pressures, a term  $(\rho_\ell / \rho_v)$  was intuitively incorporated in it. Its functional



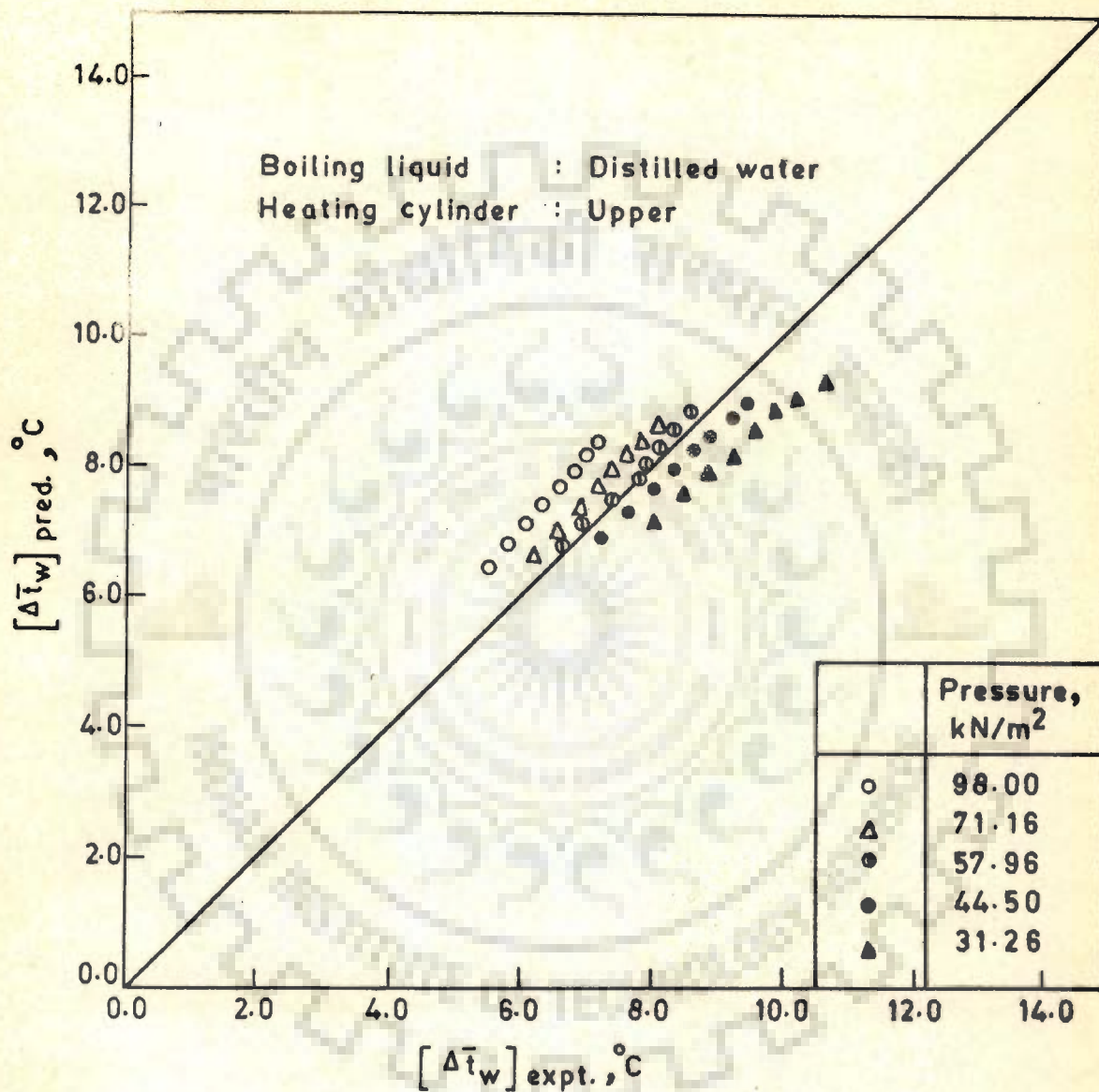


Fig 6-23 Present experimental data compared with the Alad'ev equation, Eq. (2-105)

relationship with the wall superheat  $\Delta \bar{t}_w$  was obtained from the Figure 6.24. Using this the Alad'ev correlation assumes the following form for the boiling of distilled water for a given heating surface :

$$\frac{\Delta \bar{t}_w}{T_s} = 6.92 \times 10^{-4} \left[ \frac{10^{-6} q \lambda}{k_{\ell} T_s g} \right]^{0.3} \left[ \frac{\lambda}{c_{\ell} T_s} \right]^{1.2} \left( \frac{\rho_{\ell}}{\rho_v} \right)^{0.24} \quad \dots(6.3)$$

Now a question arises. Is Eq (6.3) of general applicability? Therefore Eq (6.3) was employed to correlate the experimental data for the boiling of liquids other than distilled water. Figure 6.25 contains the experimental data of benzene and toluene conducted on the same heating surface. It is noted that Eq (6.3) correlates them excellently within  $\pm 10$  per cent, if the constant is changed to  $62.72 \times 10^{-4}$  and  $71.13 \times 10^{-4}$  respectively. Figure 6.26 represents the experimental data of earlier investigators [28,45] conducted on differing heating surfaces within  $\pm 10.0$  per cent, if the 'constant' of Eq (6.3) is changed as per Table 6.3.

Table 6.3 Values of constant,  $C_3$  in Eq (6.3)

Boiling liquid	Heating surface	Constant, $C_3$	Investigator(s)
Distilled water	Brass pipe	$4.60 \times 10^{-4}$	Cryder and Finalborgo [48]
Methanol		$6.42 \times 10^{-4}$	
Distilled water	Zirconium ribbon	$9.91 \times 10^{-4}$	Cole and Shulman [25]
Methanol		$12.94 \times 10^{-4}$	

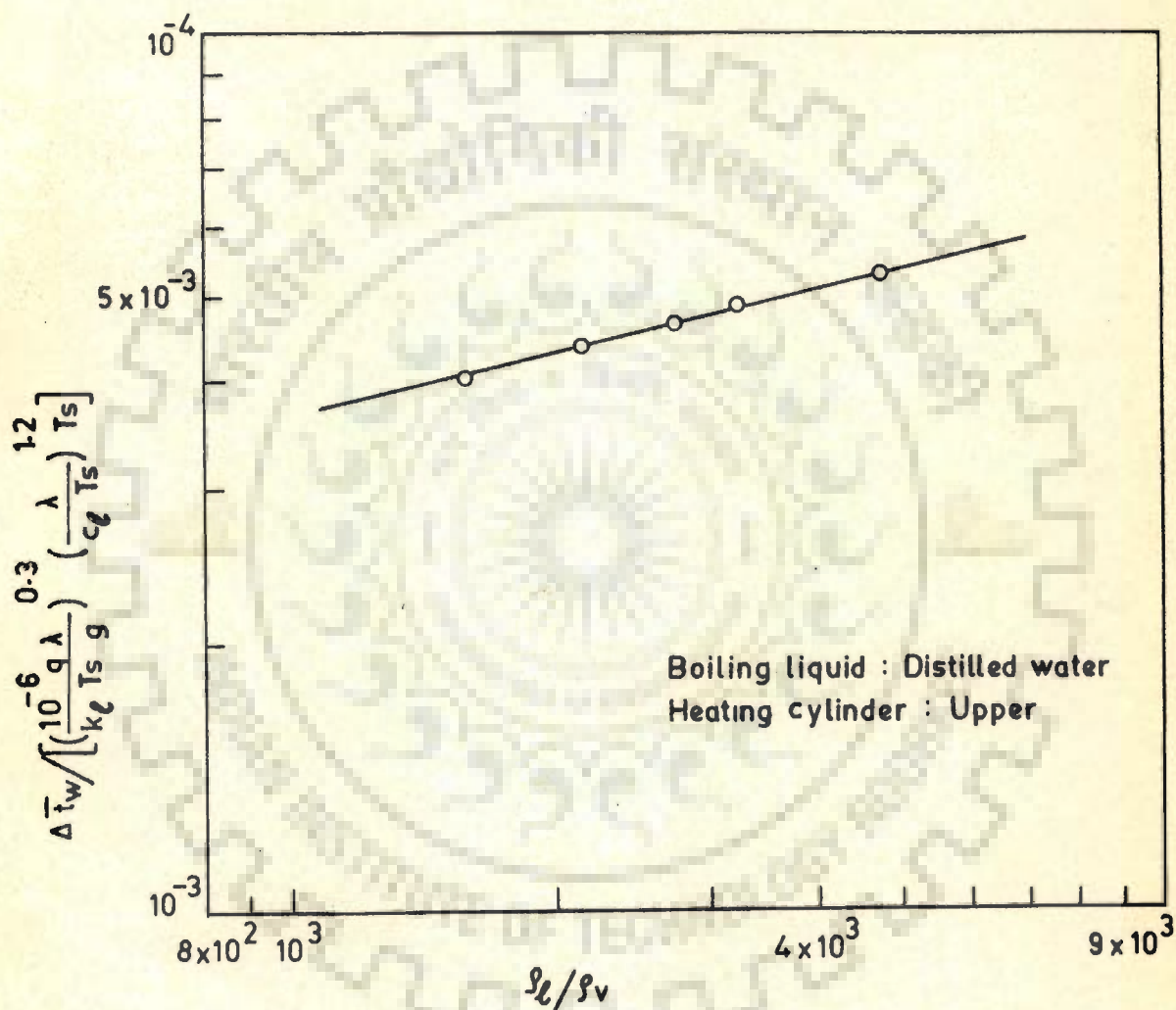


Fig 6.24 Relationship between  $\Delta \bar{t}_w / \left[ \frac{10^{-6} q \lambda}{k_l T_s g} \right]^{0.3} \left[ \frac{\lambda}{c_l T_s} \right]^{1.2} T_s$   
and  $\rho_l/\rho_v$

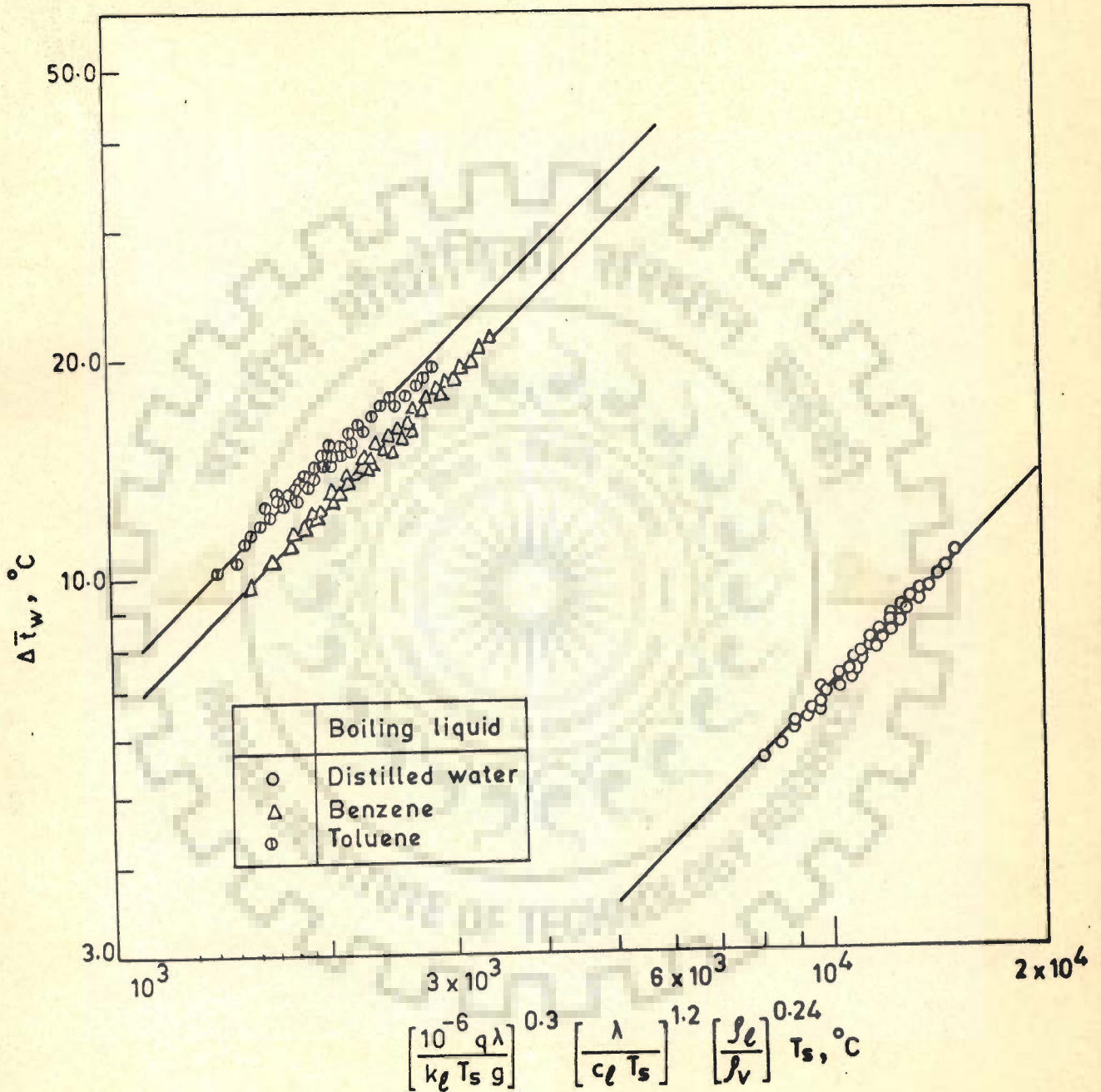


Fig 6.25 A plot of  $\Delta \bar{t}_w$  vs  $\left[ \frac{10^{-6} q \lambda}{k_l T_s g} \right]^{0.3} \left[ \frac{\lambda}{c_l T_s} \right]^{1.2} \left[ \frac{\rho_l}{\rho_v} \right]^{0.24} T_s$   
for nucleate pool boiling of saturated liquids

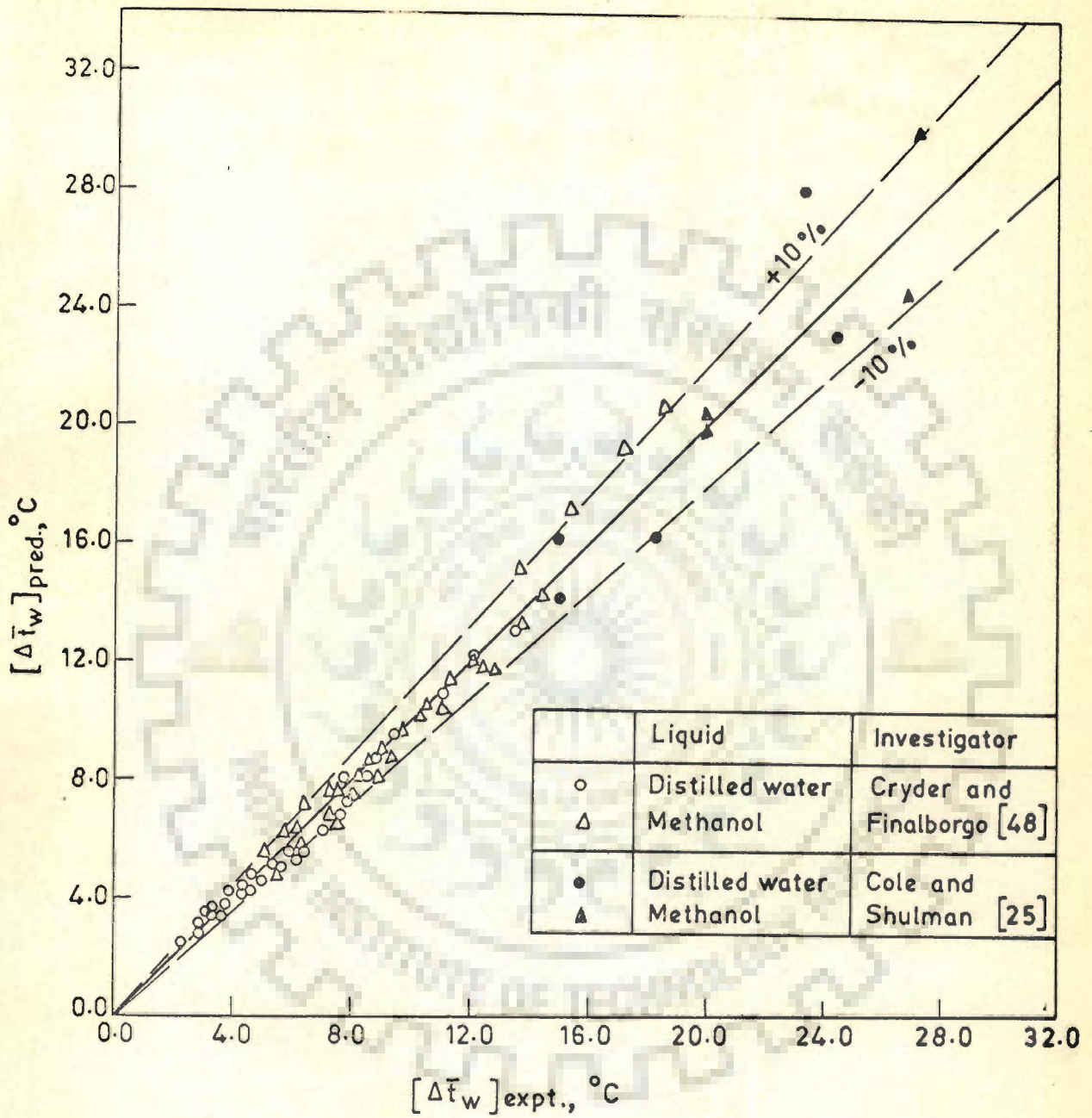


Fig 6-26 Experimental wall superheat compared with predicted values from the modified Alad'ev equation, Eq (6-4)

It may be noted that the different values of the 'constant' of Eq (6.3) are due to differing heating surface characteristics and the boiling liquids used in these investigations. Based on the above it is concluded that the Alad'ev correlation assumes the following functional relationship for determining the wall superheat for the boiling of liquids under atmospheric and subatmospheric pressures :

$$\frac{\Delta \bar{t}_w}{T_s} = C_3 \left[ \frac{10^{-6} q \lambda}{k_{\ell} T_s g} \right]^{0.3} \left[ \frac{\lambda}{c_{\ell} T_s} \right]^{1.2} \left[ \frac{\rho_{\ell}}{\rho_v} \right]^{0.24} \quad \dots(6.4)$$

where the constant,  $C_3$  depends upon the heating surface and the boiling liquid combination.

The value of the constant,  $C_3$  of Eq (6.4) is to be obtained for a given heating surface and liquid. Once the value of constant,  $C_3$  is known, one can use Eq (6.4) to predict the average wall superheat for the boiling of liquids on a given heating surface.

Eqs (6.2 and 6.4) show that the average wall superheat is proportional to heat flux raised to the power of 0.3. Hence Eq (6.4) can be reduced to Eq (6.2) if the quantities other than heat flux appearing in Eq (6.4) are expressed as functions of pressure as follows :

$$\text{Physical property} \propto (p)^n \quad \dots(6.5)$$

Accordingly, the exercise was undertaken and the values of exponent,  $n$  of Eq (6.5) for the respective physico-thermal properties of liquids appearing in Eq (6.4) were

Table 6.4 Values of exponent,  $n$  of Eq (6.5)

Boiling liquid	Range of $p$ kN/m <sup>2</sup>	$\lambda$	$k_{\ell}$	$\rho_v$	$\rho_{\ell}$	$T_s$	$c_{\ell}$
Distilled water	6.66 - 100.00	-0.0149	0.0262	0.9963	-0.0218	0.0743	0.0081
Benzene	32.64 - 98.00	-0.0207	-0.0970	0.9375	-0.0476	0.0875	0.0348
Toluene	30.47 - 98.00	-0.0255	-0.0960	0.9463	-0.0480	0.0831	0.0204
Methanol	8.4 - 100.60	-0.0149	-0.0245	1.013	-0.0349	0.0573	0.0304
Isopropanol	15.33 - 97.98	-0.0287	-0.0437	0.9393	-0.0437	0.0619	0.0218
Carbon tetrachloride	21.68 - 100.00	-0.0337	-0.0699	0.9825	-0.0480	0.0787	0.0044
Average, $n$		-0.0231	-0.0508	0.9691	-0.0407	0.0738	0.01998

determined. They are listed in Table 6.4 for different liquids from subatmospheric to atmospheric pressure and also the mean values of the exponent,  $n$ .

From Eqs (6.4) and (6.5) and Table 6.4 one gets the following :

$$\Delta \bar{t}_w \propto q^{0.3} p^{-0.32} \quad \dots(6.6)$$

It is interesting to note that Eq (6.6) is essentially the same as Eq (6.2).

#### 6.2.13 DETERMINATION OF $\Psi(p/p_1)$ OF EQ (5.17)

For this purpose the experimental data for the boiling of benzene of the present investigation were considered. The values of  $\Psi(p/p_1)$  were calculated by using the corresponding experimental values of  $\Delta \bar{t}_w / \Delta \bar{t}_{w,1}$  and the ratios of other terms appearing in Eq (5.17) as shown in Appendix C. The calculated values of  $\Psi(p/p_1)$  were plotted against  $p/p_1$  on a log-log plot in Figure 6.27. All the data points are correlated excellently by the following equation :

$$\Psi \left( \frac{p}{p_1} \right) = \left( \frac{p}{p_1} \right)^{-0.589} \quad \dots(6.7)$$

#### 6.2.14 GENERAL CORRELATION FOR WALL SUPERHEAT

Using Eq (6.7) into Eq (5.17) one gets the following equation :



$$\frac{\Delta \bar{t}_w}{\Delta \bar{t}_{w,1}} = \left[ \frac{p}{p_1} \right]^{-0.589} \left[ \frac{\rho \ell}{\rho_{\ell,1}} \right]^{-0.525} \left[ \frac{c \ell}{c_{\ell,1}} \right]^{-0.675} \\ \left[ \frac{k \ell}{k_{\ell,1}} \right]^{-0.3} \left[ \frac{T_s}{T_{s,1}} \right]^{0.024} \left[ \frac{\lambda}{\lambda_1} \right]^{0.276} \left[ \frac{\rho_v}{\rho_{v,1}} \right]^{0.276} \\ \left[ \frac{\sigma}{\sigma_1} \right]^{0.249} \left[ \frac{q}{q_1} \right]^{0.3} \quad \dots (6.8)$$

where subscript '1' represents the reference pressure. The reference pressure,  $p_1$  is that at which the value of  $\Delta \bar{t}_{w,1}$  is known. It may be noted that all the physico-thermal properties appearing in Eq (6.8) are determined at the saturation temperature.

Eq (6.8) is free from the quantities describing the surface roughness of the heating surface. In fact, its explicit determination is not possible. Figure 6.28 is a plot of experimental data pertaining to atmospheric and sub-atmospheric pressures of the present investigation for the boiling of distilled water, benzene and toluene on stainless steel heating cylinder; and of earlier investigations, namely; Sharma et al. [93] for the boiling of distilled water, ethanol, methanol and isopropanol on stainless steel cylinder; Cryder and Finalborgo [48] for the boiling of distilled water, methanol and carbon-tetrachloride on brass pipe and Cole and Shulman [25] for the boiling of distilled water and methanol on zirconium ribbon. It is found that all the data points are correlated by Eq (6.8) within  $\pm 10$  per cent irrespective

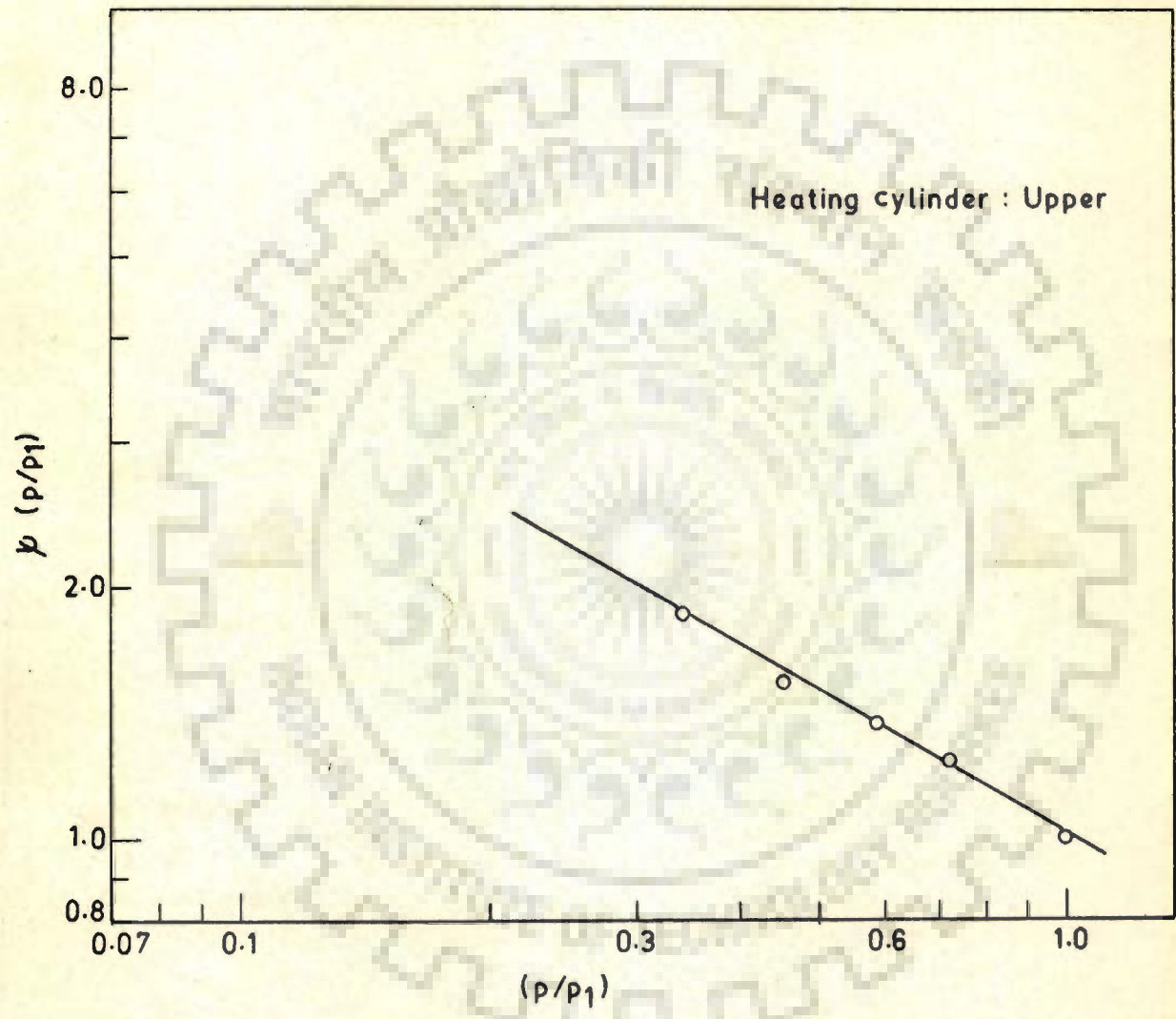


Fig 6-27 A plot of  $\psi(p/p_1)$  vs  $(p/p_1)$  for the boiling of saturated benzene of present investigation

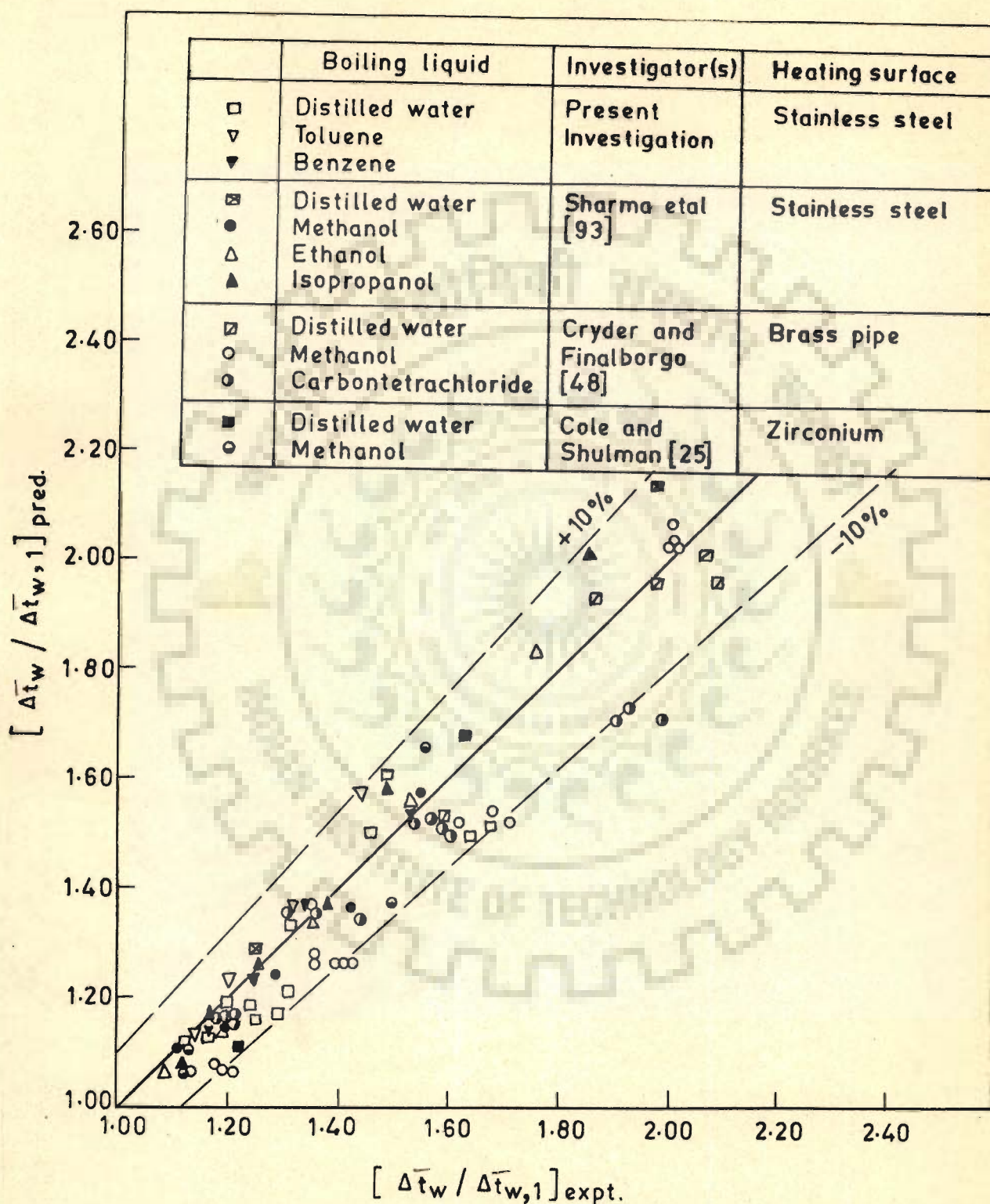


Fig 6.28 Comparison of experimental data of various investigators with present analysis, Eq (6.8)

of the characteristics of the heating surfaces and the boiling liquids. This would imply that the 'surface-liquid combination' factor does not depend upon pressure for the boiling of liquids under subatmospheric pressures.

The above result shows that the Transient Heat Conduction model due to Mikic and Rohsenow [92] and the Latent Heat Transport model due to Rallis and Jawurek [36] and the expressions of bubble departure diameter due to Cole and Rohsenow [98] of bubble emission frequency due to Hatton and Hall [20] and the nucleation site density due to Brown [13] are valid for the nucleate pool boiling heat transfer data for atmospheric and subatmospheric pressures.

#### REMARKS ON EQ (6.8)

With the knowledge of  $\Delta \bar{t}_{w,1}$  at  $p_1$  and heat flux,  $q_1$  and the physico-thermal properties of the boiling liquid at  $p_1$  and  $p$ , the value of  $\Delta \bar{t}_w$  for pressure,  $p$  and heat flux,  $q$  can be predicted from Eq (6.8). Further-more, Eq (6.8) can be used for checking the consistency of experimental data conducted at different pressures for a given boiling liquid and heating surface.

#### 6.2.15 RELATIONSHIP BETWEEN THE VALUES OF AVERAGE WALL SUPERHEAT FOR THE BOILING OF ORGANIC LIQUIDS AND THE DISTILLED WATER

The values of average wall superheat for the boiling of benzene,  $(\Delta \bar{t}_w)_b$  were compared with those for the boiling

of distilled water,  $(\Delta \bar{t}_w)_w$  under the same conditions of pressure and heat flux on a given heating surface. For this a plot between  $(\Delta \bar{t}_w)_b / (\Delta \bar{t}_w)_w$  and heat flux,  $q$  was drawn as shown in Figure 6.29. This plot reveals the following results :

A horizontal line represented by the following equation correlates all the experimental data points conducted in the present investigation :

$$\frac{(\Delta \bar{t}_w)_b}{(\Delta \bar{t}_w)_w} = 1.98 \quad \dots(6.9)$$

In other words the average wall superheat for the boiling of benzene is 1.98 times the value of average wall superheat of distilled water for a given condition of heat flux and pressure on the same heating surface. This is valid for the heat flux ranging from 20.210 kW/m<sup>2</sup> to 48.504 kW/m<sup>2</sup> and the pressure from 33.84 kN/m<sup>2</sup> to 96.86 kN/m<sup>2</sup>.

Figure 6.30 is similar to Figure 6.29 comparing the experimental data for the boiling of toluene and distilled water conducted on the same heating surface. It is found that the average wall superheat for the boiling of toluene,  $(\Delta \bar{t}_w)_t$  is 1.85 times of  $(\Delta \bar{t}_w)_w$  for all the values of pressure and heat flux studied. All the data points are correlated by the following equation :

$$\frac{(\Delta \bar{t}_w)_t}{(\Delta \bar{t}_w)_w} = 1.85 \quad \dots(6.10)$$

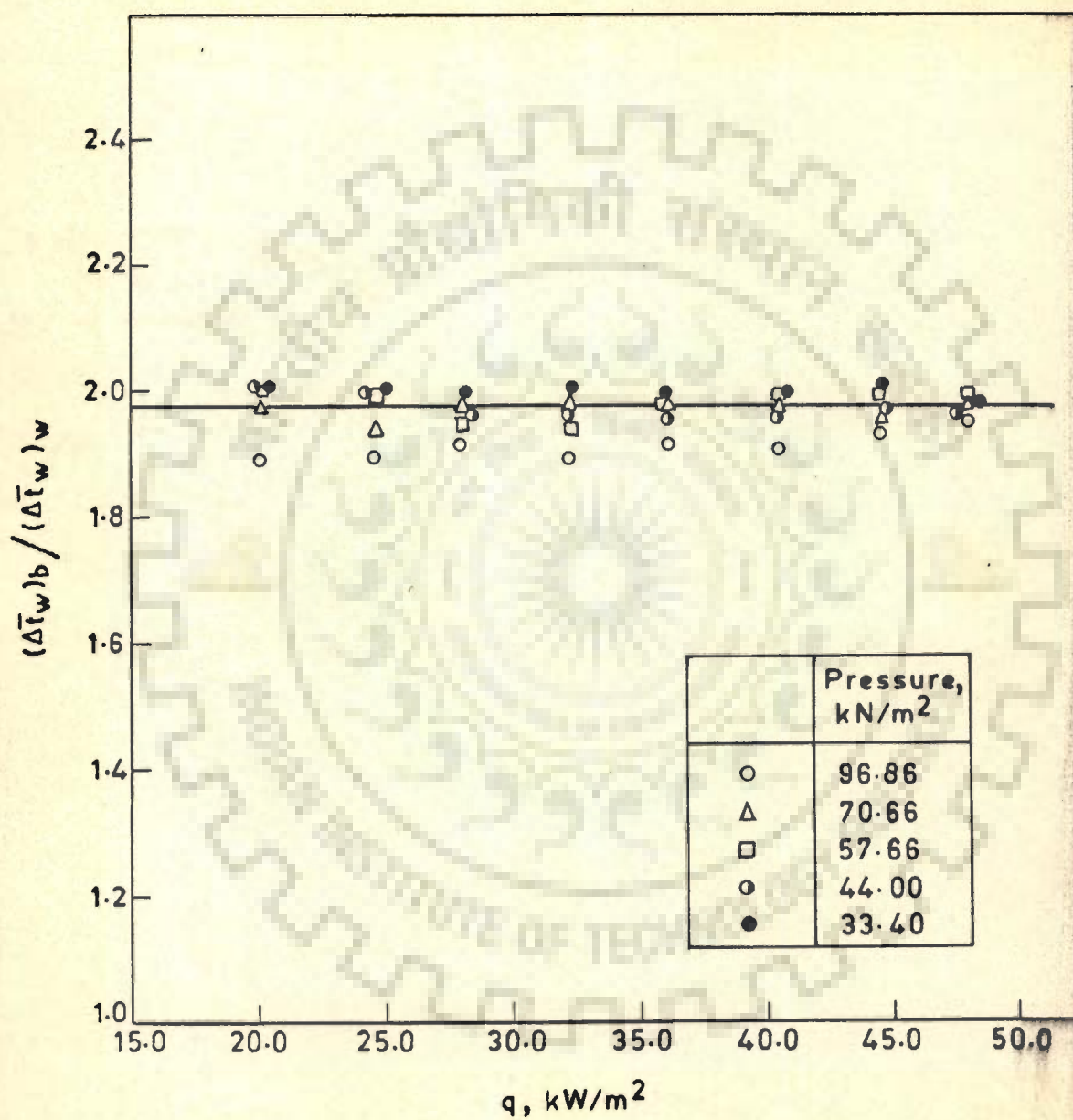


Fig 6-29  $(\Delta \bar{t}_w)_b / (\Delta \bar{t}_w)_w$  as a function of heat flux

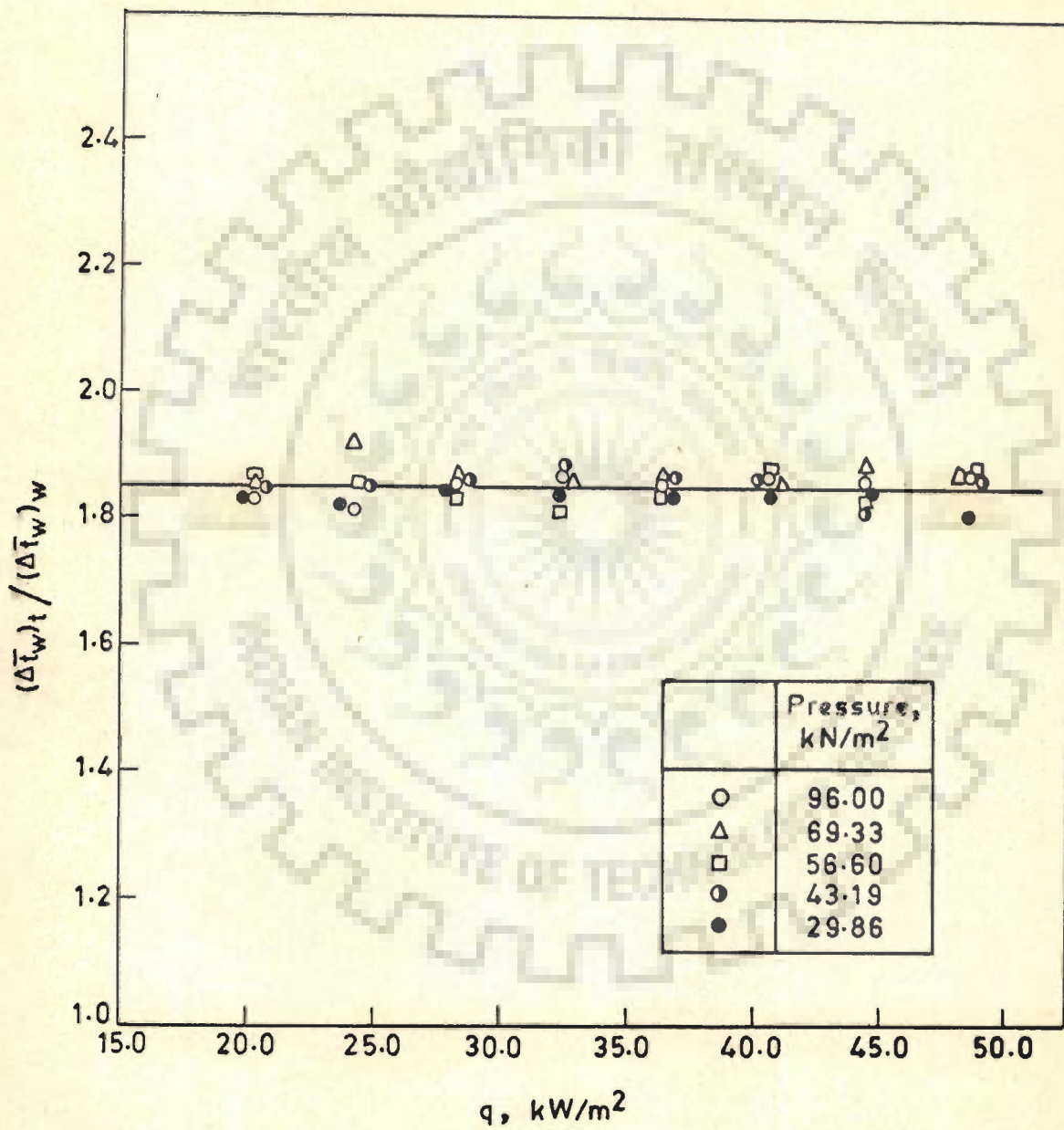


Fig 6.30  $(\Delta \bar{T}_w)_t / (\Delta \bar{T}_w)_w$  as a function of heat flux

### 6.2.16 PREDICTION OF AVERAGE WALL SUPERHEAT OF BENZENE AND TOLUENE

Eqs (6.8), (6.9) and (6.10) provide a method for the prediction of the average wall superheat for the boiling of benzene,  $(\Delta\bar{t}_w)_b$  and also for the boiling of toluene,  $(\Delta\bar{t}_w)_t$  at any pressure,  $p$  and heat flux,  $q$  on a given heating surface from the knowledge of average wall superheat for the boiling of distilled water  $(\Delta\bar{t}_{w,1})_w$  at pressure  $p_1$ , heat flux,  $q_1$  on the same heating surface and the properties of distilled water at pressures,  $p$  and  $p_1$  without resorting to experimentation as outlined below :

1. Calculate the value of  $(\Delta\bar{t}_w)_w$  for the boiling of distilled water at heat flux,  $q$  and pressure,  $p$  from Eq (6.8) by using the value of  $(\Delta\bar{t}_{w,1})_w$  and its corresponding values of heat flux,  $q_1$ ; pressure,  $p_1$  and the properties at pressures  $p_1$  and  $p$ .
2. Now use the above determined value of  $(\Delta\bar{t}_w)_w$  into respective Eqs (6.9) and (6.10) to get the value of  $(\Delta\bar{t}_w)_b$  and  $(\Delta\bar{t}_w)_t$  for the boiling of benzene and toluene.



### 6.3 BOILING HEAT TRANSFER FROM AN ASSEMBLY CONSISTING OF TWO HEATING CYLINDERS ORIENTED HORIZONTALLY ONE OVER THE OTHER

Heat transfer from a heating surface to the boiling liquids is a complex phenomenon. It is still complex when there are more than one heating surface like, in multitubular vaporisers. In the present investigation the experiments have also been conducted for the boiling of saturated liquids on the assembly of two heating cylinders placed one over the other horizontally. This has been carried out to account for as to how the vapour bubbles emerging out from the lower heating cylinder affect the wall temperature distribution, wall superheat and heat transfer coefficient of the upper heating cylinder. For this study the boiling liquids were distilled water, benzene and toluene, the heat flux ranged from  $16.168 \text{ kW/m}^2$  to  $48.504 \text{ kW/m}^2$  and pressure from  $43.19 \text{ kN/m}^2$  to  $98.40 \text{ kN/m}^2$ . Both the heating cylinders had the same identical surface characteristics as established in Section 6.2.1. They were heated such that they were under same heat flux. The experimental data are recorded in Table B.3 of Appendix B.

The following Sections discuss the important results and their interpretations pertaining to heat transfer from the assembly of two heating cylinders to the pool of boiling liquids.

### 6.3.1 WALL-AND THE LIQUID-TEMPERATURE DISTRIBUTION AROUND THE HEATING CYLINDERS

Figures 6.31 through 6.33 show the wall- and liquid-temperature distributions around the upper and the lower heating cylinders for the boiling of distilled water, benzene and toluene respectively at atmosphere pressure. From the plots the following points are noted :

1. For a given heat flux the wall temperature decreases from top- to side- to bottom- position of the upper heating cylinder, whereas it increases from top- to side- to bottom- position of the lower heating cylinder.
2. When the heat flux is raised, the curves for both the heating cylinders shift to their respective higher values of temperature for all the circumferential positions. However their characteristic behaviour does not change.
3. The liquid-temperature does not change around the heating cylinders.

The possible explanation of the wall temperature distribution of lower heating cylinder has been given in Section 6.2.2.

The typical behaviour of wall temperature of the upper heating cylinder is attributed to the fact that the vapours emerging out from the lower heating cylinder travel upward through the liquid and ultimately strike the bottom

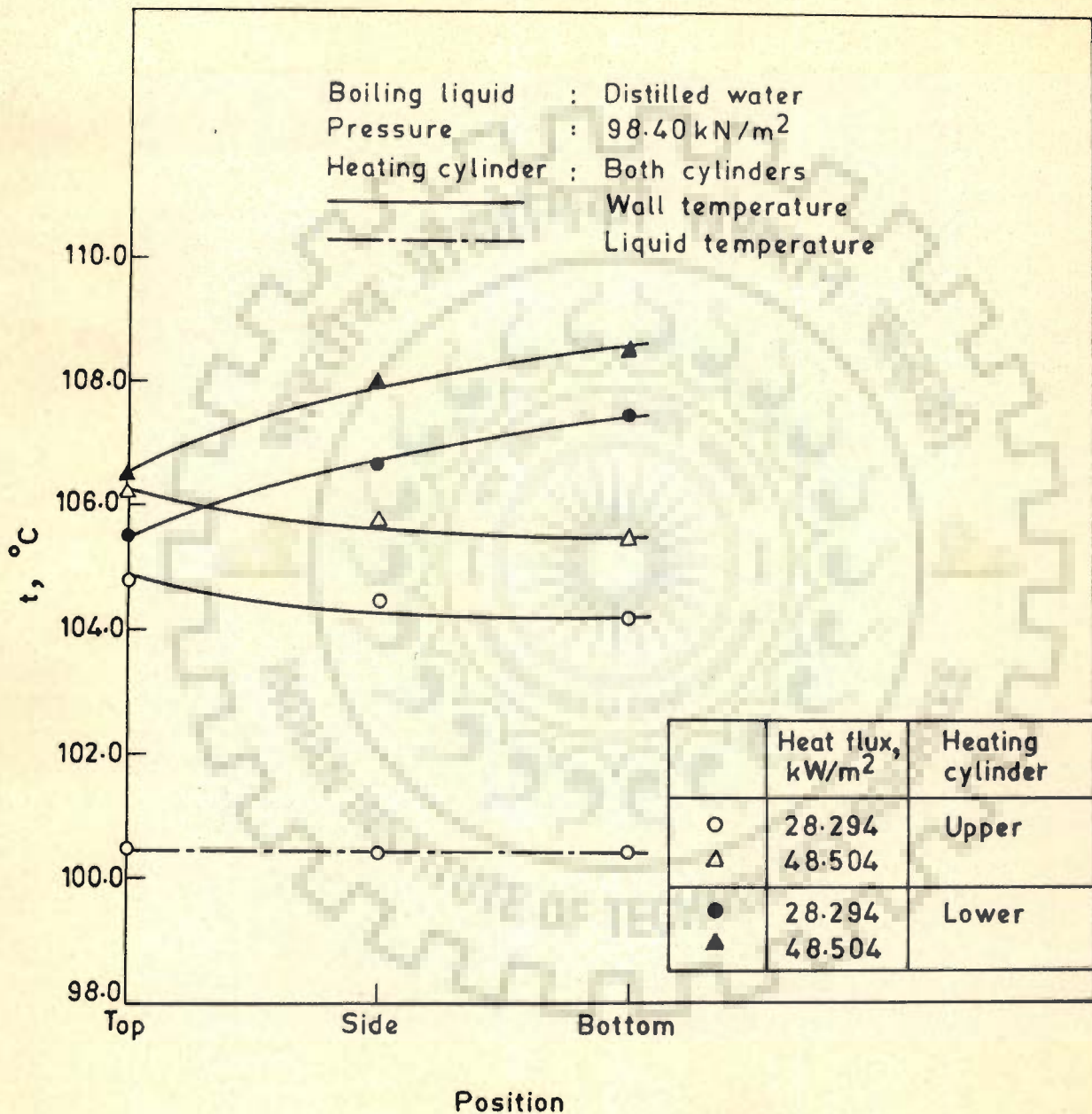


Fig 6.31 Effect of heat flux on wall and liquid temperature distribution around the upper and lower heating cylinders

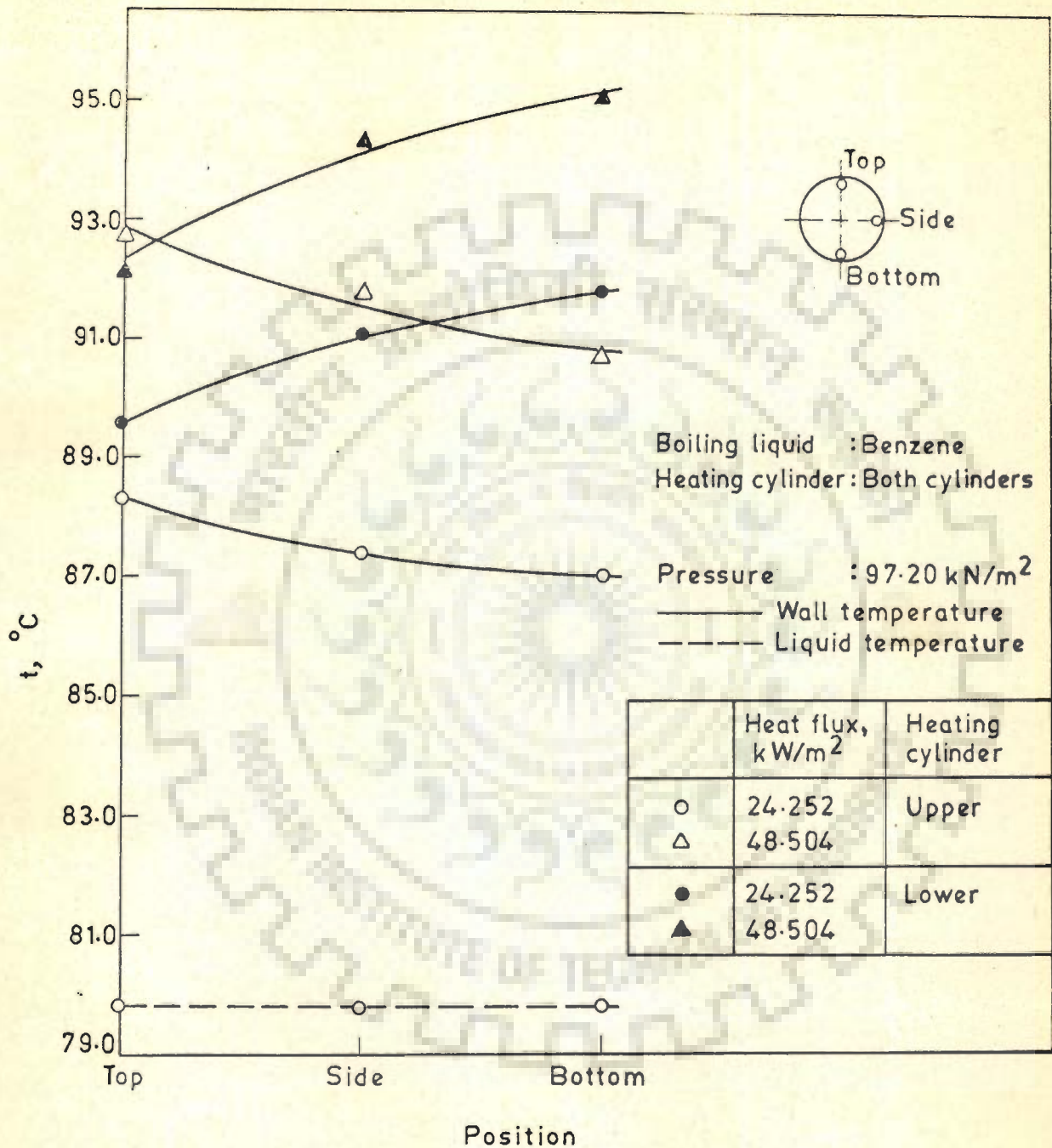


Fig 6.32 Effect of heat flux on wall and liquid temperature distribution around the upper and lower heating cylinders

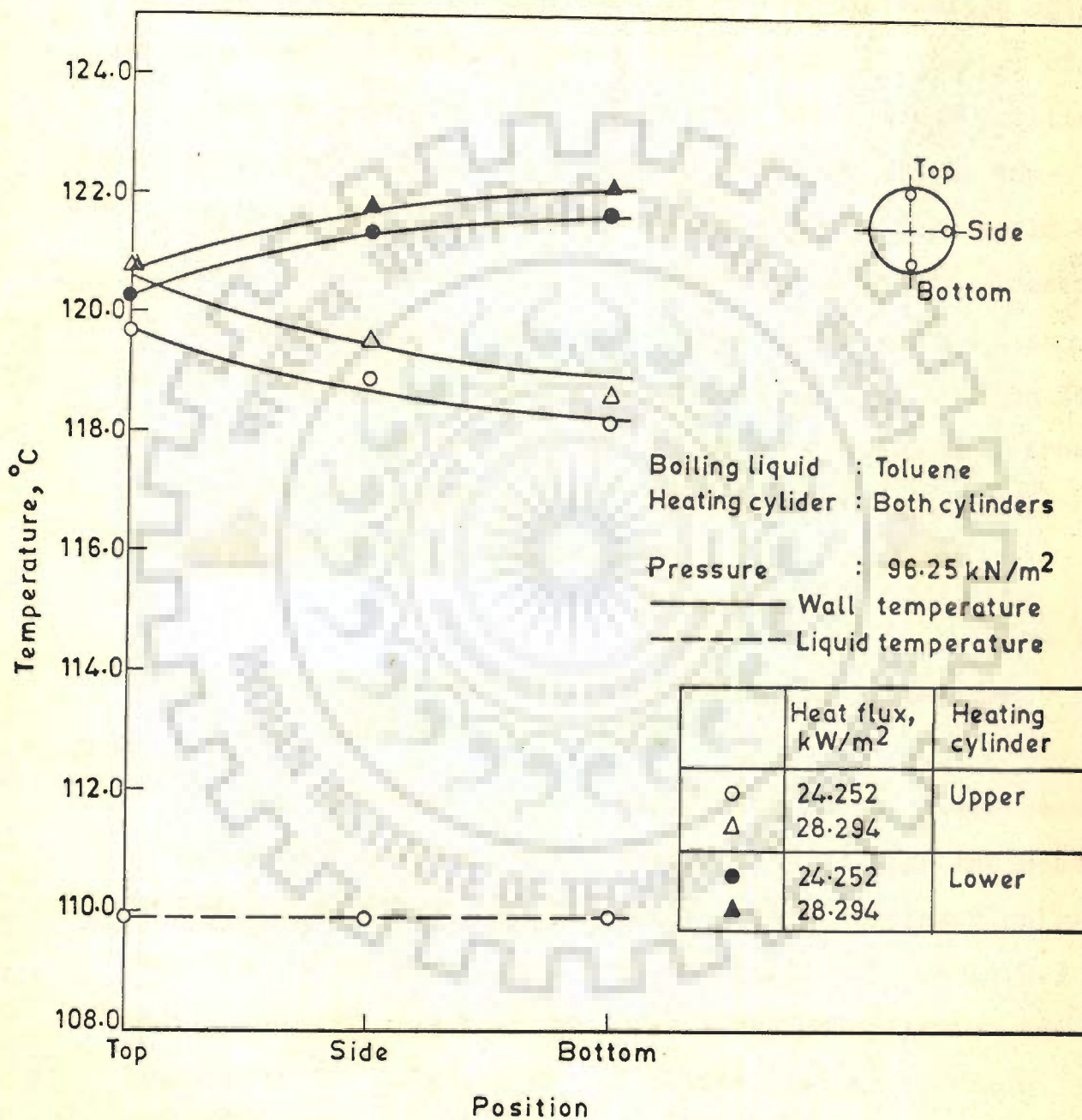


Fig 6.33 Effect of heat flux on wall and liquid temperature distribution around the upper and lower heating cylinders

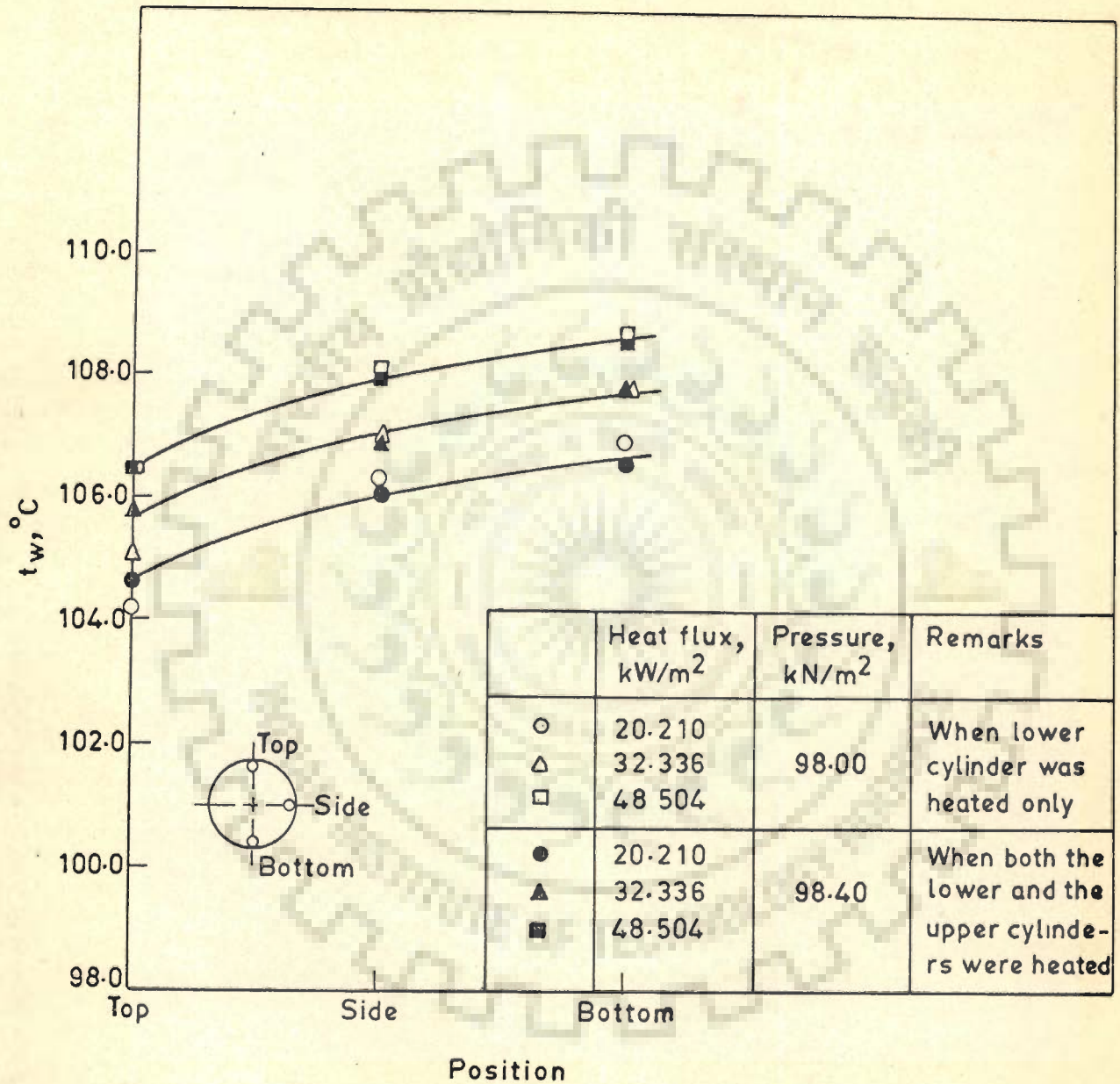


Fig 6.34 Wall temperature distribution around the lower heating cylinder for the boiling of distilled water

surface of the upper heating cylinder. Due to this the liquid in the proximity of bottom- position of the upper heating cylinder experiences induced turbulence in addition to that caused by the dynamics of the vapour bubbles originating there. Further, it is obvious that the effect of the induced turbulence decreases from the bottom- position to side- position and is likely to disappear at the top- position of the cylinder. An implication of this would be that the wall temperature corresponding to the top- position of the upper cylinder and that of the lower cylinder should be the same for a given heat flux, pressure and boiling liquid. It may be pointed out that this fact is corroborated from the experimental data for all the values of heat flux, pressure and the boiling liquids.

### 6.3.2 LOCAL WALL TEMPERATURE DISTRIBUTION AROUND THE LOWER HEATING CYLINDER

The experimental data pertaining to the lower heating cylinder were compared with those conducted when the heat transfer took place from the lower heating cylinder only. The data points were taken from the respective Table B.3 and Table B.2. Figure 6.34 shows a typical plot for the boiling of distilled water indicating that the surface characteristics of the lower heating cylinder did not change at all. Similar plots for benzene and toluene are given in Figures 6.35 and 6.36. This, as a matter of fact, is an expected behaviour as the bubble dynamics on the

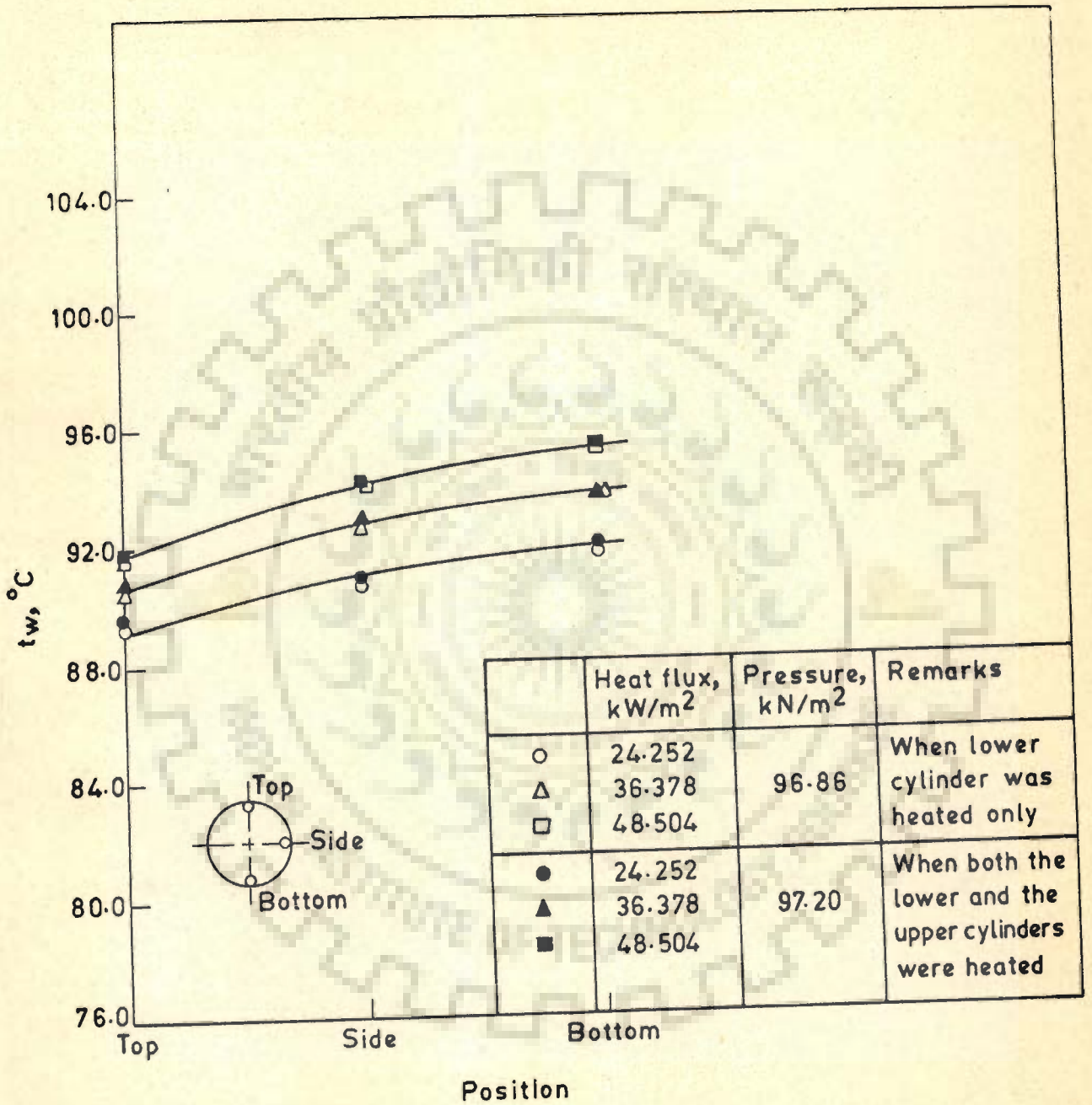


Fig 6.35 Wall temperature distribution around the lower heating cylinder for the boiling of benzene



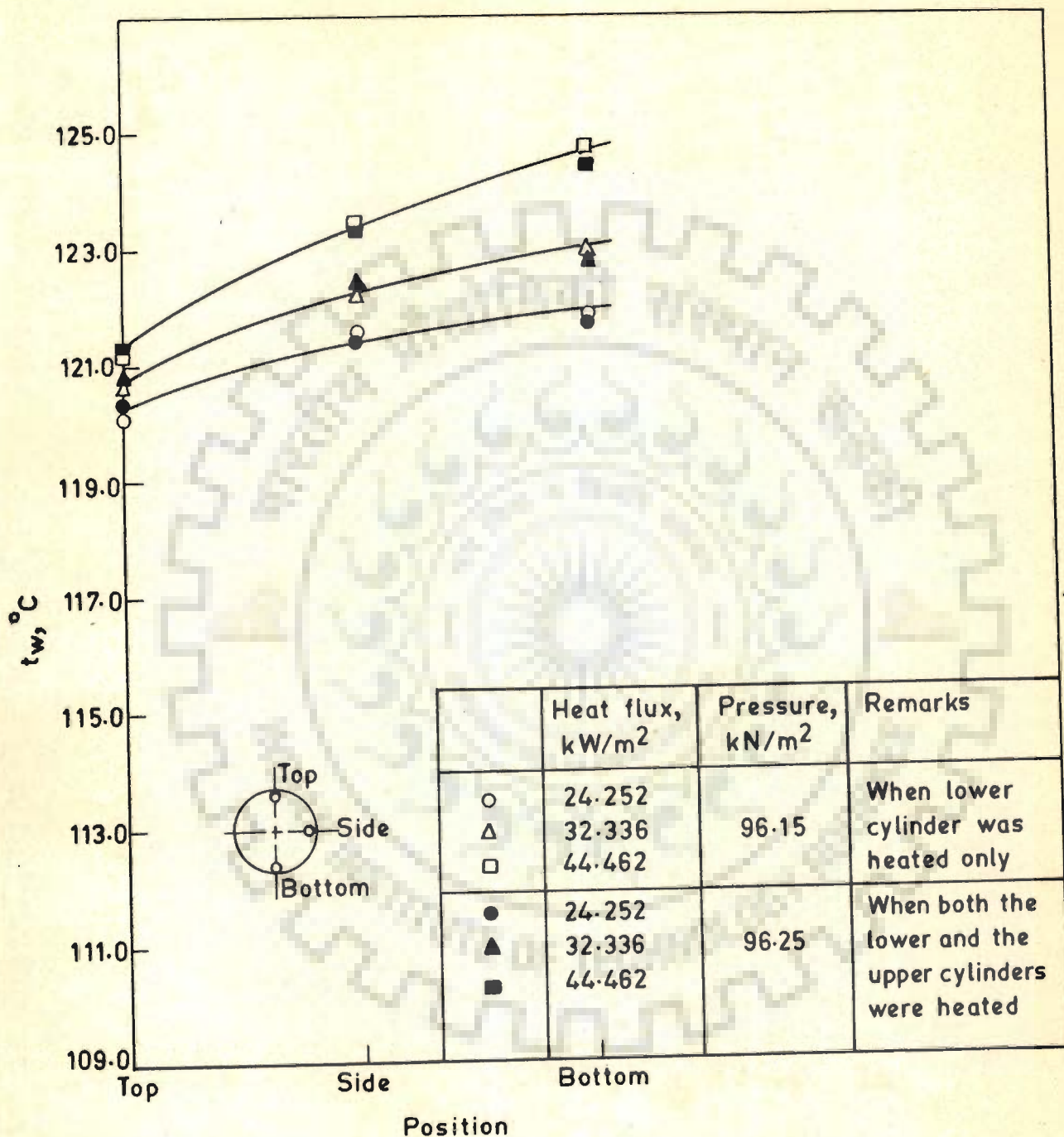


Fig 6.36 Wall temperature distribution around the lower heating cylinder for the boiling of toluene

lower heating cylinder is not affected by the bubbles originating on the upper heating cylinder which in fact find their passage upward only.

### 6.3.3 LOCAL WALL SUPERHEAT OF THE UPPER AND THE LOWER HEATING CYLINDERS

Figures 6.37 through 6.39 represent the typical plots showing the distributions of wall superheat of upper and lower heating cylinders for the boiling of distilled water, benzene and toluene respectively with pressure as a parameter for the value of heat flux equal to  $32.336 \text{ kW/m}^2$ . All the plots exhibit the following characteristic features:

1. For the upper heating cylinder the wall superheat decreases regularly from top- to side- to bottom-position for a given pressure. With the increase in pressure the curve shifts such that the value of  $\Delta t_w$  decreases for all the circumferential positions. However the nature of the curve remains unaltered.
2. For the lower heating cylinder the wall superheat increases regularly from top- to side-to bottom-position for a given pressure. As the pressure is raised, the curve shifts to lower values of wall superheat with no change in its nature.

The above behaviour depicted by the upper and the lower heating cylinders are attributed to the facts given in Sections 6.3.1 and 6.2.6.

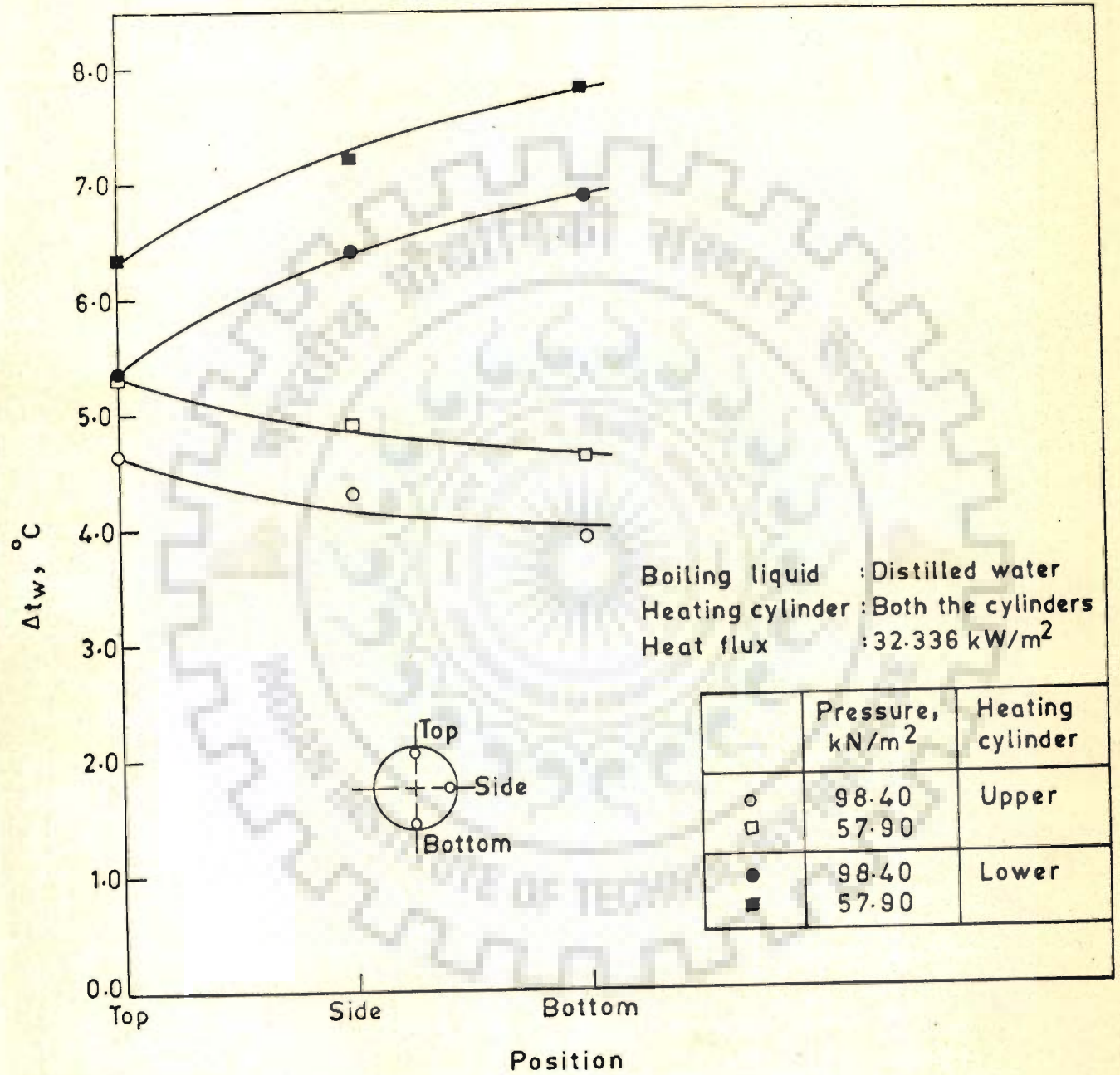


Fig 6-37 Wall superheat distribution along the circumference of the upper and lower heating cylinders

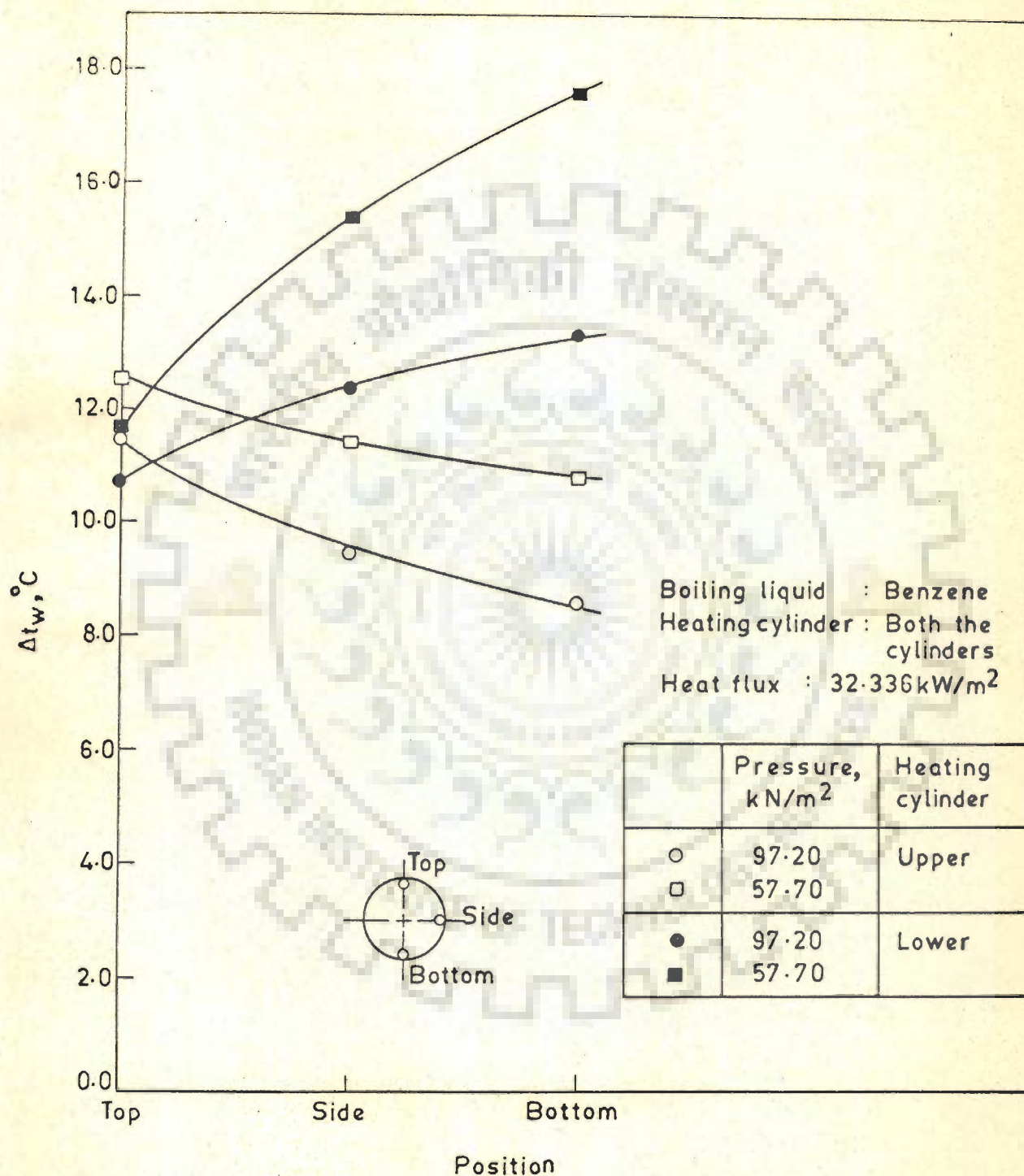


Fig 6.38 Wall superheat distribution along the circumference of the upper and lower heating cylinders

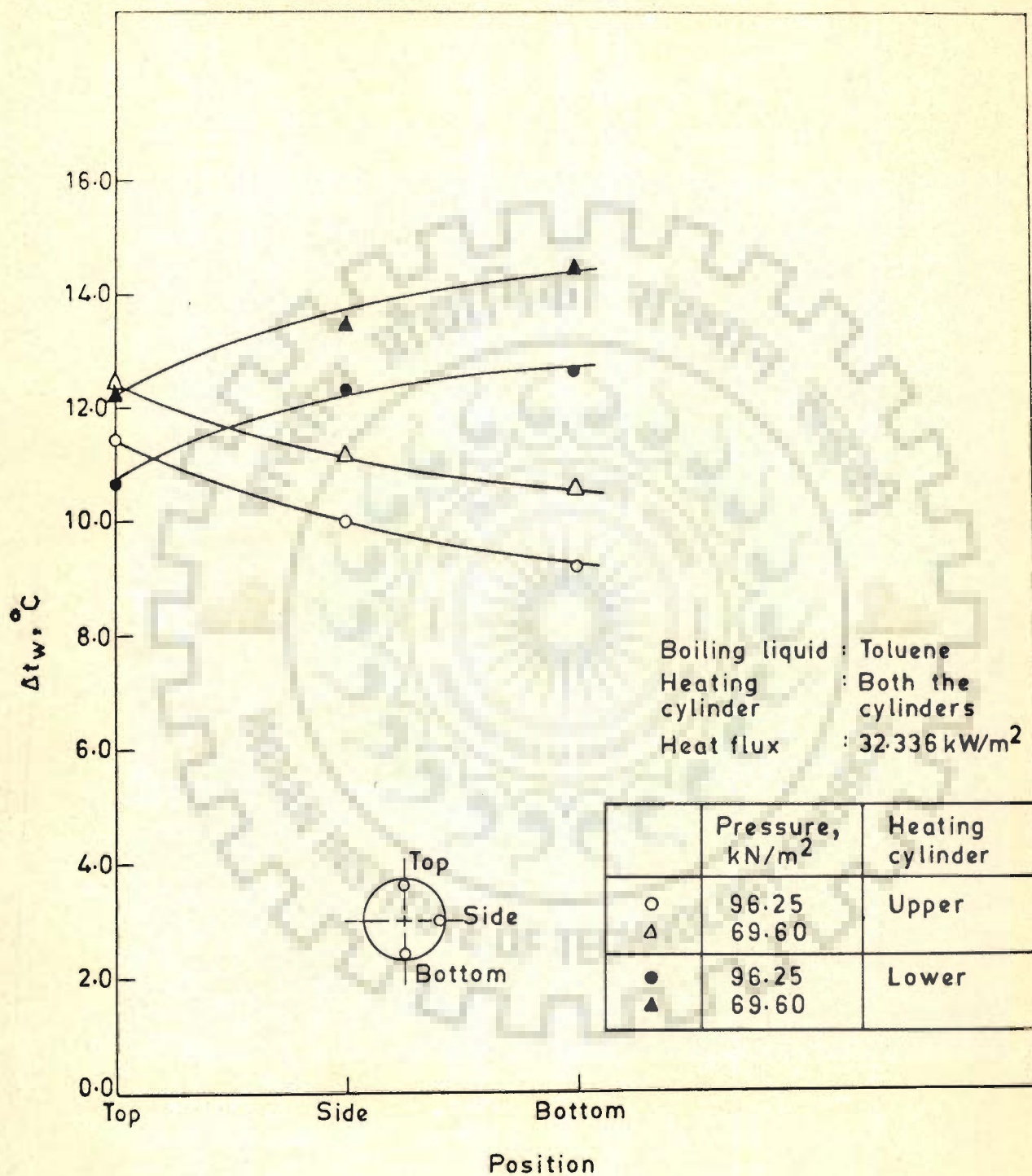


Fig 6.39 Wall superheat distribution along the circumference of the upper and lower heating cylinders

#### 6.3.4 EFFECT OF HEAT FLUX ON AVERAGE WALL SUPERHEAT

Figures 6.40 through 6.42 represent the typical effect of heat flux on average wall superheat for the boiling of distilled water, benzene and toluene respectively on a log-log plot. From these plots the following is noted :

It is seen that the wall superheat increases continuously upto a certain value of heat flux. Beyond which a 'dome' appears followed by a linear increase in the value of  $\Delta \bar{t}_w$  with  $q$ . This typical behaviour is observed for all the values of pressure.

The variation of average wall superheat with heat flux can be represented mathematically as:

$$\Delta \bar{t}_w = C_4 q^n \quad \dots(6.11)$$

where  $C_4$  is a constant which depends upon heat flux, boiling liquid and pressure for a given heating surface. The values of exponent,  $n$  are given by :

$$n = 0.45 ; \quad \text{for } q \leq 24.252 \text{ kW/m}^2$$

$$n = 0.55 ; \quad \text{for } q \geq 28.294 \text{ kW/m}^2$$

#### 6.3.5 EFFECT OF PRESSURE ON AVERAGE WALL SUPERHEAT

Figures 6.43 through 6.45 exhibit the typical variation in average wall superheat with pressure for the boiling of distilled water, benzene and toluene respectively on a log-log plot with heat flux as a parameter. An inspection of these plots leads to the following results :

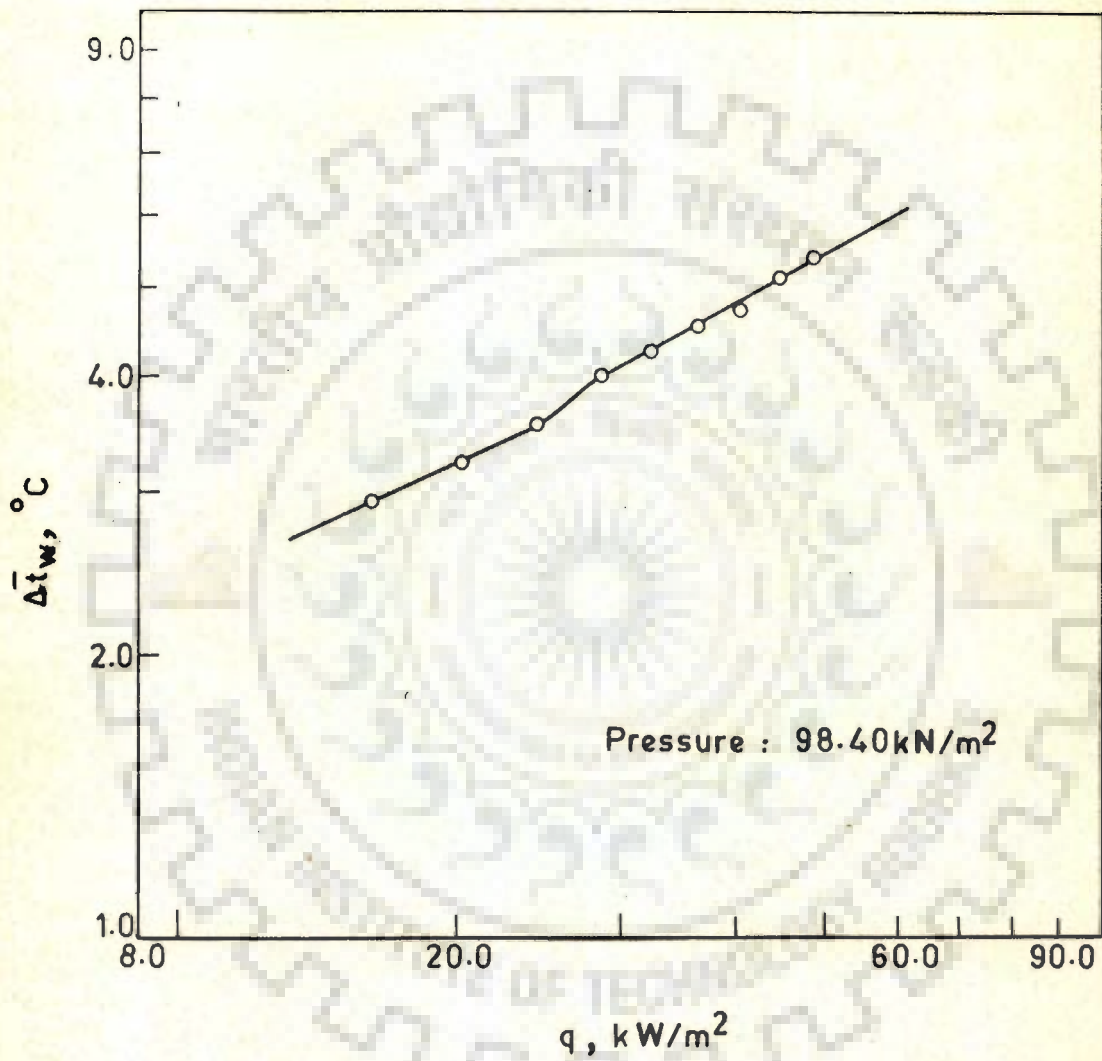


Fig 6-40 Variation of average wall superheat with heat flux for the boiling of distilled water on upper heating cylinder

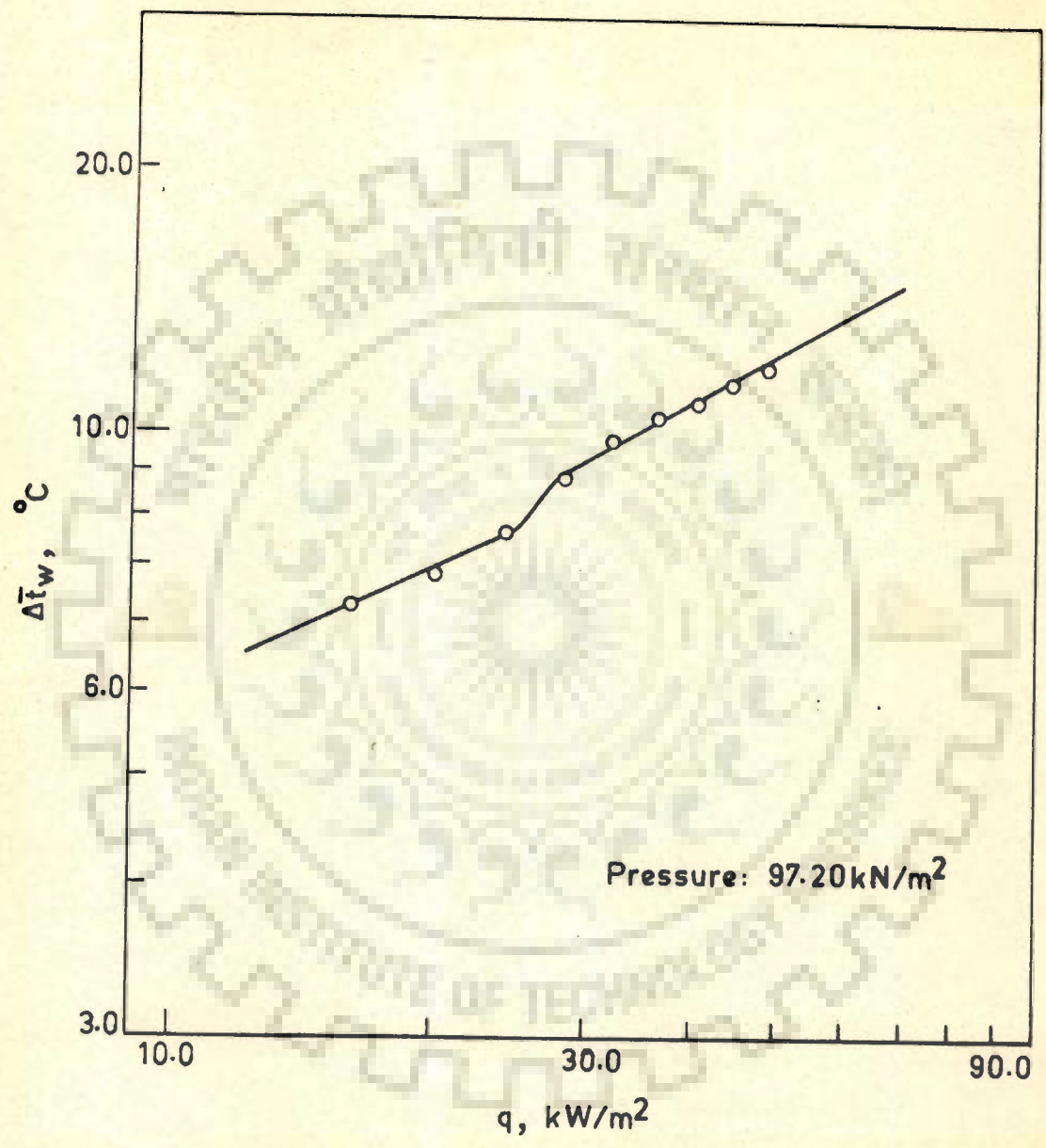


Fig 6.41 Variation of average wall superheat with heat flux for the boiling of benzene on upper heating cylinder



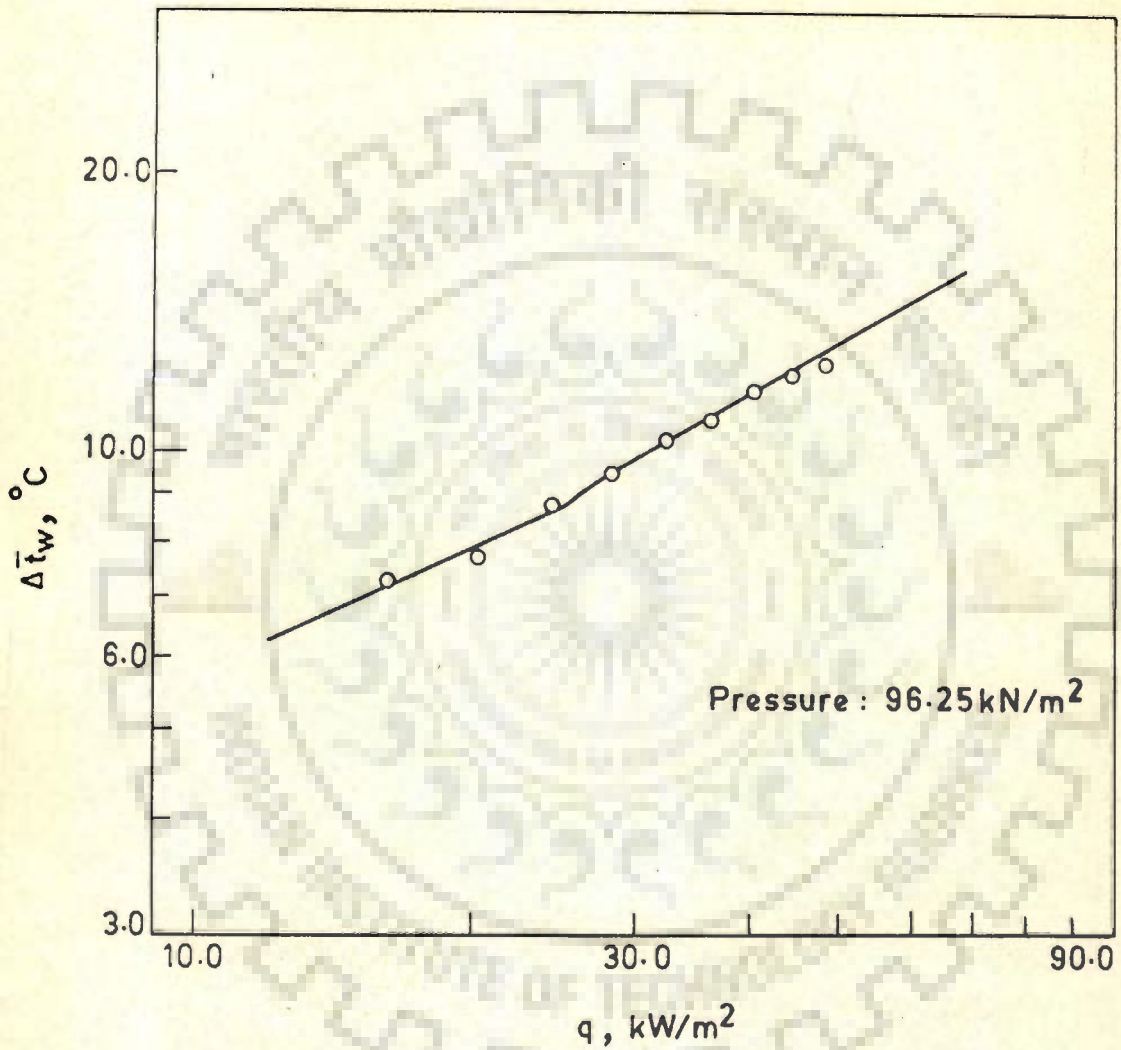


Fig 6.42 Variation of average wall superheat with heat flux for the boiling of toluene on upper heating cylinder

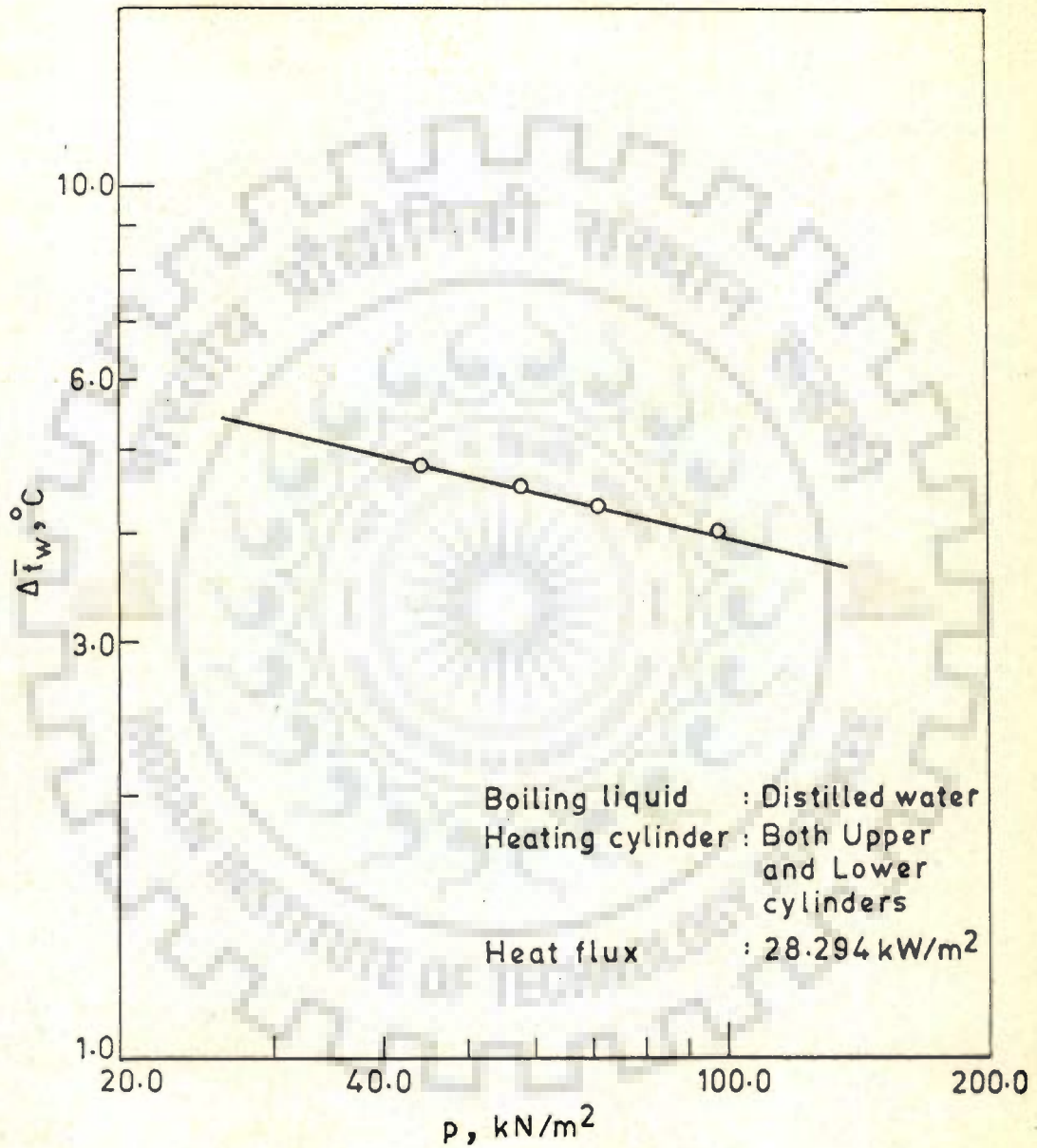


Fig 6.43 Variation of average wall superheat with pressure for upper heating cylinder

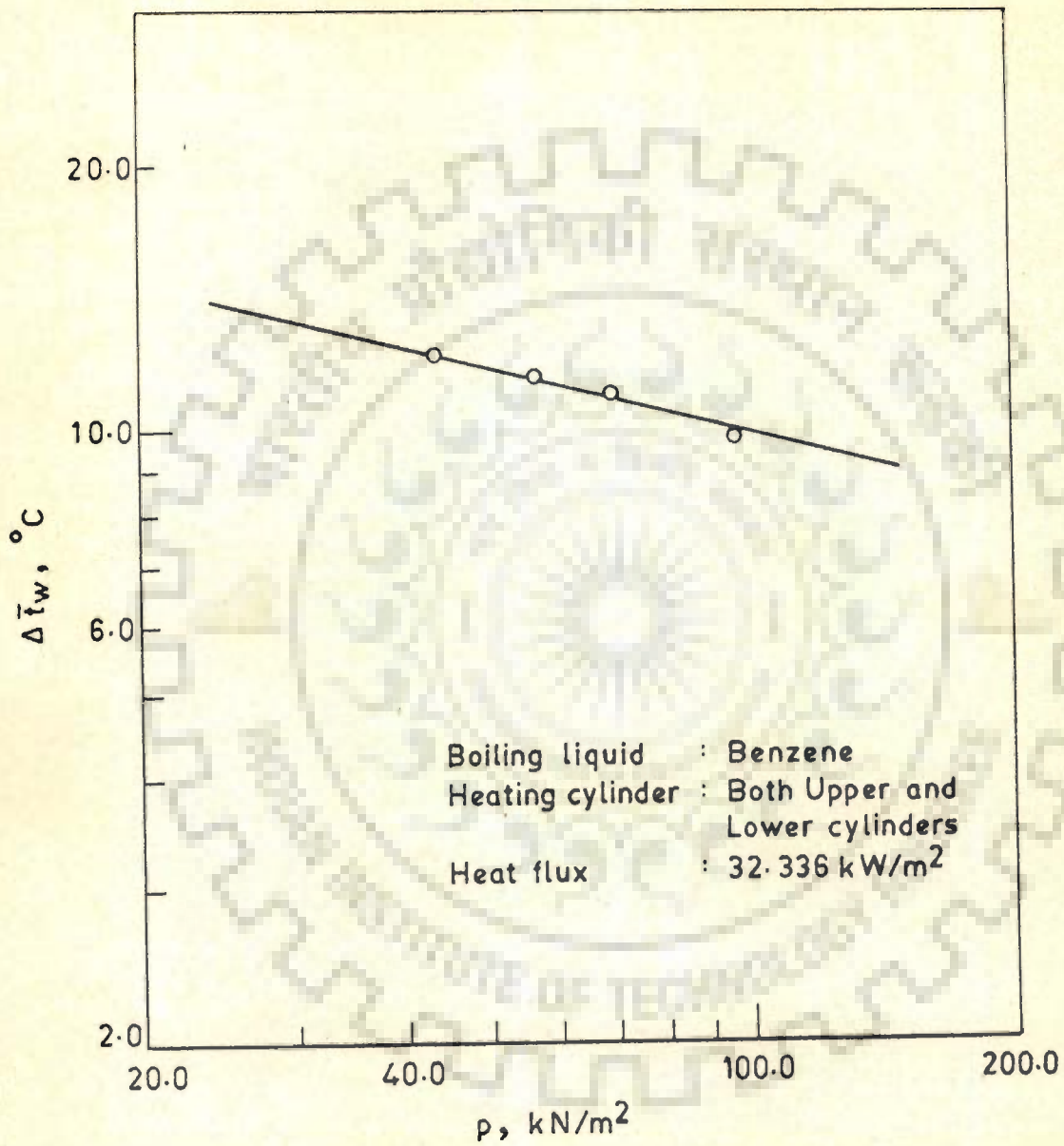


Fig 6.44 Variation of average wall superheat with pressure for upper heating cylinder

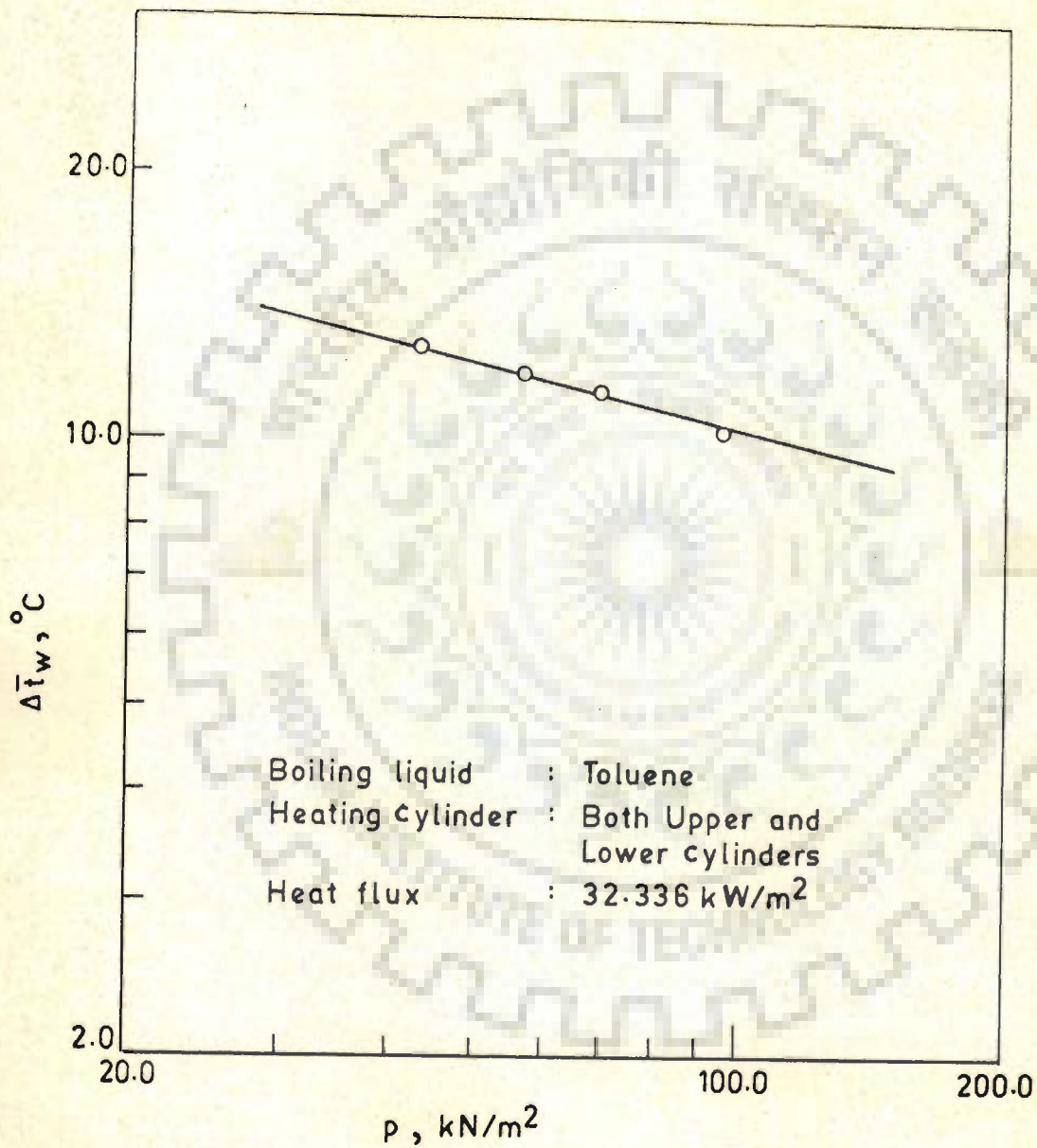


Fig 6.45 Variation of average wall superheat with pressure for upper heating cylinder

The value of average wall superheat decreases with pressure linearly according to the following equation :

$$\Delta \bar{t}_w = C_5 p^{-0.25} \quad \dots(6.12)$$

where constant,  $C_5$  is a function of boiling liquid for a given heating surface and a value of heat flux.

### 6.3.6 EFFECT OF HEAT FLUX ON HEAT TRANSFER COEFFICIENT

Figures 6.46 through 6.48 are the typical plots to represent the effect of heat flux on heat transfer coefficient for lower and the upper heating cylinders for the boiling of distilled water, benzene and toluene respectively at atmospheric pressure on a log-log plot. From these Figures the following points are observed :

1. For lower heating cylinder, heat transfer coefficient increases linearly with heat flux representing the following mathematical relationship (curve I) :

$$h = C_6 q^{0.7} \quad \dots(6.13)$$

This is the same relationship as reported in literature [63,83,92,102].

2. For upper heating cylinder, the heat transfer coefficient is higher than that of lower heating cylinder for all the values of heat flux. However,

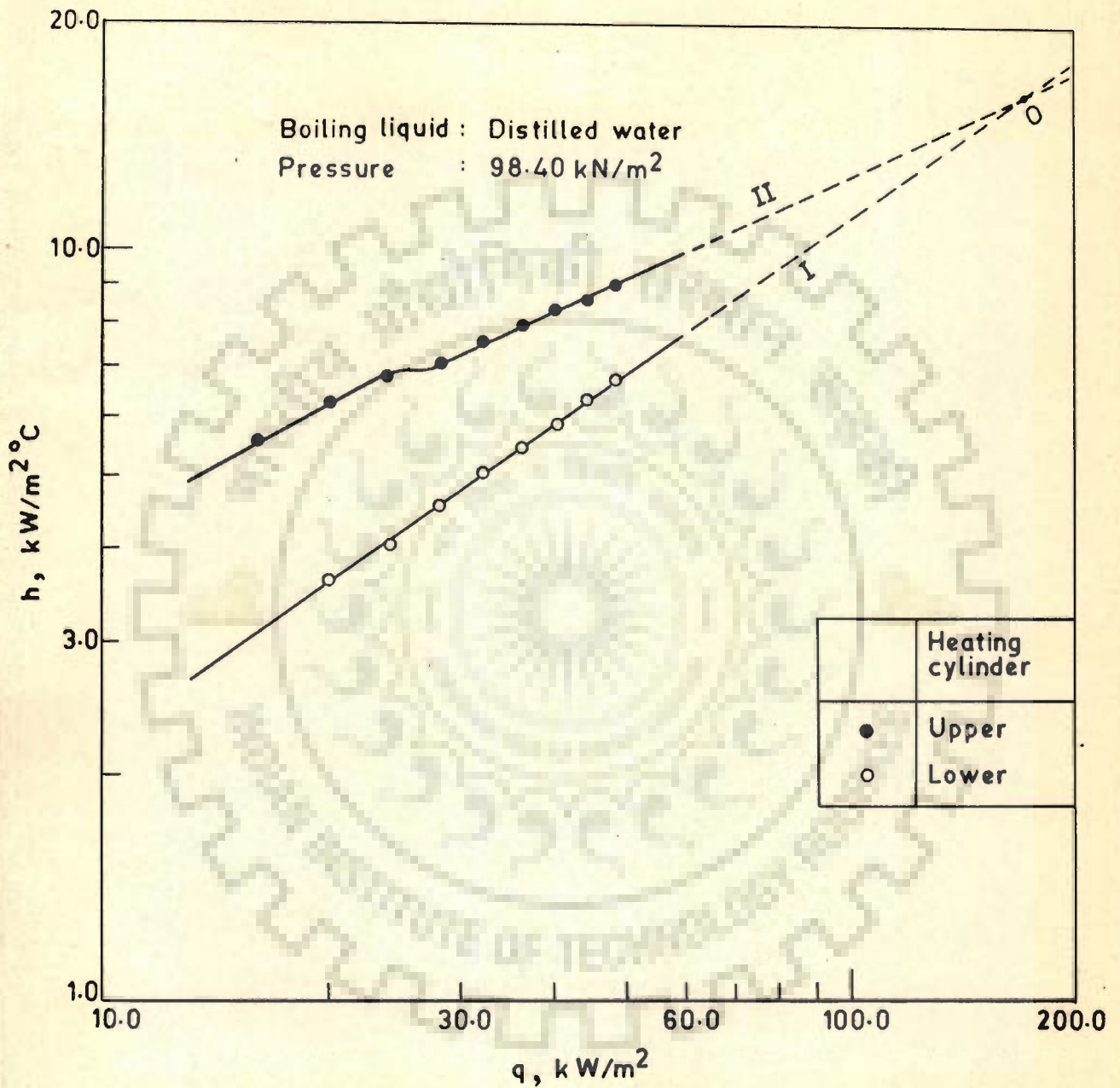


Fig 6.46 Variation of heat transfer coefficient with heat flux for upper and lower heating cylinders

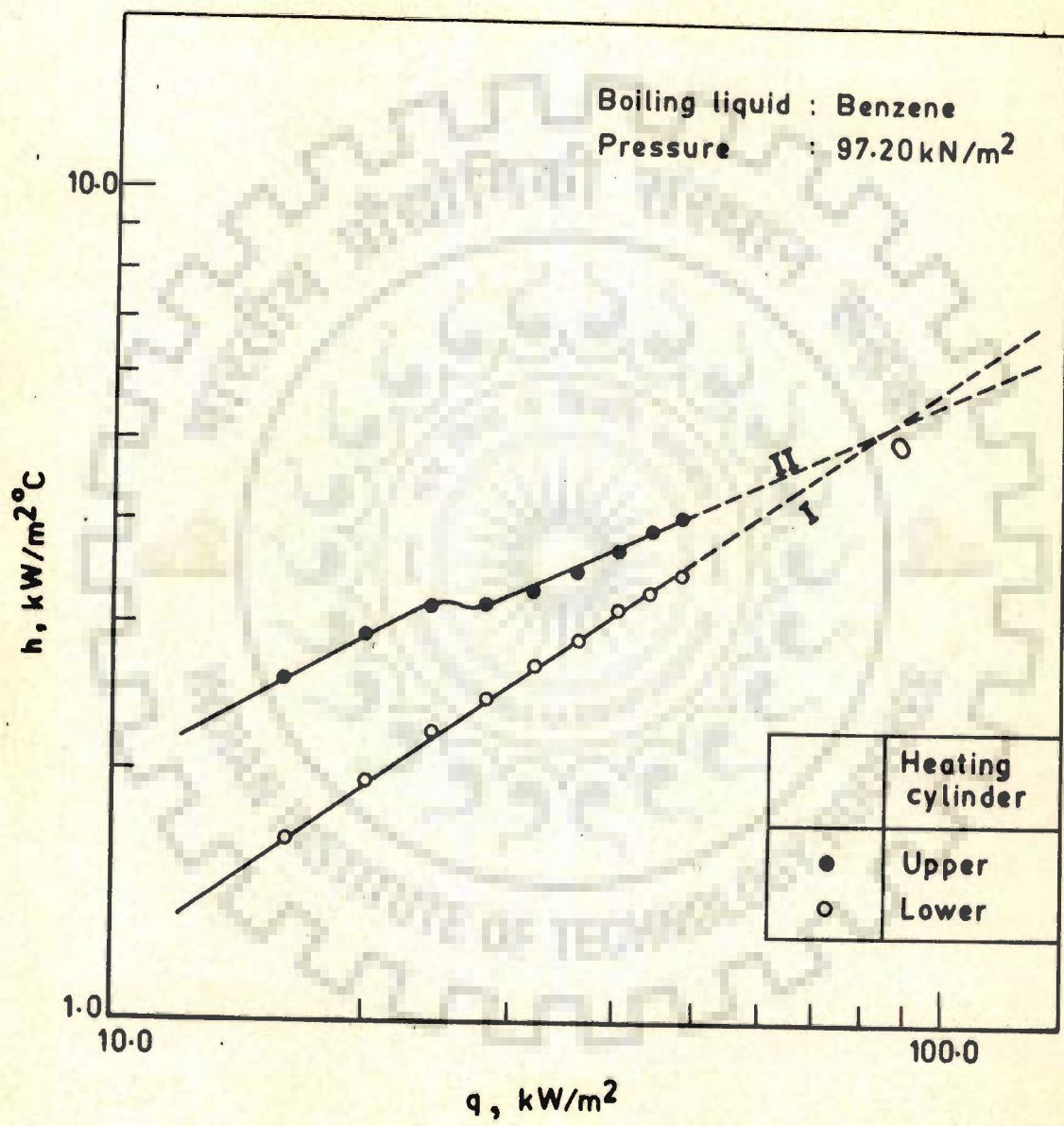


Fig 6.47 Variation of heat transfer coefficient with heat flux for upper and lower heating cylinders

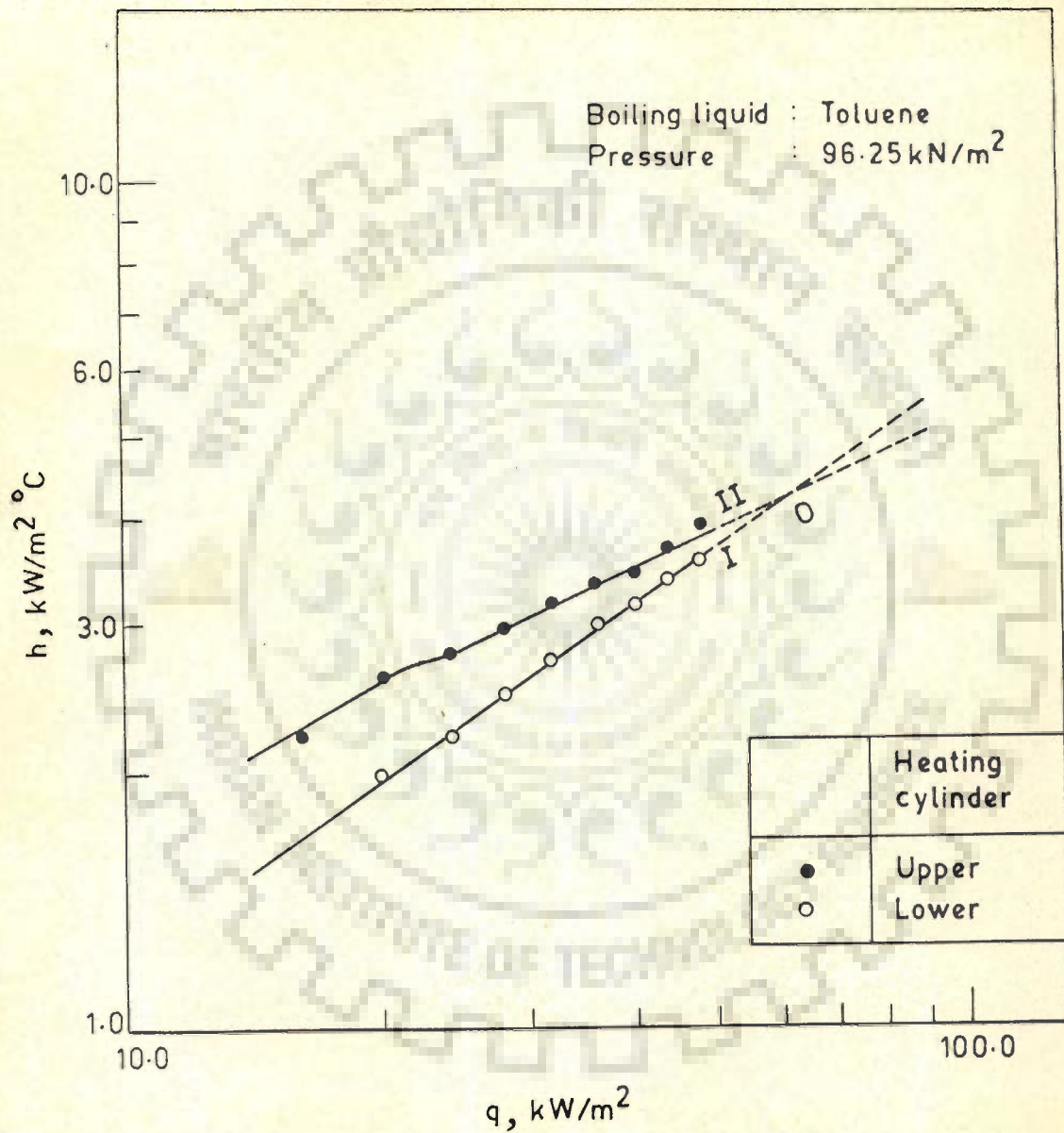


Fig 6.48 Variation of heat transfer coefficient with heat flux for upper and lower heating cylinders



the rate at which it changes with heat flux is not governed by the above relationship, Eq (6.13). This has the following relationship (curve II) :

a. For  $q \leq 24.252 \text{ kW/m}^2$

$$h = C_7 q^{0.55} \quad \dots(6.14)$$

b. For  $q \geq 28.294 \text{ kW/m}^2$

$$h = C_8 q^{0.45} \quad \dots(6.15)$$

where constants,  $C_6$ ,  $C_7$  and  $C_8$  of Eqs (6.13), (6.14) and (6.15) depends upon the boiling liquid and pressure for a given heating surface.

Further, all these curves possess a part of them represented by a 'dome' for the values of heat flux from  $24.252 \text{ kW/m}^2$  to  $28.294 \text{ kW/m}^2$ . It is interesting to mention that for this range of heat flux, data for other pressures also showed a similar behaviour.

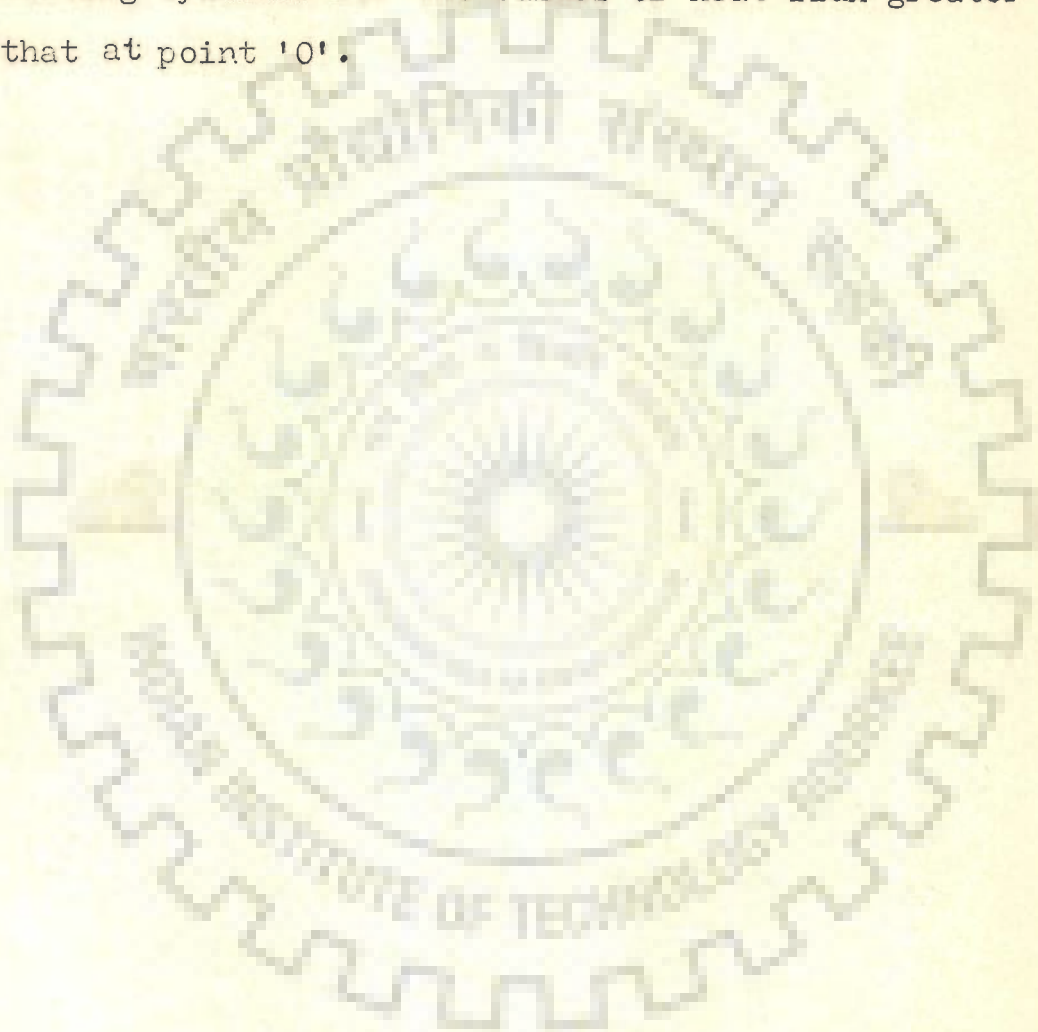
For a given heat flux, the upper heating cylinder has higher values of heat transfer coefficient than those for the lower heating cylinder due to the following reason :

The vapour bubbles from the lower heating cylinder rise up in the liquid. On their way up, they strike the upper heating surface and cause turbulence in the liquid enveloping it in addition to that due to the dynamics of the bubbles originating on the upper heating cylinder. Thus the heat transfer coefficient for the upper heating cylinder becomes greater.

The peculiar behaviour of curve II for the values of heat flux exceeding  $28.294 \text{ kW/m}^2$ , that the difference between the heat transfer coefficient of the upper and the lower heating cylinders decreases, seems to be due to the fact that the amount of vapours rising up from the lower heating cylinder to the upper heating cylinder increases with the rise in heat flux so much so that the vapours might be blanketing more and more portion of the surface of the upper cylinder to reduce its heat transfer coefficient progressively. This argument is further corroborated when curves I and II are extrapolated which shows that the difference in the values of heat transfer coefficient keeps on diminishing and ultimately disappears at a point-marked 'O'. At this 'point' the values of heat transfer coefficient for the upper and the lower heating cylinders equalise indicating that the effect of the vapour blanketing around the upper heating cylinder nullifies the increase in heat transfer coefficient of it due to induced turbulence created by the dynamics of the vapour bubbles rising up from the lower heating cylinder.

From the above it may be concluded that for an assembly of two heating cylinders the vapours from the lower heating cylinder contribute to increase the heat transfer coefficient of the upper heating cylinder appreciably only upto a certain value of heat flux. Beyond this value the heat transfer coefficient for upper cylinder is not much greater than that of the lower heating cylinder. The

difference between the two values keeps on decreasing and ultimately is expected to become zero at a heat flux corresponding to point 'O'. Further it is anticipated that the values of heat transfer coefficient for the upper heating cylinder might become smaller than those for the lower heating cylinder for the values of heat flux greater than that at point 'O'.



## CHAPTER 7

### CONCLUSIONS AND RECOMMENDATIONS

Some of the important conclusions emerging out from the present investigation pertaining to nucleate pool boiling of saturated liquids on horizontal heating cylinder(s) for subatmospheric to atmospheric pressures, ranging from  $3.82 \text{ kN/m}^2$  to  $101.33 \text{ kN/m}^2$ , and heat flux from  $6.870 \text{ kW/m}^2$  to  $48.504 \text{ kW/m}^2$  are listed below :

- A. When only one of the heating cylinders was energized electrically :
1. The value of wall superheat for the boiling of distilled water, benzene and toluene increases from top- to side-to bottom-position for all the values of pressure and heat flux.
  2. Average wall superheat for the boiling of distilled water, benzene, toluene and methanol under atmospheric and subatmospheric pressures is related to heat flux and pressure by the following equation within  $\pm 10$  per cent.

$$\bar{\Delta t}_w = \text{constant } q^{0.3} p^{-0.32}$$

where 'constant' is a function of boiling liquid and heating surface characteristics (liquid-surface combination) and its value is determined experimentally only.

3. The Alad'ev correlation for the calculation of average wall superheat for nucleate pool boiling of liquids does not correlate the experimental data for atmospheric and subatmospheric pressures. However, it is found that the correlation in its modified form succeeds to correlate the boiling heat transfer data of distilled water, benzene, toluene and methanol taken on heating surfaces of differing characteristics within  $\pm 10$  per cent. The modified correlation is given by the following equation :

$$\frac{\Delta \bar{t}_w}{T_s} = \text{constant} \left[ \frac{10^{-6} q \lambda}{g k_{\ell} T_s} \right]^{0.3} \left[ \frac{\lambda}{c_{\ell} T_s} \right]^{1.2} \left[ \frac{\rho_{\ell}}{\rho_v} \right]^{0.24}$$

where the value of 'constant' depends upon the boiling liquid and the heating surface characteristics (liquid-surface combination). All the physico-thermal properties are determined at the saturation temperatures of the boiling liquids.

4. Using the Transient Heat Conduction model and the Latent Heat Transport model with appropriate expressions for bubble departure diameter, bubble emission frequency and nucleation site density, a semi-theoretical equation for wall superheat for atmospheric and subatmospheric pressures has been recommended in the following form :

$$\frac{\bar{\Delta t}_w}{\bar{\Delta t}_{w,1}} = \left[ \frac{p}{p_1} \right]^{-0.589} \left[ \frac{\rho_\ell}{\rho_{\ell,1}} \right]^{-0.525} \left[ \frac{c_\ell}{c_{\ell,1}} \right]^{-0.675}$$

$$\left[ \frac{k_\ell}{k_{\ell,1}} \right]^{-0.3} \left[ \frac{T_s}{T_{s,1}} \right]^{0.024} \left[ \frac{\lambda}{\lambda_1} \right]^{0.276}$$

$$\left[ \frac{\rho_v}{\rho_{v,1}} \right]^{0.276} \left[ \frac{\sigma}{\sigma_1} \right]^{0.249} \left[ \frac{q}{q_1} \right]^{0.3}$$

where subscript '1' represents a reference pressure.

The above equation correlates the experimental data for the boiling of distilled water, benzene, toluene, methanol, ethanol, isopropanol and carbon tetra-chloride conducted on differing heating surfaces within  $\pm 10$  per cent implying that the effect of surface-liquid combination factor disappears when one attempts the ratio of wall superheat at different pressures. In other words surface-liquid combination factor for the boiling of liquid under subatmospheric pressures does not depend upon pressure.

This equation is advantageous to predict the value of average wall superheat,  $\bar{\Delta t}_w$  at a pressure,  $p$  and heat flux,  $q$  for the boiling of a liquid on a given heating surface from the knowledge of average wall superheat,  $\bar{\Delta t}_{w,1}$  at the reference pressure,  $p_1$  on the same heating surface for heat flux,  $q_1$  and the physico-thermal properties

appearing in the equation at pressures  $p$  and  $p_1$ . The reference pressure,  $p_1$  can be taken as atmospheric pressure or any other convenient pressure.

5. Based on the experimental data for atmospheric and subatmospheric pressures, it has been found that the ratio of average wall superheat for the boiling of benzene,  $(\Delta \bar{t}_w)_b$  to that of distilled water,  $(\Delta \bar{t}_w)_w$  for a given horizontal heating cylinder, heat flux and pressure bears a constant value equal to 1.98 whereas this ratio is equal to 1.85 for the boiling of toluene and distilled water.

In other words one can find the value of average wall superheat for the boiling of benzene,  $(\Delta \bar{t}_w)_b$  and also for the boiling of toluene,  $(\Delta \bar{t}_w)_t$  at a pressure,  $p$  and heat flux,  $q$  on a given heating surface from the knowledge of average wall superheat for the boiling of distilled water  $(\Delta \bar{t}_w)_w$  at pressure,  $p$  and heat flux,  $q$  on the same heating surface.

- B. When both the heating cylinders were energized electrically:
  1. The values of wall superheat of upper heating cylinder for the boiling of distilled water, benzene and toluene decrease regularly from the top- to the side- to the bottom-position, whereas for the lower heating cylinder they increase from the top- to the side- to the bottom-position for a given

pressure, heat flux and heating surface.

2. The vapour-bubbles emerging out from the lower heating cylinder of an assembly consisting of two heating cylinders kept one over the other show pronounced effect on the boiling heat transfer from the upper heating cylinder :

- a. For  $16.168 \leq q \leq 24.252 \text{ kW/m}^2$

The heat transfer coefficient for the boiling of liquids on the upper heating cylinder is related to heat flux by the following power law :

$$h = \text{constant } q^{0.55}$$

where the value of 'constant' is a function of boiling liquid for a given pressure and heating surface.

The heat transfer coefficient for the boiling of liquids on the lower heating cylinder is correlated by the following equation :

$$h = \text{constant } q^{0.7}$$

where the value of 'constant' depends on the boiling liquid for a given heating surface and pressure.

Further, the ratio of heat transfer coefficient from the upper heating cylinder for the boiling of distilled water to that of from the lower heating cylinder is 1.75, whereas it is



1.50 for the boiling of benzene and 1.30 for the boiling of toluene.

- b. For  $24.252 < q \leq 28.294 \text{ kW/m}^2$  :

The variation in heat transfer coefficient for the boiling of liquids on the upper heating cylinder with heat flux is represented by a 'dome' shaped curve, whereas that for the lower heating cylinder is represented by the same power law i.e.  $h = \text{constant } q^{0.7}$ .

- c. For  $28.294 < q \leq 48.504 \text{ kW/m}^2$ :

The values of heat transfer coefficient from the upper heating cylinder to the boiling liquids are governed by the following power law i.e.  $h = \text{constant } q^{0.45}$  and from the lower heating cylinder by the same power law ( $h = \text{constant } q^{0.7}$ ) where 'constant' depends on boiling liquid on a given heating surface and pressure.

Based on the results obtained in the present investigation the following is recommended for future studies :

1. The experimental data should be conducted for the assembly of two cylinder for the value of heat flux exceeding  $48.504 \text{ kW/m}^2$  to cover the situation when the upper heating cylinder will be blanketed with the vapour bubble emerging

out from the lower heating cylinder considerably resulting in a situation when the heat transfer coefficient of the upper heating cylinder becomes smaller than that of the lower heating cylinder.

2. The experimental data for the boiling of liquids on the heating cylinders should be extended to more than 2 tubes spaced on the standard triangular and square pitches as practised in shell and tube exchangers. This represents a real industrial situation and thereby the results will be of great value to the design engineers.
3. It will be worthwhile if the above data are also conducted on the tubes of different materials as commonly used in industrial reboilers and vaporizers.

## APPENDIX A

### CIRCUMFERENTIAL TEMPERATURE AVERAGING

Because of non-uniform boiling conditions around the heating cylinder the temperature of the wall and that of the liquid have been measured at the top-, at the side- and at the bottom- position of the heating cylinder. Following procedure has been used for averaging them:

The average wall temperature  $\bar{t}_w$  was obtained by the use of the following equation :

$$\bar{t}_w = \frac{1}{2\pi} \int_0^{2\pi} t_w(\theta) d\theta \quad \dots(A.1)$$

where ' $\theta$ ' denotes the circumferential position at which wall temperature was measured.

As Simpson's rule is reasonably accurate and a simple method of integration, it has been considered for the averaging purpose as given below :

$$\text{Let } t_w = F(\theta)$$

where  $F(\theta)$  is a function which represents the wall temperature  $t_{w0}, t_{w1}, t_{w2}, \dots, t_{wn}$  at the respective equidistant positions  $\theta_0, \theta_1, \theta_2, \dots, \theta_n$  on the circumference of the heating cylinder. Further, the interval between the two successive  $\theta$ 's be represented by  $h$ .

Applying Newton's interpolation formula, the following relationship is derived :

$$d\theta = h du \quad \dots(A.2)$$

$$\text{where } u = \frac{\theta - \theta_0}{h}$$

Integrating Eq (A.2) over n intervals of space h (=d $\theta$ ) the following is obtained :

$$\int_{\theta_0}^{\theta_0+nh} t_w d\theta = h \int_0^n \left[ t_{w0} + u \Delta t_{w0} + \frac{u(u-1)}{2!} \Delta^2 t_{w0} + \dots \right] du$$

$$\text{where } \Delta t_{w0} = t_{w1} - t_{w0}$$

$$\begin{aligned} \text{and } \Delta^2 t_{w0} &= \Delta t_{w1} - \Delta t_{w0} \\ &= [(t_{w2} - t_{w1}) - (t_{w1} - t_{w0})] \\ &= [t_{w2} - 2t_{w1} + t_{w0}] \end{aligned}$$

or

$$\int_{\theta_0}^{\theta_0+nh} t_w d\theta = h \left[ n t_{w0} + \frac{n^2}{2} \Delta t_{w0} + \left( \frac{n^3}{3} - \frac{n^2}{2} \right) \frac{\Delta^2 t_{w0}}{2} + \dots \right] \quad \dots(A.3)$$

The subscript, 1 refers to the top-position whereas subscripts, 0 and 2 for the two side-positions of the heating cylinder.

The present experimentation involved the measurement of the wall temperature at three circumferential positions,  $90^\circ (= \pi/2)$  apart at the top-, the side- and the bottom- of the heating cylinder. Therefore a two-step length ( $n=2$ ) is considered. With this the above equation (A.3) is written as :

$$\begin{aligned}
 \int_{\theta_0}^{\theta_0+2h} t_w d\theta &= h \left[ 2t_{w0} + \Delta t_{w0} + \left( \frac{8}{3} - 2 \right) \frac{\Delta^2 t_{w0}}{2} + \dots \right] \\
 &= h \left[ 2t_{w0} + (t_{w1} - t_{w0}) + \left( \frac{8}{3} - 2 \right) (t_{w2} - 2t_{w1} + t_{w0}) \right. \\
 &\quad \left. + \dots \right] \quad \dots(A.4)
 \end{aligned}$$

Neglecting the difference terms above the second derivative, Eq (A.4) assumes the following form :

$$\begin{aligned}
 \int_{\theta_0}^{\theta_0+2h} t_w d\theta &= h \left[ 2 t_{w0} + (t_{w1} - t_{w0}) + \left( \frac{8}{3} - 2 \right) (t_{w2} - 2t_{w1} + t_{w0}) \right] \\
 &= \frac{h}{3} \left[ t_{w0} + 4t_{w1} + t_{w2} \right] \quad \dots(A.5)
 \end{aligned}$$

Substituting  $h = \frac{\pi}{2}$  into Eq (A.5), the following is resulted :

$$\int_{\theta_0}^{\theta_0+2h} t_w d\theta = \frac{\pi}{6} \left[ t_{w0} + 4t_{w1} + t_{w2} \right] \quad \dots(A.6)$$

Inserting the value of the integral from (A.6) into (A.1), one gets

$$\begin{aligned}
 \bar{t}_w &= \frac{1}{2\pi} \left[ \frac{\pi}{6} ( t_{w0} + 4t_{w1} + t_{w2} ) + \frac{\pi}{6} ( t_{w2} + 4t_{w3} + t_{w0} ) \right] \\
 &= \frac{1}{12} ( 2t_{w0} + 4t_{w1} + 2t_{w2} + 4t_{w3} ) \quad \dots(A.7)
 \end{aligned}$$

The subscript, 3 represents the bottom- position.

Due to the symmetry of the boiling conditions about the vertical central plane of the heating cylinder, the wall temperature corresponding to the two side- positions would be equal. Therefore,

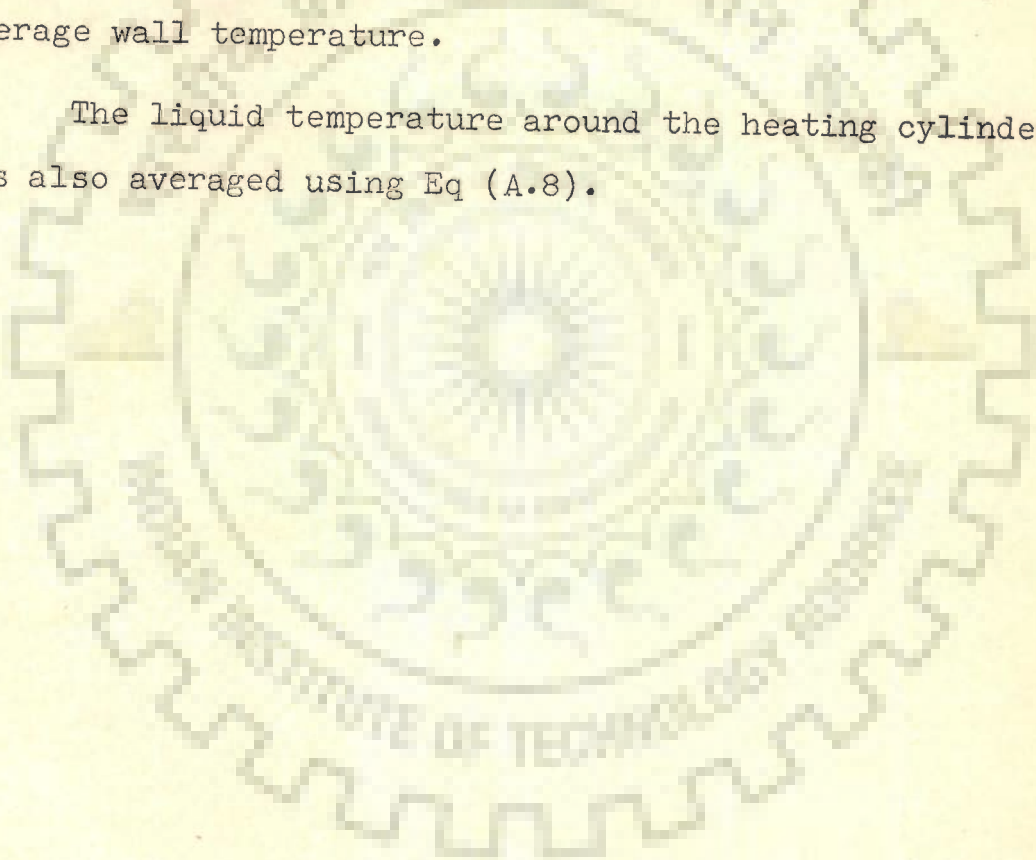
$$t_{w2} = t_{wo}$$

Using the above relationship in Eq (A.7) the following final equation is obtained :

$$\bar{t}_w = \frac{1}{3} ( t_{wo} + t_{w1} + t_{w2} ) \quad \dots(A.8)$$

Eq (A.8) is a simple equation representing the arithmetic mean of the wall temperatures as the average wall temperature. This equation has been used for getting average wall temperature.

The liquid temperature around the heating cylinder was also averaged using Eq (A.8).



## APPENDIX B

### TABULATION OF EXPERIMENTAL DATA

Table B.1 Experimental data for boiling heat transfer from the upper heating cylinder (lower heating cylinder was not heated)

Table B.2 Experimental data for boiling heat transfer from the lower heating cylinder (upper heating cylinder was not heated)

Table B.3 Experimental data for boiling heat transfer from the upper and the lower heating cylinders

#### Nomenclature

$p$	Pressure
$q$	Heat flux
$t_w$	Wall temperature
$t_l$	Liquid temperature

Subscripts 1,2 and 3 represent top-, side- and bottom-position of the heating cylinder(s) respectively.

Table B.1 Experimental data for boiling heat transfer from the upper heating cylinder (lower heating cylinder was not heated)

Run No.	Heat flux, $W/m^2$ $q$	Recorded temperatures					
		Wall temperature, $^{\circ}C$			Liquid temperature, $^{\circ}C$		
		$(t_w)_1$	$(t_w)_2$	$(t_w)_3$	$(t_l)_1$	$(t_l)_2$	$(t_l)_3$
Boiling liquid - Distilled water							
$p = 98.00 \text{ kN/m}^2$							
1	20210.19	108.40	110.50	111.10	100.25	100.25	100.25
2	24252.22	109.70	111.55	112.25	100.25	100.25	100.25
3	28294.26	110.40	112.74	113.60	100.25	100.25	100.25
4	32336.30	111.65	113.55	114.65	100.25	100.25	100.25
5	36378.33	112.60	114.75	115.80	100.25	100.25	100.25
6	40420.37	113.65	115.75	116.80	100.25	100.25	100.25
7	44462.41	114.60	116.92	117.87	100.25	100.25	100.25
8	48504.45	115.65	118.05	118.73	100.25	100.25	100.25
$p = 71.16 \text{ kN/m}^2$							
9	20210.19	100.50	102.75	103.05	91.75	91.75	91.75
10	24252.22	101.80	103.80	104.25	91.75	91.75	91.75
11	28294.26	103.00	104.90	105.45	91.75	91.75	91.75
12	32336.30	104.20	106.00	106.45	91.75	91.75	91.75



Table B.1 contd.

Run No.	Heat flux, $W/m^2$ $q$	Recorded temperatures					
		Wall temperature, $^{\circ}C$			Liquid temperature $^{\circ}C$		
		$(t_w)_1$	$(t_w)_2$	$(t_w)_3$	$(t_l)_1$	$(t_l)_2$	$(t_l)_3$
13	36378.33	105.30	107.10	107.50	91.75	91.75	91.75
14	40420.37	106.30	108.20	108.60	91.75	91.75	91.75
15	44462.41	107.35	109.20	109.70	91.75	91.75	91.75
16	48504.45	108.35	110.25	110.80	91.75	91.75	91.75
		$p = 57.93 \text{ kN/m}^2$					
17	20210.19	94.90	95.90	96.45	85.35	85.35	85.35
18	24252.22	96.40	97.18	98.15	85.35	85.35	85.35
19	28294.26	97.60	98.25	99.45	85.35	85.35	85.35
20	32336.30	98.75	99.45	100.50	85.35	85.35	85.35
21	36378.33	99.85	100.65	101.60	85.35	85.35	85.35
22	40420.37	100.83	101.70	102.75	85.35	85.35	85.35
23	44462.41	101.90	102.65	103.90	85.35	85.35	85.35
24	48504.45	103.00	103.85	104.80	85.35	85.35	85.35
		$p = 44.50 \text{ kN/m}^2$					
25	20210.19	90.40	91.80	92.95	80.25	80.25	80.25
26	24252.22	91.60	93.10	94.10	80.25	80.25	80.25
27	28294.26	92.75	94.20	95.40	80.25	80.25	80.25
28	32336.30	94.00	95.40	96.50	80.25	80.25	80.25

Table B.1 contd.

Run No.	Heat flux, $W/m^2$ $q$	Recorded temperatures					
		Wall temperature, $^{\circ}C$			Liquid temperature, $^{\circ}C$		
		$(t_w)_1$	$(t_w)_2$	$(t_w)_3$	$(t_l)_1$	$(t_l)_2$	$(t_l)_3$
29	36378.33	95.10	96.50	97.60	80.25	80.25	80.25
30	40420.37	96.30	97.50	98.70	80.25	80.25	80.25
31	44462.41	97.35	98.70	99.85	80.25	80.25	80.25
32	48504.45	98.50	99.75	101.00	80.25	80.25	80.25
$p = 31.26 \text{ kN/m}^2$							
33	20210.19	82.38	83.30	84.83	71.25	71.25	71.25
34	24252.22	83.70	83.55	86.10	71.25	71.25	71.25
35	28294.26	84.75	85.85	87.40	71.25	71.25	71.25
36	32336.30	85.77	87.15	78.70	71.25	71.25	71.25
37	36378.33	86.72	88.05	89.60	71.25	71.25	71.25
38	40420.37	87.95	89.05	92.80	71.25	71.25	71.25
39	44462.41	89.18	90.48	92.25	71.25	71.25	71.25
40	48504.45	90.25	91.65	93.35	71.25	71.25	71.25
Boiling liquid - Benzene $p = 96.86 \text{ kN/m}^2$							
41	16168.15	91.25	92.90	93.70	79.55	79.55	79.55
42	20210.19	92.75	94.40	95.20	79.55	79.55	79.55

Table B.1 contd.

Run No.	Heat flux, $W/m^2$ $q$	Recorded temperatures					
		Wall temperature, $^{\circ}C$			Liquid temperature, $^{\circ}C$		
		$(t_w)_1$	$(t_w)_2$	$(t_w)_3$	$(t_l)_1$	$(t_l)_2$	$(t_l)_3$
43	24252.22	94.15	95.80	96.60	79.55	79.55	79.55
44	28294.26	95.65	97.30	98.10	79.55	79.55	79.55
45	32336.30	96.85	98.50	99.30	79.55	79.55	79.55
46	36378.33	98.25	99.90	100.70	79.55	79.55	79.55
47	40420.37	99.40	101.25	101.90	79.55	79.55	79.55
48	44462.41	100.70	102.60	103.25	79.55	79.55	79.55
49	48504.45	102.04	103.94	104.54	79.55	79.55	79.55
$p = 70.66 \text{ kN/m}^2$							
50	16168.15	84.35	85.55	86.45	70.65	70.65	70.65
51	20210.19	85.95	87.15	88.10	70.65	70.65	70.65
52	24252.22	87.45	88.65	89.65	70.65	70.65	70.65
53	28294.26	88.90	90.10	91.10	70.65	70.65	70.65
54	32336.30	90.20	91.40	92.65	70.65	70.65	70.65
55	36378.33	91.50	92.70	94.10	70.65	70.65	70.65
56	40420.37	92.90	94.00	95.40	70.65	70.65	70.65
57	44462.41	94.00	95.20	96.80	70.65	70.65	70.65
58	48504.45	95.20	96.70	97.80	70.65	70.65	70.65

Table B.1 contd.

Run No.	Heat flux, $W/m^2$ $q$	Recorded temperatures					
		Wall temperature, $^{\circ}C$			Liquid temperature, $^{\circ}C$		
		$(t_w)_1$	$(t_w)_2$	$(t_w)_3$	$(t_l)_1$	$(t_l)_2$	$(t_l)_3$
$p = 57.66 \text{ kN/m}^2$							
59	16168.15	79.65	80.90	81.70	65.15	65.15	65.15
60	20210.19	81.15	82.50	83.75	65.15	65.15	65.15
61	24252.22	82.15	84.10	85.75	65.15	65.15	65.15
62	28294.26	83.50	85.15	87.30	65.15	65.15	65.15
63	32336.30	84.75	87.00	89.00	65.15	65.15	65.15
64	36378.33	86.05	88.05	90.73	65.15	65.15	65.15
65	40420.37	87.55	89.35	91.95	65.15	65.15	65.15
66	44462.41	88.65	91.00	93.10	65.15	65.15	65.15
67	48504.45	89.95	92.55	94.15	65.15	65.15	65.15
$p = 44.00 \text{ kN/m}^2$							
68	16168.15	73.10	74.55	76.20	57.95	57.95	57.95
69	20210.19	74.80	76.25	78.00	57.95	57.95	57.95
70	24252.22	76.30	77.85	79.70	57.95	57.95	57.95
71	28294.26	77.80	79.40	81.30	59.95	57.95	57.95
72	32336.30	79.20	80.80	82.80	57.95	57.95	57.95

Table B.1 contd.

Run No.	Heat flux, $W/m^2$ $q$	Recorded temperatures					
		Wall temperature, $^{\circ}C$			Liquid temperature, $^{\circ}C$		
		$(t_w)_1$	$(t_w)_2$	$(t_w)_3$	$(t_l)_1$	$(t_l)_2$	$(t_l)_3$
73	36378.33	80.65	82.25	84.25	57.95	57.95	57.95
74	40420.37	82.00	83.60	85.60	57.95	57.95	57.95
75	44462.41	83.35	84.95	87.00	57.95	57.95	57.95
76	48504.45	84.65	86.30	88.40	57.95	57.95	57.95
$p = 33.40 \text{ kN/m}^2$							
77	16168.15	64.95	66.60	68.45	48.30	48.30	48.30
78	20210.19	66.75	68.60	70.55	48.30	48.30	48.30
79	24252.22	68.50	70.30	72.35	48.30	48.30	48.30
80	28294.26	70.00	71.90	73.95	48.30	48.30	48.30
81	32336.30	71.60	73.50	75.65	48.30	48.30	48.30
82	36378.33	73.00	74.95	77.30	48.30	48.30	48.30
83	40420.37	74.45	76.00	78.80	48.30	48.30	48.30
84	44462.41	75.95	77.50	80.35	48.30	48.30	48.30
85	48504.45	77.00	79.50	81.45	48.30	48.30	48.30

Table B.1 contd.

Run No.	Heat flux, $W/m^2$ $q$	Recorded temperatures					
		Wall temperature, $^{\circ}C$			Liquid temperature, $^{\circ}C$		
		$(t_w)_1$	$(t_w)_2$	$(t_w)_3$	$(t_l)_1$	$(t_l)_2$	$(t_l)_3$
Boiling liquid - Toluene							
$p = 96.00 \text{ kN/m}^2$							
86	20210.19	122.53	124.30	125.65	109.90	109.90	109.90
87	24252.22	123.45	125.85	126.90	109.90	109.90	109.90
88	28294.26	125.20	127.55	128.35	109.90	109.90	109.90
89	32336.30	126.65	128.80	129.80	109.90	109.90	109.90
90	36378.33	128.05	129.90	130.74	109.90	109.90	109.90
91	40420.37	129.50	131.35	131.95	109.90	109.90	109.90
92	44462.41	130.75	132.40	133.00	109.90	109.90	109.90
93	48504.45	132.20	133.60	134.20	109.90	109.90	109.90
$p = 69.33 \text{ kN/m}^2$							
94	20210.19	113.65	115.25	116.50	99.35	99.35	99.35
95	24252.22	115.50	117.00	118.40	99.35	99.35	99.35
96	28294.26	116.50	118.15	119.40	99.35	99.35	99.35

Table B.1 contd.

Run No.	Heat flux, $W/m^2$ $q$	Recorded temperatures					
		Wall temperature, $^{\circ}C$			Liquid temperature, $^{\circ}C$		
		$(t_w)_1$	$(t_w)_2$	$(t_w)_3$	$(t_l)_1$	$(t_l)_2$	$(t_l)_3$
97	32336.30	117.70	119.55	120.70	99.35	99.35	99.35
98	36378.33	119.00	121.00	122.00	99.35	99.35	99.35
99	40420.37	120.40	122.55	123.00	99.35	99.35	99.35
100	44462.41	121.60	124.05	124.35	99.35	99.35	99.35
101	48504.45	123.00	125.00	125.50	99.35	99.35	99.35
		$p = 56.60 \text{ kN/m}^2$					
102	20210.19	109.20	110.50	111.50	93.95	93.95	93.95
103	24252.22	110.60	111.90	113.05	93.95	93.95	93.95
104	28294.26	112.10	113.30	114.60	93.95	93.95	93.95
105	32336.30	113.80	114.75	115.70	93.95	93.95	93.95
106	36378.33	114.90	116.40	117.10	93.95	93.95	93.95
107	40420.37	116.30	117.60	118.45	93.95	93.95	93.95
108	44462.41	117.80	119.00	119.60	93.95	93.95	93.95
109	48504.45	119.30	120.25	120.70	93.95	93.95	93.95

Table B.1 contd.

Run No.	Heat flux, $W/m^2$ q	Recorded temperatures					
		Wall temperature, $^{\circ}C$			Liquid temperature, $^{\circ}C$		
		$(t_w)_1$	$(t_w)_2$	$(t_w)_3$	$(t_l)_1$	$(t_l)_2$	$(t_l)_3$
$p = 43.19 \text{ kN/m}^2$							
110	20210.19	102.40	104.30	104.50	86.25	86.25	86.25
111	24252.22	104.00	105.60	106.90	86.25	86.25	86.25
112	28294.26	105.60	107.30	108.10	86.25	86.25	86.25
113	32336.30	107.40	108.70	109.30	86.25	86.25	86.25
114	36378.33	108.30	110.20	110.70	86.25	86.25	86.25
115	40420.37	110.20	111.30	112.10	86.25	86.25	86.25
116	44462.41	111.90	112.50	113.05	86.25	86.25	86.25
117	48504.45	113.30	113.60	114.45	86.25	86.25	86.25
$p = 29.86 \text{ kN/m}^2$							
118	20210.19	94.60	95.70	96.80	76.90	76.90	76.90
119	24252.22	96.15	97.45	98.50	76.90	76.90	76.90
120	28294.26	97.65	99.35	100.15	76.90	76.90	76.90



Table B.1 contd.

Run No.	Heat flux, $W/m^2$ $q$	Recorded temperatures					
		Wall temperature, $^{\circ}C$			Liquid temperature, $^{\circ}C$		
		$(t_w)_1$	$(t_w)_2$	$(t_w)_3$	$(t_l)_1$	$(t_l)_2$	$(t_l)_3$
121	32336.30	99.20	100.80	101.70	76.90	76.90	76.90
122	36378.33	100.65	102.25	102.90	76.90	76.90	76.90
123	40420.37	102.10	103.75	104.35	76.90	76.90	76.90
124	44462.41	103.30	105.15	105.65	76.90	76.90	76.90
125	48504.45	104.70	106.65	107.20	76.90	76.90	76.90

Table B.2 Experimental data for boiling heat transfer from the lower heating cylinder (upper heating cylinder was not heated)

Run No.	Heat flux, $W/m^2$ $q$	Recorded temperatures					
		Wall temperature, $^{\circ}C$			Liquid temperature, $^{\circ}C$		
		$(t_w)_1$	$(t_w)_2$	$(t_w)_3$	$(t_l)_1$	$(t_l)_2$	$(t_l)_3$
Boiling liquid -- Distilled water $p = 93.00 \text{ kN/m}^2$							
1	20210.19	108.65	110.30	110.73	100.25	100.25	100.25
2	24252.22	109.70	111.55	111.85	100.25	100.25	100.25
3	28294.26	110.80	112.45	113.20	100.25	100.25	100.25
4	32336.30	111.95	113.50	114.28	100.25	100.25	100.25
5	36378.33	112.95	114.50	115.45	100.25	100.25	100.25
6	40420.37	113.93	115.56	116.60	100.25	100.25	100.25
7	44462.41	115.00	116.50	117.61	100.25	100.25	100.25
8	48504.45	116.05	117.53	118.60	100.25	100.25	100.25
$p = 71.16 \text{ kN/m}^2$							
9	20210.19	100.80	102.65	102.85	91.75	91.75	91.75
10	24252.22	102.00	103.75	104.10	91.75	91.75	91.75
11	28294.26	103.10	104.90	105.30	91.75	91.75	91.75
12	32336.30	104.25	106.00	106.35	91.75	91.75	91.75

Table B.1 contd.

Run No.	Heat flux, $W/m^2$ $q$	Recorded temperatures					
		Wall temperature, $^{\circ}C$			Liquid temperature, $^{\circ}C$		
		$(t_w)_1$	$(t_w)_2$	$(t_w)_3$	$(t_l)_1$	$(t_l)_2$	$(t_l)_3$
13	36378.33	105.30	107.15	107.45	91.75	91.75	91.75
14	40420.37	106.35	108.25	108.45	91.75	91.75	91.75
15	44462.41	107.40	109.25	109.60	91.75	91.75	91.75
16	48504.45	108.40	110.25	110.70	91.75	91.75	91.75
$p = 57.93 \text{ kN/m}^2$							
17	20210.19	94.85	96.40	97.00	85.35	85.35	85.35
18	24252.22	95.96	97.70	98.20	85.35	85.35	85.35
19	28294.26	97.20	99.00	99.44	85.35	85.35	85.35
20	32336.30	98.45	100.25	100.65	85.35	85.35	85.35
21	36378.33	99.45	101.13	101.60	85.35	85.35	85.35
22	40420.37	100.45	102.00	102.84	85.35	85.35	85.35
23	44462.41	101.37	103.10	104.00	85.35	85.35	85.35
24	48504.45	102.40	104.20	105.05	85.35	85.35	85.35
$p = 44.50 \text{ kN/m}^2$							
25	20210.19	90.80	91.70	92.48	80.25	80.25	80.25
26	24252.22	92.00	92.95	93.75	80.25	80.25	80.25
27	28294.26	93.20	94.05	95.00	80.25	80.25	80.25
28	32336.30	94.35	95.30	96.10	80.25	80.25	80.25

Table B.2 contd.

Run No.	Heat flux, $W/m^2$ q	Recorded temperatures					
		Wall temperature, °C			Liquid temperature, °C		
		$(t_w)_1$	$(t_w)_2$	$(t_w)_3$	$(t_l)_1$	$(t_l)_2$	$(t_l)_3$
29	36378.33	95.45	96.40	97.25	80.25	80.25	80.25
30	40420.37	96.55	97.50	98.40	80.25	80.25	80.25
31	44462.41	97.60	98.65	99.50	80.25	80.25	80.25
32	48504.45	98.65	99.70	100.60	80.25	80.25	80.25
$p = 31.26 \text{ kN/m}^2$							
33	20210.19	82.70	83.33	84.20	71.25	71.25	71.25
34	24252.22	83.95	84.70	85.47	71.25	71.25	71.25
35	28294.26	84.95	86.10	86.70	71.25	71.25	71.25
36	32336.30	85.95	87.10	88.37	71.25	71.25	71.25
37	36378.33	87.20	88.10	89.60	71.25	71.25	71.25
38	40420.37	88.10	89.20	91.00	71.25	71.25	71.25
39	44462.41	89.10	90.45	92.10	71.25	71.25	71.25
40	48504.45	90.35	91.90	93.40	71.25	71.25	71.25
Boiling liquid - Benzene							
$p = 96.86 \text{ kN/m}^2$							
41	16168.15	91.55	92.40	93.75	79.55	79.55	79.55
42	20210.19	93.15	94.35	95.35	79.55	79.55	79.55
43	24252.22	94.30	95.70	96.80	79.55	79.55	79.55
44	28294.26	95.70	97.40	98.50	79.55	79.55	79.55

Table B.1 contd.

Run No.	Heat flux, $W/m^2$	Recorded temperature					
		Wall temperature, $^{\circ}C$			Liquid temperature, $^{\circ}C$		
		$(t_w)_1$	$(t_w)_2$	$(t_w)_3$	$(t_l)_1$	$(t_l)_2$	$(t_l)_3$
45	32336.30	96.35	98.55	99.60	79.55	79.55	79.55
46	36378.33	97.95	100.05	101.13	79.55	79.55	79.55
47	40420.37	99.10	101.38	102.40	79.55	79.55	79.55
48	44462.41	100.18	102.65	103.80	79.55	79.55	79.55
49	48504.45	101.70	104.13	105.20	79.55	79.55	79.55
$p = 70.66 \text{ kN/m}^2$							
50	16168.15	84.10	85.40	86.40	70.55	70.55	70.55
51	20210.19	85.25	86.95	88.20	70.55	70.55	70.55
52	24252.22	86.35	86.65	90.15	70.55	70.55	70.55
53	28294.26	87.40	90.10	91.95	70.55	70.55	70.55
54	32336.30	88.45	91.70	93.85	70.55	70.55	70.55
55	36378.33	89.35	93.20	95.80	70.55	70.55	70.65
56	40420.37	90.30	94.80	97.80	70.65	70.65	70.65
57	44462.41	91.15	96.00	99.45	70.65	70.65	70.65
58	48504.45	92.05	97.43	101.35	70.65	70.65	70.65
$p = 57.60 \text{ kN/m}^2$							
59	16168.15	79.10	81.15	81.70	65.05	65.05	65.05
60	20210.19	80.30	82.80	83.70	65.05	65.05	65.05

Table B.2 contd.

Run No.	Heat flux, $W/m^2$ q	Recorded temperatures					
		Wall temperature, °C			Liquid temperature, °C		
		$(t_w)_1$	$(t_w)_2$	$(t_w)_3$	$(t_l)_1$	$(t_l)_2$	$(t_l)_3$
61	24252.22	81.40	84.20	85.80	65.05	65.05	65.05
62	28294.26	82.50	85.50	87.60	65.05	65.05	65.05
63	32336.30	83.35	87.10	89.60	65.05	65.05	65.05
64	36378.33	84.30	88.60	91.70	65.05	65.05	65.05
65	40420.37	85.40	90.10	93.80	65.15	65.15	65.15
66	44462.41	86.40	91.47	95.75	65.15	65.15	65.15
67	48504.45	87.35	83.00	97.60	65.15	65.15	65.15
		$p = 44.00 \text{ kN/m}^2$					
68	16168.15	72.75	74.50	76.35	57.90	57.90	57.90
69	20210.19	73.90	76.10	78.38	57.90	57.90	57.90
70	24252.22	75.00	77.62	80.20	57.95	57.95	57.95
71	28294.26	76.15	79.10	82.15	57.95	57.95	57.95
72	32336.30	77.28	80.72	84.15	57.95	57.95	57.95
73	36378.33	78.20	82.10	86.05	57.95	57.95	57.95
74	40420.37	79.23	83.60	88.25	57.95	57.95	57.95
75	44462.41	80.20	85.65	90.13	57.95	57.95	57.95
76	48504.45	81.05	86.35	92.00	57.95	57.95	57.95

Table B.2 contd.

Run No.	Heat flux, $W/m^2$ $q$	Recorded temperatures					
		Wall temperature, $^{\circ}C$			Liquid temperature, $^{\circ}C$		
		$(t_w)_1$	$(t_w)_2$	$(t_w)_3$	$(t_l)_1$	$(t_l)_2$	$(t_l)_3$
$p = 33.40 \text{ kN/m}^2$							
77	16168.15	65.15	66.95	67.90	48.30	48.30	48.30
78	20210.19	66.38	68.65	70.05	48.30	48.30	48.30
79	29252.22	67.70	70.35	72.05	48.30	48.30	48.30
80	28294.26	69.23	71.95	73.98	48.30	48.30	48.30
81	32336.30	70.60	73.55	76.05	48.30	48.30	48.30
82	36378.33	71.75	75.08	78.25	48.30	48.30	48.30
83	40420.37	72.98	76.38	80.28	48.30	48.30	48.30
84	44462.41	74.20	77.80	82.05	48.30	48.30	48.30
85	48504.45	75.20	78.85	83.35	48.30	48.30	48.30
Boiling liquid - Toluene							
$p = 96.15 \text{ kN/m}^2$							
86	20210.19	123.00	125.00	125.20	109.90	109.90	110.15
87	24252.22	125.10	126.50	126.75	109.90	109.90	110.15
88	28294.26	126.40	127.50	128.10	109.90	109.90	110.15
89	32336.30	127.35	129.00	129.60	109.90	109.90	110.15
90	36378.33	128.35	130.00	130.90	109.90	109.90	110.15
91	40420.37	129.30	131.40	132.70	109.90	109.90	110.15

Table B.2 contd.

Run No.	Heat flux, $W/m^2$ $q$	Recorded temperatures					
		Wall temperature, °C			Liquid temperature, °C		
		$(t_w)_1$	$(t_w)_2$	$(t_w)_3$	$(t_l)_1$	$(t_l)_2$	$(t_l)_3$
92	44462.41	130.20	132.60	134.00	109.90	109.90	110.15
93	48504.45	131.40	133.80	135.80	109.90	109.90	110.15
$p = 69.93 \text{ kN/m}^2$							
94	20210.19	114.50	115.50	115.85	99.35	99.35	99.60
95	24252.22	116.15	117.15	117.80	99.35	99.35	99.60
96	28294.26	117.25	118.35	119.10	99.35	99.35	99.60
97	32336.30	118.55	119.75	120.65	99.35	99.60	99.60
98	36378.33	119.75	121.05	122.10	99.35	99.60	99.60
99	40420.37	120.85	122.15	123.80	99.60	99.60	99.60
100	44462.41	121.90	123.30	125.30	99.60	99.60	99.60
101	48504.45	123.40	124.35	126.40	99.60	99.60	99.60
$p = 56.60 \text{ kN/m}^2$							
102	20210.19	109.00	111.00	111.85	93.95	93.95	94.15
103	24252.22	110.00	112.75	113.45	93.95	93.95	94.15
104	28294.26	111.65	113.90	115.05	93.95	93.95	94.15
105	32336.30	113.00	115.30	116.45	93.95	93.95	94.15



Table B.2 contd.

Run No.	Heat flux, $W/m^2$ $q$	Recorded temperatures					
		Wall temperature, $^{\circ}C$			Liquid temperature, $^{\circ}C$		
		$(t_w)_1$	$(t_w)_2$	$(t_w)_3$	$(t_l)_1$	$(t_l)_2$	$(t_l)_3$
106	36378.33	114.60	116.70	117.75	93.95	94.15	94.15
107	40420.37	115.90	117.80	118.70	94.15	94.15	94.15
108	44462.41	117.40	119.20	120.20	94.15	94.15	94.15
109	48504.45	118.40	120.20	121.30	94.15	94.15	94.15
		$p = 43.45 \text{ kN/m}^2$					
110	20210.19	103.00	104.00	105.10	86.45	86.45	86.45
111	24252.22	104.50	105.60	106.95	86.45	86.45	86.45
112	28294.26	105.70	107.10	108.70	86.45	86.45	86.45
113	32336.30	106.85	108.40	110.45	86.45	86.45	86.45
114	36378.33	108.05	109.70	112.20	86.45	86.45	86.45
115	40420.37	109.35	110.95	113.95	86.45	86.45	86.45
116	44462.41	110.45	112.20	115.70	86.45	86.45	86.45
117	48504.45	111.40	113.10	117.30	86.45	86.45	86.45
		$p = 29.86 \text{ kN/m}^2$					
118	20210.19	94.60	95.90	97.20	76.90	76.90	76.90
119	24252.22	95.95	97.20	98.80	76.90	76.90	76.90
120	28294.26	97.40	98.60	100.65	76.90	76.90	76.90
121	32336.30	98.70	100.40	102.40	76.90	76.90	76.90

Table B.2 contd.

Run No.	Heat flux, $W/m^2$ $q$	Recorded temperatures					
		Wall temperature, $^{\circ}C$			Liquid temperature, $^{\circ}C$		
		$(t_w)_1$	$(t_w)_2$	$(t_w)_3$	$(t_l)_1$	$(t_l)_2$	$(t_l)_3$
122	36378.33	100.00	101.80	103.90	76.90	76.90	76.90
123	40420.37	101.20	103.40	105.50	76.90	76.90	76.90
124	44462.41	102.40	104.70	107.00	76.90	76.90	76.90
125	48504.45	103.30	106.00	108.40	76.90	76.90	76.90

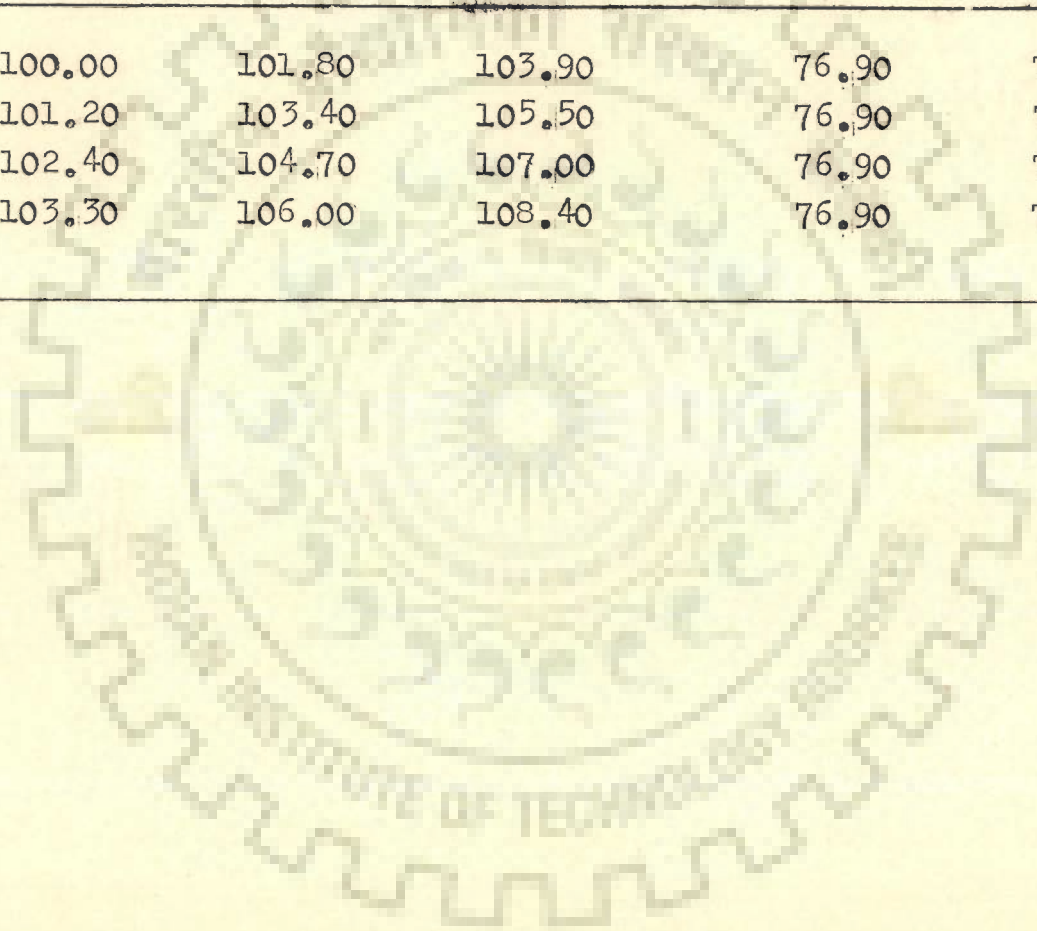


Table B.3 Experimental data for boiling heat transfer from the lower and the upper heating cylinders

Run No.	Heat flux, $W/m^2$ $q$	Heating cylinder	Recorded temperatures					
			Wall temperature, $^{\circ}C$			Liquid temperature, $^{\circ}C$		
			$(t_w)_1$	$(t_w)_2$	$(t_w)_3$	$(t_l)_1$	$(t_l)_2$	$(t_l)_3$
Boiling liquid-Distilled water								
$p = 98.40 \text{ kN/m}^2$								
1	16168.15	Upper	106.75	106.45	106.25	100.25	100.25	100.25
		Lower	107.60	109.10	109.65	100.25	100.25	100.25
2	20210.19	Upper	107.95	107.70	107.30	100.25	100.25	100.25
		Lower	108.75	110.25	110.75	100.25	100.25	100.25
3	24252.22	Upper	109.30	109.60	108.60	100.45	100.45	100.45
		Lower	110.25	111.35	112.20	100.45	100.45	100.45
4	28294.26	Upper	110.60	110.25	110.00	100.45	100.45	100.45
		Lower	111.30	112.45	113.30	100.45	100.45	100.45
5	32336.30	Upper	111.75	111.40	111.00	100.45	100.45	100.45
		Lower	112.40	113.50	114.45	100.45	100.45	100.45
6	36378.33	Upper	112.80	112.55	112.15	100.45	100.45	100.45
		Lower	113.45	114.60	115.50	110.45	100.45	100.45

Table B.5 contd.

Run No	Heat flux, $W/m^2$ $q$	Heating cylinder	Recorded temperatures					
			Wall temperature, $^{\circ}C$			Liquid temperature, $^{\circ}C$		
			$(t_w)_1$	$(t_w)_2$	$(t_w)_3$	$(t_l)_1$	$(t_l)_2$	$(t_l)_3$
7	40420.37	Upper	114.00	113.50	113.20	100.45	100.45	100.45
		Lower	114.50	115.70	116.60	100.45	100.45	100.45
8	44462.41	Upper	115.15	114.70	114.40	100.45	100.45	100.45
		Lower	115.50	116.75	117.50	100.45	100.45	100.45
9	48504.45	Upper	116.20	115.80	115.45	100.45	100.45	100.45
		Lower	116.40	117.90	118.50	100.45	100.45	100.45
$p = 71.50 \text{ kN/m}^2$								
10	16168.15	Upper	98.75	98.55	98.25	92.00	92.00	92.00
		Lower	99.40	101.80	102.20	92.00	92.00	92.00
11	20210.19	Upper	100.00	99.75	99.40	92.00	92.00	92.00
		Lower	100.95	102.85	103.25	92.00	92.00	92.00
12	24252.22	Upper	101.20	100.95	100.50	92.00	92.00	92.00
		Lower	102.25	103.90	104.45	92.00	92.00	92.00
13	28294.26	Upper	102.50	102.15	101.70	92.00	92.00	92.00
		Lower	103.35	105.20	105.70	92.00	92.00	92.00

Table B.5 contd.

Run No.	Heat flux, $W/m^2$ $q$	Heating cylinder	Recorded temperatures					
			Wall temperature, $^{\circ}C$			Liquid temperature, $^{\circ}C$		
			$(t_w)_1$	$(t_w)_2$	$(t_w)_3$	$(t_l)_1$	$(t_l)_2$	$(t_l)_3$
14	32336.30	Upper	103.65	103.35	102.95	92.00	92.00	92.00
		Lower	104.50	106.25	106.60	92.00	92.00	92.00
15	36378.33	Upper	104.75	104.35	104.15	92.00	92.00	92.00
		Lower	105.50	107.35	107.80	92.00	92.00	92.00
16	40420.37	Upper	106.00	105.50	105.20	92.00	92.00	92.00
		Lower	106.60	108.45	108.75	92.00	92.00	92.00
17	44462.41	Upper	107.03	106.55	106.25	92.00	92.00	92.00
		Lower	107.65	109.45	109.90	92.00	92.00	92.00
18	42504.45	Upper	108.15	107.60	107.35	92.00	92.00	92.00
		Lower	108.65	110.50	110.95	92.00	92.00	92.00
			$p = 57.90 \text{ kN/m}^2$					
19	16168.15	Upper	92.35	92.05	91.75	85.35	85.35	85.35
		Lower	93.40	95.35	96.00	85.35	85.35	85.35
20	20210.19	Upper	93.50	93.30	92.95	85.35	85.35	85.35
		Lower	94.80	96.45	97.00	85.35	85.35	85.35
21	24252.22	Upper	94.75	94.45	94.05	85.35	85.35	85.35
		Lower	95.90	97.65	98.30	85.25	85.35	85.35

Table B.3 contd.

Run No.	Heat flux, $W/m^2$ $q$	Heating cylinder	Recorded temperatures					
			Wall temperature, $^{\circ}C$			Liquid temperature, $^{\circ}C$		
			$(t_w)_1$	$(t_w)_2$	$(t_w)_3$	$(t_l)_1$	$(t_l)_2$	$(t_l)_3$
22	28294.26	Upper	96.05	95.80	95.35	85.35	85.35	85.35
		Lower	97.15	99.05	99.45	85.35	85.35	85.35
23	32336.30	Upper	97.30	96.90	96.60	85.35	85.35	85.35
		Lower	98.35	100.20	100.80	85.35	85.35	85.35
24	36378.33	Upper	98.40	98.00	97.75	85.35	85.35	85.35
		Lower	99.45	101.65	101.65	85.35	85.35	85.35
25	40420.37	Upper	99.55	99.10	98.85	85.35	85.35	85.35
		Lower	100.50	102.00	102.85	85.35	85.35	85.35
26	44462.41	Upper	100.70	100.20	99.85	85.35	85.35	85.35
		Lower	101.30	103.20	104.05	85.35	85.35	85.35
27	48504.45	Upper	101.70	101.20	101.00	85.35	85.35	85.35
		Lower	102.40	104.25	105.15	85.35	85.35	85.35
			$p = 44.50 \text{ kN/m}^2$					
28	16168.15	Upper	87.45	87.20	86.90	80.25	80.25	80.25
		Lower	89.05	90.50	91.30	80.25	80.25	80.25

Table B.3 contd.

Run No.	Heat flux, $W/m^2$ $q$	Heating cylinder	Recorded temperatures					
			Wall temperature, $^{\circ}C$			Liquid temperature, $^{\circ}C$		
			$(t_w)_1$	$(t_w)_2$	$(t_w)_3$	$(t_l)_1$	$(t_l)_2$	$(t_l)_3$
29	20210.19	Upper	88.70	88.40	88.05	80.25	80.25	80.25
		Lower	90.75	91.75	92.50	80.25	80.25	80.25
30	24252.22	Upper	89.85	89.55	89.25	80.25	80.25	80.25
		Lower	91.90	92.95	93.85	80.25	80.25	80.25
31	28294.26	Upper	91.25	90.25	90.45	80.25	80.25	80.25
		Lower	93.10	94.15	95.10	80.25	80.25	80.25
32	33336.30	Upper	92.55	92.00	91.70	80.25	80.25	80.25
		Lower	94.30	95.35	96.20	80.25	80.25	80.25
33	36378.33	Upper	93.60	93.00	92.85	80.25	80.25	80.25
		Lower	95.45	96.35	97.30	80.25	80.25	80.25
34	40420.37	Upper	94.75	94.25	94.00	80.25	80.25	80.25
		Lower	96.50	97.50	98.45	80.25	80.25	80.25
35	44462.41	Upper	95.90	95.30	95.05	80.25	80.25	80.25
		Lower	97.55	98.60	99.60	80.25	80.25	80.25
36	48504.45	Upper	97.00	96.40	96.15	80.25	80.25	80.25
		Lower	98.60	99.75	100.70	80.25	80.25	80.25

Table B.3 contd.

Run No.	Heat flux, $W/m^2$ $q$	Heating cylinder	Recorded temperatures					
			Wall temperature, $^{\circ}C$			Liquid temperature, $^{\circ}C$		
			$(t_w)_1$	$(t_w)_2$	$(t_w)_3$	$(t_l)_1$	$(t_l)_2$	$(t_l)_3$
Boiling liquid - Benzene $p = 97.20 \text{ kN/m}^2$								
37	16168.15	Upper	89.80	89.50	88.90	79.80	79.80	79.80
		Lower	91.80	92.85	93.80	79.80	79.80	79.80
38	20210.19	Upper	91.30	90.90	90.45	79.80	79.80	79.80
		Lower	93.50	94.60	95.50	79.80	79.80	79.80
39	24252.22	Upper	93.30	92.40	91.95	79.80	79.80	79.80
		Lower	94.60	96.10	96.80	79.80	79.80	79.80
40	28294.26	Upper	95.90	94.15	93.50	79.80	79.80	79.80
		Lower	96.00	97.70	98.60	79.80	79.80	79.80
41	32336.30	Upper	97.90	95.90	95.05	79.80	79.80	79.80
		Lower	97.15	98.80	99.80	79.80	79.80	79.80
42	36378.33	Upper	99.35	97.45	96.35	79.80	79.80	79.80
		Lower	98.30	100.40	101.20	79.80	79.80	79.80
43	40420.37	Upper	100.48	98.75	97.90	79.80	79.80	79.80
		Lower	99.40	101.65	102.60	79.80	79.80	79.80



Table B.3 contd.

Run No.	Heat flux, $W/m^2$ $q$	Heating cylinder	Recorded temperatures					
			Wall temperature, $^{\circ}C$			Liquid temperature, $^{\circ}C$		
			$(t_w)_1$	$(t_w)_2$	$(t_w)_3$	$(t_l)_1$	$(t_l)_2$	$(t_l)_3$
44	44462.41	Upper	101.55	100.25	99.15	79.80	79.80	79.80
		Lower	100.50	102.95	104.00	79.80	79.80	79.80
45	48504.45	Upper	102.70	101.75	100.70	79.80	79.80	79.80
		Lower	102.10	104.30	105.10	79.80	79.80	79.80
			$p = 70.60 \text{ kW/m}^2$					
46	16168.15	Upper	81.70	81.25	80.60	70.65	70.65	70.65
		Lower	84.10	85.50	86.60	70.65	70.65	70.65
47	20210.19	Upper	83.45	82.75	81.65	70.65	70.65	70.65
		Lower	85.35	87.10	90.35	70.65	70.65	70.65
48	24252.22	Upper	85.50	84.40	83.95	70.65	70.65	70.65
		Lower	87.50	90.20	92.10	70.65	70.65	70.65
49	28294.26	Upper	87.55	86.25	85.55	70.65	70.65	70.65
		Lower	87.50	90.20	92.10	70.65	70.65	70.65
50	32336.30	Upper	89.75	88.00	87.30	70.65	70.65	70.65
		Lower	88.60	91.75	93.95	70.65	70.65	70.65

Table B.3 contd.

Run No.	Heat flux, $W/m^2$	Heating cylinder	Recorded temperatures					
			Wall temperature, $^{\circ}C$			Liquid temperature, $^{\circ}C$		
			$(t_w)_1$	$(t_w)_2$	$(t_w)_3$	$(t_l)_1$	$(t_l)_2$	$(t_l)_3$
51	30378.33	Upper	91.00	89.20	88.35	70.65	70.65	70.65
		Lower	89.65	93.20	95.80	70.65	70.65	70.65
52	40420.37	Upper	92.70	90.70	90.05	70.65	70.65	70.65
		Lower	90.55	94.80	97.75	70.65	70.65	70.65
53	44462.41	Upper	93.80	92.05	91.60	70.65	70.65	70.65
		Lower	91.60	95.90	99.40	70.65	70.65	70.65
54	48504.45	Upper	95.70	93.40	92.95	70.65	70.65	70.65
		Lower	92.70	97.30	101.30	70.65	70.65	70.65
$p = 57.70 \text{ kN/m}^2$								
55	16168.15	Upper	76.30	75.75	75.25	65.15	65.15	65.15
		Lower	79.20	81.20	81.85	65.15	65.15	65.15
56	20210.19	Upper	78.55	77.90	77.30	65.15	65.15	65.15
		Lower	80.40	82.95	83.75	65.15	65.15	65.15
57	24252.22	Upper	80.15	79.25	78.60	65.15	65.15	65.15
		Lower	81.55	84.35	85.90	65.15	65.15	65.15

Table B.3 contd.

Run No.	Heat flux, $W/m^2$ $q$	Heating cylinder	Recorded temperatures					
			Wall temperature, $^{\circ}C$			Liquid temperature, $^{\circ}C$		
			$(t_w)_1$	$(t_w)_2$	$(t_w)_3$	$(t_l)_1$	$(t_l)_2$	$(t_l)_3$
58	28294.26	Upper	82.85	81.75	81.30	65.15	65.15	65.15
		Lower	82.65	85.65	87.65	65.15	65.15	65.15
59	32336.30	Upper	84.35	83.25	82.60	65.15	65.15	65.15
		Lower	83.45	87.20	89.40	65.15	65.15	65.15
60	36378.33	Upper	85.90	84.80	84.35	65.15	65.15	65.15
		Lower	84.50	88.60	91.75	65.15	65.15	65.15
61	40420.37	Upper	87.65	86.35	85.90	65.15	65.15	65.15
		Lower	85.65	90.25	93.75	65.15	65.15	65.15
62	44462.41	Upper	88.80	87.70	87.45	65.15	65.15	65.15
		Lower	86.70	91.60	95.75	65.15	65.15	65.15
63	48504.45	Upper	90.20	89.25	88.70	65.15	65.15	65.15
		Lower	87.80	93.00	97.60	65.15	65.15	65.15
			$p = 43.80 \text{ kN/m}^2$					
64	16168.15	Upper	70.80	70.00	68.65	57.85	57.85	57.85
		Lower	72.65	74.45	76.20	57.85	57.85	57.85

Table B.3 contd.

Run No.	Heat flux, $W/m^2$ $q$	Heating cylinder	Recorded temperatures					
			Wall temperature, $^{\circ}C$			Liquid temperature, $^{\circ}C$		
			$(t_w)_1$	$(t_w)_2$	$(t_w)_3$	$(t_l)_1$	$(t_l)_2$	$(t_l)_3$
65	20210.19	Upper	72.80	71.35	70.45	57.85	57.85	57.85
		Lower	73.80	76.10	73.25	57.85	57.85	57.85
66	24252.22	Upper	73.85	73.10	72.25	57.85	57.85	57.85
		Lower	74.95	77.50	80.05	57.85	57.85	57.85
67	28294.26	Upper	76.05	75.15	74.45	57.85	57.85	57.85
		Lower	76.00	78.90	82.00	57.85	57.25	57.85
68	32336.30	Upper	77.70	76.60	75.70	57.85	57.85	57.85
		Lower	77.10	80.65	84.00	57.85	57.85	57.85
69	36378.33	Upper	79.30	78.00	77.30	57.85	57.85	57.85
		Lower	78.05	82.00	85.90	57.85	57.85	57.85
70	40420.37	Upper	81.30	79.70	79.20	57.85	57.85	57.85
		Lower	79.15	83.50	83.15	57.85	57.85	57.85
71	44462.41	Upper	82.40	81.30	80.60	57.85	57.85	57.85
		Lower	80.20	85.30	90.25	57.85	57.85	57.85
72	48504.45	Upper	84.20	82.60	82.00	57.85	57.85	57.85
		Lower	81.15	86.30	91.80	57.85	57.85	57.85

Table B.3 contd.

Run No.	Heat flux, $W/m^2$ q	Heating cylinder	Recorded temperatures					
			Wall temperature, °C			Liquid temperature, °C		
			$(t_w)_1$	$(t_w)_2$	$(t_w)_3$	$(t_l)_1$	$(t_l)_2$	$(t_l)_3$
Boiling liquid-toluene p = 96.25 kN/m <sup>2</sup>								
73	16163.15	Upper	121.15	120.95	120.10	110.15	110.15	110.15
		Lower	121.60	123.60	124.05	110.15	110.15	110.15
74	20210.19	Upper	122.60	122.20	121.38	110.15	110.15	110.15
		Lower	123.10	125.00	125.10	110.15	110.15	110.15
75	24252.22	Upper	124.70	123.90	123.15	110.15	110.15	110.15
		Lower	125.30	126.40	126.70	110.15	110.15	110.15
76	28294.26	Upper	126.60	125.35	124.50	110.15	110.15	110.15
		Lower	126.50	127.60	127.90	110.15	110.15	110.15
77	32336.30	Upper	128.25	126.80	126.00	110.15	110.15	110.15
		Lower	127.45	129.10	129.40	110.15	110.15	110.15
78	36373.33	Upper	129.50	128.48	127.85	110.15	110.15	110.15
		Lower	128.50	130.10	130.65	110.15	110.15	110.15

Table B.3 contd.

Run No.	Heat flux, $W/m^2$	Heating cylinder	Recorded temperatures					
			Wall temperature, $^{\circ}C$			Liquid temperature, $^{\circ}C$		
			$(t_w)_1$	$(t_w)_2$	$(t_w)_3$	$(t_l)_1$	$(t_l)_2$	$(t_l)_3$
79	40420.37	Upper	130.73	130.10	129.10	109.90	109.90	109.90
		Lower	129.45	131.40	132.30	109.90	109.90	109.90
80	44462.41	Upper	131.75	131.15	130.30	109.90	109.90	109.90
		Lower	130.45	132.50	133.60	109.90	109.90	109.90
81	48504.45	Upper	132.78	132.15	131.88	109.90	109.90	109.90
		Lower	131.50	133.60	135.30	109.90	109.90	109.90
$p = 69.60 \text{ kN/m}^2$								
82	16168.15	Upper	110.80	110.40	109.75	99.35	99.35	99.35
		Lower	112.65	113.70	114.20	99.35	99.35	99.35
83	20210.19	Upper	112.40	112.00	111.35	99.35	99.35	99.35
		Lower	114.20	115.30	115.70	99.35	99.35	99.35
84	24252.22	Upper	114.15	113.70	112.90	99.35	99.35	99.35
		Lower	116.00	116.85	117.50	99.35	99.35	99.35
85	28294.26	Upper	116.30	115.65	114.80	99.35	99.35	99.35
		Lower	117.05	118.15	118.90	99.35	99.35	99.35

Table B.3 contd.

Run No.	Heat flux, $W/m^2$ $q$	Heating cylinder	Recorded temperatures					
			Wall temperature, $^{\circ}C$			Liquid temperature, $^{\circ}C$		
			$(t_w)_1$	$(t_w)_2$	$(t_w)_3$	$(t_l)_1$	$(t_l)_2$	$(t_l)_3$
86	32336.30	Upper	118.45	117.20	116.55	99.35	99.35	99.35
		Lower	118.20	119.45	120.40	99.35	99.35	99.35
87	36378.33	Upper	119.80	118.95	117.70	99.35	99.35	99.35
		Lower	119.40	120.75	121.90	99.35	99.35	99.35
88	40420.37	Upper	121.05	120.00	119.35	99.35	99.35	99.35
		Lower	120.60	121.90	123.50	99.35	99.35	99.35
89	44462.41	Upper	122.10	121.30	121.10	99.35	99.35	99.35
		Lower	121.80	123.10	125.00	99.35	99.35	99.35
90	48504.45	Upper	123.05	122.85	122.60	99.35	99.35	99.35
		Lower	122.95	124.30	126.30	99.35	99.35	99.35
			$p = 56.40 \text{ kN/m}^2$					
91	16168.15	Upper	105.85	105.25	104.70	93.95	93.95	93.95
		Lower	107.20	109.35	110.15	93.95	93.95	93.95
92	20210.19	Upper	107.50	107.00	106.70	93.95	93.95	93.95
		Lower	108.70	110.80	111.65	93.95	93.95	93.95
93	24252.22	Upper	109.45	108.85	108.30	93.95	93.95	93.95
		Lower	109.75	112.30	111.35	93.95	93.95	93.95

Table B.3 contd.

Run No.	Heat flux, $W/m^2$	Heating cylinder	Recorded temperatures					
			Wall temperature, $^{\circ}C$			Liquid temperature, $^{\circ}C$		
			$(t_w)_1$	$(t_w)_2$	$(t_w)_3$	$(t_l)_1$	$(t_l)_2$	$(t_l)_3$
94	28294.26	Upper	111.25	110.65	110.50	93.95	93.95	93.95
		Lower	111.20	113.70	114.95	93.95	93.95	93.95
95	32336.30	Upper	113.10	112.70	111.85	93.95	93.95	93.95
		Lower	112.60	115.10	116.30	93.95	93.95	93.95
96	36378.33	Upper	114.55	114.15	113.50	93.95	93.95	93.95
		Lower	114.10	116.50	117.70	93.95	93.95	93.95
97	40420.37	Upper	111.25	110.65	110.50	93.95	93.95	93.95
		Lower	115.50	117.60	118.80	93.95	93.95	93.95
98	44462.41	Upper	117.35	117.15	116.90	93.95	93.95	93.95
		Lower	117.00	118.90	120.10	93.95	93.95	93.95
99	48504.45	Upper	118.80	118.40	118.20	93.95	93.95	93.95
		Lower	118.20	120.00	121.20	93.95	93.95	93.95
			$p = 43.19 \text{ MPa}$					
100	16168.15	Upper	98.55	96.35	97.45	85.25	86.25	85.25
		Lower	101.30	102.50	103.30	86.25	85.25	85.25



Table B.3 contd.

Run No.	Heat flux, $W/m^2$	Heating cylinder	Recorded temperatures					
			Wall temperature, $^{\circ}C$			Liquid temperature, $^{\circ}C$		
			$(t_w)_1$	$(t_w)_2$	$(t_w)_3$	$(t_l)_1$	$(t_l)_2$	$(t_l)_3$
101	20210.19	Upper	100.25	100.00	99.35	86.25	86.25	86.25
		Lower	102.80	103.85	104.85	86.25	86.25	86.25
102	24252.22	Upper	102.05	101.85	101.00	86.25	86.25	86.25
		Lower	104.20	105.40	106.75	86.25	86.25	86.25
103	28294.26	Upper	104.60	103.80	103.35	86.25	86.25	86.25
		Lower	105.50	106.90	108.60	86.25	86.25	86.25
104	32336.30	Upper	106.45	105.65	105.20	86.25	86.25	86.25
		Lower	106.70	108.20	110.15	86.25	86.25	86.25
105	35378.33	Upper	107.55	107.25	106.80	86.25	86.25	86.25
		Lower	107.80	109.50	112.00	86.25	86.25	86.25
106	40420.37	Upper	109.35	108.75	108.65	86.25	86.25	86.25
		Lower	109.10	110.75	113.80	86.25	86.25	86.25

Table B.3 contd.

Run No.	Heat flux, $W/m^2$	Heating cylinder	Recorded temperatures					
			Wall temperature, $^{\circ}C$			Liquid temperature, $^{\circ}C$		
			$(t_w)_1$	$(t_w)$	$(t_w)_3$	$(t_l)_1$	$(t_l)_2$	$(t_l)_3$
107	44462.41	Upper	110.60	110.00	109.9	86.25	86.25	86.25
		Lower	110.15	112.00	115.60	86.25	86.25	86.25
108	48504.45	Upper	111.75	111.50	111.30	86.25	86.25	86.25
		Lower	111.25	113.05	117.00	86.25	86.25	86.25

## APPENDIX C

### SAMPLE CALCULATIONS

#### DIMENSIONS OF THE HEATING CYLINDER

Outside diameter,  $D_o = 0.030$  m

Inside diameter,  $D_i = 0.018$  m

Length,  $l = 0.105$  m

#### C.1 HEAT TRANSFER AREA OF THE HEATING CYLINDER, A

$$\begin{aligned} A &= \pi D_o l \\ &= 9.896 \times 10^{-3} \text{ m}^2 \end{aligned} \quad \dots(C.1)$$

#### C.2 HEAT FLUX, q

$$q = \frac{W}{A} \quad \dots(C.2)$$

#### C.3 CORRECTED WALL TEMPERATURE, $t_{wc}$

The corrected value of wall temperature,  $t_{wc}$  is obtained by subtracting the temperature drop across the thickness of the wall of the heating cylinder,  $\delta t_w$  from the measured value of wall temperature. Following equation of conductive heat transfer for thin walled cylinder has been used to calculate the value of  $\delta t_w$ :

$$\delta t_w = \frac{q D_o}{2k_w} l n \frac{D_o}{D_h} \quad \dots(C.3)$$

where  $D_h$  is thermocouple circle diameter and  $k_w$  is the thermal conductivity of the heating cylinder material.

$$D_h = 0.024 \text{ m} , \quad k_w = 16.52 \text{ W/m } ^\circ\text{C}$$

Run number 91 of Table B.1 of Appendix B as reproduced below is selected to demonstrate the calculation procedure:

Heat flux, W/m <sup>2</sup>	Wall temperature, °C			Liquid temperature, °C		
	Top	Side	Bottom	Top	Side	Bottom
40,420.37	129.5	131.35	131.95	109.90	109.90	109.90

Substitution of these values in Eq (C.3)

$$\delta t_w = \frac{40,420.37 \times 0.030}{2 \times 16.52} \ln \frac{0.030}{0.024}$$

$$= 8.187 \text{ } ^\circ\text{C}$$

Now  $t_{wc} = t_w - \delta t_w$

$$(t_{wc})_{\text{Top}} = 129.50 - 8.187 = 121.313 \text{ } ^\circ\text{C}$$

$$(t_{wc})_{\text{Side}} = 131.35 - 8.187 = 123.163 \text{ } ^\circ\text{C}$$

$$(t_{wc})_{\text{Bottom}} = 131.95 - 8.187 = 123.763 \text{ } ^\circ\text{C}$$

#### C.4 WALL SUPERHEAT, $\Delta t_w$

The value of wall superheat,  $\Delta t_w$  is obtained by subtracting the value of liquid temperature,  $t_l$  from the corresponding value of wall temperature,  $t_w$  as given below :

$$(\Delta t_w)_{\text{Top}} = (t_{wc})_{\text{Top}} - (t_l)_{\text{Top}} = 121.313 - 109.9 = 11.413 \text{ } ^\circ\text{C}$$

$$(\Delta t_w)_{\text{Side}} = (t_{wc})_{\text{Side}} - (t_l)_{\text{Side}} = 123.163 - 109.9 = 13.263 \text{ } ^\circ\text{C}$$

$$(\Delta t_w)_{\text{Bottom}} = (t_{wc})_{\text{Bottom}} - (t_l)_{\text{Bottom}} = 123.763 - 109.9 = 13.863 \text{ } ^\circ\text{C}$$

### C.5 AVERAGE WALL SUPERHEAT, $\Delta \bar{t}_w$

The value of average wall superheat,  $\Delta \bar{t}_w$  is obtained by subtracting the value of average liquid temperature,  $\bar{t}_\ell$  from the average value of wall temperature,  $\bar{t}_w$  as given by the following equation :

$$\Delta \bar{t}_w = \bar{t}_w - \bar{t}_\ell$$

The average value of wall temperature,  $\bar{t}_w$  is calculated by substituting the corrected local values of wall temperature in the following equation, Eq (A.8) of Appendix A :

$$\begin{aligned} \bar{t}_w &= \frac{1}{3} [ t_{w,top} + t_{w,side} + t_{w,bottom} ] \\ &= \frac{1}{3} ( 121.313 + 123.163 + 123.763 ) \\ &= 122.746 \text{ } ^\circ\text{C} \end{aligned}$$

The average value of local temperature,  $\bar{t}_\ell$  is obtained in a similar manner :

$$\begin{aligned} \bar{t}_\ell &= \frac{1}{3} [ 109.90 + 109.90 + 109.90 ] \\ &= 109.90 \text{ } ^\circ\text{C} \\ \Delta \bar{t}_w &= 122.746 - 109.90 \\ &= 12.846 \text{ } ^\circ\text{C} \end{aligned}$$

### C.6 PREDICTION OF $\Delta \bar{t}_w$ FROM EQ (6.2)

The experimental values of average wall superheat,  $\Delta \bar{t}_w$  are compared with the predictions from Eq (6.2) of Chapter 6 which is reproduced below :

$$\Delta \bar{t}_w = C_2 q^{0.3} p^{-0.32} \quad \dots(6.2)$$

The value of constant,  $C_2$  for the boiling of toluene is taken from Table 6.1. It is equal to 2.28.

$$q = 40,420.37 \text{ W/m}^2 ; \quad p = 96.00 \text{ kN/m}^2$$

$$\begin{aligned} \Delta \bar{t}_w &= 2.28 (40,420.37)^{0.3} (96.00)^{-0.32} \\ &= 12.752 \text{ }^\circ\text{C} \end{aligned}$$

$$\begin{aligned} \text{Deviation} &= \frac{12.752 - 12.846}{12.846} \times 100 \\ &= -0.729 \text{ per cent} \end{aligned}$$

### C.7 PREDICTION OF $\Delta \bar{t}_w$ FROM ALAD'EV EQUATION, Eq (6.4)

The experimentally-determined values of average wall superheat,  $\Delta \bar{t}_w$  are also compared with the predicted values due to Alad'ev equation, Eq (2.105) which is as follows :

$$\frac{\Delta \bar{t}_w}{T_s} = 4.7 \times 10^3 \left[ \frac{10^{-6} q \lambda}{k \rho T_s g} \right]^{0.3} \left[ \frac{\lambda}{c \rho T_s} \right]^{1.2}$$

The physico-thermal properties used in Eq (2.105) are taken at the measured liquid temperature [ 102-105].

For Run No. 4 of Table B.1 of Appendix B

$$\begin{aligned} \Delta \bar{t}_w &= 4.7 \times 10^{-3} \left[ \frac{10^{-6} \times 32336.3 \times 2256.2 \times 10^3}{0.6825 \times 373.22 \times 9.81} \right]^{0.3} \times \\ &\quad \left[ \frac{2256.2 \times 10^3}{4220.8 \times 373.22} \right]^{1.2} \times 373.22 \\ &= 7.43 \text{ }^\circ\text{C} \end{aligned}$$

$$\begin{aligned} \text{Deviation} &= \frac{7.43 - 6.48}{6.48} \times 100 \\ &= 14.66 \text{ per cent} \end{aligned}$$

### C.8 PREDICTION OF $\Delta \bar{t}_w$ FROM MODIFIED ALAD'EV EQUATION, Eq(6.4)

The modified Alad'ev equation is :

$$\frac{\Delta \bar{t}_w}{T_s} = C_3 \left[ \frac{10^{-6} q \lambda}{k_f T_s g} \right]^{0.3} \left[ \frac{\lambda}{c_f T_s} \right]^{1.2} \left[ \frac{\rho_f}{\rho_v} \right]^{0.24}$$

The value of the constant,  $C_3$  is taken from Table 6.3. For distilled water of Run No. 4 of Table B.1 of Appendix B

$$C_3 = 6.92 \times 10^{-4}$$

$$\begin{aligned} \Delta \bar{t}_w &= 6.92 \times 10^{-4} \left[ \frac{10^{-6} \times 32336.3 \times 2256.2 \times 10^3}{0.6825 \times 373.22 \times 9.81} \right]^{0.3} \times \\ &\quad \left[ \frac{2256.2 \times 10^3}{4220.8 \times 373.22} \right]^{1.2} \left[ \frac{958.24}{0.602} \right]^{0.24} \times \\ &= 373.22 \\ &= 6.42 \text{ } ^\circ\text{C} \end{aligned}$$

$$\begin{aligned} \text{Deviation} &= \frac{6.42 - 6.48}{6.48} \times 100 \\ &= -0.93 \text{ per cent} \end{aligned}$$

### C.9 PREDICTION OF $\Delta \bar{t}_w / \Delta \bar{t}_{w,1}$ USING Eq (6.8)

Data of Run Nos.20 and 4 of Table B.1 of Appendix are used :

$$\left[ \frac{\Delta \bar{t}_w}{\Delta \bar{t}_{w,1}} \right]_{\text{expt.}} = 1.3161$$

The value of  $\frac{\Delta \bar{t}_w}{\Delta \bar{t}_{w,1}}$  is calculated by Eq (6.8) which is as follows :

$$\begin{aligned}
 \left[ \frac{\Delta \bar{t}_w}{\Delta t_{w,1}} \right]_{\text{Pred.}} &= \left[ \frac{p}{p_1} \right]^{-0.589} \left[ \frac{\rho \ell}{\rho_{\ell,1}} \right]^{-0.525} \left[ \frac{c \ell}{c_{\ell,1}} \right]^{-0.675} \\
 &\quad \left[ \frac{k \ell}{k_{\ell,1}} \right]^{-0.3} \left[ \frac{\lambda}{\lambda_1} \right]^{0.276} \left[ \frac{\sigma}{\sigma_1} \right]^{0.249} \\
 &\quad \left[ \frac{\rho_v}{\rho_{v,1}} \right]^{0.276} \left[ \frac{T_s}{T_{s,1}} \right]^{0.024} \left[ \frac{q}{q_1} \right]^{0.3} \\
 &\quad \dots (6.8)
 \end{aligned}$$

$$\begin{aligned}
 \left[ \frac{\Delta \bar{t}_w}{\Delta t_{w,1}} \right]_{\text{Pred.}} &= \left[ \frac{44.50}{98.00} \right]^{-0.589} \left[ \frac{971.6895}{958.237} \right]^{-0.525} \left[ \frac{4.1956}{4.2137} \right]^{-0.675} \\
 &\quad \left[ \frac{0.6745}{0.6826} \right]^{-0.3} \left[ \frac{2.3078 \times 10^6}{2.2562 \times 10^6} \right]^{0.276} \left[ \frac{0.0625}{0.0588} \right]^{0.249} \\
 &\quad \left[ \frac{0.2948}{0.6014} \right]^{0.276} \left[ \frac{358.35}{373.25} \right]^{0.024} \left[ \frac{32336.3}{32336.3} \right]^{0.3}
 \end{aligned}$$

= 1.3351 against the experimental value of 1.3161.

$$\begin{aligned}
 \text{Deviation} &= \frac{1.3351 - 1.3161}{1.3161} \times 100 \\
 &= 1.44 \text{ per cent}
 \end{aligned}$$

#### C.10 PREDICTION OF $(\Delta \bar{t}_w)_b$ USING Eq (6.9)

The value of average wall superheat for the boiling of benzene at a given value of heat flux and pressure is calculated from Eq (6.9) by the knowledge of average wall superheat for the boiling of distilled water for the same value of heat flux, pressure and the heating surface using the



following procedure:

Eq (6.9) is reproduced below :

$$\frac{(\Delta \bar{t}_w)_b}{(\Delta \bar{t}_w)_w} = 1.98$$

Run No. 4 of Table B.1 of Appendix B corresponds to the data for the boiling of distilled water at a heat flux of  $32333.6 \text{ W/m}^2$  and a pressure of  $98.00 \text{ kN/m}^2$ . For this run the experimentally-obtained value of average wall superheat,

$$(\Delta \bar{t}_w)_w = 6.48 \text{ }^\circ\text{C}$$

Using the value of  $(\Delta \bar{t}_w)_w$  in Eq (6.9) :

$$\begin{aligned} (\Delta \bar{t}_w)_b &= 1.98 \times 6.48 \\ &= 12.83 \text{ }^\circ\text{C} \end{aligned}$$

This value is for the boiling of benzene at heat flux of  $32336.3 \text{ W/m}^2$  and pressure of  $98.0 \text{ kN/m}^2$  and thus corresponds to data of Run No. 45 of Table B.1 of Appendix B. For this Run, the experimentally-determined value of average wall superheat,

$$(\Delta \bar{t}_w)_b = 12.12$$

$$\begin{aligned} \text{Deviation} &= \frac{12.83 - 12.12}{12.12} \times 100 \\ &= 5.85 \text{ per cent} \end{aligned}$$

APPENDIX D  
ERROR ANALYSIS

The measurement of the dimensions of the heating cylinder, power input to the heater, wall temperature and the liquid temperature always has some inaccuracies due to the limitations of the measuring instruments. Therefore error is involved in the prediction of wall superheat and heat transfer coefficient. In order to obtain the degree of error in the present experimentation, error associated with all the measuring parameters was calculated for several experimental runs. This appendix presents a typical sample calculation of error analysis for Run no. 6 of Table B.2 of Appendix B.

The error in a quantity is calculated by the following equation :

$$E_x = \left[ \sum_{i=1}^n \left( \frac{\partial x}{\partial y_i} E_{y_i} \right)^2 \right]^{1/2} \quad \dots(D.1)$$

where E represents error, x represents quantity which is a function of n variables and  $y_i$  is the  $i$ th variable.

D.1 ERROR IN THE SURFACE AREA OF HEATING CYLINDER,  $E_A$  :

Since  $A = \pi D_o \ell$   
hence  $E_A = \left[ \left( \pi \ell E_{D_o} \right)^2 + \left( \pi D_o E_{\ell} \right)^2 \right]^{1/2} \quad \dots(D.2)$

where  $E_{D_o}$  and  $E_{\ell}$  denote the error associated with diameter and length respectively.

$$D_o = 0.030 \text{ m} \quad , \quad E_{D_o} = 0.0001 \text{ m}$$

$$\ell = 0.105 \text{ m} \quad , \quad E_{\ell} = 0.0001 \text{ m}$$

$$A = \pi \times 0.030 \times 0.105 \\ = 9.896 \times 10^{-3} \text{ m}^2$$

and

$$E_A = [ (\pi \times 0.105 \times 0.0001)^2 + (\pi \times 0.030 \times 0.0001)^2 ]^{1/2} \\ = 3.43 \times 10^{-4} \text{ m}^2$$

#### D.2 ERROR IN HEAT FLUX, $E_q$

$$q = \frac{Q}{\pi D_o \ell}$$

$$\text{so } E_q = \left[ \left( \frac{E_Q}{\pi D_o \ell} \right)^2 + \left( \frac{-Q}{\pi D_o^2 \ell} E_{D_o} \right)^2 + \left( \frac{-Q}{\pi D_o \ell^2} E_{\ell} \right)^2 \right]^{1/2} \quad \dots (D.3)$$

where  $E_Q$  represents error in the measurement of heat input.

$$Q = 400 \text{ W} \quad , \quad E_Q = 8 \text{ W}$$

$$q = \frac{400}{\pi \times 0.030 \times 0.105} \\ = 40,420.37 \text{ W/m}^2$$

$$E_q = \left[ \left( \frac{8}{\pi \times 0.030 \times 0.105} \right)^2 + \left( \frac{-400 \times 0.0001}{\pi \times (0.030)^2 \times 0.105} \right)^2 + \left( \frac{-400 \times 0.0001}{\pi \times 0.030 \times (0.105)^2} \right)^2 \right]^{1/2} \\ = 820.46 \text{ W/m}^2$$

### D.3 ERROR IN TEMPERATURES, $E_{t_w}$ AND $E_{t_f}$

The corrected wall temperature of the heating cylinder was calculated by subtracting the temperature drop across the wall thickness of the heating cylinder from the measured wall temperature.

To calculate the temperature drop across the wall thickness of the heating cylinder following equation was used :

$$\delta t_w = \frac{q D_o}{2k_w} \ln \frac{D_o}{D_h}$$

$$\text{hence } E_{\delta t_w} = \left[ \left\{ \frac{D_o}{2k_w} \ln \left( \frac{D_o}{D_h} \right) E_q \right\}^2 + \left\{ \left( \frac{q}{2k_w} \ln \left( \frac{D_o}{D_h} \right) + \frac{q}{2k_w} \right) E_{D_o} \right\}^2 \right. \\ \left. + \left\{ \frac{-q D_o}{2k_w^2} \ln \frac{D_o}{D_h} E_{k_w} \right\}^2 + \left\{ \frac{-q D_o}{2k_w} \frac{1}{D_h} E_{D_h} \right\}^2 \right]^{1/2} \quad \dots(D.4)$$

where  $E_{k_w}$  and  $E_{D_h}$  represent error associated with the thermal conductivity of the heating cylinder and thermocouple circle diameter respectively.

$$k_w = 16.52 \text{ W/m K} \quad , \quad E_{k_w} = 0.0$$

$$D_h = 0.024 \text{ m} \quad , \quad E_{D_h} = 0.0001 \text{ m}$$

$$\delta t_w = \frac{40,420.37 \times 0.030}{2 \times 16.52} \ln \frac{0.030}{0.024}$$

$$= 8.189 \text{ }^\circ\text{C}$$

$$\begin{aligned}
 E_{\delta t_w} &= \left[ \left\{ \frac{0.030}{2 \times 16.52} \ln \left( \frac{0.030}{0.024} \right) \times 820.46 \right\}^2 \right. \\
 &+ \left\{ \left( \frac{40,420.37}{2 \times 16.52} \ln \left( \frac{0.030}{0.024} \right) + \frac{40,420.37}{2 \times 16.52} \right) 0.0001 \right\}^2 \\
 &+ \left\{ - \frac{40,420.37}{2 \times (16.52)^2} \ln \left( \frac{0.030}{0.024} \right) \times 0.0 \right\}^2 \\
 &+ \left. \left\{ - \frac{40,420.37 \times 0.030}{2 \times 16.52} \times \frac{1}{0.024} \times 0.0001 \right\}^2 \right]^{1/2} \\
 E_{\delta t_w} &= 0.2709 \text{ } ^\circ\text{C}
 \end{aligned}$$

Corrected wall temperature,  $t_{wc}$  is given by :

$$t_{wc} = t_w - \delta t_w$$

$$\text{hence } E_{t_{wc}} = \left[ \left( E_{t_w} \right)^2 + \left( -E_{\delta t_w} \right)^2 \right]^{1/2} \quad \dots (D.5)$$

Wall temperature

$$(t_w)_{\text{top}} = 113.65^\circ\text{C} \quad , \quad E_{t_w} = 0.01^\circ\text{C}$$

$$(t_w)_{\text{side}} = 115.75^\circ\text{C} \quad , \quad E_{t_w} = 0.01^\circ\text{C}$$

$$(t_w)_{\text{bottom}} = 116.80^\circ\text{C} \quad , \quad E_{t_w} = 0.01^\circ\text{C}$$

Corrected wall temperature

$$(t_{wc})_{\text{top}} = 113.65 - 8.189 = 105.461^\circ\text{C}$$

$$(t_{wc})_{\text{side}} = 115.75 - 8.189 = 107.561^\circ\text{C}$$

$$(t_{wc})_{\text{bottom}} = 116.80 - 8.189 = 108.611^\circ\text{C}$$

Error in corrected wall temperature

$$E_{t_{wc}} = [(0.01)^2 + (-0.2709)^2]^{1/2}$$

$$= 0.2711 \text{ } ^\circ\text{C}$$

Average wall temperature

$$\bar{t}_w = \frac{(t_{wc})_{top} + (t_{wc})_{side} + (t_{wc})_{bottom}}{3}$$

$$= \frac{105.461 + 107.561 + 108.611}{3}$$

$$\bar{t}_w = 107.211 \text{ } ^\circ\text{C}$$

Error in average wall temperature

$$E_{\bar{t}_w} = \left[ 3 \times \left( \frac{E_{t_{wc}}}{3} \right)^2 \right]^{1/2} \quad \dots(D.6)$$

$$= \left[ 3 \times \left( \frac{0.2711}{3} \right)^2 \right]^{1/2}$$

$$= 0.1565 \text{ } ^\circ\text{C}$$

Liquid temperature

$$(t_{\ell})_{top} = 100.25 \text{ } ^\circ\text{C} \quad , \quad E_{t_{\ell}} = 0.01 \text{ } ^\circ\text{C}$$

$$(t_{\ell})_{side} = 100.25 \text{ } ^\circ\text{C} \quad , \quad E_{t_{\ell}} = 0.01 \text{ } ^\circ\text{C}$$

$$(t_{\ell})_{bottom} = 100.25 \text{ } ^\circ\text{C} \quad , \quad E_{t_{\ell}} = 0.01 \text{ } ^\circ\text{C}$$

Average liquid temperature

$$\bar{t}_{\ell} = 100.25 \text{ } ^\circ\text{C}$$

Error in average liquid temperature

$$E_{\bar{t}_\ell} = \left[ 3 \times \left( \frac{E_{t_\ell}}{3} \right)^2 \right]^{1/3} \quad \dots(D.7)$$

$$E_{\bar{t}_\ell} = \left[ 3 \times \left( \frac{0.01}{3} \right)^2 \right]^{1/2}$$

$$= 0.0058 \text{ } ^\circ\text{C}$$

D.4 ERROR IN AVERAGE WALL SUPERHEAT,  $E_{\Delta\bar{t}_w}$

$$\Delta\bar{t}_w = \bar{t}_w - \bar{t}_\ell$$

$$\text{hence } E_{\Delta\bar{t}_w} = \left[ \left( E_{\bar{t}_w} \right)^2 + \left( -E_{\bar{t}_\ell} \right)^2 \right]^{1/2} \quad \dots(D.8)$$

Therefore,

$$\Delta\bar{t}_w = 107.211 - 100.25$$

$$= 6.961 \text{ } ^\circ\text{C}$$

and

$$E_{\Delta\bar{t}_w} = \left[ (0.1565)^2 + (0.0058)^2 \right]^{1/2}$$

$$= 0.1567 \text{ } ^\circ\text{C}$$

Thus, average wall superheat

$$\Delta\bar{t}_w = 6.961 \pm 0.1567 \text{ } ^\circ\text{C} ; \text{ error} = \pm 2.25 \text{ per cent.}$$

D.5 ERROR IN AVERAGE HEAT TRANSFER COEFFICIENT,  $E_h$ 

$$h = \frac{q}{\Delta \bar{t}_w}$$

$$\text{hence } E_h = \left[ \left( \frac{E_q}{\Delta \bar{t}_w} \right)^2 + \left( - \frac{q}{\Delta \bar{t}_w^2} E_{\Delta \bar{t}_w} \right)^2 \right]^{1/2} \quad \dots (D.9)$$

$$\text{Therefore, } h = \frac{40,420.37}{6.961}$$

$$= 5806.69 \text{ W/m}^2 \text{ } ^\circ\text{C}$$

and

$$E_h = \left[ \left( \frac{820.46}{6.961} \right)^2 + \left( - \frac{40,420.37}{(6.961)^2} \times 0.1567 \right)^2 \right]^{1/2}$$

$$= 176.01 \text{ W/m}^2 \text{ } ^\circ\text{C}$$

Average heat transfer coefficient

$$h = 5806.69 \pm 176.01 \text{ W/m}^2 \text{ } ^\circ\text{C} ; \text{ error} = \pm 3.03 \text{ per cent.}$$

Similar calculations with some other runs showed almost the same degree of error. Therefore, it can be concluded that the error in the present experimentation is well within  $\pm 10$  per cent which is an acceptable level of error in the studies of boiling heat transfer.



## REFERENCES

1. Jakob, M., Heat Transfer , John Wiley and Sons, Inc., New York, Vol. 1, pp. 640-647 (1949).
2. Jakob, M. and Linke, W., Physik Z., Vol. 36, pp. 267-280 (1935).
3. Corty, C. and Foust, A.S., 'Surface variables in nucleate boiling', Chem. Engg. Prog. Symp. Ser., Vol. 51, No. 17, pp. 1-12 (1955).
4. Gaertner, R.F. and Westwater, J.W., 'Population of active sites in nucleate boiling heat transfer', Chem. Engg. Prog. Symp. Ser., Vol. 56, No.30, pp.39-48 (1960).
5. Nishikawa, K. and Urakawa, K., Memoirs of the Faculty of Engineering, Kyushu University, Vol. 19, p. 139 (1960).
6. Kurihara, H.M. and Myers, J.E., 'The effect of superheat and surface roughness on boiling coefficients', AIChE, J., Vol. 6, No. 1, pp. 83-91 (1960).
7. Griffith, P. and Wallis, J.D., 'The role of surface conditions in nucleate boiling', Chem. Engg. Prog.Symp.Ser., Vol. 56, No. 30, pp. 49-63 (1960).
8. Gaertner, R.F., 'Distribution of active sites in nucleate pool boiling of liquids', Chem. Engg. Prog. Symp. Ser., Vol. 59, No.41, pp. 52-61 (1963).
9. Hsu, Y.Y. and Graham, R.W., Transport Processes in Boiling and Two Phase Systems , pp. 3-46, Hemisphere Publ.Co., Washington (1976).
10. Gaertner, R.F., 'Photographic study of nucleate pool boiling on a horizontal surface', Trans. ASME, Ser. C., J. Heat Transfer, Vol. 87, pp. 17-29 (1965).
11. Kirby, D.B. and Westwater, J.W., 'Bubble and vapour behaviour on a heated horizontal plate during pool boiling near burnout', Chem.Engg. Prog. Symp. Ser., Vol. 61, No.57, pp. 238-248 (1965).

12. Wiebe, J.R. and Judd, R.L., 'Superheat layer thickness measurements in saturated and subcooled nucleate boiling', Trans. ASME, Sec. C, J. Heat Transfer, pp. 455-461 (1971).
13. Brown, W.T., Jr., 'Study of flow surface boiling', Ph.D. Thesis, Mechanical Engineering Department, M.I.T. (1967).
14. Shoukri, M. and Judd, R.L., 'Nucleation site activation in saturated boiling', Trans. ASME, Ser. C., J. Heat Transfer, Vol. 97, No. 1, pp. 93-98 (1975).
15. Danilova, G.N., 'The effect of the number of active nuclei on the rate of transfer in large volume nucleate boiling', NASA TTF-11-305, 1967; from Inz. Fizicheskiy Zhu., Vol. XI, pp. 367-370 (1966).
16. Akiyama, M., 'Dynamics of an isolated vapour bubble in saturated nucleate boiling (part II-configuration and departure)', Bulletin JSME, Vol. 13, No. 55, pp. 86-95 (1970).
17. Kiper, A.M., 'Minimum bubble departure diameter in nucleate pool boiling', Int. J. Heat Mass Transfer, Vol. 14, pp. 931-937 (1971).
18. Katto, Y. and Kikuchi, K., 'Study of forces acting on a heated surface in nucleate pool boiling at high heat flux', Heat Transfer - Japanese Research, Vol. 1, No. 4, pp. 36-46 (1972).
19. Leppert, G. and Pitts, C.C., 'Advances in Heat Transfer', Vol. 1, (Edited by T.F. Irvine, Jr. and J.P. Hartnett), pp. 185-263, Academic Press, New York - London (1964).
20. Hatton, A.P. and Hall, I.S., Third Int. heat transfer conf. Chicago, Vol. 4 (1966).
21. Hughes, R.R. and Gilliland, E.R., Chem. Engg. Prog. Vol. 48, No. 10, p. 497 (1952).

22. Hatton, A.P., James, D.D. and Liew, T.L., 'Measurement of bubble characteristics for pool boiling from single cylindrical cavities', Heat Transfer 1970, V, Elsevier, Paper B 1.2 (1970).
23. Fritz, W. and Ende, W., Physik, Z., Vol. 36, p. 379 (1935).
24. Kabanow, W. and Frumkin, A., Z. Phys., Chem.(A), 165, 316, 433 (1933).
25. Cole, R. and Shulman, H.L., 'Bubble departure diameters at subatmospheric pressures', Chem. Engg. Prog. Symp. Ser., Vol. 62, No. 64, pp. 6-16 (1966).
26. Roll, J.B. and Myers, J., 'The effect of surface tension on factors in boiling heat transfer', AIChE J., Vol. 10, No.4, pp. 530-534 (1964).
27. Cole, R., 'Bubble frequencies and departure volumes at subatmospheric pressures', AIChE J., Vol. 13, No.4, pp. 779-783 (1963).
28. Zuber, N., 'Hydrodynamic aspects of boiling heat transfer', U.S. Atomic Energy Commission Report, AECU-4439, AEC Tech. Inf. Serv., Oak Ridge, Tenn (1959).
29. Ruckenstein, E., Bulletin, Inst. Politech. Bucaresti, Vol. 33, p. 79 (1961).
30. Semeria, R.L., 'An experimental study of the characteristics of vapour bubbles', Paper-7, Symposium of Two-Phase Fluid Flow, Inst. Mech. Engrs., London (1962).
31. Tolubinskii, V.I. and Ostrovsky, J.N., 'On the mechanism of boiling heat transfer', Int. J. Heat and Mass Transfer, Vol. 9, pp. 1463-1470 (1966).
32. Siegel, R. and Keshock, E.G., 'Effects of reduced gravity on nucleate boiling bubble dynamics in saturated water', AIChE J., Vol. 10, pp.509-517 (1964).
33. Wanninger, W., Chem. Ing. Tech., Vol. 37, p. 939 (1965).

34. Perkins, H.S. and Westwater, J.W., 'Measurements of bubbles formed in boiling methanol', *AICHE J.*, Vol.2, pp. 471-476 (1956).
35. Jicina-Molazhin, L.N. and Kutateladze, S.S., 'On the problem of effect of pressure on the mechanism of vaporisation in boiling liquid', *J. Technical Physics*, Vol. 20, No.1, pp. 110-116 (1950).
36. Rallis, C.J. and Jawurek, H.H., 'Latent heat transport in saturated nucleate boiling', *Int. J. Heat and Mass Transfer*, Vol. 7, pp. 1051-1068 (1964).
37. Staniszewski, B.E., Technical Report No. 16, Div. Sponsored Res. MIT, Cambridge (1959).
38. Han, C.Y. and Griffith, P., 'The mechanism of heat transfer in nucleate pool boiling-part I : bubble initiation, growth and departure', *Int. J. Heat and Mass Transfer*, Vol. 8, pp. 887-904 (1965).
39. Plasset, M.S. and Zwick, S.A., 'The growth of vapour bubbles in superheated liquids', *J. Applied Physics*, Vol. 25, No.4, pp. 493-500 (1954).
40. Ivey, H.J., 'Relationship between bubble frequency, departure diameter and rise velocity in nucleate boiling', *Int. J. Heat and Mass Transfer*, Vol. 10, pp. 1023-1040 (1967).
41. Dunskus, T. and Westwater, J.W., 'The effect of trace additives on heat transfer to boiling isopropanol', *Chem. Engg. Prog. Symp. Ser.*, Vol. 57, No. 32, pp. 173-181 (1961).
42. Costello, C.P. and Tuthill, W.E., 'Effect of acceleration on nucleate pool boiling', *Chem. Engg. Prog. Symp. Ser.*, Vol. 57, No. 32, pp. 189-196 (1961).
43. Cryder, D.S. and Gilliland, E.R., *Ind. Engg. Chem.*, Vol. 24, pp. 1382-1387 (1937).

44. Akin, G.A. and McAdams, W.H., Trans. AIChE J., Vol. 45, pp. 137 (1937).
45. Insinger, T.H., and Bliss, H., Trans. AIChE J., Vol. 36, pp. 491-516 (1940).
46. Linden, C.M. and Montillon, G.H., Ind. Engg. Chem., Vol. 22, pp. 708 (1930).
47. Dunn, P.S. and Vincent, A.D., Thesis MIT (1953).
48. Cryder, D.S. and Finalborgo, A.C., 'Heat transmission from metal surfaces to boiling liquids : Effect of temperature of the liquid on film coefficient', Trans. AIChE, Vol. 33, pp. 346-362 (1937).
49. Bonilla, C.F. and Perry, C.W., 'Heat transmission to boiling binary liquid mixtures', Trans. AIChE, Vol. 37, pp. 685-705 (1941).
50. Cichelli, M.T. and Bonilla, C.F., 'Heat transfer to liquids boiling under pressure', Trans. AIChE, Vol. 41, pp. 755-787 (1945).
51. Sternling, C.V. and Tichacek, L.J., 'Heat transfer coefficients for boiling mixtures - experimental data for binary mixtures of large relative volatility', Chem. Eng. Sci., Vol. 16, pp. 297-337 (1961).
52. Addoms, J.N., 'Heat transfer at high rates to water boiling outside cylinders', D.Sc. Thesis, Department of Chemical Engineering, MIT (1948).
53. Farber, E.A. and Scoria, R.L., Trans. ASME, Vol. 70, p. 369 (1948).
54. Hughmark, G.A., 'Statistical analysis of nucleate pool boiling data', AIChE National Meeting, Cleveland, Abstract 41 (1961).
55. Drayers, D.E., 'Nucleate boiling of hydrogen', Ind. Engg. Chem. Fundamentals, Vol. 4, No. 2, pp. 167-171 (1965).
56. Forster, H.K. and Zuber, N., 'Bubble dynamics and boiling heat transfer', AIChE, Vol. 1, pp. 531-535 (1955).

57. Forster, K.E. and Greif, R., 'Heat transfer to a boiling liquid-mechanism and correlations', Trans. ASME, Ser.C., J. Heat Transfer, Vol. 81, p.43-53 (1959).
58. Levy, S., 'Generalised correlation of boiling heat transfer', Trans. ASME, Ser.C., J. Heat Transfer, Vol. 81, pp. 37-42 (1959).
59. Nishikawa, K., et al., Memoirs of the Faculty of Engineering, Kyushu University, Vol. 16, No. 1, pp.28 (1956).
60. Miyauchi, T. and Yagi, S., Soc. Chem.Engrs., Japan, Vol. 25, No. 1, pp.18-30 (1961).
61. Kosky, P.G. and Lyon, D.N., 'Pool boiling heat transfer data to cryogenic liquids - Nucleate regime data and a test of some nucleate boiling correlations', AIChE J., Vol. 14, No. 3, pp. 372-387 (1968).
62. Gilmour, C.H., 'Nucleate boiling - A correlation', Chem. Engg. Prog., Vol. 54, No. 10, pp. 77-79 (1958).
63. McNelly, M.J., 'A correlation of rates of heat transfer to nucleate boiling of liquids', J. Imperial Coll., Chem. Eng. Soc., Vol. 7, pp. 18-34 (1953).
64. Kutateladze, S.S., Fundamentals of Heat Transfer, Edward Arnold (Publishers) Ltd., London (1963).
65. Borishanskii, V.M., Bobrovich, G.I. and Minchenko, F.P., 'Heat transfer from a tube to water and to ethanol in nucleate pool boiling', Problems of Heat Transfer and Hydraulics of Two phase media - A symposium edited in Russian by Kutateladze, S.S. and translated by Blunn, O.M., Pergamon Press Ltd., pp. 85-106 (1969).
66. Rohsenow, W.M., 'A method of correlating heat transfer data for surface boiling of liquids', Trans. ASME, Vol. 74, pp. 969-975 (1952).

67. Sciance, C.T., Colver, C.P. and Slipecevich, C.M., 'Nucleate pool boiling and burnout of liquified hydrocarbon gases', Chem. Eng. Prog. Symp. Ser., Vol. 63, No. 77, pp. 109-114 (1967).
68. Frost, C.W. and Li, K.W., 'On the Rohsenow pool-boiling correlations', Trans. ASME, Ser.C., J. Heat Transfer, Vol. 93, pp. 232-234 (1971).
69. Rice, P. and Calus, W.F., 'Pool boiling-single component liquids', Chem. Eng.Sci., Vol. 27, pp.1677-1686 (1972).
70. Huber, D.A. and Hoehne, J.C., 'Pool boiling of benzene, diphenyl and benzene diphenyl mixtures under pressure', J. Heat Transfer, Vol. 85, No.3, pp. 215-220 (1963).
71. Labuntsov, D.A., 'Heat transfer correlations for nucleate boiling of a liquid', Teploenergetika, No. 5 (1960).
72. Veneraki, I.E., 'Heat transfer rates during the boiling of water and sugar solutions in vertical and horizontal tubes under conditions of free convection', Izvest. Kiev. Politekh. Inst., Vol. 18, pp. 344-357 (1955).
73. Chi Fang Lin, Yu Cho and Fan Kuo Kung, 'The boiling heat transfer coefficient of binary liquid mixtures', Huo Kung Hsuch Pao, No.2, pp. 137-146 (1959).
74. Kozitskii, V.I., 'Heat transfer coefficient during the boiling of n-Butane on surfaces of various roughness', Int. Chem.Eng., Vol. 12, p. 685 (1972).
75. Bankoff, S.G., 'On the mechanism of subcooled nucleate boiling', Chem. Engg. Prog. Symp. Ser., Vol. 57, pp. 156-172 (1961).
76. Zuber, N., 'Nucleate boiling : The region of isolated bubbles and the similarity with natural convection', Int. J. Heat Mass Transfer, Vol. 6, pp.53-78 (1963).

77. Judd, R.L. and Merte, H. Jr., 'Evaluation of nucleate boiling heat flux predictions at varying levels of subcooling and acceleration', Int. J. Heat Mass Transfer, Vol. 15, pp.1075-1096 (1972).
78. Tien, C.L., 'A hydrodynamic model for nucleate pool boiling', Int. J. Heat Mass Transfer, Vol. 5, pp. 533-540 (1962).
79. Yamagata, K; Hirano, F., Nichikawa, K. and Matsuoka, H., Mem. Fac. Eng., Kyushu Univ., Vol. 15, p.97(1959).
80. Gaertner, R.F. and Westwater, J.W., Chem.Eng. Prog. Symp. Ser., Vol. 56, p. 39 (1959).
81. Minchenko, F.P. and Firsova, E.V., 'Heat transfer to water and water-lithium salt solutions in nucleate pool boiling', Problems of Heat Transfer and Hydraulics of Two-Phase Media - A symposium edited in Russian by S.S. Kutateladze and translated by O.M. Blunn, Pergamon Press Ltd., pp. 137-151(1969).
82. Alam, S.S. and Varshney, B.S., 'Nucleate pool boiling of liquids', Paper No.B-5, Second National Heat and Mass Transfer Conference, December 13-15 (1973), I.I.T. Kanpur.
83. Tolubinskii, V.I. and Kostanchuk, D.M., 'Effect of pressure on heat transfer during subcooled water boiling', Vop. Tekh.Teplofic, No.3, pp. 58-61(1971).
84. Rohsenow, W.M. and Clark, J.A., 'Heat transfer and pressure drop data for high heat flux densities to water at high sub-critical pressures', Heat Transfer and Fluid Mech. Inst., Stanford University Press, Stanford, California (1951).
85. Piret, E.L. and Isbin, H.S., 'Natural-circulation evaporation', Chem. Eng. Prog., Vol. 50, pp.305-311 (1954).
86. McFadden, P.W. and Grassmann, P., 'The relation between bubble frequency and diameter during nucleate pool boiling', Int. J. Heat Mass Transfer, Vol. 5, pp.169-173 (1962).



87. Nishikawa, K., et al , Memoirs of the Faculty of Engineering, Kyushu University, Vol. 15, No. 1 (1955) .
88. Nishikawa, K., et al., Memoirs of the Faculty of Engineering, Kyushu University, Vol. 17, No.2, pp.85-103 (1958).
89. Nishikawa, K. and Yamagata, K., 'On the correlation of nucleate boiling heat transfer', Int. J. Heat Mass Transfer, Vol. 1, pp. 219-235 (1960).
90. Nishikawa, K. and Urakawa, K., Trans. JSME, Vol. 23, No.136, p.935 (1958).
91. Nishikawa, K. and Urakawa, K., 'An experiment of nucleate boiling under reduced pressures', Memoirs of the Faculty of Engineering, Kyushu University, Vol. 19, No. 3, pp. 63-71 (1960).
92. Mikic, B.B. and Rohsenow, W.M., 'A new correlation of pool-boiling data including the effect of heating surface characteristics', Trans. ASME, Ser. C., J. Heat Transfer, pp. 245-250 (1969).
93. Sharma, P.R., Kumar, P., Gupta, S.C. and Varshney, B.S., 'Nucleate pool boiling of liquids on horizontal cylinder at subatmospheric pressures', Proc. Fourth National Heat Mass Transfer Conf., University of Roorkee, Roorkee (1977).
94. Alad'ev, I.T., 'Convective and radiant heat exchange', (Konvektivnyi i Luchisty teploobmen), Izd. Akad. Nauk., USSR, pp.232-254 (1960).
95. Raben, I.A., Beaubouef, R.T. and Commerford, G.E., 'A study of heat transfer in nucleate pool boiling of water at low pressure', Chem. Eng. Prog. Symp. Ser., Vol. 61, No. 57, pp. 249-257 (1955).
96. Singh, A., Mikic, B.B., and Rohsenow, W.M., 'Relative behaviour of water and organics in boiling', Sixth Int. Heat Mass Transfer Conf., Toronto, Canada, pp. 163-168 (1978).

97. Preckshot, G.W. and Denny, V.E., Canadian J. Chem. Eng., Vol. 45, p.241 (1967).
98. Cole, R and Rohsenow, W.M., 'Correlation of bubble departure diameter for boiling of saturated liquids', Chem. Eng. Prog. Symp. Ser., Vol. 65, No. 92, pp. 211-213 (1969).
99. Saini, J.S., Gupta, C.P. and Lal, S., 'Bubble departure diameter in nucleate pool boiling', Letters in Heat and Mass Transfer, Vol. 2, No. 1, pp. 41-48 (1975).
100. Saini, J.S., Gupta, C.P. and Lal, S., 'Bubble growth in nucleate pool boiling', Proceedings of First National Heat and Mass Transfer Conference, Madras, pp. IX-31-38 (1971).
101. Saini, J.S., Gupta, C.P. and Lal, S., 'Effect of Jakob number on forces controlling bubble departure in nucleate pool boiling', Int. J. Heat Mass Transfer, Vol. 18, p. 472 (1975).
102. Mikheyev, M., Fundamentals of Heat Transfer, Mir Publishers, Moscow (1977).
103. Perry, J.H., Chemical Engineers' Handbook, IV edition, McGraw Hill Book Co. Inc. (1963).
104. Vargaftic, N.B., Handbook on Physical Properties of Gases and Liquids, Gasudarstvenace Isdalelstav Physico-Matematicheskoe Literaturee, Moskava(1963).
105. Kutateladze, S.S. and Borishanskii, V.M., A Concise Encyclopedia of Heat Transfer, Pergamon Press, pp. 202-205 (1966).

